PhD. Olga GARBUZ
Prof. Valentin GUDUMAC
Acad. Ion TODERAS
Acad. Aurelian GULEA

ANTIOXIDANT PROPERTIES OF SYNTHETIC COMPOUNDS AND NATURAL PRODUCTS. ACTION MECHANISMS.

MONOGRAPH

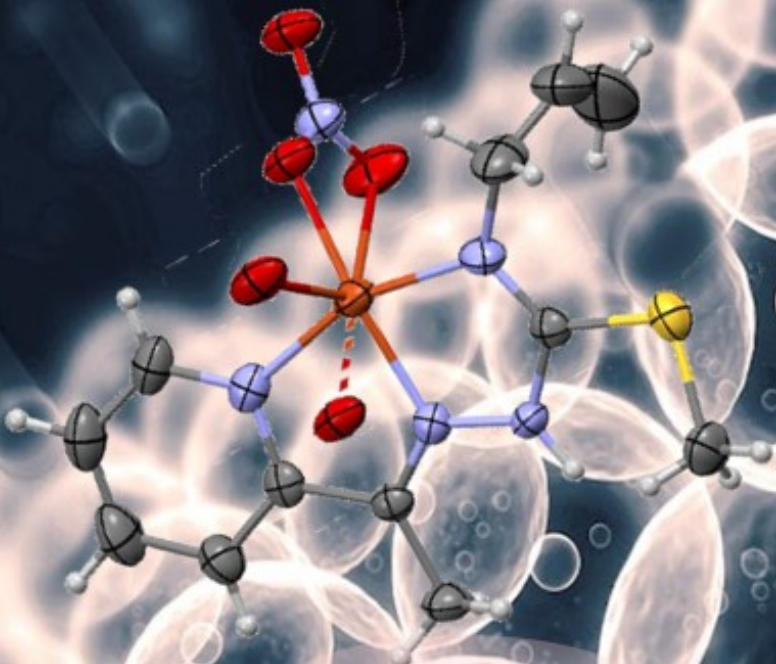

Chișinău, 2023

GULEA Aurelian
Academician, Doctor Habilitate, University Professor. Head of Scientific Research Laboratory Advanced Materials in Biopharmaceuticals and Technology, Moldova State University.
Areas of expertise: coordinative chemistry, biopharmaceutical chemistry, biochemistry
Research directions: stereochemistry of coordination compounds and inter-and intramolecular exchange mechanisms of 3d and p elements and their use in medicine, zootechny, and biotechnology
ORCID: 0000-0003-2010-7959
E-mail: guleaaurelian@gmail.com

TODERAȘ Ion
Academician, Doctor Habilitate, University Professor. Honorary Director of the Institute of Zoology, head of the Biological Invasions Research Center.
Areas of expertise: zoology, hydrobiology, functional ecology
Research directions: founder of the Ecophysiological Biogeochemistry school, establishing new principles in quantifying the functioning of poikilotherm animal populations in aquatic and terrestrial ecosystems
ORCID: 0000-0003-1599-838X
E-mail: iontoderas@yahoo.com

GUDUMAC Valentin
Doctor Habilitat of Medicine, University Professor.
Areas of expertise: biochemistry & pathobiochemistry, molecular biology, laboratory medicine
Research directions: the molecular mechanisms of action of the new Schiff bases and their combinations with 3d metals, as well as of the bioactive compounds from cyanobacteria and the argumentation of their usefulness in the chemoprevention and treatment of some multifactorial diseases, including tumor neoformations
ORCID ID: 0000-0001-9773-1878
E-mail: valentin.gudumac@usmf.md

GARBUZ Olga
Doctor in biological sciences.
Areas of expertise: biochemistry
Research directions: anticancer properties and mechanisms of action of new inorganic and organic molecular inhibitors; estimation of the antioxidant activity of synthetic compounds and natural products; evaluation of the toxicity of bioactive compounds
ORCID: 0000-0001-8783-892X
E-mail: olhamos1@gmail.com, olhamos@mail.ru

MINISTRY OF EDUCATION AND RESEARCH OF MOLDOVA

MOLDOVA STATE UNIVERSITY

INSTITUTE OF ZOOLOGY

STATE UNIERSITY OF MEDECINE AND PHARMACY NICOLAE TESTEMITANU

PhD. Olga GARBUZ, Prof. Valentin GUDUMAC,

Acad. Ion TODERAS, Acad. Aurelian GULEA

ANTIOXIDANT PROPERTIES OF SYNTHETIC COMPOUNDS AND NATURAL PRODUCTS. ACTION MECHANISMS.

MONOGRAPH

Chișinău, 2023

CZU: 544.1:577.1(075.8)

P 94

Dr. Olga Garbuz, Prof.Valentin Gudumac, Acad.Ion Toderaș, Acad. Aurelian Gulea

Monografie Proprietățile antioxidative a compușilor sintetici și naturali. Mecanisme de acțiune. Chișinău, CEP USM, 2023 - 298 p.: fig., tab.

Recomandată de către Consiliul Facultății de Chimie și Tehnologie Chimică a Universității de Stat din Moldova

Referenți: Laurenția UNGUREANU, Prof.Dr.hab. în științe biologice

Vasilii GRAUR, Dr. în științe chimice, cercetător științific superior

Proprietățile antioxidative a compușilor sintetici și naturali. Mecanisme de acțiune.

Monografia conține date originale importante despre activitatea antioxidativă a materialelor sintetice; compușilor organici, liganzilor, combinațiilor coordinative și a unor produse naturale cum ar fi produsele melifere. Un rol deosebit este acordat mecanismelor de acțiune. Monografia prezintă interes pentru specialiștii din domeniul chimiei medicinale, biofarmaceuticii, zoologiei. Este recomandată studenților de la licență, masteranzilor și doctoranzilor de la Universitatăți și colaboratorilor științiici de la Institutele de cercetare.

DESCRIEREA CIP A CAMEREI NAŢIONALE A CĂRŢII DIN REPUBLICA MOLDOVA

Proprietățile antioxidative a compușilor sintetici și naturali. Mecanisme de acțiune = Antioxidant properties of synthetic compounds and natural products. Action mechanisms : Monografie / Olga Garbuz, Valentin Gudumac, Ion Toderaş, Aurelian Gulea; Universitatea de Stat din Moldova, Institutul de Zoologie, Universitatea de Stat de Medicină şi Farmacie *Nicolae Testemiţanu*. – Chişinău: CEP USM, 2023. – 298 p.: fig., tab.

Referinţe bibliogr.: p. 229-252 (314 tit.). – [50] ex.

ISBN 978-9975-62-516-6. 544.1:577.1(075.8)

P 94

ISBN 978-9975-62-516-6

UNIVERSITATEA DE STAT DIN MOLDOVA
INSTITUTUL DE ZOOLOGIE
UNIVERSITATEA DE STAT DE MEDICINĂ ȘI FARMACIE
NICOLAE TESTEMITANU

Dr. Olga Garbuz, Prof.Valentin Gudumac,

Acad.Ion Toderaș, Acad. Aurelian Gulea

PROPRIETĂȚILE ANTIOXIDATIVE A COMPUȘILOR SINTETICI ȘI NATURALI. MECANISME DE ACȚIUNE.

MONOGRAFIE

Chișinău, 2023

ACKNOWLEDGEMENTS

We want to give special thanks to the Research Laboratory of Advanced Materials in Biopharmaceutics and Technics of the Moldova State University members: PhD TAPCOV V., PhD GRAUR V., PhD RUSNAC R., PhD student GRAUR Ia., PhD student RUSNAC A., PhD student PAHOLNITCAIA A., PhD student ERHAN T., PhD student MITKEVICH N. for providing the new inorganic and organic compounds.

We would like to acknowledge the help of the Biological Invasions Research Center members of the Institute of Zoology: Researcher RAILEAN N., PhD CEBOTARI V.

We would like to big thanks to the Institute Lavoisier de Versailles members: Professor FLOQUET S., PhD FUIOR A., PhD CEBOTARI D.

We also wish to say thanks to the members of the Research Biochemical Laboratory of the Nicolae Testemitanu State University of Medicine and Pharmacy.

This work was fulfilled with the financial support of the ANCD projects 20.80009.5007.10 and 20.80009.7007.12.

ÎN LOC DE PREFAȚĂ

În ultimele două decenii, a existat un interes semnificativ pentru rolul radicalilor liberi de oxigen, mai general cunoscuți în medicina experimentală și clinică ca specii reactive de oxigen, (SRO) și specii reactive de azot (SRA). SRO și SRA sunt generate în timpul iradierii cu lumină UV, raze X și raze gamma; sunt produse ale reacțiilor catalizate de metale; sunt prezente ca poluanți în atmosferă; sunt produse de neutrofile și macrofage în timpul inflamației; sunt produse secundare ale reacțiilor de transport de electroni catalizate de mitocondrii și ale altor mecanisme. Se știe că SRO/SRA joacă un rol dublu în sistemele biologice, deoarece pot fi atât dăunătoare, cât și benefice sistemelor vii. Efectele benefice ale SRO implică roluri fiziologice în răspunsurile celulare, de exemplu în apărarea împotriva agenților infecțioși și în funcția mai multor sisteme de semnalizare celulară. Un alt exemplu benefic de SRO la concentrații scăzute este inducerea unui răspuns mutagen. În schimb, la concentrații mari, SRO pot fi mediatori importanți ai deteriorării structurilor celulare, inclusiv lipide și membrane, proteine și acizi nucleici (numit stres oxidativ). În ciuda prezenței sistemului de apărare antioxidantă al celulei pentru a contracara daunele oxidative din SRO, daunele oxidative se acumulează în timpul ciclului de viață și s-a propus că daunele legate de radicali ai ADN-ului, proteinelor și lipidelor joacă un rol cheie în dezvoltarea bolilor dependente de vârstă, cum ar fi cancerul, ciroza hepatică, arterioscleroza, artrita, tulburările neurodegenerative și alte afecțiuni. În acest aspect, au fost cercetate peste o mie două sute substanțe chimice - compuși de coordinare ai hidrazonelor, izotiocianaților, tioureelor, triazolilor, calconelor, tiosemicarbazidelor, cu ionii următoarelor metale Zn(II), Ni(II), Co(III), Fe(III), Mn(II), Cr(III), Mo(VI) și Mo(V) sintetizați pe baza metodelor cunoscute și modificărilor acestora în Laboratorul de Cercetare a Materialelor Avansate în Biofarmaceutică și Tehnică al Universității de Stat din Moldova și Instititutului Lavoisier a Universității Paris Saclay din Franța.Produsele mielifere au fost puse la dispozitie de către Institul de Zoologie, iar testările antioxidative afost effectuate în laboratorul de biochimie a Universității de medicină și farmacie N.Testemișanu.

Autorii

CONTENTS

Introduction

In the last two decades, there has been a significant interest in the role of oxygen-free radicals, more generally known as reactive oxygen species, (ROS) and reactive nitrogen species (RNS) in experimental and clinical medicine [1]. ROS and RNS are generated during irradiation by UV light, X-rays, and gamma rays; are products of metal-catalyzed reactions; are present as pollutants in the atmosphere; are produced by neutrophils and macrophages during inflammation; are by-products of mitochondria-catalyzed electron transport reactions and other mechanisms [2]. ROS/RNS are known to play a dual role in biological systems since they can be either harmful or beneficial to living systems [3]. The beneficial effects of ROS involve physiological roles in cellular responses, for example in defense against infectious agents and the function of several cellular signaling systems. One further beneficial example of ROS at low concentrations is the induction of a mutagenic response. In contrast, at high concentrations, ROS can be important mediators of damage to cell structures, including lipids and membranes, proteins, and nucleic acids (termed oxidative stress) [4]. Despite the presence of the cell's antioxidant defense system to counteract oxidative damage from ROS, oxidative damage accumulates during the life cycle, and radical-related damage to DNA, proteins, and lipids has been proposed to play a key role in the development of age-dependent diseases such as cancer, liver cirrhosis, arteriosclerosis, arthritis, neurodegenerative disorders, and other conditions [1, 5].

An antioxidant can be defined as any substance that when present at low concentrations compared with those of an oxidizable substrate can inhibit the oxidation of lipids, proteins, or other molecules by preventing the initiation or propagation of oxidative chain reactions and can thus prevent or repair the damage done to the body's cells by oxygen [1].

Synthetic antioxidants are widely used to inhibit oxidative processes [2]. Most currently used antioxidant drugs are direct-acting antioxidants. Primary screening of direct-acting antioxidants is carried out on *in vitro* model systems, i.e. when the efficiency of their antioxidant action is determined primarily by the substance's chemical structure and does not depend, in any way, on the general homeostasis of the body [3]. Hydrophilic and lipophilic are distinguished among direct-acting antioxidants [4].

Thiosemicarbazones, thiosemicarbazides, and their derivatives and metal complexes antioxidants have recently gained attention for their capacity to protect organisms and cells from damage induced by oxidative stress or scavenge free radicals [5]. These compounds, which show considerable biological activity, may

represent an interesting approach to designing new anticancer drugs. In this aspect, one thousand two hundred and seventeen (1217) tested compounds (hydrazones, isothiocyanates, thioureas, triazoles, chalcones, thiosemicarbazides, thiosemicarbazones, Zn(II), Ni(II), Co(III), Fe(III), Mn(II), Cr(III), Mo(VI), and Mo(V) coordination compounds) were synthesized based on known methods and their modifications in the Research Laboratory of Advanced Materials in Biopharmaceutics and Technics of the Moldova State University.

The present work deals with the evaluation of new series of thiosemicarbazones, thiosemicarbazides, and their derivatives and metal complexes for their antioxidant activities using several antioxidant-capacity (AC) assays, such as ABTS, DPPH, ORAC, and LOX.

Lipoxygenases (LOXs) are key enzymes that catalyse the oxidation of polyunsaturated fatty acids (PUFAs) such as arachidic acid (AA), linoleic acid (LA), and other unsaturated fatty acids (Brash, 1999). Activation of LOX enzymes displays different physiological functions, including inflammation, erythropoiesis, epidermal differentiation, skin development, cell proliferation and carcinogenesis, tumorigenesis, and so on (Haeggstrom and Funk, 2011). Therefore, novel potent inhibitors of LOX are required to enable drug discovery efforts [6]. The tested compounds showed excellent inhibitory potential for LOX so, they showed a strong potential to be developed as new anti-inflammatory drugs.

The antioxidant potency of the tested compounds was compared to the reference antioxidant controls (Trolox, Rutin, Quercetin) and the FDA-approved anticancer drug doxorubicin (DOXO). It is known that DOXO cardiomyopathy carries a poor prognosis and is frequently fatal. DOXO induces toxic damage to the mitochondria of cardiomyocytes contributing to increased oxidative stress.

Drug-induced hemolysis and methemoglobin formation is a relatively rare but serious toxicity liability caused by oxidative stress, so the tested compounds were performed to screen for toxic hemolysis and methemoglobin formation in human red blood cells (RBCs).

Finally, direct toxic evaluation of the tested synthetic compounds was studied by acute toxicity assay against *Daphnia magna*, which is one of the most commonly used test objects in laboratory research aimed at directly determining the toxicity of chemical compounds, which are used in toxicological medicine.

There are various sources of the antioxidants like endogenous antioxidant present in the body and exogenous food sources. Bee products have been used since ancient times both for their nutritional value and for a broad spectrum of therapeutic purposes. They are deemed to be a potential source of natural antioxidants that can

counteract the effects of oxidative stress underlying the pathogenesis of many diseases. Given the growing interest in using bioactive substances from natural sources to promote health and reduce the risk of developing certain illnesses, this work aims to update the current state of knowledge on the antioxidant capacity of bee products such as honey, pollen, propolis, beeswax, royal jelly, and on the methods used. Therefore, we measured the total antioxidant capacity (TAC) in honeybee products, and hemolymph, and analysed the TAC of honeybee products and hemolymph in relation to exposure to tested compounds.

It should be noted that the assay results obtained by different methods are not always comparable, since the sensitivity of detection of individual antioxidants with different indicator reactions varies. Currently, there is no unified standard for the quantitative determination of antioxidants which makes it difficult the comparison the results obtained by different methods.

1. Oxidative stress

The idea of "oxidative stress" was originally formed about three decades ago [7, 8]. It has evolved notably since then. The occurrence of oxidative stress started in early publications of Seyle (loc. cit), which were bothered about the oxygen toxicity associated with aging, bodily responses, and processes connected with oxygen radicals, the concept of the physiology of mitochondria, and studies on their aging, as well as work on variations of redox reactions in living organisms [7]. Table 1.1 presents some definitions described by researchers over the years [9].

Hence, oxidative stress is determined by an imbalance between oxidant and antioxidant species, such as a higher weight of oxidant species, which provokes the excessive release of free radicals, or reactive species (RS) and causes cellular and molecular disruption, as well as a negative influence on redox signaling. When antioxidant protective forces are impaired or are not strong enough to overpower the production of reactive oxygen species (ROS) or Reactive nitrogen species (RNS), oxidative stress arises. The consequences of oxidative stress may be progressive and frequently dreadful. Prooxidant and antioxidant species are two underlying components of oxidative stress [9].

Metabolism and energy synthesis under oxidative stress is primarily disturbed in highly specialized and therefore the most energy consuming cells [14], which are extremely sensitive to even minimal energy disturbances and pH imbalance [15]. These include neurons (nervous system and analyzers), myocytes, as well as

cardiomyocytes (muscular system), germ cells (reproductive system), and rapidly renewing blood and skin cells [16].

Table 1.1. Some definitions of oxidative stress over time [9]**:**

Definition of Oxidative Stress
• Oxidative stress is a disturbance in the prooxidant-antioxidant balance in favor of the former [10].
• Oxidative stress is defined as a disturbance in the prooxidant-antioxidant balance that leads to potential damage [11].
• Oxidative stress is a situation when steady-state reactive oxygen species (ROS) concentration is transiently or chronically enhanced, disturbing cellular metabolism, regulation, and damaging cellular constituents [12].
• Oxidative stress is the excess ROS production relative to antioxidant defense [13].
• With the emerging knowledge that reactive oxygen species can be employed in cell regulation, the term oxidative stress has been subdivided into "oxidative eustress", providing beneficial signaling and "oxidative distress" capable of producing chemical damage [10]. Since redox signaling and redox regulation can be modulated by physiological amounts of reactive oxygen species, this has been defined as "oxidative eustress", whereas "oxidative distress" has been defined as supra physiologic loads of oxidant species bring about disrupted redox signaling or oxidative damage to biomolecules [10].

Oxidative stress is manifested by various homeostasis disorders at the cellular and tissue level:

- imbalance between pro- and anti-inflammatory cytokines (chronic systemic subclinical aseptic inflammation);
- ischemia (endothelial dysfunction);
- hypoxia (membranopathy due to activation of lipid peroxidation of cell membranes);
- disturbance of cellular reception and perception (areflexia and hyporeflexia of the cell);
- vegetative-mediator dysfunction of the cell (disturbances in the metabolism of biogenic amines);
- energy and metabolic disorders (mitochondrial dysfunction);
- disturbances of telomerase activity of cell chromosomes.

The accumulation in the cell of incompletely oxidized degradation products of proteins and lipids results in pronounced disturbances in the cellular redox potential (oxidation-reduction potential of cell membranes), which disrupts the processes of entry into the cell of substances necessary for its normal functioning, and the processes of excretion of decay products. The cell becomes acidified, as intracellular metabolic acidosis develops (the pH of the cell cytoplasm shifts to the acid side due to the accumulation of incompletely oxidized decay products in it), which exacerbates cellular dysfunction, eventually leading to accelerated apoptosis and cell death or its degeneration (the initial stages of carcinogenesis) [17, 18].

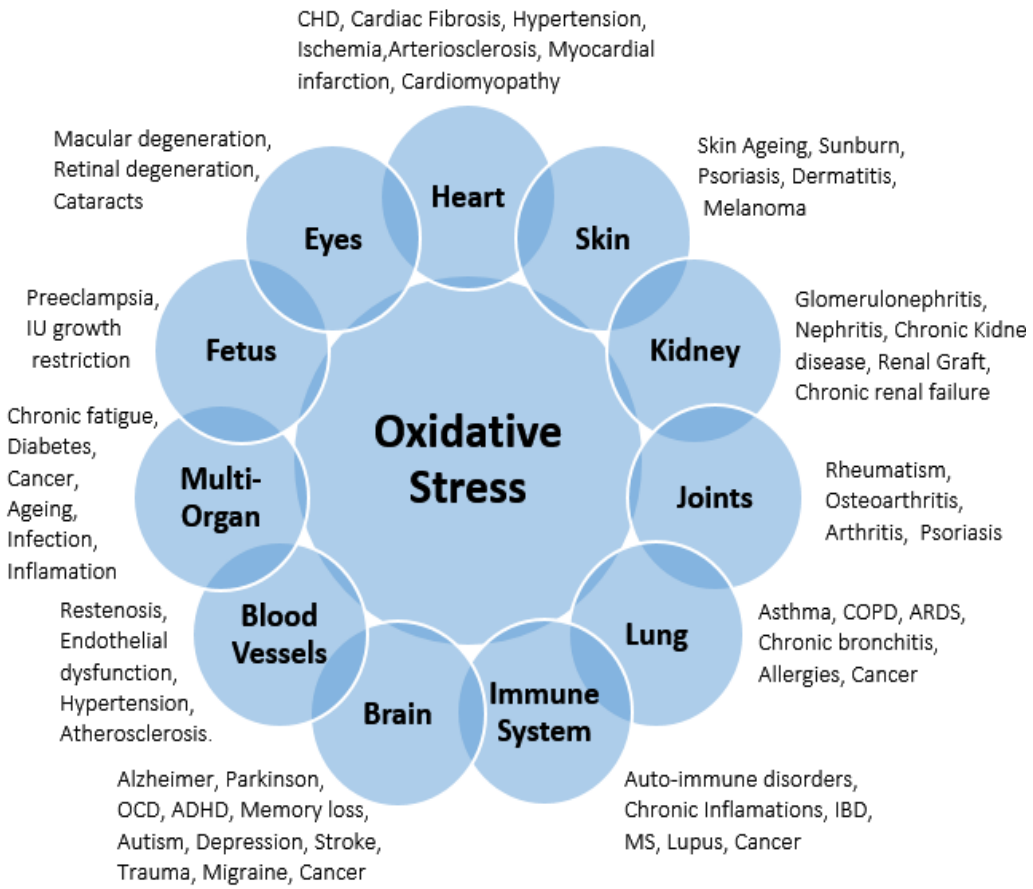

Fig. 1.1. **Oxidative stress-induced diseases in humans**

Free radicals have been evidenced to be able to accumulate throughout the body with age, triggering the aging process, as well as various neurodegenerative diseases such as Parkinson's disease, muscular dystrophy, atherosclerosis [19], and

Alzheimer's disease [20]. An imbalance between ROS and the antioxidant protective system has also been found to induce diabetes and age-related eye disease [21]. Nowadays, oxidative stress is believed to also have a significant negative impact on inflammatory diseases, ischemic diseases, hypertension, cancer, immunodeficiency syndrome, smoking-related diseases, alcoholism, and many others (Fig. 1.1) [22, 23, 24, 25].

1.1. Sources and reactions of ROS/RNS

The chai reaction underlies distinct mechanisms providing free radicals. A reaction sequence consists of interrelated stages. The first step is initiated by high temperature, ozone, superoxides, UV-radiation, air pollutants, smoking, junk foods, pesticides, or industrial chemicals [26] resulting in a free radical developed. This process may include free radical formation from stable species or they involve free radical reactions with stable species to produce distinct forms of free radicals. The next phase of the process known as prolongation starts when a sufficient amount of free radicals is developed, followed by final product synthesis. Free radicals act as accelerators during the prolongation stage while their total number stabilizes. In the end, all reactions weaken, limiting thereby the free radical number. Commonly, it happens when free radicals combine to develop more stable species [27].

ROS/RNS produced in oxygen metabolism (auto-oxidation) are indispensable for controlling gene expression, cytochrome P450 metabolism, cell proliferation, the processes of protein phosphorylation or calcium concentration in cells, apoptosis, activation of cell division controlling proteins, ensuring a bactericidal and oncostatin effect, activation of immune reactions of leukocytes, providing an anti-inflammatory systemic and local response [28]. Each disturbance of this specific equilibrium may result in the appearance of oxidative stress, a state in which the oxidizing potential elevates to a level that menaces the cellular structure stability [29]. The excess number of free radicals modifies their structure and thereby the physiological functioning of the cell by disrupting redox signaling and cytotoxic compound accumulation [30, 31].

Enzymatic reactions in the view of free radical development include prostaglandin synthesis, phagocytosis, the respiratory chain, and the cytochrome P-450 system, [32]. Some externally and internally developed sources of free radicals are shown in Figure 1.2 [33] still, but they are widely produced endogenously.

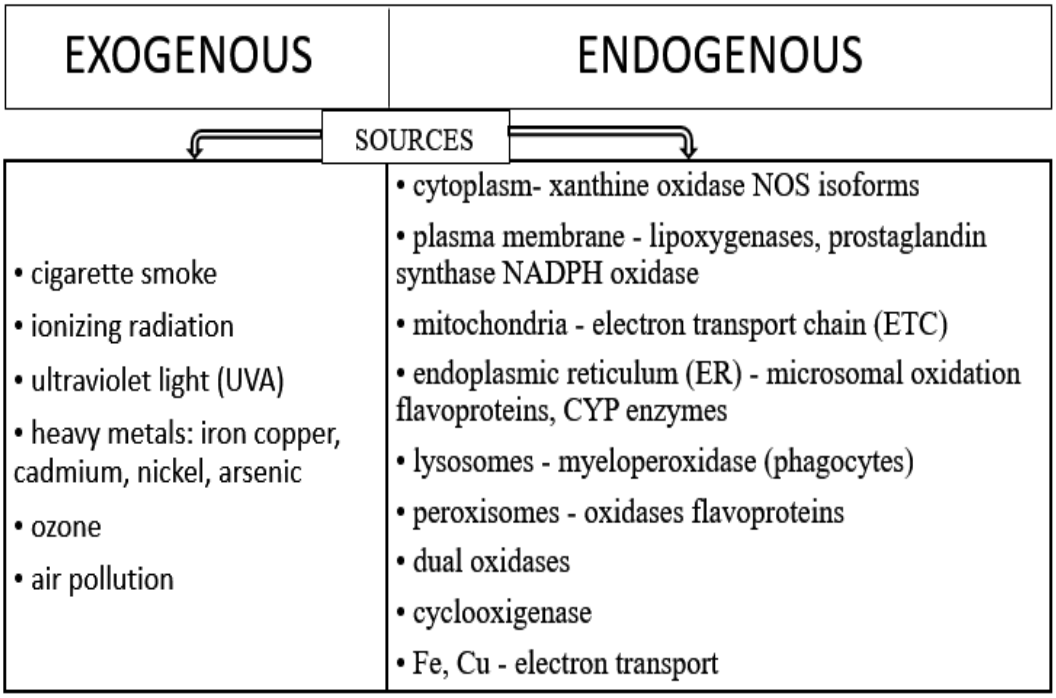

Fig. 1.2. **Exogenous and endogenous sources of free radicals** [34]

1.2. Chemistry and biochemistry of RS

Free radicals are highly reactive species (RS) containing an unpaired electron in the valence shell. They are able to donate this electron and accept it from other molecules, acting as an oxidant or reducing agent [35]. Reactive species (RS) can be separated into two groups: free radicals and non-radicals. Free radicals represent molecules that contain one or more unpaired electrons, which renders them high reactivity. ROS sharing their unpaired electrons are non-radical types. Their chemical differences are significant; still, they have resembling mechanisms for damage at the level of biomolecules [36].

Reactive species (RS) produced from nitrogen (RNS), molecular oxygen (ROS), bromine (RBS), chlorine (RCS), and sulfur-derived species have been identified (Table 1.2).

Table 1.2. Major reactive species (RS) [37, 38]**.**

Radical	Non-radical	Radical	Non-radical
Reactive oxygen species (ROS)		**Reactive nitrogen species (RNS)**	
Superoxide anion, $O_2^{\bullet-}$	Hydrogen peroxide, H_2O_2	Nitric oxide, $NO^{\bullet}$	Nitrous acid, HNO_2
Hydroxyl radical, $OH^{\bullet}$	Ozone, O_3	Nitrogen dioxide, $NO_2^{\bullet}$	Nitrosyl cation, NO^+
Hydroperoxyl radical, $HO_2^{\bullet}$	Singlet oxygen, O_2 1 Dg	Nitrate radical, $NO_3^{\bullet}$	Nitroxyl anion, NO^-
$HOO^{\bullet}$	Hypobromous acid, HOBr		Dinitrogen trioxide, N_2O_3
Singlet oxygen, $^1O_2$	Hypochlorous acid, HOCl		Dinitrogen tetroxide, N_2O_4
Carbonate, CO^-	HOI, Hypoiodous acid		Dinitrogen pentoxide, N_2O_5
$CO_2^{\bullet-}$	Organic peroxides, ROOH		Alkyl peroxynitrites, ROONO
$CO_3^{\bullet-}$	Peroxynitrous acid, ONOOH		Alkyl peroxynitrates, RO_2ONO
Alkoxyl, $RO^{\bullet}$	Peroxynitrite, $ONOO^-$		Nitryl chloride, NO_2Cl
Organic free radicals	Carbon monoxide, CO		Peroxyacetyl nitrate, $CH_3C(O)OONO_2$
Alkoxy radical, $R–O^{\bullet}$	Peroxomonocarbonate, $HOOCO_2^-$		
Peroxide radicals, $R\text{-}OO^{\bullet}$	Peroxynitrate, $O2NOO^-$	**Reactive sulfur species**	
Semiquinone radical, $^{\bullet}QH$		Thiyl radical $S^{\bullet}$	Hydrogen sulfide, H_2S
Semiquinone anion radical, $^{\bullet}QH^-$			Disulfide, RSSR
Reactive chlorine species /bromine species			Thiol/sulfide, $RSR^{\bullet}$
Atomic chlorine, Cl	Chloramines		Disulfide-S-dioxide, $RS(O)_2SR$
Atomic Bromine, Br	Chlorine gas, Cl_2		Sulfenic acid, RSOH
	Bromine gas, Br_2		Disulfide-S-monoxide, RS(O)SR
	Bromine chloride, BrCl		
	Chlorine dioxide, ClO_2		

Chemistry and biochemistry of ROS

Superoxide anion originated either during metabolic processes or as a result of oxygen "activation" through physical irradiation, is believed to be the "primary" ROS, and can continue to interact with other molecules to yield "secondary" ROS, either directly or predominantly through enzyme- or metal-catalyzed processes [39].

Superoxide radical ion is not in a direct reaction with sugars, polypeptides, or nucleic acids, and its capacity to peroxidise lipids is controversial. When it is involved in a

$$2O_2^{\bullet -} + 2H^+ \xrightarrow{SOD} H_2O_2 + O_2$$

dismutation reaction, superoxide is depleted [40]:

This biological system reaction is accelerated by SOD (superoxide dismutase) enzymes by approximately four orders of magnitude. It should be noted that SOD enzymes act in conjunction with glutathione peroxidases and catalases, as H_2O_2-removing enzymes [41].

The generation of various free radicals is strongly linked with the involvement of redox-active metals [42]. The cell redox state is tightly associated with iron (and sometimes copper) redox couple and is kept within stringent physiological ranges. Iron regulation has been suggested to ensure the nonappearance of free intracellular iron; however, an excess of superoxide induces the release of "free iron" from iron-containing molecules *in vivo*, under stress conditions. The release of iron by superoxide has been shown for [4Fe–4S] cluster-containing enzymes of the dehydrataselyase family. The released Fe(II) can take part in the Fenton reaction, producing extremely reactive hydroxyl radical (Fe(II) + H_2O_2 →Fe(III) + $^{\bullet}OH$ + OH^-). So, $O_2^{\bullet -}$ acts as an oxidant of [4Fe–4S] cluster-containing enzymes and promotes $^{\bullet}OH$ production from H_2O_2 by making Fe(II) available for the Fenton reaction under stress conditions [19–22]. The superoxide radical takes part in the Haber-Weiss reaction ($O_2^{\bullet -}$ + H_2O_2 →O_2 + $^{\bullet}OH$ + OH^-) which combines a Fenton reaction and Fe(III) reduction by superoxide, producing Fe(II) and oxygen (Fe(III) + $O_2^{\bullet -}$ →Fe(II) + O_2) [43].

Ionizing radiation induces the decomposition of H_2O, resulting in hydroxyl radicals and hydrogen atoms. $^{\bullet}OH$ is produced by the photolytic decomposition of alkylhydroperoxides, as well. Generation of $^{\bullet}OH$ close to DNA could force this radical to react with DNA bases or the deoxyribosyl backbone of DNA resulting in damaged bases or strand breaks. The extent of DNA strand breaking by $^{\bullet}OH$ has been proposed to be governed by the accessible surface areas of the hydrogen atoms present in the DNA backbone.

The majority of the hydroxyl radicals produced *in vivo* stem from the metal-catalyzed breakdown of hydrogen peroxide, by the Fenton reaction M^{n+}(Cu^+, Fe^{2+}, Ti^{3+}, Co^{2+})+H_2O_2 →$M^{(n+1)+}$(Cu^{2+}, Fe^{3+}, Ti^{4+}, Co^{3+}) + $^{\bullet}OH$ + OH^-, where Mn^+ is the transition metal ion [43].

Of additional radicals generated from oxygen that can be developed in living systems, peroxyl radicals ($ROO^{\bullet}$) are typical. The dioxyl (hydroperoxyl) radical

$HOO^{\bullet}$, which is the conjugate acid of superoxide, $O_2^{\bullet-}$ is the simplest peroxyl radical. The chemistry of this molecule type varies depending on the nature of the R group, the concentration of oxygen, the local environment, and other reactants. The diversity of the biological reactions in which they take part is possibly the most interesting trait of peroxyl radicals. The identification and assessment of lipid peroxidation are most frequently reported as evidence to support the involvement of peroxyl radical reactions in human disease and toxicology. Peroxyl radicals cause DNA cleavage and protein backbone alteration. Peroxyl radicals synergistically intensify the induction of DNA damage by superoxide [44].

Chemistry and biochemistry of RNS

Nitric oxide ($NO^{\bullet}$) is an ample reactive radical and is a significant oxidative biological signaling molecule in a high variety of various physiological processes, including neurotransmission, smooth muscle relaxation, defense mechanisms, blood pressure regulation, and immune regulation [45]. This molecule contains one unpaired electron, therefore, a radical. $NO^{\bullet}$ is produced in biological tissues via specific nitric oxide synthases (NOSs), which metabolise arginine to citrulline resulting in the formation of $NO^{\bullet}$ through a five-electron oxidative reaction. Reactive nitrogen species overproduction is called nitrosative stress. This may happen when a system's production of reactive nitrogen species exceeds its system's capacity to neutralize and eliminate them. Nitrosative stress may result in nitrosylation reactions that can modify the structure of proteins and thereby inhibit their normal function.

$NO^{\bullet}$ is soluble in both aqueous and lipid media, it easily diffuses through the cytoplasm and plasma membranes. $NO^{\bullet}$ has effects on neuronal transmission as well as on synaptic plasticity in the central nervous system. $NO^{\bullet}$ reacts with oxygen and water in the extracellular medium to form nitrate and nitrite anions.

Cells of the immune system generate both the superoxide anion and nitric oxide during the oxidative blast-induced in the course of inflammatory processes. Nitric oxide and the superoxide anion may react together under these conditions to produce essential volumes of a much more oxidatively active molecule, peroxynitrite anion ($ONOO^{-}$), an oxidizing free radical able to trigger DNA disintegration and lipid oxidation: $NO^{\bullet} + O_2^{\bullet-} \rightarrow ONOO^{-}$. So, $NO^{\bullet}$ toxicity is connected to its capacity to combine with superoxide anions. Nitric oxide easily binds certain transition metal ions; actually, many physiological effects of $NO^{\bullet}$ are induced as a result of its primary binding to Fe(II)-haem groups in the enzyme guanylate cyclase: $Fe(II) + NO^{\bullet} \rightarrow Fe(II)–NO$.

Protein S-nitrosothiols (protein-SNO) might be present in accordance with the reaction: protein-SH + RSNO → protein-SNO + RSH if cellular responses to nitrosative stress are similar to responses to oxidative stress, and indeed, protein S-nitrosothiols have been detected in animal blood and involve S-nitrosoalbumin, nitrosohaemoglobin, and the least stable S-nitrosocysteine [44].

1.3. General mechanisms of oxidative stress

Living cells are under permanent oxidative attack from RS, which results in "oxidative damage", and the complex antioxidant protection system generally maintains this attack in balance [14]. The monitoring of the redox condition is crucial for cell viability, proliferation, activation, and organ function. A pathological shift in that balance causes an increase in RS concentrations and thereby dreadful alterations to cell components, such as lipids, proteins, and DNA [46].

Lipid Peroxidation (LPO)

Lipids can be oxidized, chlorinated, and nitrated by a whole series of RS, but H_2O_2, $NO^{\bullet}$, or $O_2^{\bullet-}$, which do not react with lipids. Lipid peroxidation is a complex process providing a wide series of products generated in various amounts.

Lipid peroxidation is the most widely known biological free radical chain (FRC) reaction. The oxidation of unsaturated fatty acids or other lipids generates products, which are peroxides of these substances. It should be kept in mind that ROS does not trigger peroxidation. The process is only intensified by their presence. Peroxidation reaction, like any FRC, can be separated into three phases:

1. Initiation: Development of fatty acid radicals. Hydroxyl ($HO^{\cdot}$), peroxy ($LOO^{\cdot}$), alkoxy ($LO^{\cdot}$), and alkyl ($L^{\cdot}$), as well as O_3, SO_2, and NO_2 are the ROS that starts this reaction in living cells. Hydrogen separation causes the formation of an alkyl radical. $LH \rightarrow L^{\bullet} + H_2O$.

2. Prolongation: Unstable fatty acid radicals readily react with molecular oxygen (O_2), resulting in peroxides, which are also unstable and react with more fatty acid molecules, yielding more radicals. The reaction proceeds in a cycle, as follows: $L^{\bullet} + O_2 \rightarrow LOO^{\bullet}$ $LOO^{\bullet} + LH \rightarrow LOOH + L^{\bullet}$.

3. Termination: Increasing the number of free radicals enhances the probability of collision between them, which terminates the process: $L^{\bullet} + L^{\bullet} \rightarrow L–L$, $LOO^{\bullet} + LOO^{\bullet} \rightarrow L=O + LOH + O_2$, $LOO^{\bullet} + L^{\bullet} \rightarrow L=O + LOH$. Termination reactions afford such products as dimers of fatty acids, hydroxy acids, and oxoacids.

Lipid peroxidation products frequently react with proteins that are present in cell membranes, developing protein-lipid adducts. Ulterior reactions of lipid peroxidation products induce aldehydes syntheses such as MDA or 4-

hydroxynonenal. They readily penetrate through biological membranes and can indirectly cause DNA damage by ROS. Lipid peroxidation products are cytotoxic, mutagenic, and carcinogenic and can trigger a rupture in DNA strands. Lipid peroxidation has a negative impact on all cell membranes resulting in their damage and loss of function. The process can impair ion pumps or electron transport in the respiratory with subsequent diminished ATP production [47, 48].

Protein Oxidation

Biomolecule oxidation and protein degradation are inherent effects of aerobic cellular metabolism. Oxidative damage to proteins brings severe consequences, as it is detrimental to the function of enzymes, receptors, and transport proteins and promotes indirect damage to other biomolecules, e.g., DNA repair enzymes or polymerases in DNA replication. Oxidation of such amino acid residues, such as tyrosine, leads to the development of protein aggregation, dityrosine, cross-linking, and fragmentation. The free radical attack on proteins yields amino acid radicals, which can crosslink or react with O_2, leading to the development of peroxyl radicals, which may further transform into protein peroxides by abstracting ($H^{\bullet}$) and inducing more free radicals. The loss of activity and inactivation of the mentioned proteins damages various chemical reactions and metabolic pathways, leading to cell death. Advanced oxidation protein products (AOPP) are tyrosine-containing protein cross-linking ones. Advanced glycation end-products (AGE) are protein carbonyl substances developed through protein-ROS interaction.

These are thiol groups (-SH) that undergo mostly oxidation reactions in the course of oxidative stress. It can be triggered by such ROS as $O_2^{\bullet -}$, H_2O_2, or $HO^{\bullet}$ leading to the production of thiol radicals ($RS^{\bullet}$), which are immediately dimerized to sulfides: $RSH + O_2^{\bullet -} + H^+ \rightarrow RS^{\bullet} + H_2O_2$, $2RSH + H_2O_2 \rightarrow RS^{\bullet} + 2H_2O$, $RSH + HO^{\bullet} \rightarrow RS^{\bullet} + H_2O$, $2RS^{\bullet} \rightarrow RSSR$. Polypeptide chain oxidation is a process similar to that of lipid peroxidation. Hence, it concerns polypeptide chains or amino acid residues directly, with aromatic ones as the most reactive. When α-amino acid carbon releases a proton while interacting with hydroxyl radicals, it creates an alkyl radical transformed into alkyl hydroperoxide through a reaction with oxygen. The alkyl radical may be converted to an alkoxy radical, which activates polypeptide chain fragmentation by damaging thiol. It results in the protein function loss mentioned [47].

Nucleic Acid Oxidation

The damage caused to oxidative DNA, mostly because of the hydroxyl radical, results in a huge range of base and sugar modification products [49]. Under normal conditions, each cell is estimated to be the target of several thousand attacks on its

DNA every day. Free radicals attacking DNA purines, deoxyribose, and pyrimidines develop primary products, which are further transformed. Damage to DNA by free radicals is observed much less frequently than oxygen damage to proteins and lipids. However, the consequences are more severe because of mutagenic or immunogenic modifications. 8-hydroxy-2′-deoxyguanosine (8-OHdG) and 8-oxoguanine (8-oxo-Gua) are two of the major products of DNA oxidation [50]. Guanine, an aromatic heterocyclic substance, and purine (systematic the name is 2-amino-6-hydroxypurine) are the main building blocks of both DNA and RNA making a complementary pair with cytosine, both in a free state and as a nucleoside, are especially susceptible to the impacts of free radicals in the C8 position. Therefore, 8OHdG is the most favorable and best-known mutagenic modification of DNA [47].

ROS and metal ions-induced signaling pathways

Cells communicate with each other and react to extracellular stimuli using biological mechanisms called cell signaling or signal transduction [51]. Signal transduction is a process allowing the transmission of information from the outside of a cell to diverse functional elements inside the cell. Signal transductions are initiated by extracellular signals such as growth factors, neurotransmitters, hormones, and cytokines [52]. Signals transmitted to the transcription tools responsible for the expression of particular genes are generally forwarded to the cell nucleus through a class of proteins called transcription factors. These factors monitor the activity of RNA polymerase II. By binding to specific DNA sequences, these signal transduction processes can trigger a variety of biological activities, such as gene expression, nerve transmission, cell growth, and muscle contraction [53].

ROS also play a significant physiological role in several facets of intracellular signaling and regulation while they are preponderantly involved in producing cell damage. ROS has been clearly shown to interfere with the expression of a number of genes and signal transduction pathways. Being oxidants by nature, ROS have an impact on redox status and may, depending on their concentration, initiate either a positive response (cell proliferation) or a negative cell response (growth arrest or cell death). As mentioned above, the ROS impact on cell proliferation occurs entirely at low or transient radical concentrations while high concentrations produce cell death or even necrosis. Low concentrations of superoxide radical and hydrogen peroxide actually stimulate proliferation and boost survival in a wide variety of cell types. Hence, ROS can have a very essential physiological role as secondary messengers. Besides, can be involved in the control of the cytosolic calcium concentration, monitoring of protein phosphorylation, and activation of certain transcription factors such as NF-B and the AP-1 family factors [54].

ROS and metal ions, first of all, suppress phosphoserine/threonine-, phosphotyrosine- and phospholipid-phosphatases most likely through interacting with sulfhydryl groups on their cysteine residues, which are oxidized to develop either intramolecular or intermolecular disulphide bonds [44]. These structural modifications change protein conformation, which results in the upregulation of several signaling cascades, the most significant growth factor kinase-, src/Abl kinase-, MAPK- and PI3-kinase-dependent signaling pathways. These signaling cascades cause the activation of several redox-regulated transcription factors (AP-1, NF-B, p53, HIF-1, NFAT). Figure 1.3 summarizes ROS-induced signaling pathways [44].

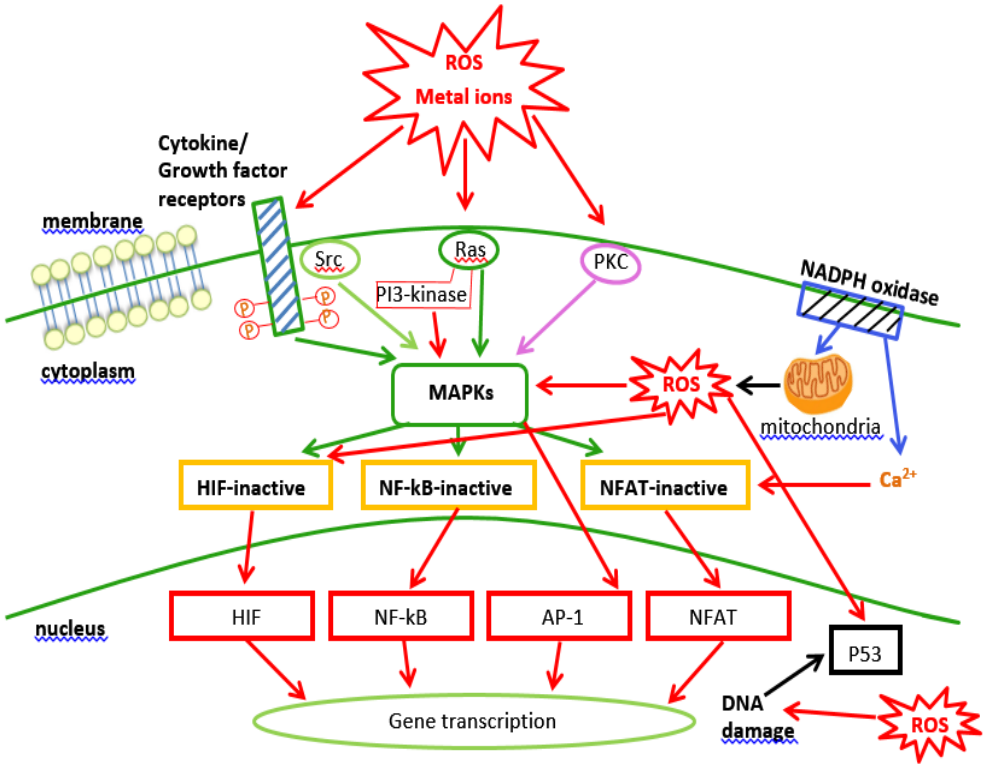

Fig. 1.3. **ROS and metal ions-induced signaling pathways** [44]

Oxidative stress activates multiple intracellular signaling, which results in apoptosis or cell overgrowth [55]. Various pathways are involved including apoptotic genes: caspase-3, -8, -9, Bim, Bcl-2, Bak, and Bax; and oxidative stress genes: CYGB (cytoglobin), GSTP1 (glutathione S-transferase pi 1), NCF1 (neutrophil cytosolic factor 1), GPX1 (glutathione peroxidase 1), SOD1 (superoxide dismutase 1), SOD2, CCS (copper chaperone for superoxide dismutase), and NOS2 (nitric oxide synthase 2) [56]. GSTP1 expression and apoptotic signaling through

activation of c-Jun N-terminal kinase (JNK) are likely to be mechanisms connecting oxidative stress [57].

Some Metal-induced oxidative stress and cancer

Many works have concentrated on metal-induced toxicity and carcinogenicity, accentuating their role in the production of reactive oxygen and nitrogen species in biological systems, and the importance of this therein [42, 58]. Metal-mediated development of free radicals may lead to diverse changes in DNA bases, increased lipid peroxidation, and alterations in calcium and sulfhydryl homeostasis.

Iron

Biochemical, animal and human data have suggested connections between increased rates of iron in the body and an elevated risk of multiple diseases including vascular disorders, cancer, and certain neurological conditions [59]. Iron-mediated ROS production causing DNA and lipid damage seems to arise from an exaggeration of the normal iron function that is to transport oxygen to tissues. Iron-induced free radical damage to DNA turns out to be essential for the development of cancer, while cancer cells are recognized to develop rapidly in response to iron. Hence, pre-menopausal women and children are assumed to be at a lower risk of common diseases since the iron volumes are not likely to be excessive in the body at these times.

Copper

The impact of dietary copper levels on the development of cancer has been investigated since copper is a significant component of several endogenous antioxidant enzymes, while free radicals have been suggested to play a role in the initiation of cancer development.

In vitro and *in vivo* assays have clearly demonstrated that copper (as copper salts) is not genotoxic. Nevertheless, *in vitro* studies have revealed that cancer cells find it easy to proliferate into tumors in a high copper environment. Thus, copper-lowering drugs have been suggested to be able to stabilize advanced cancer. Copper is a well-known prooxidant, like iron, and may be involved in the metal-catalyzed peroxidation of lipids.

Chromium

Chromium(III), which is a naturally-occurring metal, is a significant trace element that plays a major role in regulating glucose levels in the blood. When at high rates, chromium(VI) is potentially toxic and carcinogenic. All chromates, Cr(VI), can actively penetrate the cells via channels for the transfer of isoelectric and isostructural anions, such as those for SO_4^{2-} and HPO_4^{2-}. Through phagocytosis, insoluble chromates are absorbed by cells. The chromium transport through the cell

membrane was believed to refer to solely Cr(VI) species until recently. However, very recent models have also regarded the uptake of reduced Cr species produced by extracellular redox mechanisms. Some extracellularly produced Cr(V) and Cr(III) complexes also possess high permeability through the cell membrane. Chromates can develop free radicals once inside the cell [60].

Just chromium (VI) is unreactive with DNA *in vitro* or isolated nuclei. Still, it causes a wide range of DNA damage including DNA–protein crosslinks, Cr–DNA adducts, DNA–DNA crosslinks, and oxidative damage once inside the cell, in the presence of cellular reductants. Glutathione rapidly develops a complex with Cr(VI), followed by a slow reduction of Cr(VI) to produce Cr(V) within the cell [42].

Cobalt

Some workers have examined the possibility that cobalt-mediated free radical production promotes cobalt toxicity. The superoxide radical has been revealed to be generated by the reaction of H2O2 with Co(II), but when Co(II) was chelated with adenosine diphosphate or citrate, this was impeded. The nitrilotriacetate cobalt (II) complex was discovered to catalyze H_2O_2 decomposition accompanied by the production of hydroxyl radicals and slow oxidation of Co(II) [61].

Injection of Co(II) into rats results in a pattern of oxidative DNA base damage characteristic of hydroxyl radical attack through the Fenton reaction. Additionally, cobalt was revealed to interfere with DNA repair processes. Still, trace cobalt amounts are indispensable in the diet since cobalt is an integral metal of vitamin B12 composition.

Nickel

Nickel is a human carcinogen that can modify gene expression by elevated DNA methylation and compaction, rather than through mutagenic mechanisms. Nickel may intervene with DNA repair processes, while toxic rates of nickel are confirmed to trigger lipid peroxidation and protein carbonyl production in animals [62].

2. Methodologies for antioxidant activity screening and antioxidants analysis *in vitro*

Assessment of antioxidant status attracts growing attention for clinical purposes [63, 64]. But, in this case, the determination of antioxidative potential is difficult to accomplish due to the complex action mechanisms in individual anti-oxidants. Some of them act as free radical scavengers, and some prevent ROS formation or induce signaling pathways, or repair oxidative damage. Currently, there

exists no direct method for accurate measurement of oxidative stress in vivo conditions, as well. That is why oxidative stress is evaluated with the aid of multiple in vitro assays [65], including electron paramagnetic resonance (EPR) or electron spin resonance (ESR) spectroscopy, enabling the direct identification of free radicals; fluorescent probes; or indirect methods used to identify the stable products derived due to the free radical attack, such as chromatography, colorimetry, and immune, or enzymatic tests [66].

In a critical review [67], Bunaciu et al. indicated that the terms "antioxidant activity" and "antioxidant capacity" require some more clarification as they are often used interchangeably despite the fact that their meanings vary. It should be mentioned that the term "antioxidant activity" refers to kinetic-based assays estimating the rate constant of a reaction between reactants or scavenging percentages per unit of time. Hence, the term characterizes a specific antioxidant and oxidant, expressed as reaction rate value. In its turn, the antioxidant capacity defines the efficiency of antioxidants to inhibit the oxidative degradation of various bio-compounds. Measurements are based on the reaction between antioxidants under study and free radicals (reactive species inactivation, quenching, or scavenging) or the sample and transition metals reaction. Antioxidant capacity expresses the concentration of a given free radical scavenged by a sample.

As for the heterogeneous mixture, the antioxidant capacity of each individual component cannot be measured since all antioxidants react simultaneously to produce the total scavenging ability of the sample. The most reasonable way to their antioxidant capacity in the case of the complex samples involves the usage of a variety of methods that enable the different mechanisms of individual component actions to be addressed [68, 69]. The total antioxidant capacity (TAC) measured results from the collaborative effect of all sample components (i.e., synergistic or antagonistic effects).

Antioxidant capacity can be assessed by considering the final effects of their presence, usage of *in vitro* tests, or directly through applying more complex methods that involve exogenic probes to detect oxidation. The estimation of the total antioxidant capacity (TAC) level with such a variety of mechanisms involved in the antioxidant actions is one of the major challenges in antioxidant testing. So far, no universal method has been developed to gain general and univocal acceptance. Hence, one should be aware of the kind of antioxidant function being measured when choosing a specific method [70].

The estimated activity of primary antioxidants reflects their ability to scavenge ROS/RNS throughout hydrogen atom ($H^{\bullet}$) or electron (e^{-}) transfer or both types

simultaneously (i.e., proton-coupled electron transfer). Secondary antioxidants, known as preventive ones, are assessed by the chelating ability of selected transition metal ions e.g., Fe(II) or Cu(I). The action of preventive antioxidants includes inhibition of Fenton reactions as a source of hydroxyl radicals or a Lewis acid-base neutralization (metal ion—antioxidant). Endogenous antioxidative enzymes, in its turn, as "first-line defense antioxidants" (ex. SOD, CAT, and GPx), capable to scavenge superoxide anion radicals and hydrogen peroxides, require enzymatic methods for estimation of the antioxidant activity [70].

The non-enzymatic primary antioxidant assays *in vitro* can generally be non-competitive or competitive (Fig. 1) [71]. The action of the competitive assays such as TRAP, ORAC, TOSC, and peroxyl radical trapping antioxidant parameters, is ensured by the competition between a fluorogenic or chromogenic probe and antioxidants for the reactive species (ROS/RNS). The probe undergoes weaker oxidation in the presence of antioxidants, which is reflected in the changes in its measurable characteristics (absorbance, fluorescence, luminescence) [72] (Scheme 2.1.a).

The target species in the competitive scheme is defined here as a compound representing a biomolecule that may be attacked *in vivo* and the antioxidant compounds compete for the reactive species (radical or non-radicals). The antioxidant capacity assessment is based on the quantification of an analytical measurement facilitating compound defined here as the probe. The target species or its oxidized form is a probe in most of the competitive assays. Nevertheless, a compound added following the above-mentioned reaction that allows the quantification of the remaining reactive species or target molecules can also serve as a probe.

The antioxidant capacity of the compounds tested in these assays depends on: (1) the rate of reaction between them and the reactive species, (2) the rate of reaction between the target molecule and the reactive species, and (3) the concentration ratio between antioxidants and target. The following should be singled out among the requirements for these types of assays,: (1) the target/probe must be reactive with oxidants at low concentrations; (2) the spectroscopic change between the native and oxidized probe (to maximize the sensitivity) must be dramatic; (3) no radical chain reaction should occur beyond target/probe oxidation; (4) the antioxidant should not react with the target species.

The non-competitive (Scheme 2.1. b) schemes based on the Folin−Ciocalteu reaction, ABTS/TEAC, CUPRAC, FRAP, DPPH, and ABTS differ in the lack of any competing target molecule. TAC assessments are considered non-competitive if they

rely on an electron transfer (ET) mechanism, whereas competitive measurements are usually based on a hydrogen atom transfer (HAT) [72]. Putative antioxidant compounds interact with reactive species, in non-competitive assays, without the presence of any other competing target molecule. Thus, these assays involve two components in the initial reaction mixture: the antioxidant compounds and the reactive types, which may also serve as a probe for reaction monitoring. Differently, the remaining reactive species may be measured following the addition of some derivative reagents.

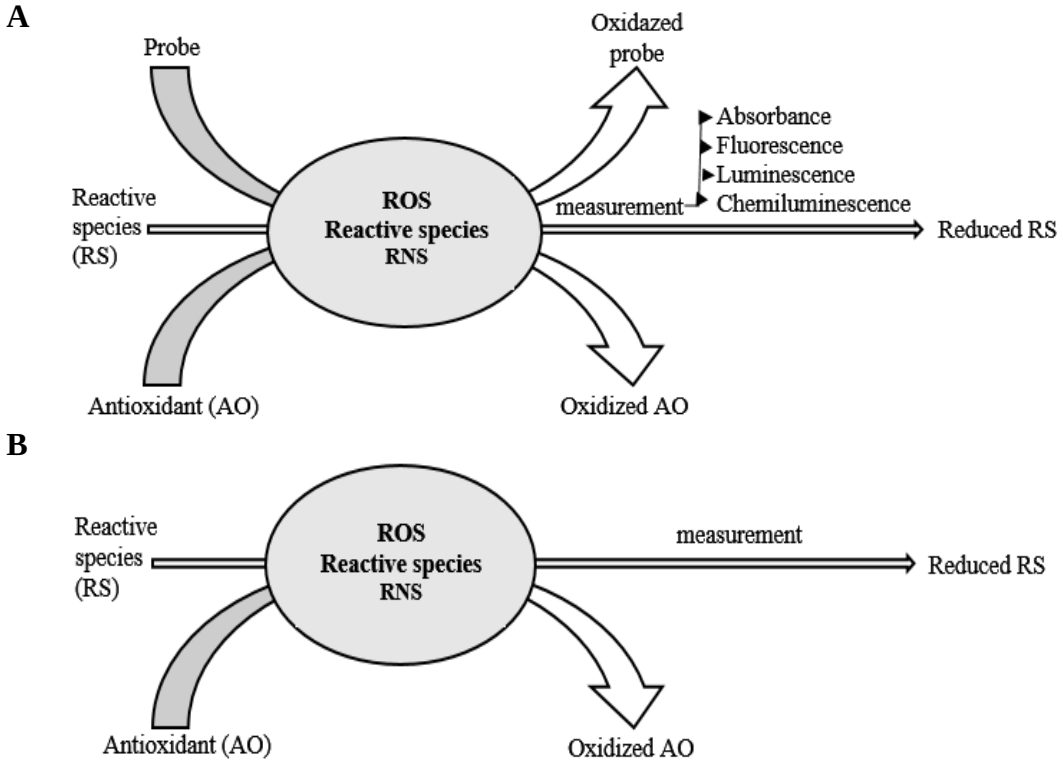

Scheme 2.1. **Schematic illustration of competitive (a) and non-competitive (b) approaches for *in vitro* assessment of antioxidant capacity**

Methods for estimation of antioxidant capacity vary in terms of reaction mechanisms, oxidant, and target/probe types, reaction conditions, and in the mode, the results are expressed. Different antioxidant standard compounds, solvents, reaction time, and pH are frequently applied even when only one of these assays is considered. Moreover, assays measuring various aspects of the antioxidant behavior are strongly recommended to ensure a complete antioxidant profile as the total antioxidant capacity depends on a multitude of factors. Putative antioxidant compounds interact in non-competitive assays with reactive types without the

presence of any other competing target molecule. Thus, these assays involve two components in the initial reaction mixture: antioxidant compounds and reactive species that may also serve as a probe for reaction monitoring. Alternatively, the remaining reactive types may be evaluated following the addition of some derivative reagents. The most common methods are described in Table 2.1.

Table 2.1. Examples of the non-enzymatic assays used for *in vitro* determination of antioxidant capacity with distinguished chromogenic agents, observed changes, the principle, mode, and mechanism of the assay [73]

Assay	The Chromogenic Agents	Observed Changes	Principle of Assay	Mode	Mech	Ref
Total antioxidant capacities						
Crocin bleaching	crocin	bleaching of crocin	The ability of AOs to inhibit oxidation of crocin.	Abs 443 nm pH 7.0–7.5	HAT	[74, 75]
ORAC (Oxygen radical absorbance capacity)	fluorescein, dichloro-fluorescein	fluorescence decay	The fluorescence caused by oxidation of the probe by peroxyl-radical initiated by the thermal decomposition of AAPH, is delayed/inhibited by AOs.	Fl. λex = 485 nm λem = 538 nm pH 7.4	HAT	[76]
TRAP (Total peroxyl radical trapping antioxidant parameter)	β-phycoerythrin	fluorescence decay	Fluorescence decay along time due to oxidation of the probe is delayed by AOs.	Fl. λex = 495 nm λem = 575 nm pH 7.5	HAT	[77, 78]
β-carotene bleaching assay	β-carotene	bleaching yellow color of β-carotene	The ability of AOs to slow down the rate of βcarotene bleaching due to its reaction with peroxyl radicals, which are formed by linolenic acid oxidation.	Abs 470 nm pH 5.5–7.5	HAT	[79, 80]
PCL (Photoche-miluminescen c)	luminol	blue light emission	An AO-sensitive inhibition of a photo-induced, chemiluminescence accompanying autooxidation of luminol.	Cl 360 nm pH 10.5	HAT	[81, 82]
Reducing antioxidant power (RP)						
FRAP (Ferric reducing antioxidant potential)	ferric tripyridyl triazine	yellow color to blue	AOs as reductant at low pH can reduce ferric tripyridyl triazine to ferrous form, causing an absorbance increase.	Abs 593 nm pH 3.6	ET	[83]
CUPRAC (cupric ion reducing antioxidant capacity)	Cu(II) complex	light blue to orange-yellow	Ability of AO for the reduction of Cu(II) in bathocuproine(2,9-dimethyl-4,7-diphenyl-1,10-phenanthroline) or neocuproine (2,9-dimethyl-1,10- phenanthroline) complexes to Cu(I) forms.	Abs 490 nm 450 nm pH 7	ET	[84]
CERAC (Ce(IV)-based	Ce(IV)	fluorescence	The ability of AO to reduce Ce(IV) to Ce(III) is	Fl λex =	ET	[85, 86]

Table 2.1. Continued

reducing capacity)			accompanied by fluorescence elevation.	256 nm λem = 360 nm pH acidic		
CHROMAC (Chromium reducing antioxidant capacity)	Cr(VI) with DPC	red–violet product	The reduction of chromate(VI) to Cr(III) in an acidic solution. The remaining Cr(VI) reacts with DPC to produce a chelate complex. The Cr(VI) consumption was correlated with AO concentration.	Abs 540 nm pH 2.8	ET	[87]
Phosphomo-lybdenum assay	Phosphormol yb-denum complex	green product	The reduction of Mo(Vl) to Mo(V) by AO.	Abs 695 nm pH acidic	ET	[8
The Folin–Ciocalteu (FC) assay	Tungstate–molybdate complexes	from yellow to dark blue	FC reagent in a basic medium is able to oxidize reducing substances, mainly phenolic and polyphenolic AOs. The change in color is connected with the transformation of Mo(VI) to Mo(V), causing an absorbance increase.	Abs 750 nm – 765 nm pH 10	ET	[72]
PFRAP (Potassium ferricyanide reducing power assay)	Ferricyanide reagent: Fe(III), $Fe(CN)6^{3-}$	prussian blue	The AOs react with potassium ferricyanide $Fe(CN)6^{3-}$) forming potassium ferrocyanide $Fe(CN)_6{}^{4-}$ – which further reacts with $FeCl_3$ to form prussian blue $KFe[Fe(CN)_6]$.	Abs 700 nm pH 6.6	ET	[89]
FTC (Ferric thiocyanate)	Fe(S-CN)2	red color	A hydroperoxide formed from a lipid (linoleic acid) oxidizes a ferrous ion to a ferric ion. The AO causes an inhibitory effect on hydroperoxide formation or by its ability to donate an electron to a ferric ion.	Abs 500 nm	ET	[90, 91]
FOX (Ferrous Oxidation-Xylenol Orange Assay)	ferric-XO complex	blue-purple color	The presence of hydroperoxides oxidizes ferrous ions to ferric ions, which subsequently react with xylenol orange (XO).	Abs 550 nm	ET	[92]
Radical scavenging assays						
DPPH	2,2-diphenyl-1-picrylhydrazyl radical	deep violet to pale yellow or colorless	The decrease in DPPH absorbance depends linearly on AO concentration.	Abs 515–517 nm pH 7	HAT/ ET	[79]
ABTS	2,2'-azino-bis(3-ethylbenzothiazoline-6-sulfonic acid (ABTS+.)	bluish-green to colorless	ABTS treated with Na/K persulphate or MnO2 gives a radical cation ($ABTS^{\cdot+}$). $ABTS^{\cdot+}$ is reduced by antioxidants. The decrease in absorbance depends linearly on AO' concentration.	Abs 734 nm pH 7.4	HAT/ ET	[93]
DMPD (N,N-dimethyl-phenylene-diamine)	$DMPD^{\cdot+}$ radical cation	reduction of purple color	$DMPD^{\cdot+}$ is generated through a reaction between DMPD and potassium persulphate the assay measures scavenging of free radicals by AOs.	Abs 517 nm pH 5.25	HAT	[94]
SOSA (Superoxi-de Anion Radical	NBT	yellow to blue	The ability of the AO to compete with NBT to scavenge $O_2^{\bullet-}$ generated by an enzymatic	Abs 560 nm pH 7.4	ET	[95]

Table 2.1. Continued

Scavenging Capacity)			HPXXOD, X-XOD or PMS/NADH systems.			
Nitric oxide free radical scavenging activity	Griess reagent	colorless to light pink to deep purple	NO was generated from sodium nitroprusside and measured by the Greiss reaction. AO reduces the amount of nitrite.	Abs 546 nm pH 7.4	ET	[96]
Peroxyni-trite Scavenging Capacity Assay	Evans Blue	dye bleaching	The percentage of scavenging of ONOO− by the Evans Blue was measured in presence of AO.	Abs 611 nm pH < 7	ET	[97]
HORAC (Hydroxyl Radical Averting Capacity Assay)	fluorescein	fluorescence decay	OH radicals are generated by a Co(II)-mediated Fenton-like reaction. The reaction is confirmed by the hydroxylation of p-hydroxybenzoic acid. Metal ion-induced OH radical generation reaction can be monitored by the fluorescence decay of fluorescein. In the presence of AO, the formation of OH radicals can be inhibited because the metal is deactivated due to coordination with AO.	Fl. λex = 493 λem = 515 nm	HAT	[83] [98]
HRS (Deoxyri-bose Degradation Assay)	MDA-TBA adducts	pink	A mixture of Fe(III)-EDTA, H2O2, vit. C generates OH radical, is able to degrade deoxyribose. The products heated under acidic conditions form MDA detected by adduct with TBA. AO can inhibit deoxyribose damage.	Abs 532 nm pH 7.4	ET	[99]
Hydroxyl Radical Scavenging Capacity Assay	Fenton-like system Fe(II)/ H_2O_2		The Fenton system generates a constant flux of pure OH radicals. ESR measurements evaluate the OH radicals scavenging capacity of AOs.	Electron spin reso-nance (ESR)	ET	[100]
CAA (Cellular Antioxidant Activity Assays)	DCFH-DA	fluorescence decay	The ability of AOs to prevent oxidation of DCFH by azide generated peroxyl radicals in human hepatocarcinoma HepG2 cells.	Fl λex.502 nm, λem 520 nm	ET	[101]
Nonradical reactive oxygen species scavenging assay						
Hydrogen peroxide scavenging activity	hydrogen peroxide	UV absorbance	Hydroxyl radicals are the byproducts of H2O2 decomposition. They initiate lipid peroxidation. After the addition of AO, the absorbance is measured against blank (phosphate buffer).	Abs 230 nm pH 7.4	ET	[102]
Singlet oxygen scavenger	RNO	bleaching of RNO	Production of singlet oxygen (1O2) was achieved by monitoring RNO bleaching. Singlet oxygen was generated by a reaction between NaOCl and H2O2.	Abs 440 nm pH 7.1	ET	[103]
ACA (Aldehyde/ carboxylic acid assay)	Alkylaldehyde/ alkylcarboxylic acid -		The stoichiometric conversion from alkylaldehyde (hexanal) to alkylcarboxylic acid in the presence of radicals induced by heat, O_2, or H_2O_2	GC	ET	[104]

Table 2.1. Continued

Metal chelating capacity assays (MCA)						
Ferrous ions chelating assay	Fe(II) with 2,2-bipyridine or ferrozine	blue	The capacity to chelate ferrous ions can be disturbed by the presence of other complexing agents (AOs), which decreased the intensity of the complex (Fe(II) and ferrozine).	Abs 562 nm 522 nm pH 4–10	ET	[105]
Copper(II) chelating capacity assay	Cu(II)- PV	dark to yellow	The chelating activity can be estimated by the measurement of the rate of color reduction.	Abs 632 nm pH 6	ET	[106]
Nanoparticles (NPs)-based assays						
Gold nanoparticles (Au-NPs)	NPs	No color into dark red	The highest capacity of reducing gold(III) to gold NPs corresponds to the highest antioxidant activity. Alternatively, cyclic voltammetry measures anodic peak potentials	Abs 555 nm pH 8	ET	[107, 108]
Silver nanoparti-cles (AgNPs)	NPs	no color into pale yellow	Nanoparticles generated from metal salts upon reduction with antioxidants in the presence of citrate-stabilized silver seeds.	Abs 423 nm pH 7	ET	[108]

Abbreviations: AAPH (2,2'-azobis–2–methyl-propanimidamide, dihydrochloride); Abs. (Absorbance); DPC (1,5-diphenylcarbazide); XO (xylenol orange); MDA (malondialdehyde); HAE (4-hydroxyalkenals); NBT (nitroblue tetrazolium); Griess reagent (1% sulfanilamide, 2% H_3PO_4, and 0.1% naphthylethylenediamine dihydrochloride); DCFH (dichlorofluorescein); Luminol (5-amino-2,3-dihydrophthalazine-1,4-dione); Cl. (Chemiluminescence), Abs. (Absorbance); Fl. (Fluorescence); HPX-XOD (hypoxanthine–xanthine oxidase); X-XOD (xanthine–xanthine oxidase); PMS/NADH (phenazine methosulphate systems); AO (antioxidant); PV (pyrocatechol violet); RNO (N, N-dimethyl-p-nitrosoaniline); DCFH-DA (2',7'-dichloro-dihydrofluorescein diacetate); triazine (2,3,5- triphenyl-1,3,4-triaza-azoniacyclopenta-1,4-diene chloride).

2.1. Scavenging capacity assays against specific ROS/RNS

Peroxyl radical (ROO•) scavenging capacity assays

Peroxyl radicals (ROO•) commonly occur in food and biological samples, being developed during lipid oxidation chain reactions. They have noxious effects on health and are also associated with food quality deterioration. Their impact on food quality has stimulated the development of several methods for the estimation of the peroxyl radical (ROO•) scavenging capacity [109].

Generally, methods for the studies on ROO• scavenging capacity measure the ability of an antioxidant to scavenge peroxyl radicals by hydrogen atom transfer (HAT) reactions. A competitive scheme is applied in these assays, where antioxidants or target molecules react with ROO•. Consequently, the assay system has three components: (1) thermolabile azo-compound (R N N R), which ensures

carbon-centered radicals ($R^{\bullet}$) that react rapidly with O_2 to give a steady $ROO^{\bullet}$ radical flux; (2) oxidizable target (PH); (3) antioxidant compounds (AH), as sown schematically in Scheme 2.2.

Water-soluble 2,2 -azobis(2-amidinopropane) dihydrochloride (AAPH) and lipid-soluble 2,2 -azobis(2,4-dimethylvaleronitrile) (AMVN) are the most frequently applied peroxyl radical generators. The rate of their spontaneous decomposition and production of $ROO^{\bullet}$ radicals is primarily estimated by the reaction medium temperature [110].

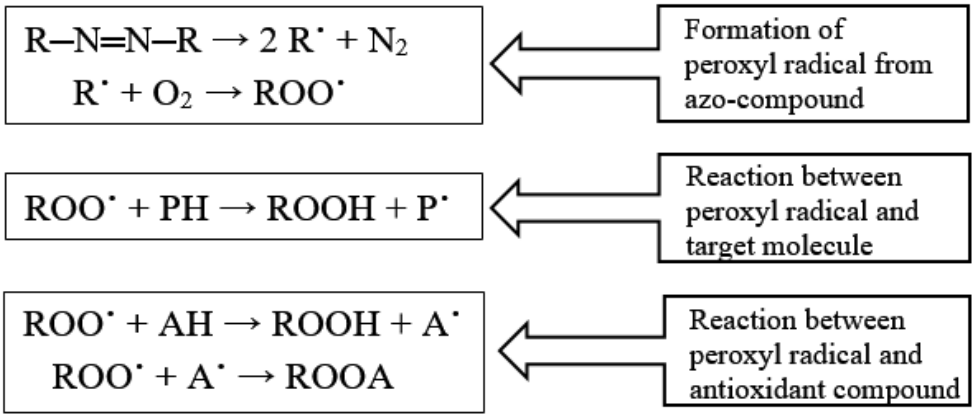

***Scheme 2.2*. Schematic representation of competitive scheme for determination of $ROO^{\bullet}$ scavenging capacity. PH: target molecule, AH: antioxidant compound**

The presence of antioxidant compounds in these competitive assays inhibits or retards the oxidation of the target/probe induced by peroxyl radicals. That is why insignificant spectroscopic changes in the target/probe would be observed (induction period or lag phase) at the beginning of the assay. The antioxidants are consumed by the constant flux of $ROO^{\bullet}$ and the oxidation of the target/probe would progress at a slower rate as the reaction proceeds, compared with the control (absence of antioxidant compounds/samples). Finally, the reaction rate of the target oxidation is similar to that obtained for the control when the antioxidants are depleted.

The concentration of the target types is usually smaller than that of antioxidants although the competitive scheme applied resembles *in vivo* conditions. This contradicts the "definition of antioxidant" [111] and what is observed in real situations, where the antioxidant concentration is much smaller than that of the oxidizable substrate (lipids or proteins, for instance). Additionally, these assays involve a $ROO^{\bullet}$ reaction without taking into consideration the essential propagation step in lipid autoxidation, such as the breakdown of hydroperoxides (ROOH) yielding peroxyl and alkoxyl ($RO^{\bullet}$) radicals [112].

ORAC (oxygen radical absorbance capacity) assay is one of the most common methods for estimating $ROO^{\bullet}$ scavenging capacity. The intensity of fluorescence decrease of the target/probe over time under the reproducible and constant flux of peroxyl radicals, generated from the thermal decomposition of AAPH in an aqueous buffer is the basis of its principle. The decay of fluorescence is inhibited when a sample that contains chain-breaking antioxidants is present [113]. The protein isolated from *Porphyridium cruentum*, β-phycoerythrin (β-PE), was initially used as the fluorescent target/probe, which reacts with $ROO^{\bullet}$ to form a non-fluorescent product [113]. However, large lot-to-lot variability, photobleaching of the β-PE after exposure to the excitation light, and interaction with polyphenols by non-specific protein binding were some shortcomings observed. The synthetic, non-protein fluorescein has been used as the fluorescent target/probe rather than the original β-PE to overcome these limitations [114]. Both lipophilic and hydrophilic chain-breaking antioxidants were applied using an acetone/water mixture containing 7% of randomly methylated β-cyclodextrin as a water solubility enhancer [115]. The ORAC assay was also used to quantify lipophilic compounds by involving AAPH or AMVN as a lipophilic peroxyl radical generator, and 4,4-difluoro-5-(4-phenyl-1,3-butadienyl)-4-bora-3a,4a-diaza-s-indacene-3-undecanoic acid as a fluorescent target/probe [116]. Huang et al. developed a high-throughput assay using a multichannel liquid handling system coupled with a microplate fluorescence reader in a 96-well format to improve the throughput [117].

The reaction in the ORAC assay is regulated for extended periods (≥30min) and the estimation is based on the area under the AUC curve that represents the probe oxidation over time. The antioxidant protective effect is assessed using the net integrated area under the fluorescence decay curves ($AUC_{sample}–AUC_{blank}$). The AUC approach advantage consists of the fact that it can be applied to antioxidants demonstrating distinct lag phases and those lacking them. Furthermore, the initial reaction rate and the total extent of inhibition are taken into account, which includes the action of slow-reacting or secondary antioxidant products resulting.

The reaction in the ORAC assay is regulated for extended periods (≥30min) and the estimation is based on the area under the AUC curve that represents the probe oxidation over time. The antioxidant protective effect is assessed using the net integrated area under the fluorescence decay curves ($AUC_{sample}–AUC_{blank}$). The AUC approach advantage consists of the fact that it can be applied to antioxidants demonstrating distinct lag phases and those lacking them. Furthermore, the initial reaction rate and the total extent of inhibition are taken into account, which includes the action of slow-reacting or secondary antioxidant products resulting [118].

To estimate the antioxidant status of human plasma, Wayner et al. [119] have proposed a total radical-trapping antioxidant parameter (TRAP) assay. This technique was based on the evaluation of the period in which oxygen uptake was inhibited by plasma during a monitored $ROO^{\bullet}$ peroxidation reaction resulting from the thermal decomposition of an azo compound. This assay targeted the human plasma while the oxygen consumed for its oxidation is the probe molecule used to follow the antioxidant action. The evaluation is based on the "lag time" corresponding to the period between the beginning of the assay and the starting point of the target molecule's oxidation. Dichlorofluorescein-diacetate (DCFH-DA) was employed by Valkonen and Kuusi as the fluorescent oxidizable substrate [120]. The oxidation of DCFH-DA by peroxyl radicals results in a highly fluorescent dichlorofluorescein (DCF) product. The presence of antioxidant compounds in this case competitively inhibits fluorescence signal increase. The antioxidant capacity that is expressed as Trolox equivalents (X_{AO}) is calculated as $X_{AO} = (C_{Trolox}/T_{Trolox}) \times T_{AO}$, where C_{Trolox} is the Trolox concentration, while T_{Trolox} and T_{AO} are the lag time of the kinetic curve of target oxidation in the presence of either Trolox or the antioxidant/sample, respectively; X_{AO} is then multiplied by 2.0, the stoichiometric factor of Trolox, and by the sample dilution factor to give the TRAP value (μM).

Some authors have also proposed the utilization of biologically occurring low-density lipoproteins (LDL) as the oxidizable target/probe [121, 122, 123]. The oxidation of LDL, isolated from blood samples, is triggered by the thermal decomposition of AAPH, a water-soluble diazo $ROO^{\bullet}$ initiator, or by a transition element such as Cu(II), and estimated through the formation of conjugated dienes, measured spectrophotometrically at 234 nm following HPLC separation [124]. The use of AAPH rather than Cu(II), as a peroxyl radical generator, is preferable in this assay since it ensures a strong resemblance with oxidative reactions that are possible in biological systems. The oxidation of Cu(II) induced LDL was studied by Sanchez-Moreno et al. who proposed several oxidizability indexes to assess the antioxidant activity of dietary polyphenols [125]. The concentration of the antioxidants that account for the lag time increases by 50% compared to the control (CLT_{50}) and was measured graphically upon representation of the ratio antioxidant lag time/control lag time as a function of antioxidant concentration. Though, the major limitation is that the LDL has to be regularly isolated from different individuals, and hence, a high inter-batch variation is verified. In addition, problems with this assay arise because it is difficult to measure the small lag times that occur, and many substances also absorb at the wavelength of the determination.

The original total oxyradical scavenging capacity (TOSC) assay involves peroxyl radicals generated by thermal homolysis of AAPH that are responsible for the oxidation of -keto-γ-methiolbutyric acid (KMBA) to ethylene, which is controlled by gas chromatographic analysis of headspace from the reaction vessel [126]. The antioxidant capacity of the substances under study is estimated by their ability to inhibit ethylene production in comparison with a control reaction. The approach for quantification of antioxidant capacity in the TOSC assay is similar to that of the ORAC assay. It is based in this case on the area under the curve representing the ethylene production inhibition as a time function (>100min The time course of ethylene production was monitored by Lichtenthaler et al. through utilizing automated headspace gas chromatography [127]. Chemiluminescence (CL) has been utilized as a detection system in peroxyl radical scavenging capacity assays. Alho and Leinonen also describe in detail the principles of $ROO^{\bullet}$-induced luminol-CL assays [128], while Lu et al. present a recent outlook on chemiluminescent methods for ROS [129]. In brief, antioxidant/sample addition induces a CL-lag phase (time during which CL emission was not detected), its magnitude is directly related to the antioxidant concentration [130, 131] or it is accountable for CL emission decrease, expressed as inhibition percentage [132].

Superoxide radical anion ($O_2^{\bullet-}$) scavenging capacity assays

Superoxide radical anion ($O_2^{\bullet-}$) results from the donation of one electron to oxygen. This radical emerges either from several metabolic processes or following oxygen activation caused by irradiation. The analytical methods for assessment of $O_2^{\bullet-}$ scavenging capacity employ the XOD/hypoxanthine system or xanthine at pH 7.4 to produce superoxide anion radical. $O_2^{\bullet-}$ is also produced, to a minor extent, with the help of a non-enzymatic reaction of phenazine methosulphate (PMS) in the presence of nicotinamide adenine dinucleotide (NADH). $O_2^{\bullet-}$ may reduce in both generation systems nitroblue tetrazolium (NBT) into formazan, which is spectrophotometrically controlled at 560 nm [133]. Antioxidant substances compete with NBT for $O_2^{\bullet-}$ and decrease the reaction rate. Cytochrome c is another widely used probe for $O_2^{\bullet-}$. The kinetic analysis of the reduction of ferricytochrome c to ferrocytochrome c was regulated at 550 nm [134]. Factually, Aruoma et al. noticed that NBT reduction inhibition was generally higher than that of cytochrome c. This is explained by the fact that $O_2^{\bullet-}$ reacts much more rapidly with cytochrome c than it does with NBT, thus, a given concentration of added $O_2^{\bullet-}$scavenger competes less efficiently in the cytochrome c system and causes less inhibition. This is clear proof that the assessment of antioxidant capacity is influenced by the nature of the probe. Hydroxylammonium chloride was used by Wang and Jiao [135] with subsequent

production of nitrite that was evaluated spectrophotometrically at 530 nm following the addition of sulfanilic acid and -naphthylamine (Griess reaction) [136]. The XOD/xanthine generating system has also been used to assess the scavenging capacity towards O_2 through reaction with KMBA to produce ethylene, which is measured using gas chromatography [137, 138]. Electron spin resonance (ESR) spectrometry can also be used to measure the scavenging capacity against this radical [139]. In this case, 5,5-dimethyl-1-pyrroline-N-oxide (DMPO) traps $O_2^{\bullet -}$ resulting in DMPO-OOH adduct detected by ESR [140].

Hydrogen peroxide (H_2O_2) scavenging capacity assays

Under physiological conditions, hydrogen peroxide (H_2O_2) is generated *in vivo* by peroxisomes and several oxidative enzymes including glucose oxidase and d-amino acid oxidase, and by the dismutation of superoxide radical that is catalyzed by superoxide dismutase.

One of the most common methods used to assess the scavenging capacity against this molecule is based on the intrinsic H_2O_2 absorption in the UV region [141]. The absorbance value at 230 nm decreases with the decrease of the H_2O_2 concentration due to scavenger compounds. Nonetheless, it is quite usual that samples are also absorbed in this wavelength, which requires "blank" measurement. This can compromise both the precision and the accuracy of the method. Primarily, it may be difficult to distinguish between minor changes when the background absorption is much higher.

Horseradish peroxidase (HRP) is used in another common assay where scopoletin is oxidized by H_2O_2 into a non-fluorescent product [142]. Scopoletin oxidation is inhibited in the presence of putative scavenger compounds and the scavenging reaction can be fluorimetrically monitored.

Arnous et al. proposed a valid alternative to these methods [143]. The enzyme-free methodology involves peroxy oxalate chemiluminescence (POCL) using 9,10-diphenylanthracene and imidazole as a fluorophore (probe) and catalyst, respectively. In short, POCL utilizes hydrogen peroxide imidazole-catalyzed oxidation of an aryl oxalate ester, which provides a high-energy intermediate (dioxetanedione) to transfer its energy into a fluorophore. The transition of the fluorophore excited state to its ground state leads to light emission.

Thus, any compound capable of scavenging H_2O_2 contributes to CL inhibition. The method has been developed to evaluate mainly the H_2O_2 scavenging capacity of lipophilic antioxidants. Assessment of H_2O_2 scavenging capacity is based on chemiluminometric detection with the help of either luminol [144] or lucigenin [145].

Hydroxyl radical (HO•) scavenging capacity assays

Nearly anything in biological systems can be regarded as a HO• scavenger due to the high reactivity of hydroxyl radicals. Thus, no specific molecule or enzyme is responsible for this task. Hence, the assessment of direct HO• scavenging capacity may be irrelevant in case of evaluation of the antioxidant action of a compound or matrix, simply since very high concentrations of scavenger are needed to compete with adjacent molecules *in vivo* or the food matrix for any HO• generated. Therefore, it is more relevant and useful to consider the capacity of putative antioxidants to scavenge or impede the development of its precursors ($O_2^{\bullet -}$, H_2O_2, HOCl) and/or to isolate free metal ions related to HO• production. Scavenger compounds that act like this would behave as preventive antioxidants.

Still, several in vitro methodologies for the determination of HO• scavenging capacity are available, most of them based on Fe^{3+} + EDTA + H_2O_2 + ascorbic acid system to ensure a constant flux of HO• radicals. Those radicals attack sugar 2-deoxy-d-ribose (used as the target), breaking it into fragments, some or all of which react upon heating with thiobarbituric acid at low pH to give a pink chromogen [146]. HO• scavenger will compete with deoxyribose for HO• radicals if it is added to the reaction mixture, suppressing the degradation of the target species. It should be emphasized that the substance(s) under study may interfere with the hydroxyl radical's generation system. In this way, compounds may inhibit the HO• generation through direct reaction with H_2O_2 or chelation of the metal ion. Thus, the performance of the deoxyribose assay with no EDTA ensures the identification of compounds that chelate metal ions [147]. In this case, iron (III) ions are chelated by deoxyribose causing "site-specific" hydroxyl radical damage, and when the test compounds are iron-chelating agents the hydroxyl radical damage of deoxyribose is inhibited. Alternatively, substances (such as ascorbic acid) can reduce Fe^{3+} to Fe^{2+} thereby enhancing the generation of hydroxyl radicals and acting as pro-oxidant agents. Truly, the deoxyribose method was also modified by Hagerman et al. by excluding ascorbic acid to assess the potential of certain tannins to behave as pro-oxidants [148].

Zhu et al. presented a metal-independent, organic Fenton reaction [149]. Salicylic acid is hydroxylated by the mixture of tetrachloro-hydroquinone (TCQH) and H_2O_2 and this process is suppressed by HO• scavenging agents. The HPLC-ED quantification of dihydroxybenzoic acid (DHBA) assessed the extension of salicylic acid oxidation. No iron chelators affect the oxidation reaction. Thereby, this metal-free TCQH/H_2O_2 system ensures the generation of HO• with fewer redox species implicated, which makes it more specific for estimating the HO• scavenging capacity.

A fluorimetric assay was developed by Ou et al. to evaluate "hydroxyl radical prevention capacity" employing fluorescein as the target/probe. $HO^{\bullet}$ radical in this assay is generated by a Co^{2+}-mediated Fenton-like reaction and the $HO^{\bullet}$ scavenging capacity originates mainly from the metal-chelating capability of the compounds. The quantification approach is similar to that of the ORAC assay except that gallic acid serves as a reference standard substance. ESR spectrometry involving DMPO can also be used to evaluate HO• scavenging capacity as in the case of $O_2^{\bullet-}$. Antioxidant compounds, in this case, inhibit the production of the DMPO-OH adduct.

The CL-based evaluation of scavenging capacity against $HO^{\bullet}$ employing luminol has also been reported [150, 151]. $HO^{\bullet}$ originates, in these cases, from the reaction between ferrous iron with molecular oxygen-inducing luminol CL. But, other ROS, including $O_2^{\bullet-}$ and H_2O_2 are produced simultaneously, thereby making it difficult to detect $HO^{\bullet}$ specifically through this detection process.

Hypochlorous acid (HOCl) scavenging capacity assays

This oxidant is derived from the enzymatic myeloperoxidase/H_2O_2/Cl^- system or by acidifying commercial sodium hypochlorite to pH 6.2 using sulphuric acid and is used in the analytical methods for *in vitro* evaluation of HOCl scavengers [152]. The former approach can be useful in the case the sample species are not involved in HOCl generation (e.g. inhibition of myeloperoxidase activity or direct reaction with H_2O_2). The second approach, i.e. assessment of the HOCl solution concentration must be conducted on a daily basis.

Yan et al. have developed a protein carbonyl assay [153]. The method is based on the observation that the content of bovine serum albumin carbonyl is elevated when it is oxidized by HOCl and that this increase is suppressed in the presence of HOCl scavengers. Scavenger compounds impede the HOCl-oxidation of human serum albumin in the assay developed by Gatto et al. [154]. These effects were estimated using reversed-phase high-performance liquid chromatography (HPLC) with spectrophotometric detection at 280 nm. Luminol-elicited CL-based methods have also been proposed, where HOCl scavengers contribute to the reduction of the analytical signal [155]. Finally, based on para-aminobenzoic acid chlorination, a fluorimetric competition assay has been developed to estimate the HOCl scavenging rate constants and implemented on some non-steroidal anti-inflammatory drugs [156].

Singlet oxygen ($^1O_2$) scavenging capacity assays

Singlet oxygen ($^1O_2$) is an excited state of molecular oxygen that has no unpaired electrons and is known to be a powerful oxidizing agent, reacting directly with a wide range of biomolecules [157].

Costa et al. have developed a fluorescence-based microplate screening assay for evaluating $^1O_2$ scavenging activity [158]. The $^1O_2$, that is selectively generated by the thermal decomposition of the endoperoxide disodium 3,3 - (1,4-naphthalene)bispropionate ($NDPO_2$), oxidizes the highly sensitive target/probe dihydroergotamine 123 (DHR) to the fluorescent form rhodamine 123. The assay was successfully conducted for screening the scavenging activity of several recognized antioxidant compounds against $^1O_2$.

Nitric oxide radical ($NO^{\bullet}$) scavenging capacity assays

Nitric oxide radical ($NO^{\bullet}$) has a crucial role in the control of diverse physiological and pathophysiological processes [159].

Vriesman et al. developed a relatively simple method for the assessment of $NO^{\bullet}$ scavenging capacity of sulfur-containing compounds in an aqueous solution with the aid of an amperometric $NO^{\bullet}$ sensor [160]. $NO^{\bullet}$ is introduced into buffered solutions of the scavenger (glutathione, glutathione disulfide, S-methyl glutathione, N-acetyl cysteine, lipoic acid, and dihydrolipoic acid) and its concentration is observed as a function of time. The natural logarithm of the $NO^{\bullet}$ concentration and time are in a linear relation. The second-order rate kinetics of the scavenging reaction was assessed following correction for the spontaneous $NO^{\bullet}$ degradation. Only the compounds, which contained a thiol group, were observed to demonstrate a considerable $NO^{\bullet}$ scavenging capacity. There is a non-competitive reaction mechanism in this method since the reaction medium only presents the reactive species ($NO^{\bullet}$) and the scavenger molecule(s).

The Griess reaction is frequently utilized for the estimation of $NO^{\bullet}$ production by intact cells or enzymes [161, 162]. It is also frequently exploited *in vitro* to quantify $NO^{\bullet}$ scavenging capacity. The nitric oxide remnants of the reaction with the test sample are measured as nitrite in this case. It should be emphasized that nitrate may also be produced and it is important to reduce it to nitrite ahead of evaluation. Keeping this in mind, Perez et al. used NADH-dependent nitrate reductase to eliminate NADH interference by adding lactate dehydrogenase and pyruvate [163]. The chromophoric azo derivative produced from nitrite following the Griess reaction is afterward estimated spectrophotometrically at 540 nm.

For screening of $NO^{\bullet}$ scavenging capacity the fluorescent target/probe 4,5-diaminofluorescein (DAF2), widely employed for *in vivo* $NO^{\bullet}$ detection and imaging,

has also been applied [164]. The nitrosation of the weak fluorescent target/probe DAF-2 by derivative $NO^{\bullet}$ species resulted in the formation of a strong green-fluorescent triazolofluorescein product (DAF-2T). The $NO^{\bullet}$ scavenging capacity was estimated by the capacity of compounds to exclude the $NO^{\bullet}$-induced nitrosation of DAF-2. The results are expressed as the percentage of DAF-2 oxidation inhibition as a function of the scavenger compound concentration [165].

Peroxynitrite ($ONOO^{-}$) scavenging capacity assays

Techniques for assessing the $ONOO^{-}$ scavenging capacity are commonly dependable on either tyrosine nitration [166] or dihydrorhodamine 123 (DHR) [167]. The first method is based on the formation of 3-nitrotyrosine that is detected spectrophotometrically along with the unreacted tyrosine following HPLC separation. The 3-nitrotyrosine concentration is estimated after tyrosine incubation with various concentrations of putative $ONOO^{-}$ scavengers and the inhibition percentage of 3-nitrotyrosine production is measured. The non-fluorescent DHR is oxidized by peroxynitrite to yield fluorescent rhodamine 123 in the second method. The fluorescence intensity is lower in the presence of $ONOO^{-}$ scavengers than that of the control and the inhibition percentage of DHR oxidation is evaluated [168].

2.2. Scavenging capacity assays against stable, non-biological radicals and evaluation of total reduction capacity

Scavenging of 2,2 -azinobis-(3-ethylbenzothiazoline-6-sulphonate) radical cation ($ABTS^{\bullet+}$) assay

The ($ABTS^{\bullet+}$) assay considers the generation of long-lived radical cation chromophore 2,2 -azinobis-(3- ethylbenzothiazoline-6-sulphonate) ($ABTS^{\bullet+}$) with absorption maxima at 414 nm, 645 nm, 734 nm, and 815 nm. The primary ($ABTS^{\bullet+}$) assay, developed by Miller et al., involved the activation of metmyoglobin, acting as peroxidase, with the aid of H_2O_2 to provide ferryl myoglobin radical, which afterward reacted with ABTS to yield $ABTS^{\bullet+}$ radical cation [169]. A sample to be tested is added before the formation of the $ABTS^{\bullet+}$ in this strategy. The compounds reduce the $ABTS^{\bullet+}$ radicals developed and the lag phase, which corresponds to the delay time in radical formation, is estimated (competitive scheme). This technique was commercialized by Randox Laboratories (San Francisco, USA) as the world's first kit for the standardization of total antioxidant status evaluation in individual serum or plasma. The order of addition of reagents and sample was later criticized as a major trap since antioxidants (quercetin, for example) can react with H2O2 and/or with oxidizing species derived which inhibit the ABTS•+ radical production resulting in an overestimation of antioxidant capacity [170].

Hence, a post-addition assay or decolorization strategy was proposed to impede the interference of antioxidant compounds with radical production, thereby making the assay more reliable and less susceptible. The sample to be tested in this case was added after yielding a certain amount of $ABTS^{\bullet+}$ radical cation and the remaining $ABTS^{\bullet+}$ concentration was estimated following the reaction with the antioxidant compound [171].

In regards to assay conditions, different strategies have been developed for $ABTS^{\bullet+}$ generation, reaction time applied, detection wavelength used for regulating the reaction, and the reference antioxidant screened. $ABTS^{\bullet+}$ radical cation can be produced through a reaction with manganese dioxide [172], potassium persulfate [173], AAPH [171], or using enzymatic reaction with metmyoglobin or horseradish peroxidase [174], or through electrochemical production [175]. Reaction times varying between 1 min and 30 min have been approved throughout the protocols reported in the literature. As for the wavelength of detection, the measurement at 734 nm is preferable as the interference from other absorbing components and the sample, turbidity is minimized. Regarding quantification, the absorbance value, proportional to the remaining $ABTS^{\bullet+}$ concentration, is quantified after a fixed reaction time.

This spectrophotometric assay is technically simple, which justifies its usage for screening and routine measurements. The $ABTS^{\bullet+}$ scavenging can be conducted over a wide pH range, which is helpful for studies on the impact of pH on antioxidant mechanisms. Moreover, the $ABTS^{\bullet+}$ radical is soluble in water and organic solvents, which makes it feasible in estimating the antioxidant capacity of both hydrophilic and lipophilic compounds/samples. However, the results of this assay depend on the time of analysis as the sample results are related to an antioxidant standard compound with different kinetic behavior.

Scavenging of 2,2-diphenyl-1-picrylhydrazyl radical ($DPPH^{\bullet}$) assay

The purple chromogen radical 2,2-diphenyl1-picrylhydrazyl ($DPPH^{\bullet}$) is lowered in this assay with the help of antioxidant/reducing compounds to the appropriate pale yellow hydrazine [176]. The scavenging capacity is usually assessed in organic media by regulating the absorbance decline at 515 nm –528 nm until it stays constant [177] or through electron spin resonance.

Milardovic et al. have recently proposed the antioxidant capacity to be measured based on an amperometric $DPPH^{\bullet}$ decrease on a glassy carbon electrode [178]. Following the reaction with the antioxidants the resulting current on a glassy carbon electrode polarized at fixed potential was proportional to the $DPPH^{\bullet}$ residual

concentration. There was also presented an amperometric method using DPPH/DPPH$^{\bullet}$ redox couple and two identical glassy carbon disc electrodes [179]. Contrary to what was initially regarded as true, the reaction mechanism is based on an electron transfer (ET) reaction while the hydrogen atom abstraction is a marginal reaction pathway since it proceeds slowly in strong hydrogen-bond-accepting solvents, such as methanol and ethanol.

The scavenging capacity against DPPH$^{\bullet}$ radical is under a strong influence of the solvent and reaction pH value as in the case of other ET-based assays. Stasko et al. screened for appropriate conditions and limits of water as a component of a mixed water-ethanol solvent in DPPH$^{\bullet}$ radical assay [180]. [50% (v/v) aqueous/ethanol solutions are a fitting choice for lipophilic and hydrophilic antioxidants while the reaction between DPPH$^{\bullet}$ and the antioxidant may accelerate considerably with a water ratio increase. However, the antioxidant capacity decreased at water content over 60% (v/v) as a portion of DPPH$^{\bullet}$ coagulates becoming hard to reach to the reaction with antioxidants. This spectrophotometric method is considered an easy and useful technique regarding screening/measuring the antioxidant capacity of both pure substances and complex samples.

Ferric reducing antioxidant power (FRAP) assay

The FRAP assay estimates the capacity of antioxidants to reduce the ferric 2,4,6-tripyridyl-s-triazine complex [Fe(III)- $(TPTZ)_2]^{3+}$ to the intensely blue colored ferrous complex [Fe(II)-$(TPTZ)_2]^{2+}$ in the acidic medium [181]. This technique has also been adapted to a 96-well microplate reader resulting in better reproducibility and higher sample performance [182]. As for its limitations, any substance (even lacking antioxidant properties) with redox potential lower than that of the redox pair Fe(III)/Fe(II), can theoretically reduce Fe(III) to Fe(II), making a contribution to the FRAP value and inducing falsely high results. Not all antioxidants, on the other hand, reduce Fe(III) at a rate rapid enough to allow the measurement to be taken within the observation time (usually 4 min). Antioxidants that act by radical quenching (H transfer), particularly thiols and carotenoids, will not be identified as the FRAP assay measures the reducing capacity based upon the reduction of ferric ions [183].

Folin–Ciocalteu reducing capacity (FC) assay

The Folin–Ciocalteu reagent is accepted to contain phosphomolybdic/phosphotungstic acid complexes though its exact chemical nature is unknown. The chemistry behind the FC assay is based on the transfer of electrons in an alkaline medium from phenolic and other reducing substances to molybdenum, forming thereby blue complexes detectable spectrophotometrically at 750 nm –765 nm [184].

2.3. Electrochemical Methods

Electrochemical measurements possess some major advantages in comparison to spectrophotometric methods mainly because they are fast, less tedious, cheaper, and safer for the environment. They include electrochemical techniques of antioxidant characterization such as potentiometry, amperometry, cyclic voltammetry (CV), square-wave voltammetry (SWV), and differential pulse (DPV). These methods utilize the fact that antioxidants are involved in redox reactions acting as reducing agents. The electrochemical techniques can measure their redox potentials [185].

2.4. Antioxidant Capacity in Cultured Cells

Cultured cells have been frequently employed as a substrate to elucidate the underlying mechanisms of oxidative stress and to estimate the defensive effects of antioxidants against different oxidative stressors. The species capable of oxidizing the biological molecules produce oxidative damage, and some species which do not provoke oxidation directly by themselves are capable of triggering a disturbance in the cellular redox equilibrium and causing oxidative stress [186].

The advantage of using cultured cells consists in the fact that various stressors and cell types including model systems for some specific diseases can be employed for the estimation of antioxidant effects. It should be also mentioned that cultured cells may become more significant as the involvement of experimental animals will be more difficult in the future. The effects of antioxidants have been evaluated against oxidative stress in cultured cells to inhibit ROS production, oxidation of lipids, proteins, and DNA, and cell death. Antioxidants are added to the cell culture medium together with the stressor or are preincubated to be inserted into cells. It is quite essential to estimate the intake of antioxidants into cells for precise evaluation of the antioxidant effect since the rate of intake into cells varies significantly depending on the antioxidants.

2.5. Antioxidant capacity *in vivo*

The capacity of antioxidants *in vivo* is determined by many factors which should be considered in its evaluation. Bioavailability is one such factor. The antioxidants should be absorbed, transported, distributed, and retained properly in biological material (fluids, cells, and tissues). The bioavailability of various antioxidants and the effect of dosage and duration have been investigated by analyzing biological fluids and tissues of humans and experimental animals following the consumption of antioxidants. The studies were focused on the time-

course change in the concentrations of metabolites as well as the parent antioxidant. Quite different capacity is observed *in vitro* and *in vivo* in some antioxidants, Metabolism also impacts the antioxidant capacity *in vivo*. Some antioxidants may experience biotransformation due to enzymatic conjugation with sulfate, methyl, or glucuronide groups [187].

The capacity and efficacy of antioxidants *in vivo* may be evaluated most precisely by the influence of antioxidant substances and materials on the oxidation level in biological fluids and tissues, such as erythrocytes, plasma, cerebrospinal fluids, and urine sampled from humans and experimental animals. Saliva and tear may also be analyzed. Reliable biomarkers are important for this purpose and many oxidative stress ones have been utilized to quantify the level of oxidation *in vivo* [188]. Lipid oxidation products [189], oxidative modification and expression of proteins and sugars [130], strand breaks of DNA, and oxidation products of DNA bases [190] have been employed as oxidative stress biomarkers. Some examples of biomarkers are summarized in Table 2.2. Free radicals cause the isomerization of unsaturated lipids from cis to trans form and increase trans fatty acids.

Table 2.2. Biomarkers of oxidative stress [191, 192]

Biomarkers of lipid peroxidation	
TBARS TBA-reactive substances	The oldest and one of the most widely used nonspecific by-products of lipid peroxidation, reacts with thiobarbituric acid (TBA), forming a pink chromogen (TBARS) measured at 532–535 nm
MDA malondialdehyde	$CH_2(CHO)_2$, colorless liquid, highly reactive, a product of LPO of polyunsaturated fatty acids, form covalent protein adducts referred to as advanced lipoxidation end-products (ALE), in analogy to advanced glycation end-products (AGE)
4-HNE 4-hydroxynonenal	α,β-unsaturated hydroxyalkenal, produced by lipid peroxidation (arachidonic or linoleic groups) in cells in higher quantities during oxidative stress, possible role in cell signal transduction.
ACR acrolein (propenal)	The simplest unsaturated aldehyde, named and characterized in 1839, electrophilic, reactive, and toxic, contact herbicide to weeds, present in tobacco smoke increases the risk of cancer, produced during cyclophosphamide treatment
F2-isoprostanes	Prostaglandin-like compounds formed in vivo from the free radical-catalyzed peroxidation of arachidonic acid
F4-isoprostanes	Prostaglandin-like compounds formed in vivo from the free radical-catalyzed peroxidation of docosahexaenoic acid, potent biological activity as anti-inflammatory mediators
CRA crotonaldehyde	CH_3CH, a representative carcinogenic aldehyde formed endogenously through lipid peroxidation, CRA is a highly reactive aldehyde and reacts with a lysine residue in the protein, reaction with CRA and lysine residue leads to the formation of numerous numbers of adducts

Table 2.2. Continued

HHE 4-hydroxy-trans-2-hexenal	Oxygenated α,β-unsaturated aldehyde, other coming from omega-3 fatty acids: 4-oxo-trans-2-nonenal, 4-hydroperoxy-trans-2-nonenal, and 4,5-epoxy-trans-2-decenal
7KC 7-ketocholesterol (7-oxocholesterol)	Toxic oxysterol, produced from oxidized cholesterol, induces: NOX, pro-inflammatory cytokines and TNF-α
Biomarkers of proteins peroxidation	
DiBrY dibromotyrosine	Product of the reaction of hypobromous acid (HOBr) from hydrogen peroxide (H_2O_2) and bromide ion (Br–)
DiY/DT dityrosine (bityrosine)	Biphenyl compound comprising two tyrosine residues linked at carbon-3 of their benzene rings
m-Tyrosine o-Tyrosine	Abnormal tyrosine isomers, derive from oxidation of the benzyl ring of the phenylalanine by hydroxyl radical, adversely affect cells and tissues
NY 3-nitrotyrosine	Specific marker of attack of peroxynitrite ($ONOO^-$) upon proteins, measured by immunostaining, HPLC, and MS in human tissues
protein carbonyls	Measurement of protein CO groups after their derivatization with DNPH is the most widely utilized measure of protein oxidation
Biomarkers of nucleic acids peroxidation	
Comet assay	
DNA fragmentation	
8OHdG 8-hydroxy-2′ -deoxyguanosine	Oxidized derivative of deoxyguanosine, a major product of DNA oxidation, increased levels are found during carcinogenesis, increase with age, linked to the enzyme OGG1 and transcription factor NFκB
8-oxo-Gua 8-hydroxyguanine	One of the most common DNA lesions resulting from reactive oxygen species, modifying guanine and can result in a mismatched pairing with adenine resulting in G to T and C to A → mutation

The impact of various antioxidants on the levels of oxidative stress biomarkers has been assessed in many studies on humans and experimental animals under normal and oxidative stress conditions. The influence of antioxidants has been also estimated in some clinical intervention studies and model animals for specific diseases.

3. Classification of antioxidants

Antioxidants are hydrophilic and lipophilic. Water-soluble antioxidants are oxidized in the cell cytosol and blood plasma, while fat-soluble antioxidants protect cell membranes from lipid peroxidation on the surface. Different antioxidants are present in a wide range of concentrations in body fluids and tissues, while some (glutathione or ubiquinone) are mainly localized inside the cells, while others (uric acid) are more evenly distributed [193, 194, 195]. Today in clinical practice are being used a huge number of different preparations with antioxidant activity. The clinical

value of an antioxidant is enhanced if the molecule is both hydro-, and lipophilic at the same time, which makes it possible to provide antioxidant effects, both inside the cell and in the intercellular space.

The regulator of the level of lipid peroxidation (LPO) in the body is the antioxidant system, in the composition of which it is quite conditionally possible to distinguish endogenous antioxidants, metal-binding proteins, and food antioxidants (Table 3.1).

There are different attributes to classify the antioxidants. The first attribute is based on the function (primary and secondary antioxidants).

Table 3.1. Level regulating antioxidants (LPO).

<table>
<tr><th colspan="2">Endogenous antioxidants</th><th>Metal-binding proteins</th><th>Food antioxidants</th></tr>
<tr><td>Non-enzymatic</td><td>Enzymatic</td><td>Albumin (copper)</td><td>Ascorbic acid (vitamin C)</td></tr>
<tr><td>Bilirubin</td><td>Copper/zinc-and magnesium-dependent superoxide dismutase</td><td>Ceruloplasmin (copper)</td><td>α- tocopherol (vitamin E)</td></tr>
<tr><td>Thiols (glutathione, α-lipoic acid, N-acetylcysteine)</td><td>Iron-dependent catalase</td><td>Metallothionein (copper)</td><td rowspan="2">β-carotene (carotenoids and oxycarotenoids, lycopene and lutein)</td></tr>
<tr><td>Thioredoxin</td><td>Selenium-dependent glutathione peroxidase</td><td>Ferritin (iron)</td></tr>
<tr><td>NADP and NAD</td><td rowspan="2">Selenium-dependent thioredoxin reductase</td><td>Transferrin (iron)</td><td rowspan="3">Polyphenols (flavonoids, flavones, and proanthocyanidins)</td></tr>
<tr><td>Ubiquinone (coenzyme Q10)</td><td rowspan="2">Myoglobin (iron)</td></tr>
<tr><td>Uric acid</td><td>Thioredoxin peroxidase</td></tr>
</table>

Primary antioxidants

They are the chain-breaking antioxidants that react with lipid radicals and convert them into more stable products. Antioxidants of this group are mainly phenolics, in structure and include the following: Antioxidant minerals, antioxidant vitamins, and phytochemicals which include flavonoids, catechins, carotenoids, β-carotene, lycopene, diterpene of, black pepper, thyme, garlic, cumin, and their derivatives.

Secondary antioxidants

The second attribute is based on enzymatic and non-enzymatic antioxidants. These phenolic compounds perform the function of capturing free radicals and stopping chain reactions. The compounds include butylated hydroxyanisole (BHA), butylated hydroxytoluene (BHT), and propyl gallate (PG).

The body's endogenous defense system against these free radicals plays an imperative role, which can be further supported by the supplementation of antioxidants in the diet. Generally, antioxidants can be divided into two major categories such as synthetic and natural.

Notwithstanding, antioxidants can be divided into two classes: enzymatic antioxidants and nonenzymatic antioxidants. Some enzymatic antioxidants are endogenously produced, including enzymes, low molecular weight molecules, and enzyme cofactors.

Among nonenzymatic antioxidants, many are obtained from dietary sources. Dietary antioxidants can be classified into various classes of which polyphenols present the largest class. Polyphenols consist of phenolic acids and flavonoids. The other classes of dietary antioxidants include vitamins, carotenoids, organosulfur, and minerals.

It should be emphasized that there is a great difference between antiradical and antioxidant activity. Antiradical activity characterizes the ability of compounds to react with free radicals while antioxidant activity represents the ability to inhibit the process of oxidation.

Consequently, all the tested systems using a stable free radical (DPPH, ABTS, etc.) give information on the radical scavenging or antioxidant activity. Mode of action of antioxidants: Based on the mode of action, antioxidants can be classified into two main groups, namely, hydrogen atom transfer (HAT) and single electron transfer (SET) assays [196].

3.1. Synthetic antioxidants

Synthetic antioxidants are widely used to inhibit oxidative processes. Most currently used antioxidant drugs are direct-acting antioxidants. Primary screening of direct-acting antioxidants is carried out on *in vitro* model systems, i.e. when the efficiency of their antioxidant action is determined primarily by the chemical structure of the substance and does not depend, in any way, on the general homeostasis of the body.

There has been much less work on the systematic study of synthetic antioxidants designed to optimize the antioxidant activity, while at the same time satisfying other important criteria, including solubility, bioavailability, and lack of toxicity (or selective toxicity in the case of cancer chemopreventive antioxidants).

Representatives of synthetic active substances of a non-enzymatic, with antioxidant properties, are Acetylcysteine, Tirilazad, Dimethyl Sulfoxide, Polydihydroxyphenylenethiosulfonate Sodium,

Pentahydroxyaethylnaphthoquinonum, Ethylmethylhydroxypyridine Succinate, Butylated Hydroxytoluene, Pyridoxine, Methylethylpiridinol, Thiotriazoline, Probucol (Vidal-2022).

Thiosemicarbazides, thiosemicarbazones, as well as their derivatives and complexes.

The steady increase in the number of diseases poses a challenge for modern chemistry in the search for new biologically active substances that will allow the treatment of these diseases and enhance the duration and quality of life. Therefore, great attention is paid to the new compounds [193].

Scientists in various disciplines have become more interested in new compounds, either synthesized or obtained from natural sources, which could provide active components to prevent or reduce the impact of oxidative stress on cells. There has been much less work on the systematic study of synthetic antioxidants designed to optimize the antioxidant activity, while at the same time satisfying other important criteria, including solubility, bioavailability, and lack of toxicity (or selective toxicity in the case of cancer chemopreventive antioxidants). Schiff bases have often been used as chelating ligands in the field of coordination chemistry, and their metal complexes have been of great interest to researchers for many years. It is well known that *N* and *S* atoms play a key role in the coordination of metals at the active sites of many metallobiomolecules. The importance of metal ions in biological systems is well established.

Cuprum, nickel, cobalt, ferum, manganese, chromium, and molybdenum are essential microelements that play various important roles in living organisms. Many crucial biological redox processes in nature are efficiently performed by these complexes that incorporate either Cu(II) Zn(II) Ni(II) Co(III) Fe(III) Mn(II) Cr(III) Mo(VI) or Mo(V) metallic center usually embedded within a coordination sphere including sulfur, oxygen, and nitrogen atoms. Since these metals play an active and important role in the metabolism of the majority of Earth's life forms, they are very interesting for biochemical and biomedical research.

Therefore, developing new Cu(II), Zn(II), Ni(II), Co(III), Fe(III), Mn(II), Cr(III), Mo(VI) or Mo(V) - based compounds appears as a good strategy for developing new drugs and there are many examples in the literature of the biological activity of Cu(II), Zn(II), Ni(II), Co(III), Fe(III), Mn(II), Cr(III), Mo(VI) or Mo(V) -based compounds, including coordination complexes.

The biological activity of complex compounds can be affected by the type and number of ligands, the geometry of the complex, the strength of bonds between the metal and donor atoms of the ligand, the degree of oxidation of the central atom, the

ability of ligands to exchange, and the outer sphere of the complex. By modifying these parameters, it is possible to achieve a change in the biological activity of the complex.

In the past couple of decades, thiosemicarbazones and thiosemicarbazides coordination complexes have received considerable attention in many domains such as biology or medicine. In particular, thousands of studies gathered in more than 200 reviews were focused in the area of biology and medicine because of the promising biological implications and remarkable pharmacological properties of thiosemicarbazone complexes as antitumor, antiviral, antimalarial, antibacterial, antifungal, or antioxidant agents.

From their side, thiosemicarbazone molecules are polydentate organic ligands that contain an imine group linked to a thiosemicarbazide moiety (Scheme 3.1) [197]. R1, R2, and R3 groups can be modified as desired, which gives thousands of possibilities [198].

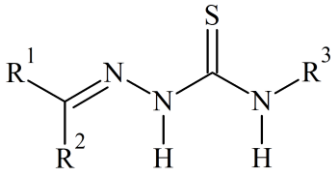

Scheme 3.1. **General Representation of Thiosemicarbazone Ligands**

Copper complexes are the most studied among the transition metal complexes with thiosemicarbazones from the biological point of view. In many cases, the coordination of thiosemicarbazones to the copper(II) ion leads to the greatest enhancement of anticancer and antimicrobial activity. Even though the selectivity of the described copper complexes in many cases exceeds the selectivity of anticancer drugs such as doxorubicin and cisplatin, in most cases, the selectivity index does not exceed. Among N^4-substituted thiosemicarbazones, more attention is paid to N^4-alkyl, N^4-arylthiosemicarbazones. N^4-allylthiosemicarbazones are described less frequently. However, N^4-allylthiosemicarbazones exhibit high biological activity and are comparatively more soluble in water. Based on this, it is important to continue the systematic study of thiosemicarbazones and biometal complexes with them to identify new substances with high anticancer, antimicrobial, and antifungal properties, which at the same time will be free from such significant drawbacks as high toxicity.

Induced toxic hemolysis and elevated index of methemoglobin are the results of the effect of oxidative stress of free-radical nature caused by chemotherapy. It is known from the literature that the biological action of the anticancer anthracyclines

doxorubicin and daunorubicin is frequently connected with their ability to induce oxidative stress through RF generation and reactive oxygen species [199]. This property is due to the presence of a quinone moiety in the drugs' structures, which may cause metabolic reduction generating superoxide via aerobic redox cycling and, subsequently, other more reactive oxygen forms. ROS are believed to possibly play a role in cardiotoxicity induced by anthracycline. This is not surprising, as the drugs contain an electron-donating hydroquinone moiety in their chromophores. An anticancer compound should not be prooxidant as it may produce adverse modifications to cell components [200].

Synthetic antioxidants are widely used to inhibit oxidative processes. Most currently used antioxidant drugs are direct-acting antioxidants. Primary screening of direct-acting antioxidants is carried out on *in vitro* model systems, i.e. when the efficiency of their antioxidant action is determined primarily by the chemical structure of the substance and does not depend, in any way, on the general homeostasis of the body.

The work discussed herein describes the in vitro antioxidant and in vivo toxicity activities for thiosemicarbazones and thiosemicarbazides and their metal complexes.

3.2. Natural antioxidants

Nature is always a significant and rich source of countless ingredients that can be served as health-promoting agents. Many of these natural sources include routinely used fruits, vegetables, herbs, spices, nuts, seeds, leaves, roots, barks, cereals, beans, beekeeping products, and edible mushrooms that can be part of a routine diet. In addition to that, there is a huge list of medicinal plants reported to have extensive health-boosting potentials. One of the most beneficial effects of these natural sources is due to their potential antioxidant properties. Regarding the antioxidant capability, the researchers have focused their studies to explore the potential sources along with their active ingredients. The researchers have added some marine sources such as algae and seagrass as well to the list of these natural sources. Recent studies have also explored the role of naturally occurring microbiomes in the gut in the body's antioxidant pool denoted as good bugs. These good bugs can also be used as a supplement called probiotics.

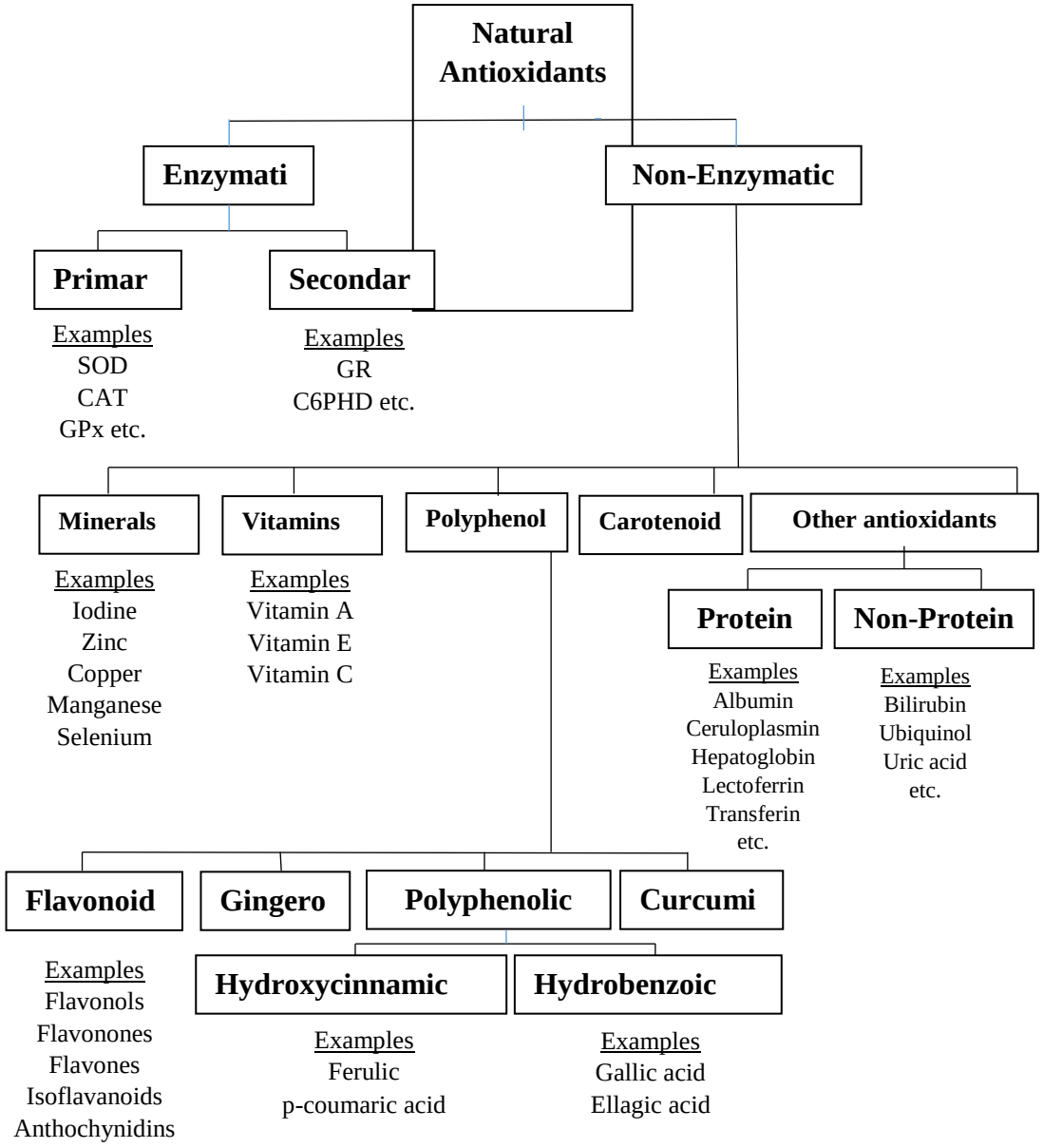

Fig. 3.1. **Classification and sub-classification of natural antioxidants (Carocho & Ferreira, 2013)**

The main targeted site of free radicals damage and the defensive approach of antioxidants in the body is at the cellular level. Based on this, these antioxidants can also be classified as enzymatic and nonenzymatic antioxidants. Enzymatic antioxidants primarily include glutathione peroxidase, catalase, and superoxide dismutase. Several other enzymes in the body contribute to the total antioxidant

capacity, which reflects in the serum [201]. Nonenzymatic antioxidants contain several subdivisions mainly vitamins such as A, E, C, and D, enzyme cofactors (Q10), peptides, and some minerals (zinc and selenium). The major ingredients from natural sources are polyphenolic compounds, which are reported to have significant antioxidant potential [202]. A detailed classification and sub-classification have been displayed in Figure 3.1.

3.3. Antioxidant activity of bee products

Beekeeping products have been among the most commonly used naturally-occurring products in folk medicine since ancient times. Honey, propolis, pollen, royal jelly, beeswax, and bee venom have been strongly appreciated for their powerful healing properties and high bioactive molecule content [203]. This area of traditional medicine, having scientific foundations, is now called apitherapy and is widely used to prevent or treat several different conditions, such as wounds, rheumatic diseases, immune and neurologic conditions, alimentary tract disorders, etc. [204]. Currently, diet and a balanced lifestyle are widely admitted to having a significant contribution to preventing and healing diseases. Modern consumers increasingly seek and use naturally-occurring functional foods that contain bioactive substances of natural origin to improve their quality of life, thanks in part to their higher safety compared to synthetic drugs [205]. Scientific studies have demonstrated a wide range of beneficial health effects of bee products, among them antioxidant, antibacterial, anti-inflammatory, antitumor, antiviral properties, and many others [206]. Their antioxidant capacity is one of the most important properties and it contributes to the prevention of some diseases. Naturally occurring antioxidants that are present in honey, beeswax, royal jelly, bee uterus, propolis, and pollen manifest great bioactivity and molecular diversity [207]. Various substances are transferred from plants and accumulated in food since bees produce honey from nectar or plant secretions. Hence, the honey composition, including its physical, chemical, organoleptic, and nutraceutical properties, is directly associated with the geographical, climatic, and environmental characteristics of the production areas. These variations are important for classifying and identifying honey.

Plants synthesize antioxidants to counteract biotic (pathogenic, predatory, competitive species) and abiotic (UV radiation, desiccation, thermal shock) stresses. They have a noxious impact on the health of people who consume them through food, this to include honeybee products produced by bees from floral nectar, pollen, or plant secretions [208]. Plant antioxidants are highly bioactive and present great molecular diversity, while the content of phenolic compounds (phenolic acids,

flavonoids) and their antiradical activity are the highest. Phenolic substances extend from simple, low molecular weight, single aromatic-ringed compounds to large, complex tannins and derived polyphenols. By chemical structure, phenolic acids can fall into hydroxybenzoic acids, with a C1–C6 nuclear structure derived from benzoic acid, with different aromatic ring methylation and hydroxylation (e.g., vanillic acid, benzoic acid, and gallic acid); and hydroxycinnamic acids, with a C3–C6 general structure and differences in the originating ring substituents (e.g., p-coumaric acid, caffeic acid, cinnamic acid, and ferulic acid,). Flavonoids have a C6–C3–C6 general structure, connecting two benzene rings linked by a pyran ring, and according to the type of substituent present on the ring can be classified into flavones, flavanones, and flavonols (e.g., catechin, myricetin, quercetin, apigenin, kaempferol, luteolin, rutin, isorhamnetin, pinocembrin, or gallocatechin) [209].

The antioxidant capacity of phenols is based on different mechanisms, including hydrogen donation, metal ion chelation, free-radical scavenging, single oxygen quenching, and action as a substrate for superoxide and hydroxyl radicals. These mechanisms are strongly connected with the metabolites and their molecular structure, e.g., hydrogen donation readiness may be prejudiced by the steric impediment of the carboxyl group, located next to the hydroxyl group. This points out that the hydroxyl group number and position in phenolic compounds are of supreme importance to the antioxidant scavenging capacity. AOA is highly correlated with phenolic compounds, but bee products are multicomponent natural substances and therefore other substances presenting AOA, including minerals, amino acids, peptides, proteins, organic acids, and enzymes are also contained in them, but at lower concentrations than phenols. The bee product in question has a primary impact on the type and concentration, followed by botanical source, geographical and entomological origin, and climatic conditions [210, 211].

There is a high number of assays available to assess phenolic content and AOA within plant extracts and pure compounds. No official method for AOA determination has been proposed so far and none of the techniques employed are perfect, each of them estimating a different group of antioxidants. Different results can be obtained when using different methods as oxidation is a complex process occurring in several stages *in vivo* and AOA can be estimated by different mechanisms. For example, some methods investigate the electron or hydrogen transfer reaction, and others evaluate the ability to suppress the development of ROS or the chelation of metal ions. Several laboratory assays have been developed and are often conducted on the same sample to closely study the antioxidant potential of natural products taking into consideration the complexity of *in vivo* antioxidant

action mechanisms and the complex interrelations between intrinsic and extrinsic factors present in biological matrices. The antioxidant responses can differ to different radical or oxidant sources, and in a mixed or complex system, no single assay will accurately reflect all radical sources or all antioxidants. Figure 3.2 summarizes the techniques of quantifying the bioactive molecules and AOA of the honey bee products encountered most commonly [212, 213].

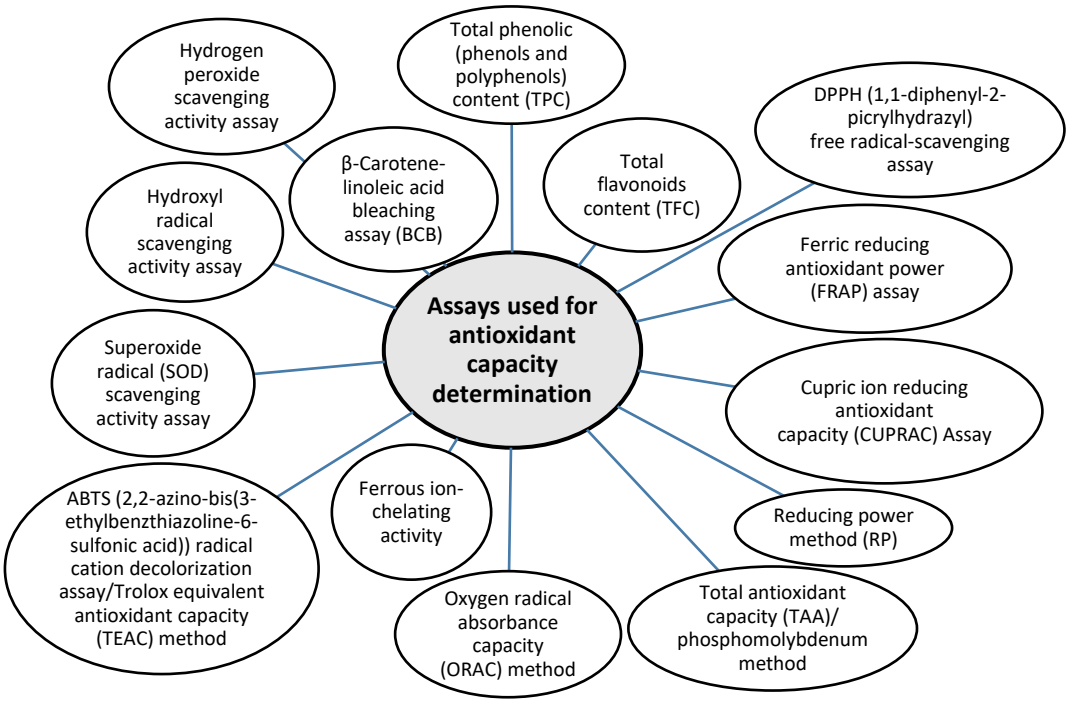

Fig. 3.2. **Methods of quantifying the bioactive molecules and AOA of the beehive products**

Plant polyphenols can act as hydrogen atom donators, reducing agents, transition-metal ion chelators, or singlet oxygen scavengers. Generally, techniques can be divided into single electron transfer (SET) and hydrogen atom transfer (HAT) methods according to the reaction mechanisms. SET methods discover the ability of an antioxidant compound to transfer an electron to reduce a substance, including carbonyls, radicals, and metals. In SET methods relative reactivity is based primarily on deprotonation and the ionization potential of the reactive functional group, consequently SET reactions are Ph-dependent. Among others, SET techniques include total phenolic content (TPC) quantification, the ferric reducing/antioxidant power (FRAP) assay, and the DPPH$^{\bullet}$ free-radical scavenging assay. HAT techniques evaluate the potential of an antioxidant to quench free radicals by hydrogen donation. HAT reactions are pH-independent, solvent, and usually rapid. HAT assays are

complicated by the presence of reducing agents, including metals, which can lead to erroneously high apparent reactivity [214]. These techniques include ORAC and β-carotene bleaching assays. For example, other methods reflect the scavenging potential of different radicals, such as hydroxyl, superoxide, or hydrogen peroxide radicals [215, 216, 217].

The results are often expressed as equivalents, calculated with the aid of calibration curves using standard antioxidant compounds, such as gallic acid (GAE) for the TPC assay; catechin (CAE), quercetin (QE), and rutin (RE) for TFC assessment; Trolox (6-hydroxy-2,5,7,8- tetramethylchroman-2-carboxylic acid, TE), a water-soluble analog of vitamin E, and ascorbic acid (AAE) for ABTS, ORAC, DPPH, and CUPRAC assays.

AOA can be expressed as a percentage of radical scavenging activity (RSA) %, calculated as follows: RSA(%) = [(B−A/B)] × 100, where B means "before" absorbance and refers to absorbance from the reagents only without the sample (blank), and A means "after" absorbance, which refers to the absorbance of the sample following the reaction.

There is another way to express the results involving the extract concentration providing 50% of radical scavenging activity (e.g., the concentration of honey sample needed to scavenge 50% of $DPPH^{\bullet}$, $ABTS^{\bullet+}$), defined as IC_{50}. The lower the IC_{50} value, the higher the scavenging capacity of the sample, since a less amount of radical scavenger is needed to reduce $DPPH^{\bullet}$ or $ABTS^{\bullet+}$.

3.4. The antioxidative system of *Apis mellifera*

Global climate change is a significant problem, the effects of which are being felt in every corner of the planet. The calendar dates for the end of winter, the melting of ice, the flowering, and the vegetation of plants change noticeably. The excessive use of pesticides, uneven distribution of rainfall, and early spring led to a rapid decline in the population of bees around the world.

Winter is quite a risky season for honey bee colonies. Long-lasting winter can lead to food reserve exhaustion, while a high density of often-weakened bee populations facilitates disease. The high mortality of honey bee colonies, explained largely by synergistic interactions between a high density of weakened *Apis mellifera* bees and parasitic mites (*Varroa destructor*), has become a critical issue for agriculture and the maintenance of natural biodiversity. Due to these, many countries encounter extended losses in bee colonies following winter [218].

It is known from literature sources that a short period of sub-optimal temperature (25°C) causes increases by about 40% of the mortality of honey bee brood reared *in vitro* [219].

The transcript levels of Cytochrome C, an electron carrier in mitochondria, are elevated in cold-stressed honey bee broods, suggesting an increase in the metabolic rate (MR). Cold-stressed broods were also shown to experience high MR. Higher MR levels have been associated with greater ROS production and have been suggested to be a physiological cost of compensatory growth following the cold stress period. Hence, keeping the MR level high may represent an imbalance of ROS and an increase in antioxidant responses in cold-stressed honey bee larvae.

The estimation of antioxidative capability for the honey bee *Apismellifera* became more simple after sequencing their genome. Corona and Robinson (2006) showed at least 39 genes coding for antioxidative proteins on this basis.

Superoxide dismutase (SOD), catalase (CAT), and peroxidases (POX) are the most significant antioxidative enzymes in the honeybee body. Genes coding for two important antioxidative enzymes, glutathione peroxidase, and glutathione reductase have been lost by insects. Their functions are performed by very active thioredoxin peroxidase and thioredoxin reductase. Glutathione S-transferases (GST) also function with peroxidase activity in insects [220].

The insect antioxidant system is also composed of such non-enzymatic components as glutathione, ascorbic acid, vitamin E, uric acid, and thioredoxin, besides antioxidant enzymes. Being universal, they can have interchangeable protective functions. A glutathione-ascorbic acid redox cycle is active in insects, as in plants. This cycle provides efficient scavenging of hydrogen peroxide produced in enzymatic reactions. Vitamin C has been confirmed to take part in proline and tyrosine hydroxylation in insects. It is sometimes recommended for honey bee artificial diets based on the lack of vitamin C demand estimation. The whole number of these antioxidants that are present in a particular biological matrix may be evaluated by measuring the total antioxidant status (TAS) [221].

Total antioxidant capacity (TAC) may be used as an alternative assessment of the entire antioxidative status. The antioxidant assay is based on the ferryl myoglobin radical derived from myoglobin and hydrogen peroxide, which oxidizes ABTS to form the radical cation $ABTS^{\bullet+}$, which is a soluble green chromogen that can be estimated spectrophotometrically. Sample antioxidants inhibit the development of this radical cation in a concentration-dependent mode. Lately, TAC has been successfully employed to quantify antioxidant levels of honeybee intact-body

extracts following dietary supplementation with vitamin C and parasitization with *Varroa destructor* (Farjan et al. 2014).

TAC quantitative measurements seem to be a good indicator for the evaluation of the changes in the oxidation status of the honeybee body. The antioxidant levels and antioxidative enzyme activity, which protect cells from the damage provoked by oxidation, are essential factors ensuring the good health of *Apis mellifera*.

Many diseases including parasitosis are the basis or result of oxidative stress. In honeybees, the symptoms of oxidative stress have been observed in drone prepupae parasitized with *Varroa destructor*. *Varroa destructor* (Acari: Varroidae) is a hematophagous mite and one of the most noxious pests of honeybees. The disease provoked by varroa mite – varrosis –reduces beekeeping productivity considerably. Mites parasitize capped brood and adult bees at all stages of their life. The infestation hurts bee immunity and longevity. The symptoms observed during varrosis are as follows: body weight reduction, fertility decrease, negative changes in the immune system, and deformations of wings and limbs. Dangerous bacterial, viral, and fungal infections often accompany Varrosis.

Untreated varrosis results in the collapse of the whole colony within 3–4 years in most cases. Conventional acaricides appear to be less and less effective since the parasite has developed resistance to them. These compounds also prejudice the quality of bee products and their safety for consumers. Hence, the search for efficient and safe methods of controlling varrosis is crucial. The protective forces of an organism can be supported by the prevention methods facilitating the effects of oxidative stress. The administration of exogenous compounds with antioxidative characteristics may become one of these methods. In this regard, we have developed a method for stimulating the status of the general hemolymph antioxidant activity of *Apis mellifera* bees and their larvae with the help of such new synthetic coordination compounds as $Na_2[Mo_2O_4EDTA]\cdot 5H_2O$, $Li_2[Mo_2O_4EDTA]\cdot 5H_2O$, and $[Co(C_4H_9N_3S)_3](NO_3)_3$. The results of our studies show that supplementation of the honey bee diet with the tested coordination compounds increases the efficiency of their antioxidative system, and the tested compounds also exhibit acaricidal properties.

4. Experimental

The studies of this work were implemented in the Research Laboratory of Advanced Materials in Biopharmaceutics and Technics of the Moldova State

University, Biological Invasions Research Center, Laboratory of Systematics and Molecular Phylogeny, Institute of Zoology, and the Research Biochemical Laboratory of the Nicolai Testemitanu State University of Medicine and Pharmacy.

4.1. Characteristics of research objects

One thousand two hundred and seventeen (1217) tested compounds (hydrazones, isothiocyanates, thioureas, triazoles, chalcones, thiosemicarbazides, thiosemicarbazones, Zn(II), Ni(II), Co(III), Fe(III), Mn(II), Cr(III), Mo(VI), and Mo(V) coordination compounds) were synthesized based on known methods and their modifications.

The Ligands were characterized by NMR (^{1}H and ^{13}C) spectroscopy. The complexes were characterized by electronic, FT-IR, and EPR spectroscopy, molar conductivity, magnetic susceptibility measurements, and elemental analysis of *C, H, N,* and *S*. In addition, the crystal structure of complexes was determined by single-crystal X-ray diffraction analysis. Melting points, IR, and NMR spectra of the tested compounds correspond to the literature data

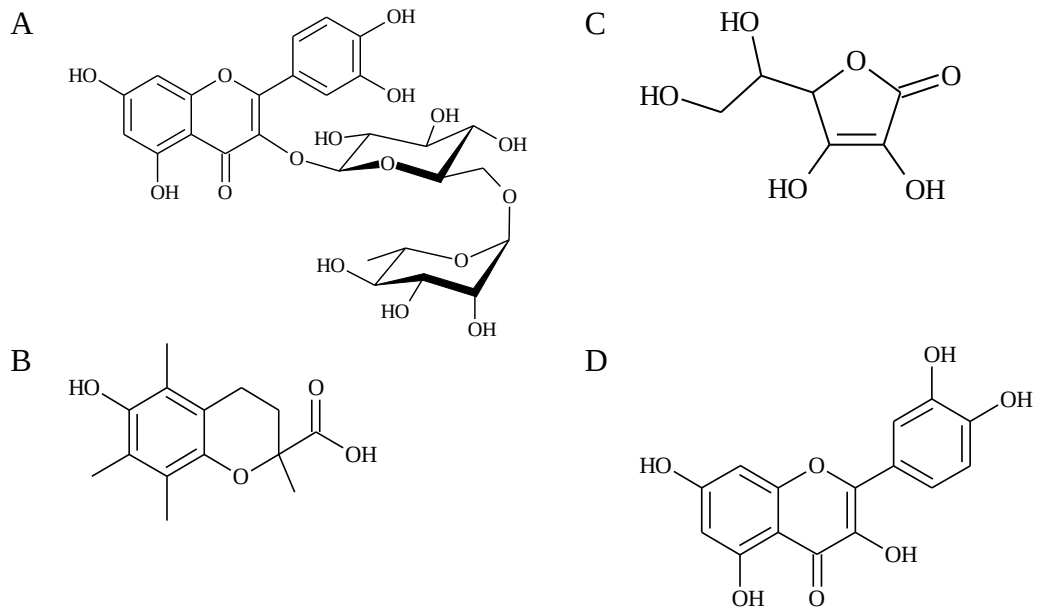

Fig. 4.1. **Structural formula of the reference compounds: A – Trolox; B – Rutin; C – Vitamin C; D – Quercetin**

The tested compounds and the reference controls were each dissolved in dimethylsulfoxide (DMSO) to create 10 mM stock solutions that were stored at a

prescribed temperature of 7°C. The stock solutions were further diluted with culture medium or DMSO to obtain 1, 10, 100, and 1000 μM solutions used for biological testing. The maximum final concentration of DMSO (<0.1%) did not induce toxicity on the test objects.

The biological activities of the tested compounds were compared with the used in biological or biochemical applications antioxidants such as Trolox (6-Hydroxy-2,5,7,8-tetramethylchroman-2-carboxylic acid), Rutin (2-(3,4-dihydroxyphenyl)-5,7-dihydroxy-3-[α-L-rhamnopyranosyl-(1→6)-β-D-glucopyranosyloxy]-4*H*-chromen-4-one), Vitamin C (lat: *Acidum ascorbinicum*) and Quercetin (2-(3,4-Dihydroxyphenyl)-5,7-dihydroxy-4*H*-1-benzopyran-4-one) (Figure 4.1 A, B, C, D).

4.2. $ABTS^{\bullet+}$ radical cation scavenging method

The antioxidant activity by the $ABTS^{\bullet+}$ method was assessed according to the method described by Re et al. with modifications. An $ABTS^{\bullet+}$ assay is an excellent tool for determining the antioxidant activity of hydrogen-donating antioxidants and chain-breaking antioxidants.

The $ABTS^{\bullet+}$ radical was formed through the reaction of ABTS (2,2'-azino-bis(3-ethylbenzothiazoline-6-sulphonic acid)) (Sigma) solution 7 mM with potassium persulfate ($K_2S_2O_8$) (Sigma) solution 2.45 mM, incubated at 25°C in the dark for 12-20 h at room temperature. The resulting solution was further diluted by mixing with acetate-buffered saline (0.02 M, pH 6,5) to obtain an absorbance of 0.70 ± 0.01 units at 734 nm.

Were prepared dilutions of the tested compounds in DMSO at concentrations ranging from 1 to 100 μM. After that, 20 μl of each tested compound's dilution was transferred to a 96-well microtiter plate and 180 μl of working solution of $ABTS^{\bullet+}$ was dispensed with the dispense module of the hybrid reader (BioTek). The decrease in absorbance at 734 nm was measured exactly after 30 min of incubation at 25°C. All the determination was made in triplicate. DMSO was used as a negative control. Blank samples were run by solvent without $ABTS^{\bullet+}$.

The measurement was made by a hybrid reader (Synergy H1, BioTek). All tests were performed in triplicate and the obtained results were averaged. The percent of inhibition (I %) of free radical cation production of ABTS was calculated by using the following equation:

$$I\ (\%)\ = \frac{Abs_{734\ nm_0} - Abs_{734\ nm_1}}{Abs_{734\ nm_0}} \times 100\ \ \text{, where} \qquad (4.1)$$

$Abs_{734\ nm0}$ is the absorbance of the control solution;

Abs $_{734\ nm1}$ is the absorbance in the presence of sample solutions or standards for positive controls.

4.3. Procedure for stimulating the total antioxidant status of the hemolymph of *Apis mellifera* bees and larvae, as well as bee products using biologically active substances

The essence of the process consists in adding a biologically active substance to 50% sugar syrup for feeding colonies of *Apis mellifera* bees in late winter or early spring. The bees are fed in the amount of 120 mL of the mixture placed on a bee frame every two days, for two weeks.

The result obtained is because, after the first collection of honey, the biological material is sampled from 10 groups in a triplet for the additional study of the total antioxidant status by $ABTS^{\bullet+}$ or $DPPH^{\bullet}$ radical cation scavenging assays.

Before starting the AOA antioxidant analysis, the samples are centrifuged for 5 minutes at 2000 r/min, then the supernatant is removed with a dispenser without disturbing the precipitate. $ABTS^{\bullet+}$ free radicals must be added in 95% ethanol to avoid precipitation after the addition of test samples. Working free radical solutions are added in 180 μL per 96-well plates.

4.4. $DPPH^{\bullet}$ radical scavenging method

The DPPH assay was done according to the method of Brand-Williams et al. with some modifications. The effect of antioxidants on $DPPH^{\bullet}$ radical scavenging is due to the hydrogen-donating ability or radical scavenging activity of the samples. The scavenging reaction between (DPPH) and an antioxidant (H-D) can be written as: (DPPH) + (H-D) → DPPH-H + (D). The DPPH reagent was diluted with a methanolic solution to give an absorbance of 0.7 ± 0.01 at 517 nm.

Were prepared dilutions of the tested compounds in DMSO at concentrations ranging from 1 to 100 μM. After that, 20 μl of each tested compounds dilution was transferred in a 96 wells microtitre plate, and 180 μl of $DPPH^{\bullet}$ (1,1-diphenyl-2-picrylhydrazyl) reagent 0.002% w/v (Sigma) with a methanolic solution was dispensed with dispense module of the hybrid reader (Synergy H1, BioTek), shake 10 s. The decrease in absorbance at 515 nm was measured exactly after 30 min of incubation at 25°C (Hybrid reader, Synergy H1, BioTek).

All the determination was made in triplicate. DMSO was used as a negative control. Blank samples were run by solvent without $DPPH^{\bullet}$ radical. The measurement was made by a hybrid reader (Synergy H1, BioTek). All tests were performed in triplicate and the obtained results were averaged. The percent of

inhibition (I %) of free radical production of DPPH was calculated by using the following equation:

$$I\ (\%)\ = \frac{Abs_{517\ nm_0} - Abs_{517\ nm_1}}{Abs_{517\ nm_0}} \times 100\ \ \text{, where} \qquad (4.2)$$

Abs $_{517\ nm\ 0}$ is the absorbance of the control solution;
Abs $_{517\ nm\ 1}$ is the absorbance in the presence of sample solutions or standards for positive controls.

4.5. Oxygen radical absorbance capacity (ORAC-Fluorescein) method

The Oxygen Radical Absorbance Capacity (ORAC) assay is a sensitive method based on the detection of chemical damage to fluorescein through the decrease in its fluorescence emission by peroxyl radicals that are generated in situ by the thermal decomposition of the free radical initiator 2,2′-azobis(2-methylpropionamidine) dihydrochloride (AAPH). The ORAC procedure used an automated plate reader (Synergy H1, BioTek, USA) with 96-well plates (Prior et al). The ORAC assay is unique in that its reactive oxygen species (ROS) generator, AAPH produces a peroxyl free radical upon thermal decomposition that is commonly found in the body, making the reaction biologically relevant. Furthermore, since AAPH is reactive with both water and lipid-soluble substances it can be used to measure the total antioxidant potential. The radicals can oxidize fluorescein to generate a product without fluorescence [222].

The automated ORAC assay was performed on a microplate reader with fluorescence filters FP (485 nm / 528 nm). The experiment was conducted at 37^0 C under pH 7.4 conditions with a blank sample in parallel. The tested compounds were prepared in DMSO for use as a stock solution. Trolox (2 mM methanolic stock solution) was used as a reference at dilution concentrations ranging from 3,125 to 100 μM in phosphate-buffered saline (PBS, sigma) (pH 7.4). A blank was used phosphate buffer instead of the antioxidant solution.

The reaction was carried out in phosphate-buffered saline (PBS) (10 mM, pH 7.4) and the final reaction mixture was 200μl. 25 μl of each tested compounds dilution were transferred in a 96-well black microtitre plate (Nunc black microwell, Denmark) and 150 μl of working solution of fluorescein disodium (3’,6’-dihydroxy-spiro[isobenzofuran-1[3H], 9’[9H]-xanthen]-3-one) (sigma) (15 nM final concentration) were dispensed with dispense module of the hybrid reader (Synergy H1, BioTek). The mixture was preincubated for 30 min at 37°C before shaking at 700 rpm (Shaker-thermostat, Sky Line, Elmi ST-3L). After that, 25 μl AAPH (2,2’-

Azobis (2-methylpropionamidine) dihydrochloride) (Sigma) solution (240 mM final concentration) was dispensed with the dispense module of the hybrid reader (Synergy H1, BioTek). The plate was immediately placed in the hybrid reader (Synergy H1, BioTek) and the fluorescence was recorded every minute for 100 min. The black microtitre plate was automatically agitated prior to each reading.

The antioxidant capacity, expressed as the area under the curve (AUC), was calculated by a statistical program following the formula:

$$AUC = 1 + \frac{RFU_1}{RFU_0} + \frac{RFU_2}{RFU_0} + \frac{RFU_3}{RFU_0} + \ldots + \frac{RFU_n}{RFU_0} \text{ , where} \qquad (4.3)$$

RFU_0 is the relative fluorescence units at time point zero;
RFU_n is the relative fluorescence units at time points.
The Net AUC was calculated by subtracting the blank AUC from the AUC of each sample, the standards, and the positive control:

$$Net\ AUC = AUC\ (sample) - AUC(blank) \qquad (4.4)$$

The correlation coefficient (R^2) was obtained using a least means squared linear regression analysis.
The slope (m) was calculated as follows:

$$Slope\ (m) = \frac{dy}{dx} \qquad (4.5)$$

To determine Trolox equivalents (TE) of each sample range the ratio of the slope (m) of the linear regression analysis of the compound to the slope of the linear regression of Trolox was used:

$$TE = \frac{m_{(compound)}}{m_{(trolox)}} \qquad (4.6)$$

4.6. Lipoxygenase (LOX) assay

Lipoxygenases (LOXs) comprise a class of non-heme iron-containing dioxygenases that stereospecifically insert molecular oxygen into cis-cis-1,4-pentadiene-containing polyunsaturated fatty acids. Among the six identified functional LOX gene isoforms in humans, 5-lipoxygenase (5-LOX), platelet 12-lipoxygenase (p 12-LOX), and 15-lipoxygenase (15-LOX) were originally discovered in leukocytes, platelets, and reticulocytes, respectively. Linoleic or arachidonic, the substrate of LOXs, is an essential constituent of cellular membranes that are released by tightly regulated phospholipase cleavage.

The LOX method system is widely employed to determine the antioxidant activity of the tested compounds. In the LOX assay, LOX-derived lipid

hydroperoxides oxidize the ferrous ion (Fe^{2+}) to the ferric ion (Fe^{3+}), the latter of which binds with thiocyanate $[SCN]^-$ to generate a red ferrothiocyanate (FTC) complex [223].

LOX method was carried out with some modifications. LOX colorimetric assay was performed in 96-well flat-bottom plates with a total assay volume of 210 µl.

Various concentrations of the tested compounds, DOXO as well as the positive assay control Quercetin were premixed with soybean lipoxidase 500-1000 U/mL in Tris–HCl buffer (50 mM, pH 7.5) and were incubated for 5 min at room temperature with shaking at 1000 rpm (Shaker-thermostat, Sky Line, Elmi ST-3L). Then, a solution of 2 mM linoleic acid in MeOH was dispensed with the dispense module of the hybrid reader (Synergy H1, BioTek) to induce the enzymatic reaction. After 6 min of incubation at room temperature, the enzymatic reaction was stopped by adding 100 µl of ferrithiocyanate complex (FTC; chromogen) with a dispensing module (MultiFlo, Biotek). The FTC was prepared *ex tempore* by mixing the equivalent volumes of 4.5 mM $FeSO_4$ in 0.2 M HCl with 3% NH_4SCN methanolic solution.

The absorbance at 500 nm was measured, using a hybrid reader (Synergy H1, BioTek). The percentage inhibition was calculated according to the formula:

$$\%\ inhibition = \frac{Abs_{500\ nm_0} - Abs_{500\ nm_1}}{AAbs_{500\ nm_0}} \times 100 \quad , where \qquad (4.7)$$

$Abs_{500\ nm0}$ is the absorbance of the control (100% activity LOX)
$Abs_{500\ nm1}$ is the absorbance of the sample.

4.7. *In vitro* toxic red blood cells (RBCs) hemolysis assay

To determine the resistance of red blood cells to oxidative stress (hemolysis) was used human blood (cod.140080991). The hemolytic activity was carried out by the detection of hemoglobin release from erythrocytes in response to various concentrations of the tested compounds and DOXO. Human venous blood was incubated at room temperature with gentle shaking at 500 rpm for 30 min. Then, the samples were centrifuged at 1000 rpm for 10 min. The hemoglobin absorbance of the supernatant was measured at 540 nm. For negative (0% lysis) and positive (100% lysis) controls, isotonic solution (0.9%) and hypotonic solution (0.1%) of NaCl were used, respectively. The absorbance value of the positive should be 0.8 ± 0.3, while the negative one should be less than 0.03. The hemolytic rates of the compounds were calculated as the following equation:

$$Hemolytic\ rate\ \ (\%) = \frac{A_t}{A_c} \times 100, where \qquad (4.8)$$

A_t is the absorbance value of the tested compound;
A_c is the absorbance value of the positive control.

4.8. *In vitro* formation of methemoglobin (metHb) in intact erythrocytes assay

The assay was performed as described with minor modifications. Briefly, human venous blood (cod.140080991). The blood sample's methemoglobin concentration was measured using the method below, which is based on that of Evelyn and Malloy.

The serum was removed after centrifugation at 1000g for 5 min, and the red blood cells (RBCs) were washed in cold phosphate-buffered saline (PBS) at 1000g for 5 min. The washed erythrocytes were diluted in physiological saline (1:1) with various concentration of the tested compound as well as DOXO were incubated at 37^0C with gentle shaking at 500 rpm for 3 h.

After that, a solution of 2% digitonin ($C_{56}H_{92}O_{29}$) was used to induce hemolysis. The measurement was made by a hybrid reader (BioTek), in absorbance at 540 and 630 nm. Then, the hemolysate was divided into two parts. The absorbance of the first part was read at 630 nm and then read again at 630 nm after the addition of 2% potassium cyanide (KCN), to convert the metHb into cyanmethemoglobin. Change in the intensity of light absorption after the addition of potassium cyanide is directly proportional to the concentration metHb.

Finally, 10 μL of 2% potassium ferricyanide ($K_3Fe(CN)_6$) (causes translation of remaining oxyhemoglobin to methemoglobin) was applied and the absorbance was measured at 540 nm. The measurement was obtained by a plate reader (BioTek) at 540/630 nm.

The ability to induce MetHb formatted in human RBCs was calculated using the following equation:

$$MetHb\ (mM)\ = \frac{A_1 - A_2}{4.3 - 0.71}, where \qquad (4.9)$$

A_1 – the maximum absorbance value of MetHb at 630 nm (pH 6.8);
A_2 - the absorbance value of the test sample at 630 nm, where cyanmethemoglobin is directly proportional to the concentration MetHb
4.30 - millimolar absorbance coefficient of MetHb at 630 nm (pH 6.8)
0.71 - millimolar absorbance coefficient of cyanmethemoglobin at 630 nm (pH 6.8).

The Hb (mM) was calculated by the equation:

$$Hb\ (mM) = \frac{A_t}{11} \times 100, where \quad (4.10)$$

A_t - absorbance value of test sample at 540 nm;
11- millimolar absorbance coefficient of cyanmethemoglobin at 540 nm.

The MetHb (percentage total Hb) was calculated by the equation:

$$Total\ Hb\ (\%) = \frac{MetHb}{Hb} \times 100 \quad (4.11)$$

4.9. Acute Toxicity Assay against *Daphnia magna*

The general toxicity of the analyzed compounds was evaluated using *Daphnia magna* (Straus, 1820). *Daphnia magna* originated from a culture maintained parthenogenetically at the Institute of Zoology, Center of Research of Biological Invasions. The tested organisms *Daphnia magna* were fed with *Chlorella vulgaris.* These unicellular algae were grown using aseptic technology to exclude contamination of the culture by bacteria, algae, or protozoa. Chlorella vulgaris were cultivated in Prat's growth medium containing KNO_3 (1μM), $MgSO_4 \cdot 7H_2O$ (40μM), $K_2HPO_4 \cdot 3H_2O$ (400μM), $FeCl_3 \cdot 6H_2O$ (3.6μM) in H_2O distilled (adjusted the pH to7.0, autoclaved and stored at 5°C) [224, 225, 226].

D. magna was maintained in aerated aqueous straw infusion growth media supplemented with $CaCl_2$ (11.76g/L), NaHCO3 (2.59g/L), KCl (0.23g/L), and $MgSO_4$, $7H_2O$ (4.93 g/L). (pH~7.5±0.2; $O_2 \geq 6.0$mg/L).

Juveniles were chosen according to their size and placed in fresh medium for 24 -48 h. *D. magna* was cultured in Costar® 24-well culture transparent sterile plates covered by a lid to avert the capacity of pollution and evaporation but to supply gaseous exchange between air and culture medium. Each well contained 10 organisms in 1000 μL final volume of each dilution of the tested compounds.

The bioassay was then repeated at the concentrations ranging from 0.1 to100μM (0.1, 1, 10, and100μM) in order to determine LC_{50} for each compound. Aqueous straw infusion growth media was used to dilute the stock solutions to the required concentrations.

The final test solutions contained up to 0.1% DMSO and had a final volume of 1 mL. 0.1% solution of DMSO in aerated medium (pH~7.5±0.2; $O_2 \geq 6.0$mg/L) was used as a negative control. The juvenile daphnids were incubated throughout the experiment at 22 ± 2^0C, using a 16h / 8h light / dark cycle (500 – 1000 lx). The mobility (viability) of the test organisms was observed after the 24-h and 48-h exposure. The experiment was performed in triplicate. The daphnids were considered

immobilized only if they did not float during the 15 s, following gentle mixing of the test and control solutions, even if they could still move their antennae. The percentage of viability (V (%)) of *Daphnia magna* was calculated according to the formula:

$$V(\%) = \frac{\text{N (sample)}}{\text{N (control)}} \times 100, \text{ where} \qquad (4.12)$$

N- number of the viability of *Daphnia magna*.

The compound's median lethal concentration (LC_{50}) values were calculated from the dose-response equation determined by the least squares fit method.

4.10. Statistical Analysis

The half-maximal inhibitory concentration (IC_{50}) was used as an indicator of the effectiveness of the inhibition of free radicals of the tested substances. The toxicity of compounds was presented in the form of the median lethal concentration values (LC_{50}) that were calculated from the dose-response equation determined by the least-squares fit method using the *GraphPad* software. All data are presented as means ± standard deviation (SD).

5. Antioxidant properties of synthetic compounds

Antioxidants are extensively studied for their capacity to protect organisms and cells from damage induced by oxidative stress. Scientists in various disciplines have become more interested in new compounds, either synthesized or obtained from natural sources that could provide active components to prevent or reduce the impact of oxidative stress on cells. There has been much less work on the systematic study of synthetic antioxidants designed to optimize the antioxidant activity, while at the same time satisfying other important criteria, including solubility, bioavailability, and lack of toxicity (or selective toxicity in the case of cancer chemopreventive antioxidants).

Synthetic antioxidants are widely used to inhibit oxidative processes. Most currently used antioxidant drugs are direct-acting antioxidants. Primary screening of direct-acting antioxidants is carried out on *in vitro* model systems, i.e. when the efficiency of their antioxidant action is determined primarily by the chemical structure of the substance and does not depend, in any way, on the general homeostasis of the body. Thiosemicarbazones, thiosemicarbazides, their derivatives, and complexes have gained attention recently for their capacity to protect organisms and cells from damage induced by oxidative stress or scavenge free radicals [227].

These compounds, which show considerable biological activity, may represent an interesting approach to designing new anticancer drugs [228].

In this regard, we have studied the biological activity of synthesized substances such as thiosemicarbazones, thiosemicarbazides, their derivatives, and complexes [229, 230, 231, 232, 233, 234, 235, 236, 237]. Many of the studied substances have significant antiproliferative, antituberculosis, antibacterial, and anti-fungal activities, which we have previously identified [238, 239, 240, 241, 242, 243, 244, 245, 246, 247].

To exclude the eventual presence of concomitant adverse effects associated with oxidative stress, the tested compounds were investigated by several antioxidant-capacity (AC) assays [248], such as ABTS, DPPH, ORAC, and LOX [249]. The antioxidant potency of the tested compounds was compared to the FDA-approved anticancer drug doxorubicin (DOXO) and the reference antioxidant controls Trolox, Rutin и Quercetin. It is known that doxorubicin-induced cardiomyopathy carries a poor prognosis and is frequently fatal. Doxorubicin induces toxic damage to the mitochondria of cardiomyocytes contributing to increased oxidative stress [250, 251].

Drug-induced hemolysis and methemoglobin formation is a relatively rare but serious toxicity liability caused by oxidative stress, so thiosemicarbazones, thiosemicarbazides, their derivatives, and complexes were performed to screen for toxic hemolysis and methemoglobin formation in human red blood cells (RBCs).

Finally, direct toxic evaluation of thiosemicarbazones, thiosemicarbazides, their derivatives, and complexes, and anticancer drug doxorubicin was studied using the *Daphnia magna* bioassay by ISO 6341: 2012, which is one of the most commonly used test-objects in laboratory research aimed at directly determining the toxicity of chemical compounds, which are used in toxicological medicine [252].

5.1. $ABTS^{\bullet+}$ radical cation scavenging activity of the tested compounds

Antioxidant activity reportedly affects various bioactivities (whitening, anti-inflammation, and high blood pressure). The ABTS assay is a widely used method for the assessment of the total antioxidant capacities of the anticancer compound *in vitro* [253].

The ABTS method is based on the measurement in the long wavelength absorption (λ max = 734 nm) of a radical cation 2,2'-azobis-(3-ethylbenzothiazoline-6-sulfonate) ($ABTS^{\bullet+}$) [254]. The free radical $ABTS^{\bullet+}$ is generated by the oxidation of ABTS, commonly using potassium persulfate (Scheme 5.1). Antioxidants inhibit the oxidation of ABTS by electron transfer radical scavenging and hydrogen

donating [255, 256] and play a critical role in stabilizing detrimental free radicals in the human body. In terms of antioxidant activity, the ability to eliminate hydroxyl radicals or superoxide radicals through a physiologic action or oxidation is evaluated, and a high index indicates strong antioxidant activity.

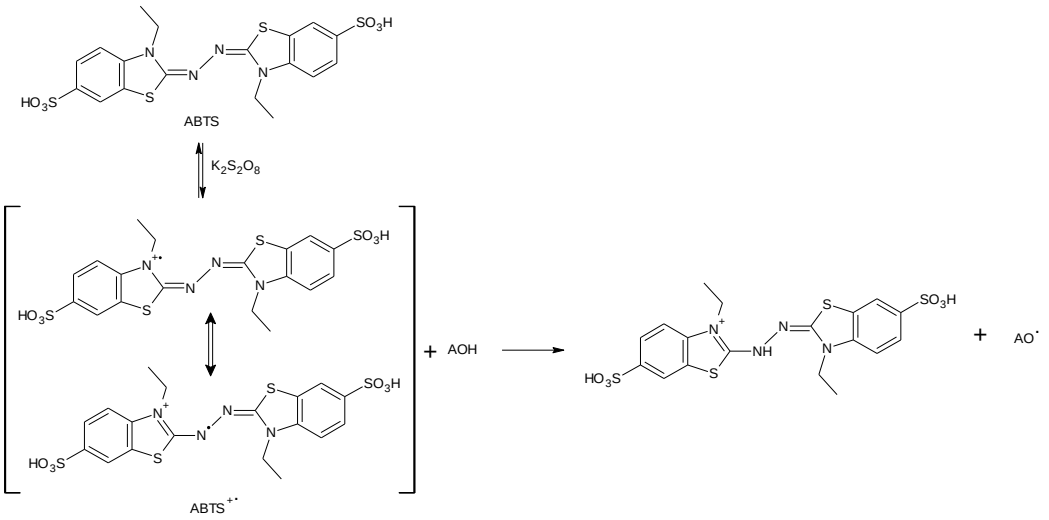

Scheme 5.1. **Oxidation of ABTS by potassium persulfate to generate radical cation $ABTS^{\bullet+}$ and its reaction with an antiradical compound (AOH)**

So, the tested compounds as well as the reference antioxidant compounds Trolox, Rutin, and the FDA-approved anticancer drug doxorubicin (DOXO) were screened for free radical scavenging activity by the $ABTS^{\bullet+}$ method.

According to this work, the tested compounds were capable of scavenging $ABTS^{\bullet+}$ radical in a concentration-dependent manner. The IC_{50} values of the tested compounds are represented in table 5.1.

Table 5.1. $ABTS^{\bullet+}$ scavenging activity of the tested compounds

№	Formula	$IC_{50} \pm SD$ (μM)
1	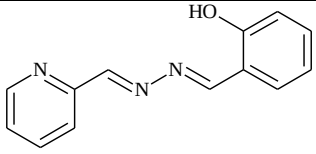	21.0 ± 0.4
2	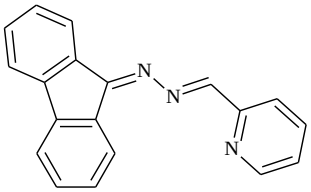	≥100

Table 5.1. Continued

№	Formula	IC_{50} (μM)
3	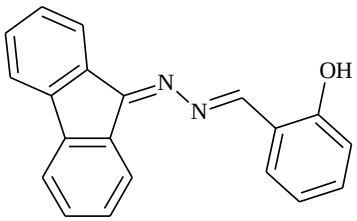	27.9 ± 0.9
4	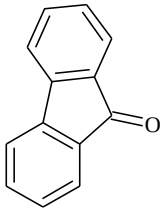	≥100
5	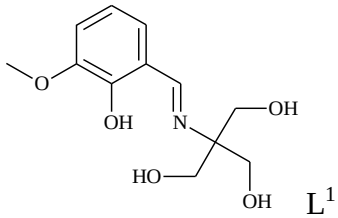 L^1	17.2 ± 0.2
6	$Cu(L^1\text{-}H)_2$	77.5 ± 2.1
7	$Ni(L^1\text{-}H)_2$	0.6 ± 0.2
8	$Co(L^1\text{-}H)_2Cl$	21.4 ± 0.3
9	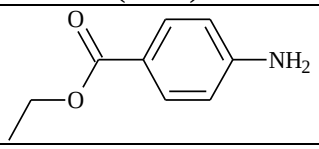	71.4 ± 2.5
10	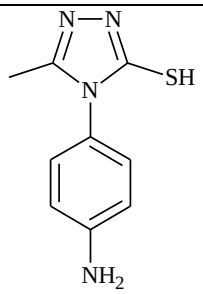	14.1 ± 0.2
11	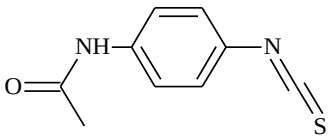	19.2 ± 1.1
12	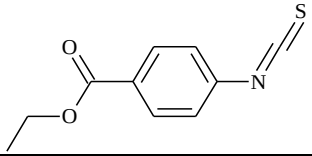	≥100

Table 5.1. Continued

№	Formula	IC_{50} (μM)
13	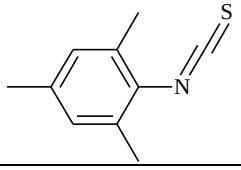	≥100
14	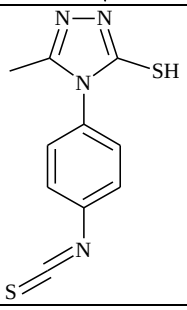	14.1 ± 0.2
15	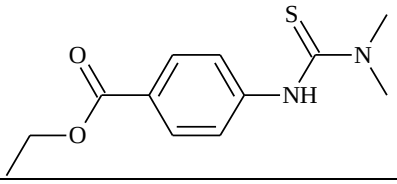	70.4 ± 1.5
16	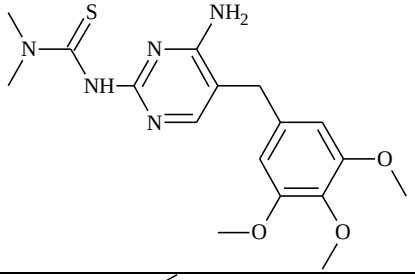	3.2 ± 0.3
17	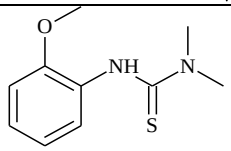	19.5 ± 0.2
18	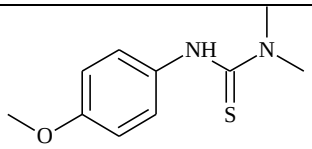	18.3 ± 1.1
19	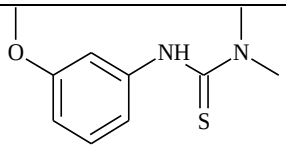	24.6 ± 0.3
20	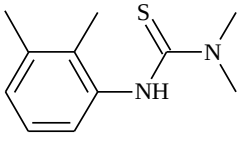	17.1 ± 0.1

Table 5.1. Continued

№	Formula	IC_{50} (μM)
21	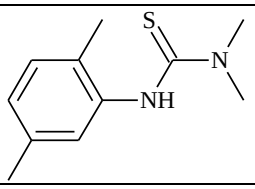	26.9 ± 0.1
22	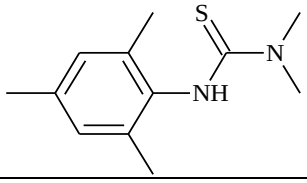	12.2 ± 0.2
23	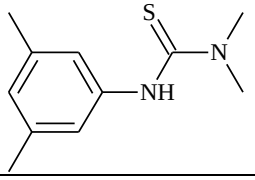	20.3 ± 0.8
24	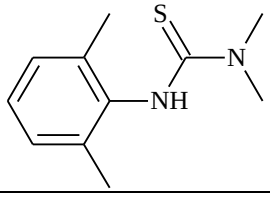	17.8 ± 0.4
25	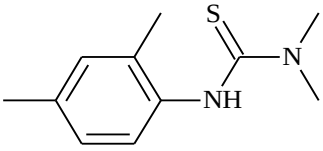	19.0 ± 0.3
26	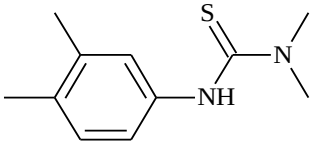	19.3 ± 1.0
27	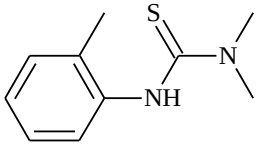	15.0 ± 0.1
28	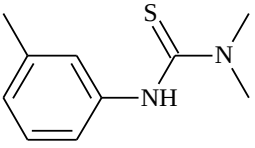	21.8 ± 0.8
29	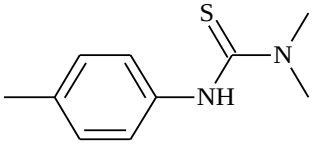	17.3 ± 0.5

Table 5.1. Continued

№	Formula	IC_{50} (μM)
30	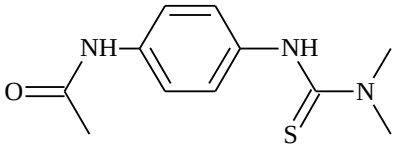	34.6 ± 0.9
31	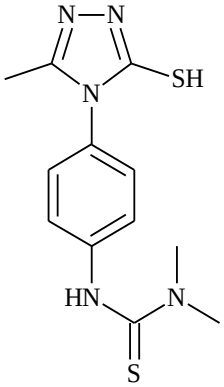	13.6 ± 0.3
32	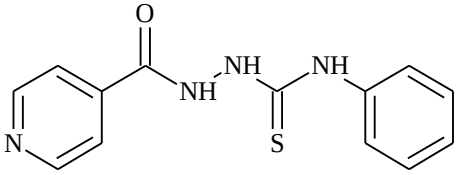	7.8 ± 0.6
33	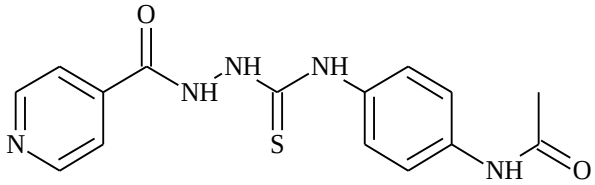	11.0 ± 0.3
34	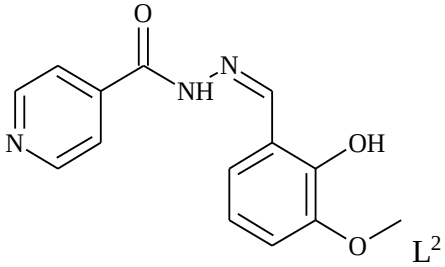	11.0 ± 0.7
35	$Cu(L^2\text{-}H)Cl$	53.6 ± 0.3
36	$Cu(L^2\text{-}2H)\cdot 2H_2O$	≥100
37	$Cu(L^2\text{-}H)Br$	≥100
38	$Ni(L^2\text{-}H)Cl\cdot 2H_2O$	33.1 ± 0.9
39	$Ni(L^2\text{-}2H)\cdot 4H_2O$	≥100
40	$Co(L^2\text{-}H)_2Cl\cdot 4H_2O$	22.4 ± 0.6
41	$Co(L^2\text{-}H)_2NO_3\cdot H_2O$	34.3 ± 0.5
42	$Co(L^2\text{-}2H)(L^2\text{-}H)\cdot H_2O$	80.6 ± 0.5

Table 5.1. Continued

№	Formula	IC_{50} (μM)
43	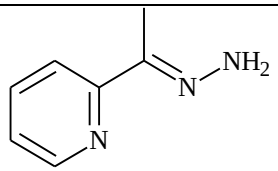	72.2 ± 1.3
44	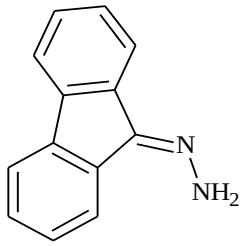	22.3 ± 0.4
45	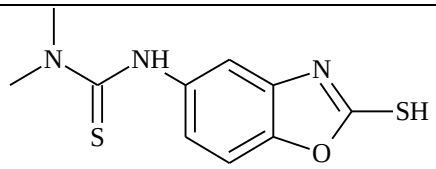	13.8 ± 0.7
46	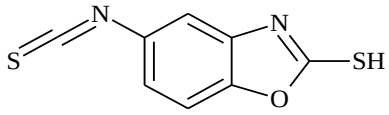	23.5 ± 0.1
47	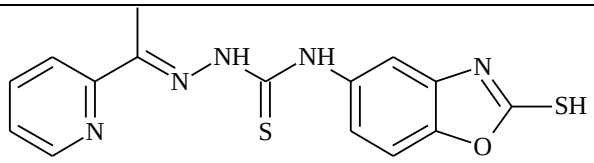	17.1 ± 0.7
48	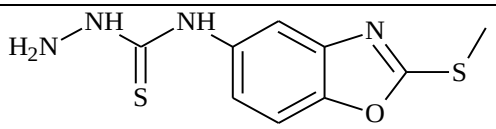	13.5 ± 0.5
49	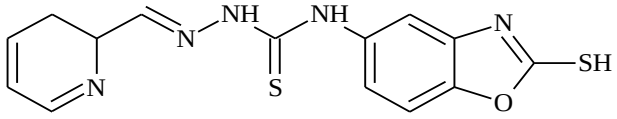	16.9 ± 0.6
50	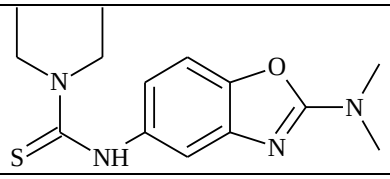	23.8 ± 0.7
51	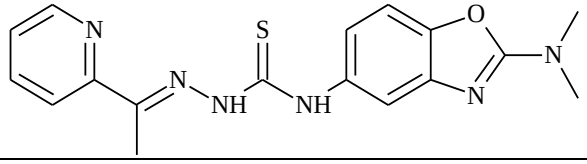	20.1 ± 0.9

Table 5.1. Continued

№	Formula	IC_{50} (μM)
52	$Cu(L^3)Cl_2$ 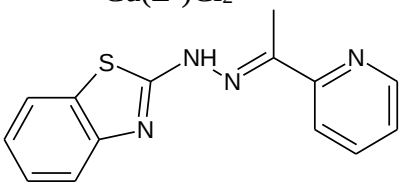 L^3 -	≥100
53	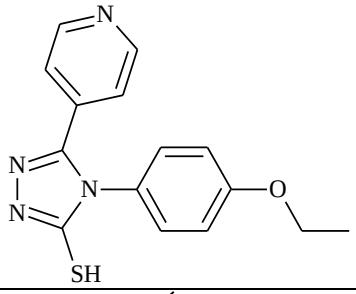	16.4 ± 0.2
54	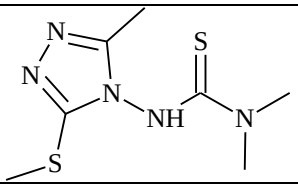	9.6 ± 0.2
55	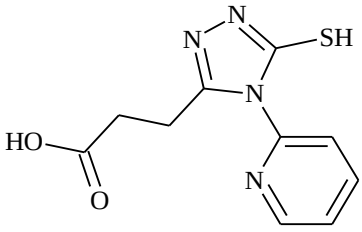	10.3 ± 0.1
56	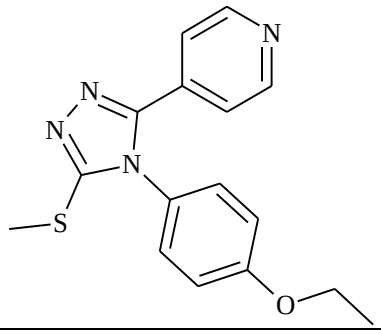	≥100
57	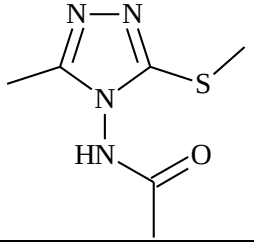	≥100

Table 5.1. Continued

№	Formula	IC_{50} (μM)
58	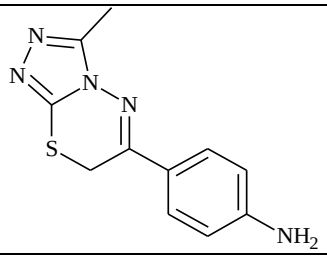	≥100
59	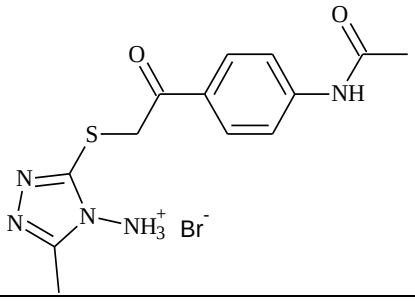	≥100
60	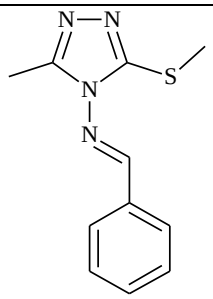	≥100
61	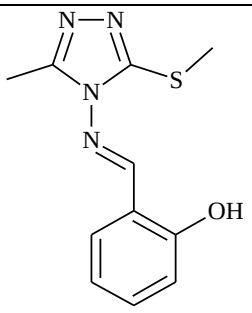	25.6 ± 0.6
62	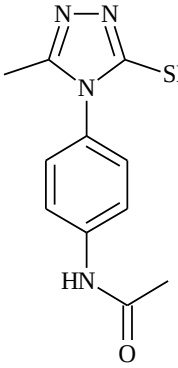	17.4 ± 0.5

Table 5.1. Continued

№	Formula	IC_{50} (μM)
63	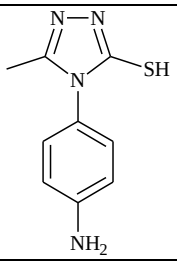	14.1 ± 0.1
64	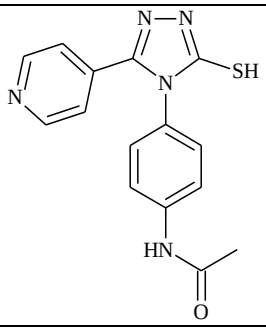	11.5 ± 0.5
65	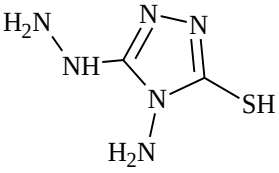	7.6 ± 0.3
66	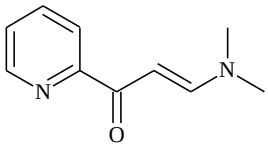	≥100
67	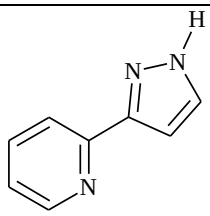	≥100
68	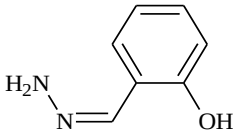	8.6 ± 0.3
69	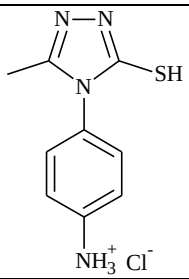	19.0 ± 0.6

Table 5.1. Continued

№	Formula	IC_{50} (μM)
70	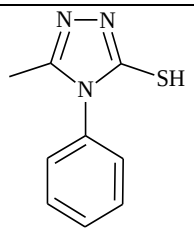	12.3 ± 0.2
71	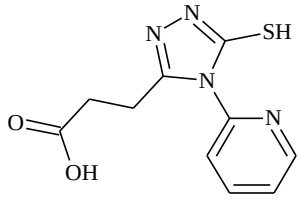	10.3 ± 0.1
72	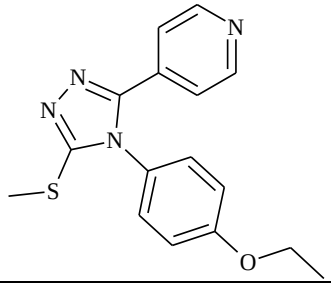	≥100
73	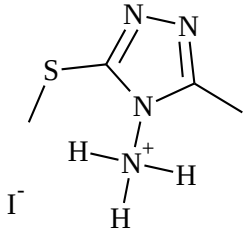	≥100
74	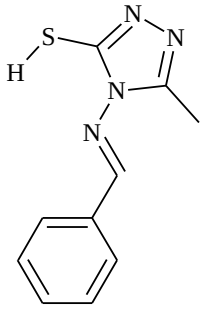	9.3 ± 0.5
75	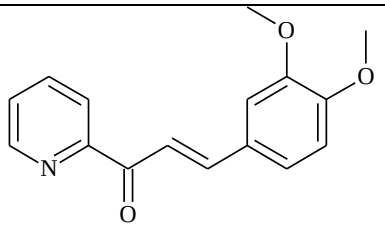	≥100

Table 5.1. Continued

№	Formula	IC_{50} (μM)
76	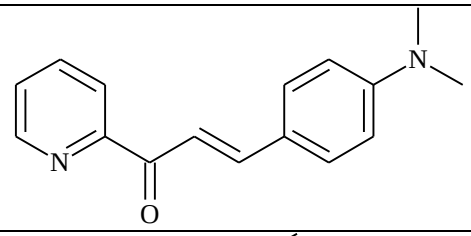	9.3 ± 0.8
77	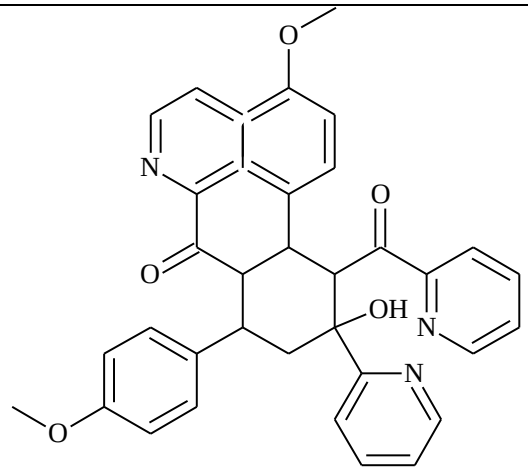	≥100
78	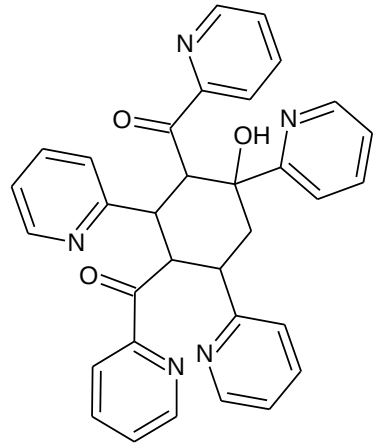	82.1 ± 1.2
79	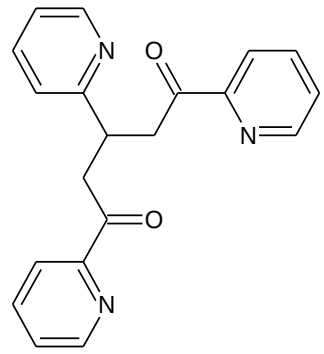	≥100

Table 5.1. Continued

№	Formula	IC_{50} (μM)
80	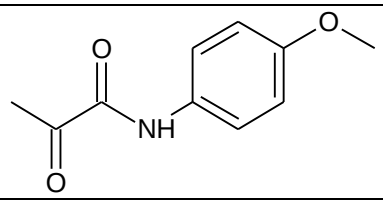	≥100
81	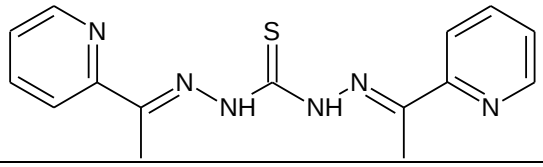	7.1 ± 0.1
82	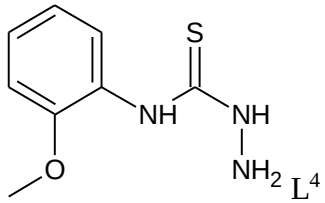 L^4	6.3 ± 0.1
83	$[Cu(L^4)_2]Br_2$	9.1 ± 0.8
84	$[Cu(L^4)_2]Cl_2$	16.1 ± 0.5
85	$[Cu(L^4)_2](NO_3)_2$	38.9 ± 0.4
86	$[Ni(L^4)_2]Cl_2$	1.7 ± 0.3
87	$Ni(L^4\text{-}H)_2$	13.4 ± 0.3
88	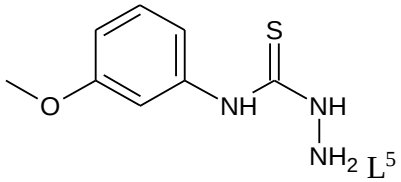 L^5	6.2 ± 0.4
89	$[Cu(L^5)_2]Br_2$	5.5 ± 0.3
90	$[Cu(L^5)_2](NO_3)_2$	14.3 ± 0.2
91	$[Cu(L^5)_2](ClO_4)_2$	21.9 ± 0.1
92	$[Ni(L^5)_2]Cl_2$	3.6 ± 0.5
93	$Cu(L^5\text{-}H)_2$	4.4 ± 0.1
94	$Ni(L^5\text{-}H)_2$	2.9 ± 0.6
95	$Co(L^5\text{-}H)_3$	3.8 ± 0.9
96	$[Co(L^5)_3]Cl_3$	12.2 ± 0.8
97	$[Co(L^5)_3]Br_3$	3.7 ± 0.2
98	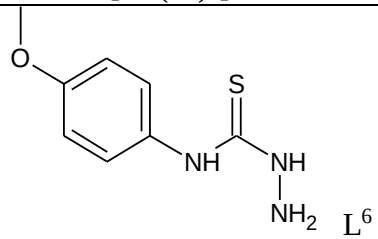 L^6	2.2 ± 0.2

Table 5.1. Continued

№	Formula	IC_{50} (μM)
99	$[Cu(L^6)_2]Cl_2$	5.9 ± 0.1
100	$[Cu(L^6)_2](NO_3)_2$	15.9 ± 0.3
101	$[Cu(L^6)_2](ClO_4)_2$	6.3 ± 0.1
102	$[Ni(L^6)_2]Cl_2$	3.7 ± 0.6
103	$Cu(L^6\text{-}H)_2$	5.1 ± 0.3
104	$Ni(L^6\text{-}H)_2$	5.8 ± 0.4
105	$Co(L^6\text{-}H)_3$	12.1 ± 0.4
106	$[Co(L^6)_3]Cl_3$	2.3 ± 0.2
107	$[Co(L^6)_3]Br_3$	2.3 ± 0.4
108	$[Co(L^6)_3](NO_3)_3$	2.7 ± 0.3
109	$[Fe(L^6)_3]Br_3$	2.1 ± 0.7
110	$[Fe(L^6)_3]Cl_3$	2.8 ± 0.3
111	$[Mn(L^6)_2]Cl_2$	≥100
112	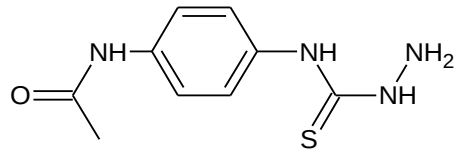	15.3 ± 0.6
113	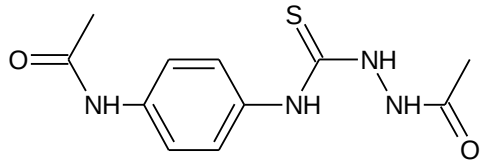	10.3 ± 0.8
114	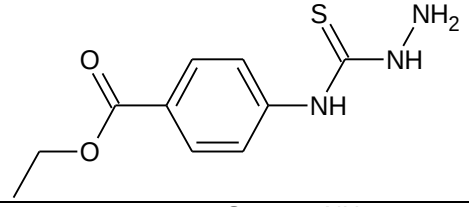	11.5 ± 0.6
115	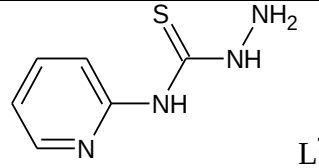 L^7	8.6 ± 0.9
116	$Cu(L^7)_2(NO_3)_2$	19.0 ± 0.2
117	$Cu(L^7)_2Cl_2$	16.1 ± 0.3
118	$Cu(L^7)_2SO_4$	18.5 ± 0.4
119	$Cu(L^7)_2(CH_3COO)_2$	19.0 ± 0.3
120	$Zn(L^7)_2Cl_2$	2.9 ± 0.1
121	$Ni(L^7)_2Cl_2$	4.8 ± 0.2
122	$Ni(L^7)_2(NO_3)_2$	5.7 ± 0.7
123	$Ni(L^7)_2SO_4$	4.8 ± 0.2
124	$Co(L^7)_2(ClO_4)_2$	≥100

Table 5.1. Continued

№	Formula	IC_{50} (μM)
125	$Co(L^7)_2Cl_2$	22.8 ± 0.2
126	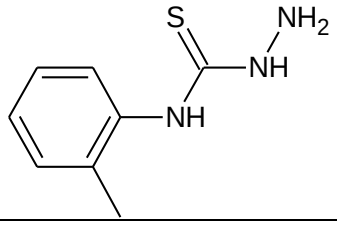	16.2 ± 0.1
127	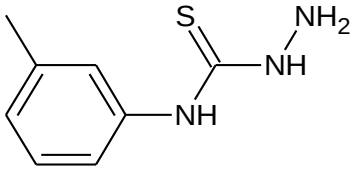	13.2 ± 0.2
128	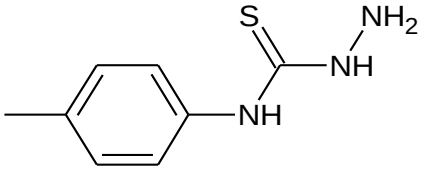	18.1 ± 0.6
129	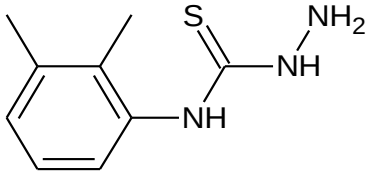	14.5 ± 0.1
130	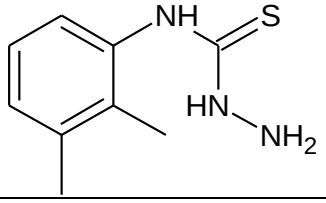	6.9 ± 0.9
131	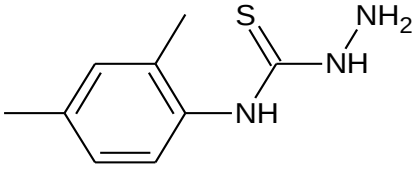	15.3 ± 0.8
132	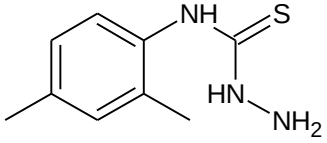	3.9 ± 0.1
133	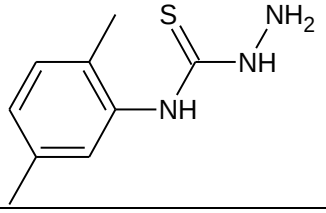	6.9 ± 0.2

Table 5.1. Continued

№	Formula	IC_{50} (μM)
134	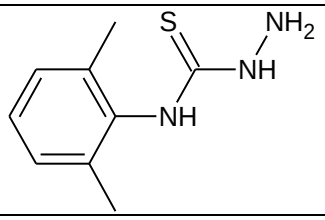	15.5 ± 0.2
135	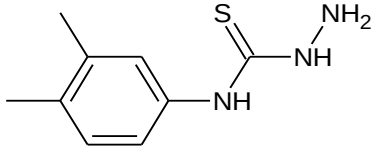	13.6 ± 0.5
136	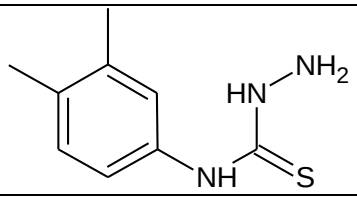	5.5 ± 0.1
137	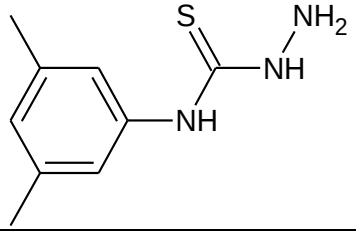	14.2 ± 0.2
138	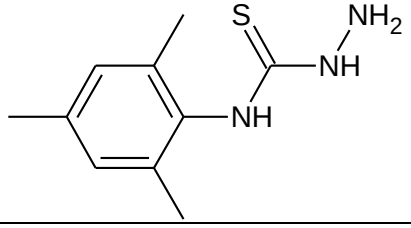	14.4 ± 1.3
139	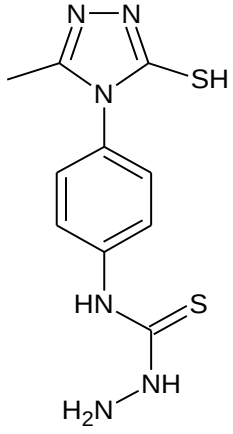	7.1 ± 0.1

Table 5.1. Continued

№	Formula	IC_{50} (μM)
140	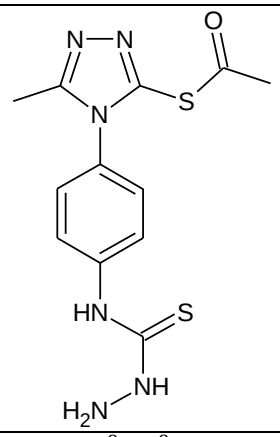	42.3 ± 0.5
141	$Cu(L^8)(L^8\text{-}H)Cl$ 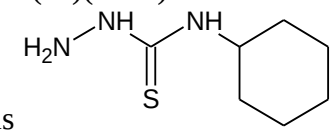 Where L^8 is	≥100
142	$Cu(L^8)(L^8\text{-}H)Br$	≥100
143	$Cu(L^8)(L^8\text{-}H)(OAc)$	16.7 ± 0.5
144	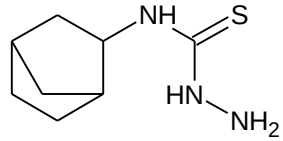	13.6 ± 0.5
145	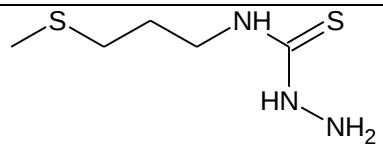	16.8 ± 0.6
146	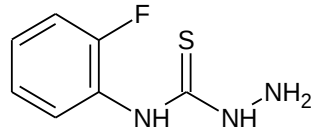	18.7 ± 0.9
147	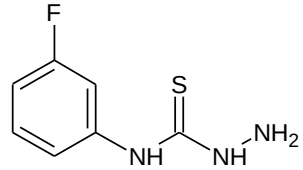	38.5 ± 0.6
148	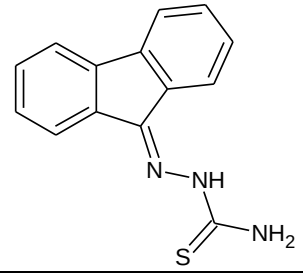	18.4 ± 0.7

Table 5.1. Continued

№	Formula	IC_{50} (μM)
149	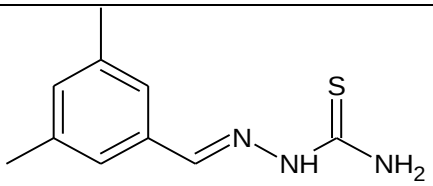	21.6 ± 0.3
150	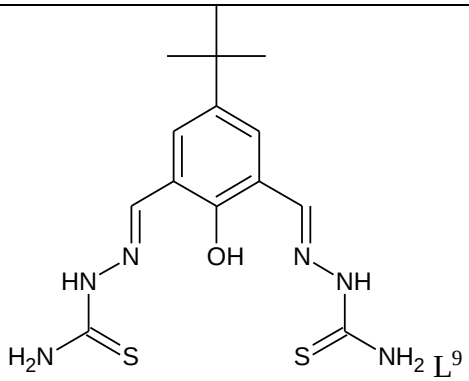 L^9	20.3 ± 1.6
151	$Cu_2(L^9\text{-}3H)Br\cdot 2H_2O\cdot 3C_2H_5OH$	≥100
152	$Cu_2(L^9\text{-}3H)Cl\cdot 4H_2O$	≥100
153	$Cu_2(L^9\text{-}3H)NO_3\cdot H_2O\cdot 2\ C_2H_5OH$	≥100
154	$Cu_2(L^9\text{-}3H)ClO_4$	≥100
155	$Cu_2(L^9\text{-}3H)(OAc)$	≥100
156	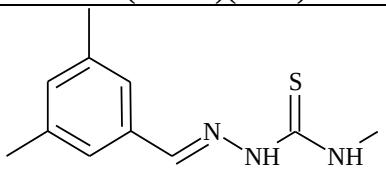	27.8 ± 0.3
157	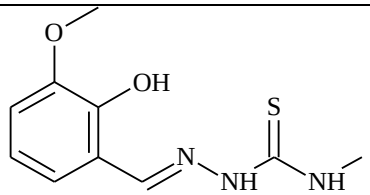	7.7 ± 0.1
158	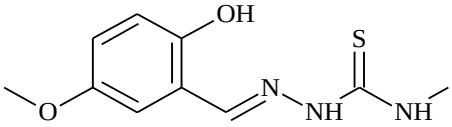	9.8 ± 0.1
159	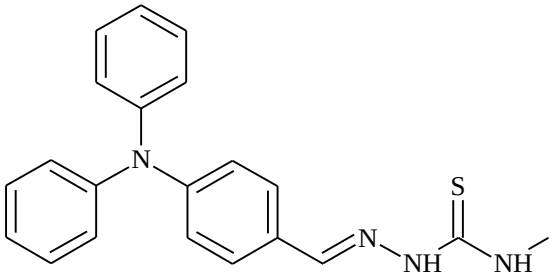	21.2 ± 0.4

Table 5.1. Continued

№	Formula	IC_{50} (μM)
160	$Cu_2(L^{10}\text{-}3H)(OAc)\cdot H_2O$ 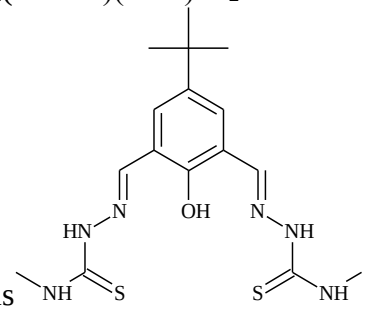 Where L^{10} is	≥100
161	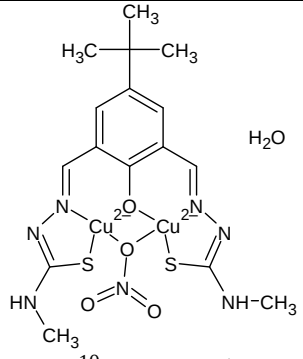 $Cu_2(L^{10}\text{-}3H)(NO_3)\cdot H_2O$	≥100
162	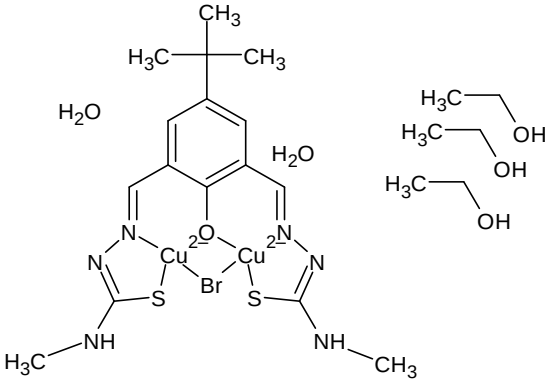 $Cu_2(L^{10}\text{-}3H)Br\cdot 2H_2O\cdot 3C_2H_5OH$	≥100
163	$Cu_2(L^{10}\text{-}3H)Cl\cdot 4H_2O$	≥100
164	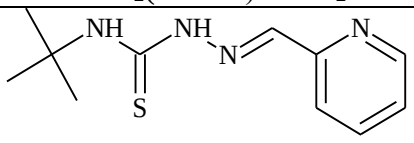 L^{11}	18.5 ± 0.2
165	$Ni(L^{11}\text{-}H)Cl$	11.6 ± 0.3
166	$Ni(L^{11}\text{-}H)_2$	2.9 ± 0.1
167	$Ni(L^{11}\text{-}H)Br$	12.2 ± 0.2
168	$Co(L^{11}\text{-}H)_2(OAc)$	≥100
169	$Co(L^{11}\text{-}H)_2(NO_3)$	≥100

Table 5.1. Continued

№	Formula	IC_{50} (μM)
170	$Cu(L^{11}\text{-}H)(OAc)$	71.1 ± 0.4
171	$Cu(L^{11}\text{-}H)(NO_3)$	≥100
172	$Cu(L^{11}\text{-}H)Cl$	89.9 ± 1.5
173	$Cu(L^{11}\text{-}H)Br$	75.4 ± 0.7
174	$Ni(L^{11}\text{-}H)(NO_3)$	11.0 ± 0.5
175	$Ni(L^{11}\text{-}H)(OAc)$	19.1 ± 0.1
176	$Co(L^{11}\text{-}H)_2Br$	≥100
177	$Co(L^{11}\text{-}H)_2Cl$	≥100
178	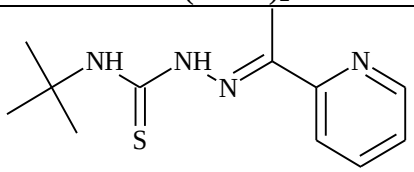 L^{12}	12.5 ± 0.1
179	$Ni(L^{12}\text{-}H)Cl$	6.7 ± 0.1
180	$Ni(L^{12}\text{-}H)Br$	8.1 ± 0.1
181	$Cu(L^{12}\text{-}H)Cl$	16.4 ± 0.9
182	$Cu(L^{12}\text{-}H)(NO_3)$	23.8 ± 0.2
183	$Cu(L^{12}\text{-}H)(OAc)$	48.9 ± 1.0
184	$Ni(L^{12}\text{-}H)(NO_3)$	16.2 ± 0.3
185	$Ni(L^{12}\text{-}H)(OAc)$	17.4 ± 0.2
186	$Co(L^{12}\text{-}H)_2Br$	≥100
187	$Co(L^{12}\text{-}H)_2(OAc)$	≥100
188	$Co(L^{12}\text{-}H)_2(NO_3)$	≥100
189	$Co(L^{12}\text{-}H)_2Cl$	≥100
190	$Ni(L^{13}\text{-}H)(NO_3)$ 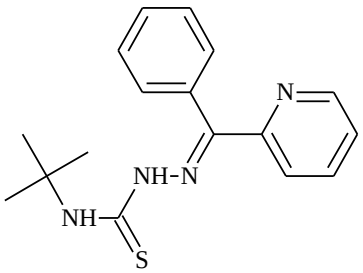 Where L^{13} is	126.7 ± 2.3
191	$Ni(L^{13}\text{-}H)Cl$	13.0 ± 0.1
192	$Co(L^{13}\text{-}H)_2(NO_3)$	20.8 ± 0.1
193	$Co(L^{13}\text{-}H)_2Cl$	19.4 ± 0.2
194	$Cu(L^{13}\text{-}H)(OAc)$	55.3 ± 0.4
195	$Cu(L^{13}\text{-}H)(NO_3)\cdot H_2O$	66.2 ± 0.6
196	$Cu(L^{13}\text{-}H)(ClO_4)\cdot H_2O$	≥100
197	$Cu(L^{13}\text{-}H)Br$	100.2 ± 4.3
198	$Cu(L^{13}\text{-}H)Cl$	114.5 ± 1.7

Table 5.1. Continued

№	Formula	IC_{50} (μM)
199	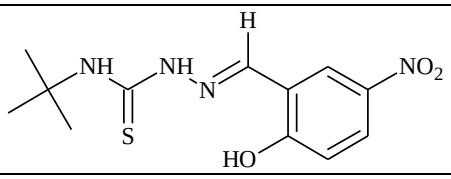	9.6 ± 0.1
200	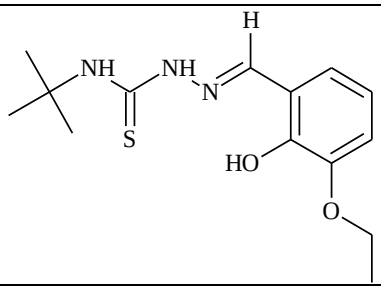	5.6 ± 0.1
201	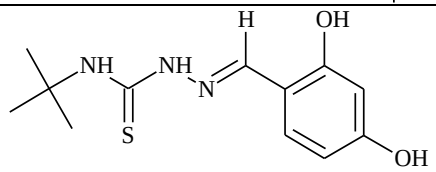	5.2 ± 0.1
202	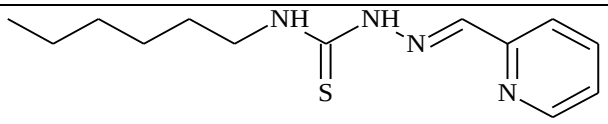 L^{14}	15.6 ± 0.3
203	$Cu(L^{14}\text{-}H)ClO_4 \cdot H_2O$	≥100
204	$Cu(L^{14}\text{-}H)(OAc)$	91.3 ± 0.8
205	$Cu(L^{14}\text{-}H)Br$	≥100
206	$Cu(L^{14}\text{-}H)NO_3$	72.6 ± 0.3
207	$Cu(L^{14}\text{-}H)Cl$	≥100
208	$Ni(L^{14}\text{-}H)Cl$	18.5 ± 0.1
209	$Ni(L^{14}\text{-}H)NO_3$	≥100
210	$Ni(L^{14}\text{-}H)(OAc)$	16.7 ± 0.4
211	$Fe(L^{14}\text{-}H)_2Cl$	≥100
212	$Zn(L^{14}\text{-}H)Cl \cdot H_2O$	68.0 ± 1.0
213	$Co(L^{14}\text{-}H)_2Cl$	54.8 ± 2.4
214	$Co(L^{14}\text{-}H)_2Br$	≥100
215	$Co(L^{14}\text{-}H)_2(NO_3)$	≥100
216	$Mn(L^{14}\text{-}H)_2$	48.5 ± 1.8
217	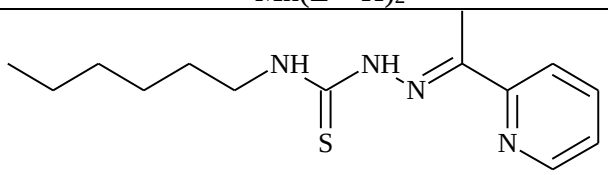 L^{15}	10.2 ± 0.6
218	$Cu(L^{15}\text{-}H)ClO_4 \cdot H_2O$	≥100
219	$Cu(L^{15}\text{-}H)NO_3$	≥100

Table 5.1. Continued

№	Formula	IC_{50} (μM)
220	$Cu(L^{15}\text{-}H)(OAc)$	88.6 ± 0.3
221	$Cu(L^{15}\text{-}H)Cl$	≥100
222	$Cu(L^{15}\text{-}H)Br$	≥100
223	$Ni(L^{15}\text{-}H)NO_3$	18.3 ± 0.2
224	$Ni(L^{15}\text{-}H)Br$	24.5 ± 0.1
225	$Co(L^{15}\text{-}H)_2(NO_3)$	≥100
226	$Co(L^{15}\text{-}H)_2Cl$	≥100
227	$Fe(L^{15}\text{-}H)_2Cl$	≥100
228	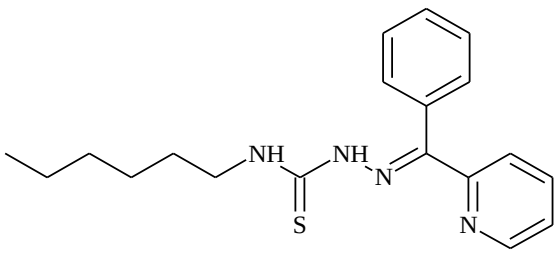 L^{16}	23.3 ± 0.4
229	$Cu(L^{16}\text{-}H)Br$	≥100
230	$Cu(L^{16}\text{-}H)(NO_3)$	≥100
231	$Cu(L^{16}\text{-}H)Cl$	≥100
232	$Cu(L^{16}\text{-}H)(OAc)$	≥100
233	$Cu(L^{16}\text{-}H)(ClO_4)\cdot H_2O$	≥100
234	$Ni(L^{16}\text{-}H)(NO_3)$	16.7 ± 0.1
235	$Co(L^{16}\text{-}H)_2Br$	≥100
236	$Co(L^{16}\text{-}H)_2(NO_3)$	129.1 ± 2.6
237	$Co(L^{16}\text{-}H)_2Cl$	100.9 ± 4.9
238	$Co(L^{16}\text{-}H)_2Br$	≥100
239	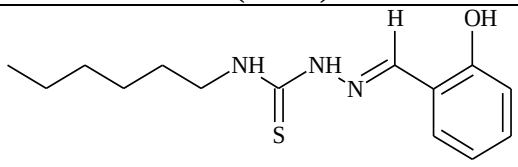 L^{17}	0.4 ± 0.1
240	$Cu(L^{17}\text{-}H)(ClO_4)\cdot H_2O$	≥100
241	$Cu(L^{17}\text{-}H)Br$	≥100
242	$Cu(L^{17}\text{-}H)(HSO_4)$	103.0 ± 5.3
243	$Ni(L^{17}\text{-}H)(NO_3)$	5.7 ± 0.1
244	$Ni(L^{17}\text{-}H)Br$	5.3 ± 0.3
245	$Ni(L^{17}\text{-}H)(OAc)$	7.7 ± 0.1
246	$Ni(L^{17}\text{-}H)_2$	6.9 ± 0.1
247	$Cu(L^{17}\text{-}H)(NO_3)$	≥100
248	$Cu(L^{17}\text{-}H)Cl$	≥100
249	$Ni(L^{17}\text{-}H)Cl$	19.8 ± 0.4

Table 5.1. Continued

№	Formula	IC_{50} (μM)
250	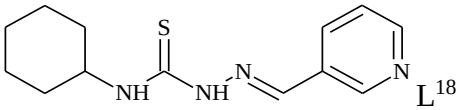 L^{18}	21.0 ± 0.3
251	$Cu(L^{18}\text{-}H)Cl\cdot H_2O$	25.1 ± 0.6
252	$Cu(L^{18}\text{-}H)ClO_4\cdot H_2O$	72.1 ± 2.4
253	$Cu(L^{18}\text{-}H)(OAc)\cdot H_2O$	25.5 ± 0.1
254	$Ni(L^{18}\text{-}H)_2$	11.2 ± 0.7
255	$Ni(L^{18}\text{-}H)(OAc)$	7.2 ± 0.1
256	$Ni(L^{18}\text{-}H)(NO_3)$	17.6 ± 0.6
257	$Co(L^{18}\text{-}H)_2(NO_3)$	≥100
258	$Co(L^{18}\text{-}H)_2Br$	≥100
259	$Co(L^{18}\text{-}H)_2(OAc)$	≥100
260	$Fe(L^{18}\text{-}H)_2Cl$	38.9 ± 1.1
261	$Fe(L^{18}\text{-}H)_2(NO_3)$	≥100
262	$Mn(L^{18}\text{-}H)_2$	6.7 ± 0.6
263	$Zn(L^{18}\text{-}H)_2$	14.1 ± 0.4
264	$Zn(L^{19}\text{-}H)Cl\cdot H_2O$ 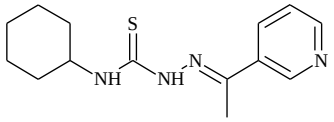 Where L^{19} is	21.6 ± 1.0
265	$Fe(L^{19}\text{-}H)_2(NO_3)$	23.4 ± 0.7
266	$Mn(L^{20}\text{-}H)_2$ 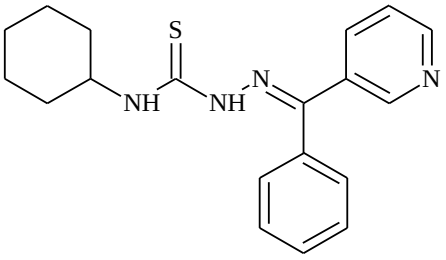 Where L^{20} is	13.9 ± 0.4
267	$Zn(L^{20}\text{-}H)_2$	13.9 ± 0.4
268	$Cu(L^{20}\text{-}H)NO_3$	98.1 ± 1.5
269	$Cu(L^{20}\text{-}H)ClO_4\cdot H_2O$	93.5 ± 1.5
270	$Cu(L^{20}\text{-}H)NO_3\cdot H_2O$	92.4 ± 2.4
271	$Cu(L^{20}\text{-}H)Br$	69.8 ± 1.3
272	$Cu(L^{20}\text{-}H)Cl$	54.0 ± 1.2
273	$Ni(L^{20}\text{-}H)Cl$	≥100
274	$Ni(L^{20}\text{-}H)(OAc)$	≥100
275	$Co(L^{20}\text{-}H)_2(NO_3)$	8.9 ± 0.4
276	$Co(L^{20}\text{-}H)_2Br$	≥100

Table 5.1. Continued

№	Formula	IC_{50} (μM)
277	$Co(L^{20}\text{-}H)_2Cl$	≥100
278	$Zn(L^{20}\text{-}H)(OAc)\cdot H_2O$	15.8 ± 0.3
279	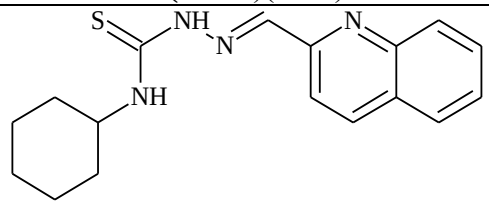 L^{21}	27.9 ± 0.4
280	$Ni(L^{21}\text{-}H)_2$	19.4 ± 0.1
281	$Ni(L^{21}\text{-}H)Cl$	≥100
282	$Ni(L^{21}\text{-}H)OAc$	≥100
283	$Co(L^{21}\text{-}H)_2(NO_3)$	≥100
284	$Co(L^{21}\text{-}H)_2Br$	≥100
285	$Co(L^{21}\text{-}H)_2Cl$	≥100
286	$Fe(L^{21}\text{-}H)_2Br$	≥100
287	$Fe(L^{21}\text{-}H)_2Cl$	60.8 ± 1.0
288	$Mn(L^{21}\text{-}H)_2$	7.7 ± 0.6
289	$Zn(L^{21}\text{-}H)OAc$	17.3 ± 0.1
290	$Cu(L^{21}\text{-}H)OAc$	≥100
291	$Cu(L^{21}\text{-}H)Cl\cdot H_2O$	25.8 ± 1.0
292	$Cu(L^{21}\text{-}H)ClO_4\cdot H_2O$	8.1 ± 0.3
293	$Cu(L^{21}\text{-}H)Br\cdot H_2O$	14.9 ± 1.3
294	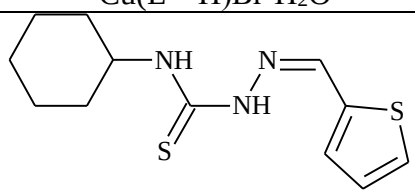	28.6 ± 0.3
295	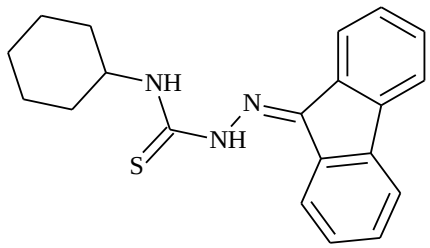 L^{22}	26.0 ± 1.1
296	$Cu(L^{22}\text{-}H)Br\cdot H_2O$	37.3 ± 0.6
297	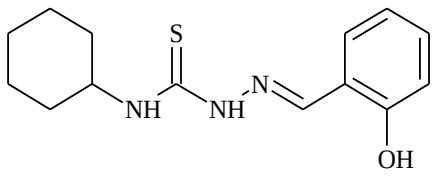 L^{23}	6.7 ± 0.4
298	$Cu(L^{23}\text{-}H)Cl\cdot H_2O$	14.7 ± 0.1

Table 5.1. Continued

№	Formula	IC_{50} (μM)
299	$Cu(L^{23}\text{-}H)Br\cdot H_2O$	21.7 ± 0.3
300	$Cu(L^{23}\text{-}2H)\cdot H_2O$	10.8 ± 0.2
301	$Cu(L^{23}\text{-}H)(NO_3)\cdot H_2O$	14.9 ± 0.4
302	$Cu(L^{23}\text{-}H)(ClO_4)\cdot H_2O$	5.9 ± 0.4
303	$Ni(L^{23}\text{-}H)_2\cdot 2H_2O$	2.1 ± 0.5
304	$Ni(L^{23}\text{-}H)(OAc)$	3.0 ± 0.7
305	$Ni(L^{23})(L^{23}\text{-}H)Br$	12.3 ± 0.2
306	$Co(L^{23}\text{-}H)_2(NO_3)$	62.5 ± 1.3
307	$Co(L^{23}\text{-}H)_2Br$	≥100
308	$Co(L^{23}\text{-}H)_2Cl$	7.3 ± 0.5
309	$Co(L^{23}\text{-}H)_2(OAc)$	3.7 ± 0.3
310	$Fe(L^{23}\text{-}H)_2Br$	≥100
311	$Fe(L^{23}\text{-}H)_2Cl$	2.1 ± 0.1
312	$Fe(L^{23}\text{-}H)_2(NO_3)$	55.9 ± 1.3
313	$Mn(L^{23}\text{-}H)_2$	22.6 ± 0.3
314	$Zn(L^{23}\text{-}H)Cl$	7.5 ± 0.1
315	$Zn(L^{23}\text{-}H)(OAc)$	7.1 ± 0.1
316	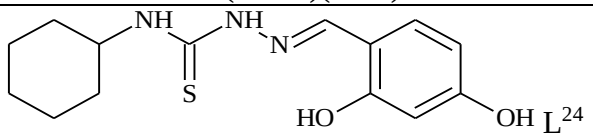 L^{24}	4.8 ± 0.3
317	$Cu(L^{24}\text{-}H)(NO_3)$	6.4 ± 0.1
318	$Cu(L^{24}\text{-}H)Cl$	7.1 ± 0.7
319	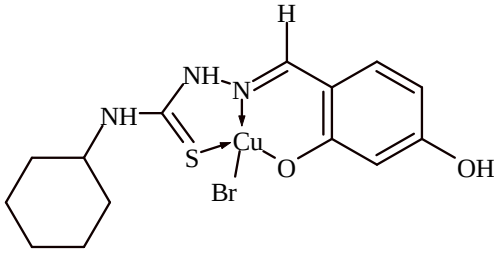 $Cu(L^{24}\text{-}H)Br$	11.9 ± 0.9
320	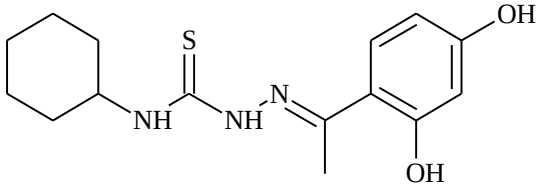 L^{25}	3.6 ± 0.1
321	$Cu(L^{25}\text{-}H)NO_3\cdot H_2O$	20.7 ± 0.8
322	$Cu(L^{25}\text{-}H)Br$	≥100
323	$Cu(L^{25}\text{-}H)(OAc)\cdot H_2O$	36.4 ± 0.5
324	$Cu(L^{26}\text{-}H)NO_3$	1.9 ± 0.3
325	$Cu(L^{26}\text{-}H)Cl$	6.5 ± 0.4

Table 5.1. Continued

№	Formula	IC_{50} (μM)
326	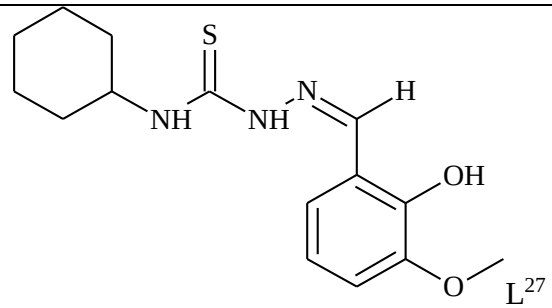 L^{27}	22.3 ± 0.6
327	$Cu(L^{27}\text{-}H)(ClO_4)\cdot H_2O$	13.4 ± 0.1
328	$Ni(L^{27}\text{-}H)_2$	10.2 ± 0.6
329	$Cu(L^{27}\text{-}H)Br\cdot H_2O$	5.9 ± 0.1
330	$Cu(L^{27}\text{-}2H)\cdot 2H_2O$	10.4 ± 0.2
331	$Cu(L^{27}\text{-}H)(NO_3)$	12.2 ± 0.5
332	$Cu(L^{27}\text{-}H)Cl\cdot H_2O$	37.0 ± 0.4
333	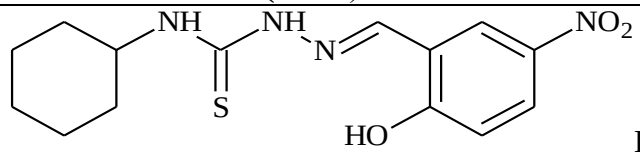 L^{28}	23.1 ± 0.4
334	$Cu(L^{28}\text{-}H)Br$	≥100
335	$Cu(L^{28}\text{-}H)Cl$	≥100
336	$Cu(L^{28}\text{-}H)(NO_3)$	20.1 ± 0.2
337	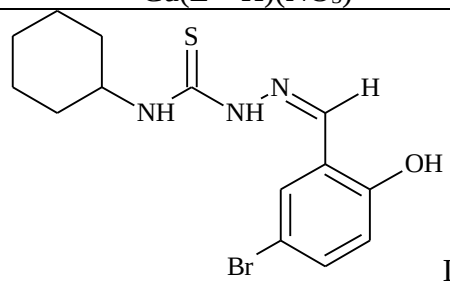 L^{29}	35.0 ± 1.3
338	$Cu(L^{29}\text{-}H)Cl\cdot H_2O$	≥100
339	$Mn(L^{29}\text{-}H)_2$	9.4 ± 0.5
340	$Ni(L^{29}\text{-}H)(NO_3)$	59.7 ± 1.7
341	$Zn(L^{29}\text{-}H)(OAc)$	≥100
342	$Cu(L^{29}\text{-}2H)\cdot H_2O$	≥100
343	$Cu(L^{29}\text{-}H)(NO_3)\cdot H_2O\cdot C_2H_5OH$	≥100
344	$Cu(L^{29}\text{-}H)(ClO_4)\cdot H_2O$	≥100
345	$Ni(L^{29}\text{-}H)_2$	69.5 ± 1.3
346	$Ni(L^{29}\text{-}H)(OAc)$	45.3 ± 1.7
347	$Co(L^{29}\text{-}H)_2(NO_3)$	57.2 ± 0.1
348	$Fe(L^{29}\text{-}H)_2Br$	44.7 ± 0.6
349	$Co(L^{29}\text{-}H)_2Cl$	22.8 ± 0.2

Table 5.1. Continued

№	Formula	IC_{50} (μM)
350	$Fe(L^{29}\text{-}H)_2Cl$	63.2 ± 0.2
351	$Cu(L^{29}\text{-}H)Br\cdot H_2O$	57.1 ± 1.2
352	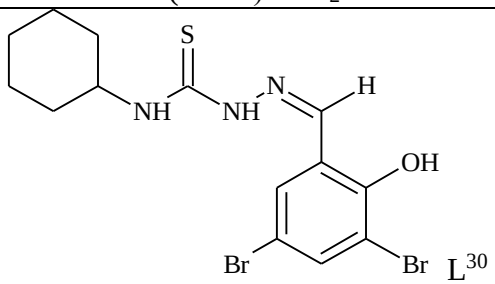 L^{30}	64.1 ± 1.4
353	$Ni(L^{30}\text{-}H)_2$	69.9 ± 1.9
354	$Zn(L^{30}\text{-}2H)\cdot 2H_2O$	15.9 ± 1.1
355	$Cu(L^{30}\text{-}H)(NO_3)\cdot H_2O$	94.8 ± 2.1
356	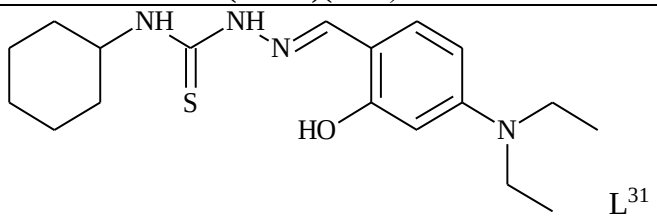 L^{31}	4.5 ± 0.4
357	$Cu(L^{31}\text{-}H)Br$	1.8 ± 0.2
358	$Cu(L^{31}\text{-}H)Cl$	11.4 ± 0.9
359	$Cu(L^{31}\text{-}H)(NO_3)$	13.6 ± 0.6
360	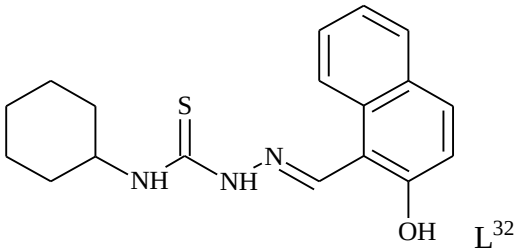 L^{32}	37.6 ± 1.3
361	$Cu(L^{32}\text{-}2H)\cdot H_2O$	45.0 ± 1.5
362	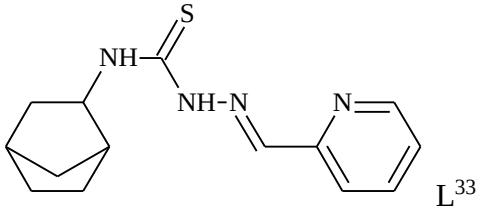 L^{33}	54.5 ± 0.2
363	$Ni(L^{33})_2Cl_2$	5.0 ± 0.6
364	$Ni(L^{33}\text{-}H)Cl$	15.8 ± 0.4
365	$Cu(L^{33}\text{-}H)(NO_3)$	≥100
366	$Cu(L^{33}\text{-}H)Br$	≥100
367	$Cu(L^{33}\text{-}H)Cl$	≥100
368	$Cu(L^{33}\text{-}H)(OAc)$	≥100

Table 5.1. Continued

№	Formula	IC_{50} (μM)
369	$Co(L^{33}\text{-}H)_2(NO_3)$	≥100
370	$Co(L^{33}\text{-}H)_2Br$	≥100
371	$Co(L^{33}\text{-}H)_2Cl$	≥100
372	$Ni(L^{33})_2(NO_3)_2$	16.7 ± 0.9
373	$Fe(L^{33}\text{-}H)_2(NO_3)$	≥100
374	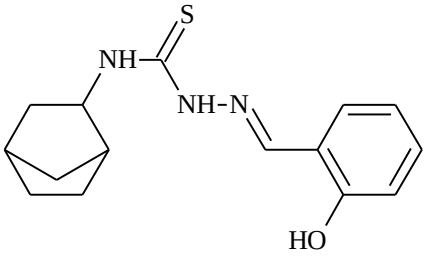 L^{34}	25.9 ± 1.1
375	$Cu(L^{34}\text{-}H)(NO_3)$	≥100
376	$Cu(L^{34}\text{-}H)Cl$	≥100
377	$Cu(L^{34}\text{-}H)Br$	≥100
378	$Cu(L^{34}\text{-}H)(Cl_2CHCOO)$	≥100
379	$Cu(L^{34}\text{-}H)(ClO_4)$	≥100
380	$Cu(L^{34}\text{-}2H)(H_2O)$	16.1 ± 0.8
381	$Ni(L^{34}\text{-}H)_2$	3.9 ± 0.1
382	$Fe(L^{34}\text{-}H)_2Cl$	8.6 ± 0.2
383	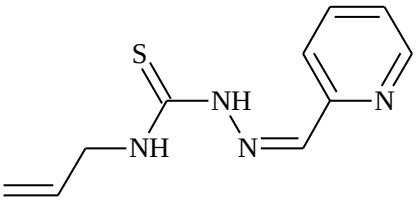 L^{35}	14.2 ± 0.8
384	$L^{35}\cdot HCl$	9.8 ± 1.0
385	$L^{35}\cdot HNO_3$	12.9 ± 0.4
386	$2L^{35}\cdot H_2SO_4$	12.3 ± 0.9
387	$L^{35}\cdot HClO_4$	12.4 ± 0.1
388	$L^{35}\cdot NH_2SO_3H$	12.8 ± 0.3
389	$L^{35}\cdot ClCH_2COOH$	13.4 ± 0.8
390	$L^{35}\cdot Cl_2CHCOOH$	10.9 ± 0.1
391	$L^{35}\cdot Cl_3CCOOH$	12.1 ± 0.7
392	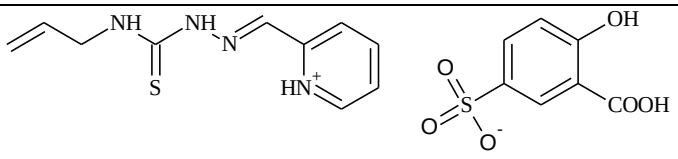	15.0 ± 0.3

Table 5.1. Continued

№	Formula	IC_{50} (μM)
393	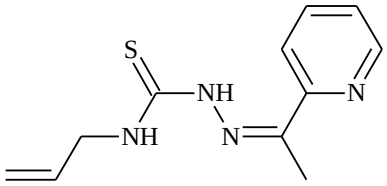 L^{36}	11.6 ± 0.3
394	$L^{36}\cdot HCl$	28.6 ± 0.2
395	$L^{36}\cdot HNO_3$	18.1 ± 0.5
396	$2L^{36}\cdot H_2SO_4$	29.8 ± 0.6
397	$L^{36}\cdot HClO_4$	16.2 ± 0.3
398	$L^{36}\cdot NH_2SO_3H$	21.3 ± 0.1
399	$L^{36}\cdot ClCH_2COOH$	41.0 ± 0.9
400	$L^{36}\cdot Cl_2CHCOOH$	15.1 ± 0.4
401	$L^{36}\cdot Cl_3CCOOH$	13.6 ± 0.7
402	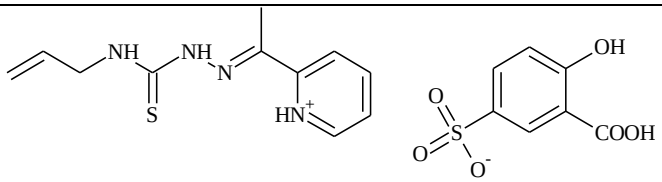	18.4 ± 0.5
403	$Cu(L^{36})(NO_3)_2$	29.8 ± 1.2
404	$Cu(L^{36}\text{-}H)(OAc)$	26.8 ± 0.5
405	$Cu(L^{36}\text{-}H)Cl$	≥100
406	$Cu(L^{36}\text{-}H)Br$	≥100
407	$(Cu(L^{36}\text{-}H))_2SO_4$	38.7 ± 1.0
408	$Cu(L^{36}\text{-}H)(NO_3)$	45.5 ± 0.1
409	$Cu(Im)(L^{36}\text{-}H)(NO_3)$ 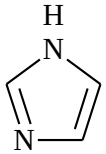 Where Im is	37.4 ± 2.0
410	$Cu(3.4\text{-}Lut)(L^{36}\text{-}H)(NO_3)$ 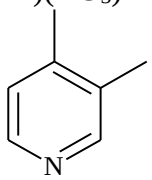 Where 3.4-Lut is	36.6 ± 0.5

Table 5.1. Continued

№	Formula	IC_{50} (μM)
411	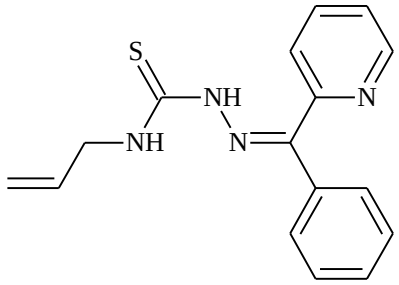 L^{37}	18.7 ± 0.4
412	$L^{37}\cdot HCl$	13.6 ± 0.8
413	$L^{37}\cdot HNO_3$	17.3 ± 0.7
414	$2L^{37}\cdot H_2SO_4$	17.5 ± 0.8
415	$L^{37}\cdot HClO_4$	19.0 ± 0.7
416	$L^{37}\cdot NH_2SO_3H$	32.7 ± 1.6
417	$L^{37}\cdot ClCH_2COOH$	7.2 ± 0.5
418	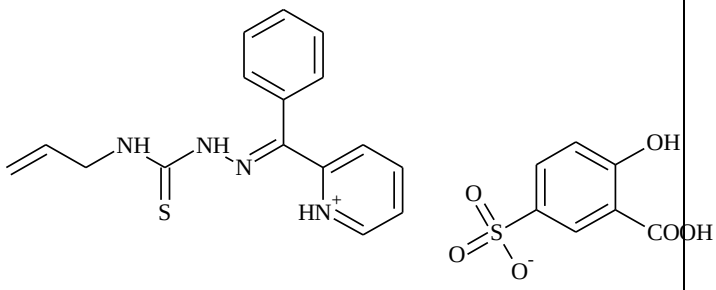	8.9 ± 0.9
419	$Cu(L^{37}\text{-}H)(NO_3)$	≥100
420	$Cu(L^{37}\text{-}H)Cl$	52.9 ± 0.2
421	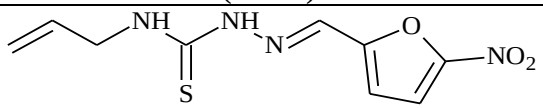	22.1 ± 0.2
422	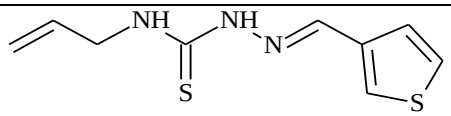	17.5 ± 0.4
423	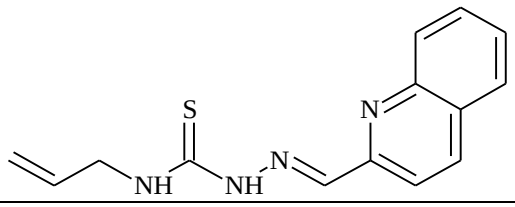	≥100
424	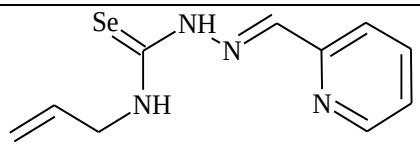	14.6 ± 0.7

Table 5.1. Continued

№	Formula	IC_{50} (μM)
425	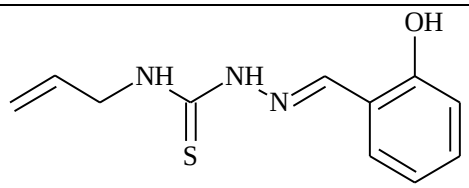 L^{38}	13.8 ± 0.4
426	$Cu(L^{38}\text{-}H)Cl$	51.8 ± 0.3
427	$Cu(L^{38}\text{-}H)Br$	52.7 ± 0.4
428	$Cu(L^{38}\text{-}H)(NO_3)$	76.2 ± 0.8
429	$Cu(L^{38}\text{-}2H)H_2O$	44.9 ± 1.5
430	$Co(L^{38}\text{-}H)_2Cl$	21.4 ± 0.6
431	$Co(L^{38}\text{-}H)_2(NO_3)$	8.7 ± 0.3
432	$Ni(L^{38})(L^{38}\text{-}H)Cl$	3.6 ± 0.1
433	$Zn(L^{38}\text{-}H)Cl$	9.2 ± 1.1
434	$Fe(L^{38}\text{-}H)_2(NO_3)$	2.4 ± 0.1
435	$Cu(Im)(L^{38}\text{-}H)(NO_3)$	5.8 ± 0.1
436	$Cu(3.5Br_2Py)(L^{38}\text{-}H)(NO_3)$ 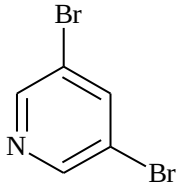 Where $3.5Br_2Py$ is	7.5 ± 0.5
437	$Cu(4\text{-}Pic)(L^{38}\text{-}H)(NO_3)$ 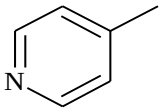 Where 4-Pic is	5.8 ± 0.1
438	$Cu(3\text{-}Pic)(L^{38}\text{-}H)(NO_3)$ 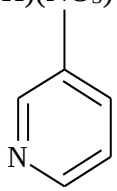 Where 3-Pic is	3.4 ± 0.8
439	$Cu(2.2'\text{-}BPy)(L^{38}\text{-}2H)$ 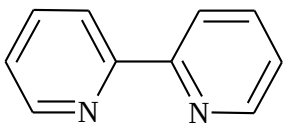 Where 2.2'-BPy is	10.2 ± 0.1

Table 5.1. Continued

№	Formula	IC_{50} (μM)
440	Cu(1.10-Phen)(L^{38}-2H) 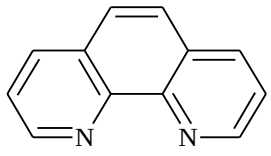 Where 1.10-Phen is	22.8 ± 0.6
441	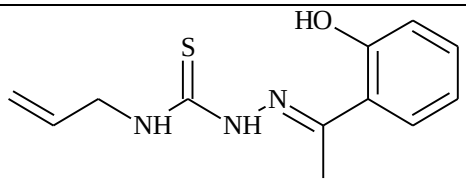 L^{39}	92.8 ± 0.7
442	Cu(1.10-Phen)(L^{39})$(NO_3)_2$	7.7 ± 0.7
443	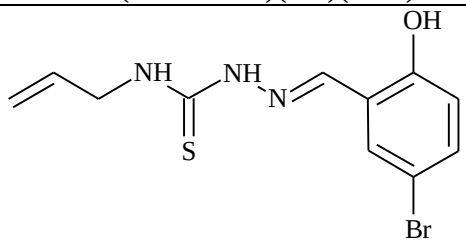 L^{40}	8.5 ± 0.6
444	Cu(L^{40}-H)Cl	≥100
445	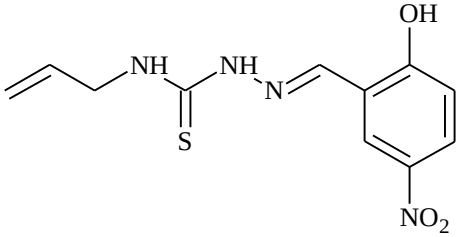 L^{41}	8.0 ± 0.2
446	Cu(L^{41}-H)Cl	68.3 ± 0.4
447	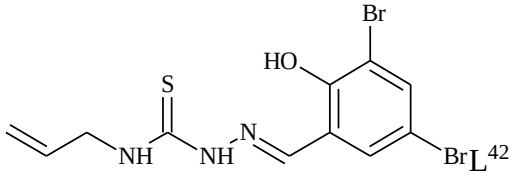 L^{42}	11.9 ± 0.1
448	Cu(L^{42}-H)$NO_3 \cdot H_2O$	18.7 ± 0.8
449	Cu(1.10-Phen)(L^{42}-H)NO_3	19.9 ± 0.1
450	Cu(2.2'-BPy)(L^{42}-H)NO_3	13.4 ± 0.5
451	Cu(L^{42}-2H)H_2O	≥100
452	Cu(1.10-Phen)(L^{42}-2H)	14.8 ± 0.7
453	Cu(2.2'-BPy)(L^{42}-2H)	19.7 ± 0.6
454	Cu(3.4-Lut)(L^{42}-2H)	≥100
455	Cu(4-Pic)(L^{42}-2H)	16.8 ± 0.7
456	Cu(3-Pic)(L^{42}-2H)	23.9 ± 0.8

Table 5.1. Continued

№	Formula	IC_{50} (μM)
457	$Cu(Py)(L^{42}\text{-}2H)$ 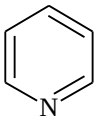 Where Py is	18.7 ± 0.1
458	$Cu(L^{42}\text{-}H)Br$	≥100
459	$Co(L^{42}\text{-}H)_2NO_3$	59.4 ± 0.7
460	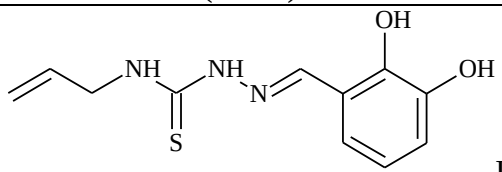 L^{43}	5.7 ± 0.5
461	$Cu(L^{43}\text{-}H)NO_3$	7.1 ± 0.1
462	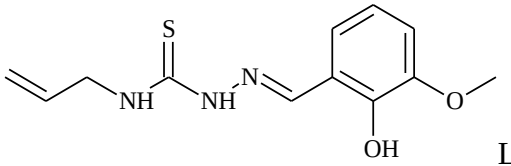 L^{44}	20.0 ± 0.1
463	$Cu(L^{44}\text{-}H)Cl$	24.6 ± 0.3
464	$Cu(L^{44}\text{-}2H)H_2O$	13.9 ± 0.3
465	$Cu(1.10\text{-}Phen)(L^{44}\text{-}2H)$	5.2 ± 0.2
466	$Cu(2.2'\text{-}BPy)(L^{44}\text{-}2H)$	7.3 ± 0.2
467	$Cu(Im)(L^{44}\text{-}2H)$	6.9 ± 0.8
468	$Cu(3.5\text{-}Br_2Py)(L^{44}\text{-}2H)$	7.0 ± 0.8
469	$Cu(3.4\text{-}Lut)(L^{44}\text{-}2H)$	7.6 ± 0.3
470	$Cu(4\text{-}Pic)(L^{44}\text{-}2H)$	18.7 ± 0.6
471	$Cu(3\text{-}Pic)(L^{44}\text{-}2H)$	12.8 ± 0.6
472	$Cu(Py)(L^{44}\text{-}2H)$	8.4 ± 0.5
473	$Cu(L^{44}\text{-}H)NO_3\cdot H_2O$	21.5 ± 0.2
474	$Cu(2.2'\text{-}BPy)(L^{44}\text{-}H)NO_3$	6.8 ± 0.2
475	$Cu(3.5\text{-}Br_2Py)(L^{44}\text{-}H)NO_3$	6.7 ± 0.5
476	$Cu(Py)(L^{44}\text{-}H)NO_3$	16.4 ± 0.4
477	$Cu(4\text{-}Pic)(L^{44}\text{-}H)NO_3$	12.8 ± 0.2
478	$Cu(3\text{-}Pic)(L^{44}\text{-}H)NO_3$	18.7 ± 0.5
479	$Cu(3.4\text{-}Lut)(L^{44}\text{-}H)NO_3$	3.2 ± 0.1
480	$Cu(Im)(L^{44}\text{-}H)NO_3$	8.6 ± 0.7
481	$Cu(1.10\text{-}Phen)(L^{44}\text{-}H)NO_3$	7.8 ± 0.3
482	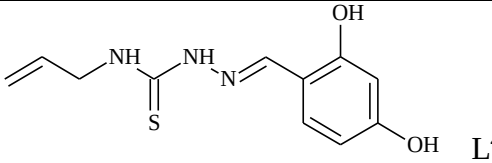 L^{45}	5.5 ± 0.8

Table 5.1. Continued

№	Formula	IC_{50} (μM)
483	$Cu(L^{45}\text{-}H)Cl$	12.8 ± 0.2
484	$Cu(L^{45}\text{-}2H)H_2O$	6.5 ± 0.8
485	$Cu(1.10\text{-}Phen)(L^{45}\text{-}2H)$	≥100
486	$Cu(2.2'\text{-}BPy)(L^{45}\text{-}2H)$	7.4 ± 0.8
487	$Cu(3.4\text{-}Lut)(L^{45}\text{-}2H)$	4.5 ± 0.2
488	$Cu(4\text{-}Pic)(L^{45}\text{-}2H)$	23.9 ± 0.9
489	$Cu(3\text{-}Pic)(L^{45}\text{-}2H)$	17.3 ± 0.8
490	$Cu(L^{45}\text{-}H)NO_3$	8.6 ± 0.3
491	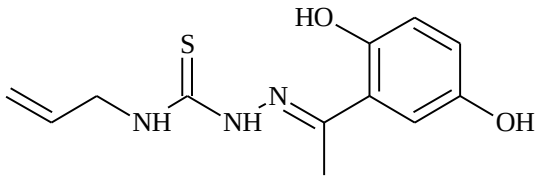 L^{46}	11.5 ± 0.1
492	$Cu(L^{46}\text{-}H)NO_3$	17.4 ± 0.3
493	$Cu(L^{46}\text{-}H)Cl$	17.8 ± 0.8
494	$Co(L^{46}\text{-}H)_2NO_3$	7.6 ± 0.6
495	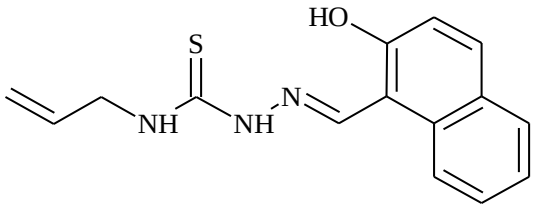 L^{47}	13.6 ± 0.2
496	$Cu(L^{47}\text{-}H)Cl$	14.2 ± 0.6
497	$Cu(L^{47}\text{-}H)NO_3$	14.4 ± 0.4
498	$Co(L^{47}\text{-}H)_2NO_3$	8.5 ± 0.8
499	$Ni(L^{47})(L^{47}\text{-}H)Cl$	8.5 ± 0.3
500	$Cr(L^{47}\text{-}H)_2NO_3$	0.9 ± 0.1
501	$Cu(1.10\text{-}Phen)(L^{47}\text{-}H)NO_3$	14.5 ± 0.5
502	$Cu(2.2'\text{-}BPy)(L^{47}\text{-}H)NO_3$	87.3 ± 1.1
503	$Cu(L^{47}\text{-}2H)H_2O$	18.9 ± 0.8
504	$Cu(1.10\text{-}Phen)(L^{47}\text{-}2H)$	33.7 ± 0.3
505	$Cu(2.2'\text{-}BPy)(L^{47}\text{-}2H)$	11.6 ± 0.5
506	$Cu(3.4\text{-}Lut)(L^{47}\text{-}2H)$	8.9 ± 0.1
507	$Cu(4\text{-}Pic)(L^{47}\text{-}2H)$	≥100
508	$Cu(3\text{-}Pic)(L^{47}\text{-}2H)$	15.4 ± 0.2
509	$Cu(Py)(L^{47}\text{-}2H)$	9.5 ± 0.7

Table 5.1. Continued

№	Formula	IC_{50} (μM)
510	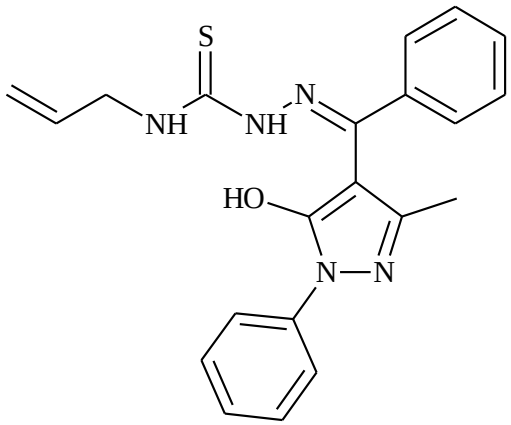 L^{48}	19.7 ± 0.9
511	$Cu(L^{48}\text{-}H)NO_3$	≥100
512	$Cu(L^{48}\text{-}H)(OAc)$	31.4 ± 1.8
513	$Cu(L^{48}\text{-}H)Br$	55.8 ± 2.6
514	$Cu(L^{48}\text{-}H)Cl$	42.1 ± 1.6
515	$Co(L^{48}\text{-}H)_2Br$	≥100
516	$Co(L^{48}\text{-}H)_2Cl$	12.4 ± 0.7
517	$Co(L^{48}\text{-}H)_2NO_3$	13.8 ± 0.1
518	$Fe(L^{48}\text{-}H)_2Cl$	≥100
519	$Fe(L^{48}\text{-}H)_2Br$	≥100
520	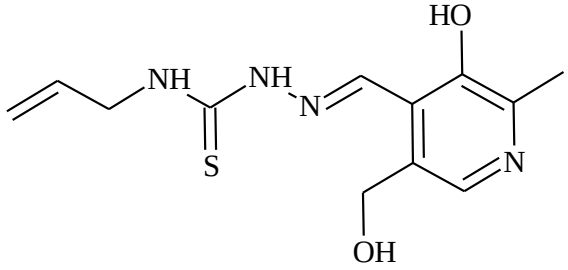 L^{49}	16.7 ± 0.2
521	$L^{49}\cdot HCl$	13.5 ± 0.2
522	$Cu(L^{49}\text{-}H)NO_3$	≥100
523	$Cu(L^{49}\text{-}H)(OAc)$	≥100
524	$Cu(L^{49}\text{-}H)Br$	≥100
525	$Cu(L^{49}\text{-}H)Cl$	≥100
526	$Ni(L^{49}\text{-}H)_2$	93.6 ± 4.9
527	$Co(L^{49}\text{-}H)_2Cl$	≥100
528	$Fe(L^{49}\text{-}H)_2Cl$	8.2 ± 0.2
529	$Fe(L^{49}\text{-}H)_2Br$	6.2 ± 0.3

Table 5.1. Continued

№	Formula	IC_{50} (μM)
530	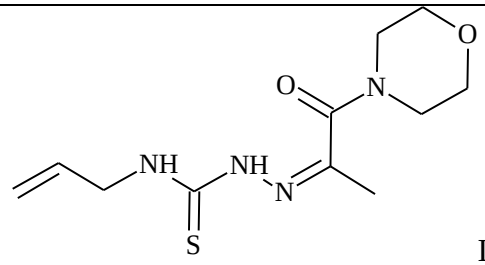 L^{50}	94.4 ± 4.8
531	$Cu(L^{50}\text{-}H)Cl$	128.3 ± 3.4
532	$Cu(L^{50}\text{-}H)Br$	168.4 ± 5.0
533	$Cu(L^{50}\text{-}H)(NO_3)$	140.3 ± 3.4
534	$Cu(L^{50}\text{-}H)(OAc)$	≥100
535	$Cu(L^{50}\text{-}H)(Cl_2CHCOO)$	≥100
536	$Ni(L^{50})_2(NO_3)_2$	19.6 ± 0.1
537	$Ni(L^{50})(L^{50}\text{-}H)Cl$	≥100
538	$Cu(1.10\text{-}Phen)(L^{50}\text{-}H)(NO_3)$	23.0 ± 0.2
539	$Cu(2.2'\text{-}BPy)(L^{50}\text{-}H)(NO_3)$	22.3 ± 0.3
540	$Ni(L^{50}\text{-}H)Cl$	30.6 ± 0.8
541	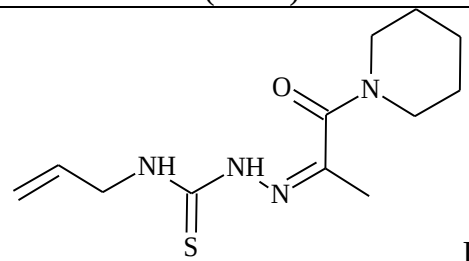 L^{51}	56.4 ± 1.5
542	$Cu(L^{51})Cl_2$	105.9 ± 0.5
543	$Cu(L^{51}\text{-}H)Br$	≥100
544	$Cu(1.10\text{-}Phen)(L^{51})(NO_3)_2$	≥100
545	$Ni(L^{51})_2(NO_3)_2$	38.6 ± 1.1
546	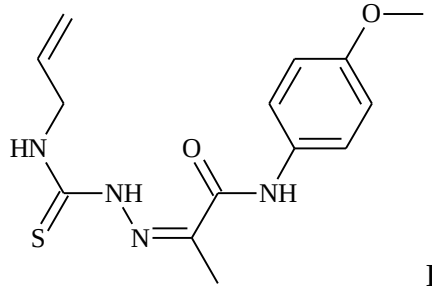 L^{52}	68.6 ± 0.6
547	$Cu(L^{52}\text{-}H)Cl$	≥100
548	$Cu(L^{52}\text{-}H)Br$	≥100
548	$Cu(L^{52}\text{-}H)(NO_3)$	≥100
549	$Cu(L^{52}\text{-}H)(Cl_2CHCOO)$	78.5 ± 2.0
550	$Cu(L^{52}\text{-}H)(OAc)$	96.4 ± 1.6

Table 5.1. Continued

№	Formula	IC_{50} (μM)
551	$Cu(L^{52}\text{-}H)(ClO_4)$	≥100
552	$Fe(L^{52}\text{-}H)_2NO_3$	62.5 ± 1.3
553	$Ni(L^{52})_2Cl_2$	58.4 ± 1.1
554	$Ni(L^{52}\text{-}H)Cl$	75.6 ± 3.1
555	$Ni(L^{52})_2(NO_3)_2$	29.2 ± 0.2
556	$Cu(1.10\text{-}Phen)(L^{52}\text{-}H)(NO_3)$	72.3 ± 3.2
557	$Cu(2.2'\text{-}BPy)(L^{52}\text{-}H)(NO_3)$	97.2 ± 1.4
558	$Cu(3.4\text{-}Lut)(L^{52}\text{-}H)(NO_3)$	99.3 ± 0.4
559	$Cu(4\text{-}Pic)(L^{52}\text{-}H)(NO_3)$	61.3 ± 1.3
560	$Cu(3\text{-}Pic)(L^{52}\text{-}H)(NO_3)$	68.4 ± 1.7
561	$Cu(Py)(L^{52}\text{-}H)(NO_3)$	83.4 ± 0.9
562	$Cu(Im)(L^{52}\text{-}H)(NO_3)$	68.5 ± 1.4
563	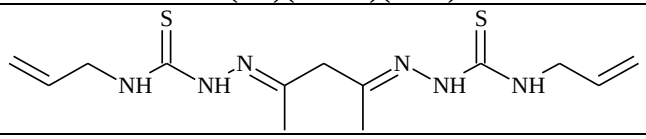	18.9 ± 0.7
564	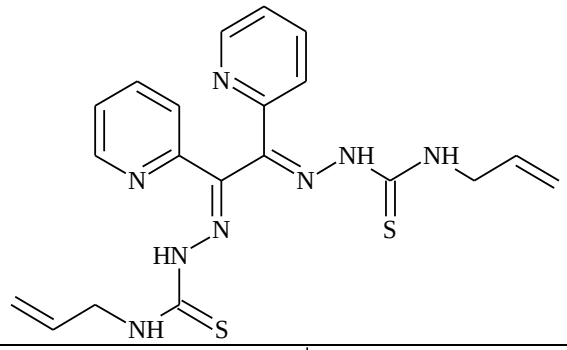	13.1 ± 0.4
565	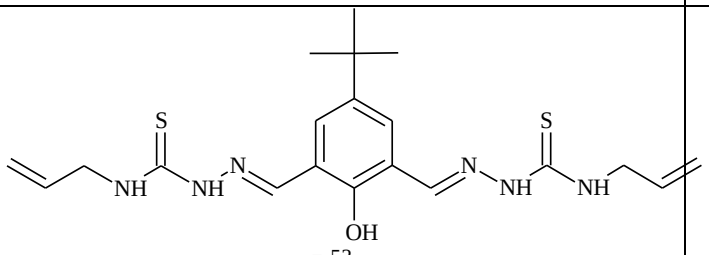 L^{53}	51.1 ± 1.4
566	$Cu_2(L^{53}\text{-}3H)NO_3 \cdot 5CH_3OH$	≥100
567	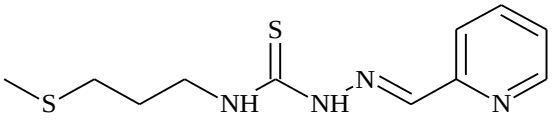 L^{54}	32.4 ± 1.3
568	$Cu(L^{54}\text{-}H)NO_3$	≥100
569	$Cu(L^{54}\text{-}H)Br$	≥100
570	$Cu(L^{54}\text{-}H)Cl$	≥100

Table 5.1. Continued

№	Formula	IC_{50} (μM)
571	$Cu(L^{54}\text{-}H)(Cl_2CHCOO)$	≥100
572	$Cu(L^{54}\text{-}H)(OAc)$	≥100
573	$Ni(L^{54})_2Cl_2$	2.7 ± 0.1
574	$Fe(L^{54}\text{-}H)_2Cl$	61.1 ± 0.6
575	$Co(L^{54}\text{-}H)_2Cl$	≥100
576	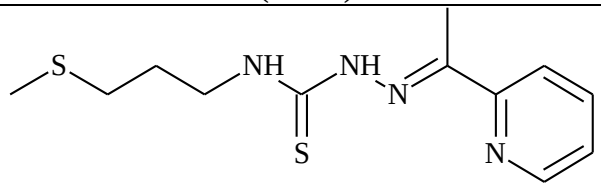 L^{55}	23.5 ± 0.1
577	$Cu(L^{55}\text{-}H)(OAc)$	32.3 ± 0.1
578	$Cu(L^{55}\text{-}H)Br$	≥100
579	$Cu(L^{55}\text{-}H)Cl$	≥100
580	$Cu(L^{55}\text{-}H)(NO_3)$	≥100
581	$Cu(L^{55}\text{-}H)(Cl_2CHCOO)$	≥100
582	$Ni(L^{55})(L^{55}\text{-}H)Cl$	9.1 ± 0.1
583	$Ni(L^{55})(L^{55}\text{-}H)(NO_3)$	8.7 ± 0.1
584	$Cu(1.10\text{-}Phen)(L^{55}\text{-}H)(NO_3)$	≥100
585	$Cu(2.2'\text{-}BPy)(L^{55}\text{-}H)(NO_3)$	160.3 ± 3.2
586	$Ni(L^{55}\text{-}H)Cl$	8.7 ± 0.4
587	$Ni(L^{55}\text{-}H)(NO_3)$	9.7 ± 0.2
588	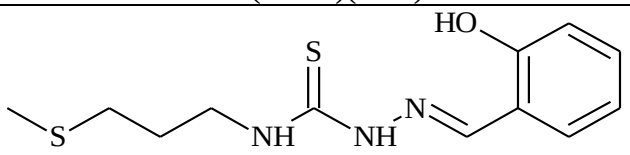 L^{56}	15.2 ± 0.1
589	$Cu(L^{56}\text{-}H)(NO_3)$	≥100
590	$Cu(L^{56}\text{-}H)Br$	≥100
591	$Cu(L^{56}\text{-}H)Cl$	≥100
592	$Cu(L^{56}\text{-}H)(Cl_2CHCOO)$	66.9 ± 1.5
593	$Co(L^{56}\text{-}H)_2(NO_3)$	18.0 ± 0.2
594	$Fe(L^{56}\text{-}H)_2(NO_3)$	27.6 ± 0.5
595	$Cu(L^{57})(ClO_4)_2$ 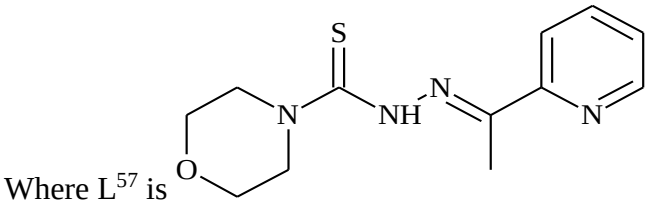 Where L^{57} is	16.7 ± 0.3

Table 5.1. Continued

№	Formula	IC_{50} (μM)
596	$Co(L^{58})Cl_2$ 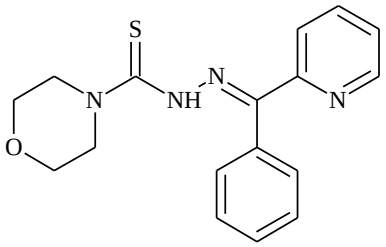 Where L^{58} is	8.1 ± 0.5
597	$Co(L^{58})(NO_3)_2$	7.3 ± 0.3
598	$Ni(L^{58})Cl_2$	19.1 ± 0.4
599	$Cu(L^{58})Br_2$	20.9 ± 1.0
600	$Cu(L^{58})(NO_3)_2$	83.6 ± 0.6
601	$Cu(L^{59})(NO_3)_2$ 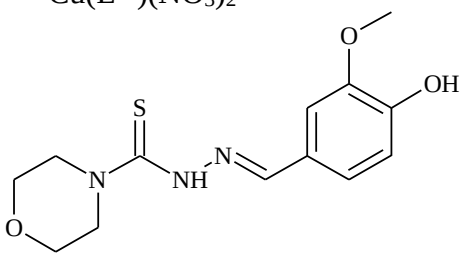 Where L^{59} is	63.2 ± 0.2
602	$Cu(L^{59})Br_2$	38.5 ± 0.4
603	$Co(L^{59})(NO_3)_2$	18.0 ± 0.3
604	$Ni(L^{59})Cl_2$	15.2 ± 0.4
605	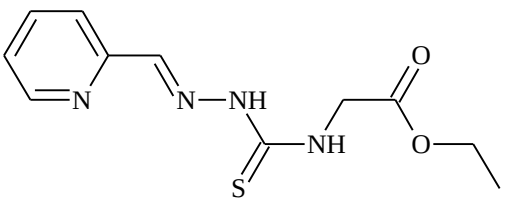 L^{60}	52.8 ± 0.3
606	$Cu(L^{60}\text{-}H)Cl$	≥100
607	$Cu(L^{60}\text{-}H)(NO_3)$	≥100
608	$Cu(L^{60}\text{-}H)Br$	≥100
609	$Cu(L^{60}\text{-}H)(OAc)$	≥100
610	$Cu(L^{60}\text{-}H)(ClO_4)\cdot H_2O$	≥100
611	$Ni(L^{60}\text{-}H)Cl$	22.7 ± 0.6
612	$Co(L^{60}\text{-}H)_2Cl$	≥100
613	$Fe(L^{60}\text{-}H)_2Cl$	24.6 ± 0.8
614	$Mn(L^{60}\text{-}H)_2$	40.4 ± 0.9
615	$Zn(L^{60}\text{-}H)Cl\cdot H_2O$	37.7 ± 1.6

Table 5.1. Continued

№	Formula	IC_{50} (μM)
616	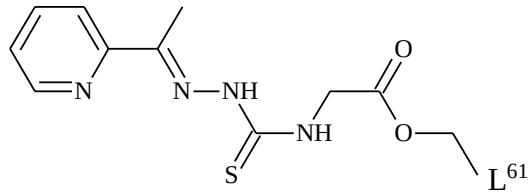 L^{61}	46.7 ± 0.4
617	$Cu(L^{61}\text{-}H)(NO_3)$	≥100
618	$Cu(L^{61}\text{-}H)Cl$	≥100
619	$Cu(L^{61}\text{-}H)(ClO_4)\cdot H_2O$	43.7 ± 0.3
620	$Cu(L^{61}\text{-}H)Br$	≥100
621	$Cu(L^{61}\text{-}H)(OAc)$	≥100
622	$Ni(L^{61}\text{-}H)Cl$	15.1 ± 0.1
623	$Fe(L^{61}\text{-}H)_2Br$	≥100
624	$Fe(L^{61}\text{-}H)_2Cl$	≥100
625	$Fe(L^{61}\text{-}H)_2(NO_3)$	≥100
626	$Co(L^{61}\text{-}H)_2Cl$	≥100
627	$Mn(L^{61}\text{-}H)_2$	32.1 ± 1.5
628	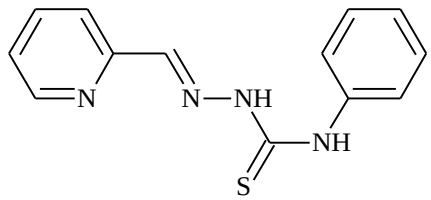 L^{62}	14.9 ± 0.4
629	$2L^{62}\cdot H_2SO_4$	10.0 ± 0.1
630	$L^{62}\cdot HCl$	10.8 ± 0.2
631	$L^{62}\cdot HNO_3$	9.4 ± 0.3
632	$L^{62}\cdot HClO_4$	9.9 ± 0.1
633	$L^{62}\cdot Cl_2CHCOOH$	6.6 ± 0.2
634	$L^{62}\cdot NH_2SO_3H$	6.4 ± 0.2
635	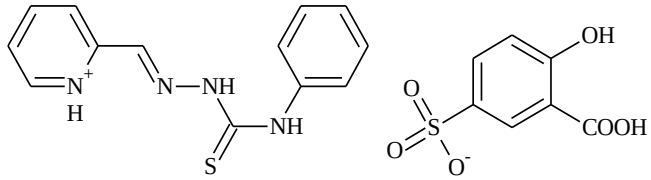	8.6 ± 0.9
636	$Cu(L^{62}\text{-}H)Cl$	4.5 ± 0.6
637	$Cu(Str)(L^{62}\text{-}H)Cl$ 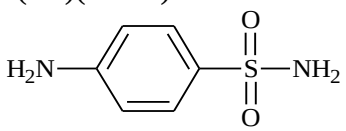 Where Str is	6.2 ± 0.7

Table 5.1. Continued

№	Formula	IC_{50} (μM)
638	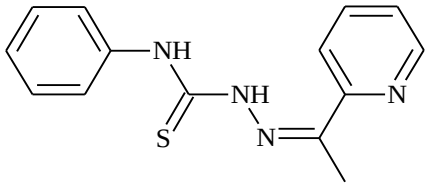 L^{63}	13.6 ± 0.3
639	$L^{63}\cdot HNO_3$	11.2 ± 0.6
640	$L^{63}\cdot HCl$	15.6 ± 0.1
641	$L^{63}\cdot NH_2SO_3H$	10.8 ± 0.2
642	$L^{63}\cdot Cl_2CHCOOH$	10.6 ± 0.3
643	$L^{63}\cdot HClO_4$	10.9 ± 0.7
644	$2L^{63}\cdot H_2SO_4$	11.0 ± 0.4
645	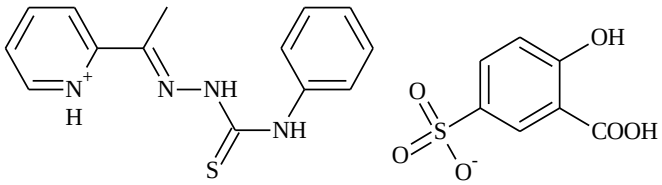	12.1 ± 0.6
646	$L^{64}\cdot HClO_4$ 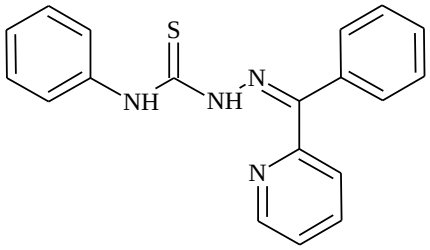 Where L^{64} is	23.6 ± 0.3
647	$L^{64}\cdot HNO_3$	25.6 ± 0.4
648	$L^{64}\cdot HCl$	20.1 ± 0.1
649	$2L^{64}\cdot H_2SO_4$	15.0 ± 0.7
650	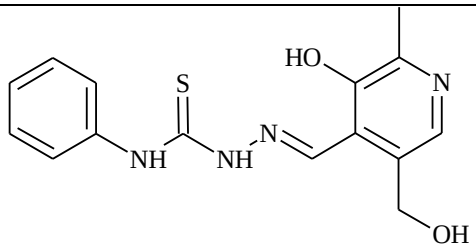 L^{65}	14.1 ± 0.4
651	$Cu(L^{65}\text{-}H)(NO_3)$	53.1 ± 0.1
652	$Cu(L^{65}\text{-}H)Br$	34.9 ± 0.3
653	$Cu(L^{65}\text{-}H)(OAc)$	47.4 ± 0.2
654	$Cu(L^{65}\text{-}H)(Cl_2CHCOO)$	26.9 ± 0.4

Table 5.1. Continued

№	Formula	IC_{50} (μM)
655	$Cu(L^{65}\text{-}H)Cl$	43.3 ± 0.7
656	$Co(L^{65}\text{-}H)_2Cl$	≥100
657	$Ni(L^{65}\text{-}H)_2$	≥100
658	$Fe(L^{65}\text{-}H)_2(NO_3)$	14.2 ± 0.4
659	$Fe(L^{65}\text{-}H)_2Cl$	7.9 ± 0.4
660	$Fe(L^{65}\text{-}H)_2Br$	8.7 ± 0.1
661	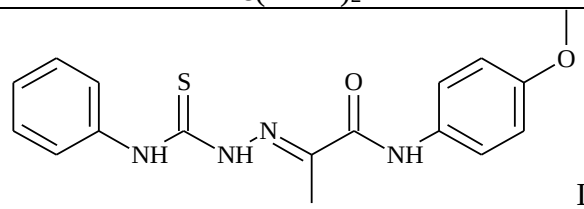 L^{66}	33.8 ± 1.6
662	$Cu(L^{66}\text{-}H)Br$	90.3 ± 1.0
663	$Cu(L^{66}\text{-}H)(NO_3)$	≥100
664	$Cu(L^{66}\text{-}H)Cl$	87.8 ± 0.7
665	$Cu(L^{66}\text{-}H)(OAc)$	66.3 ± 2.0
666	$Cu(L^{66}\text{-}H)(ClO_4)$	88.2 ± 2.1
667	$Cu(L^{66}\text{-}H)(Cl_2CHCOO)$	94.8 ± 3.8
668	$Ni(L^{66})(NO_3)_2$	≥100
669	$Cu(1.10\text{-}Phen)(L^{66}\text{-}H)(NO_3)$	77.2 ± 2.4
670	$Cu(3\text{-}Pic)(L^{66}\text{-}H)(NO_3)$	53.6 ± 1.2
671	$Cu(3.4\text{-}Lut)(L^{66}\text{-}H)(NO_3)$	86.7 ± 1.3
672	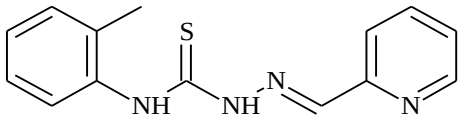	11.2 ± 0.1
673	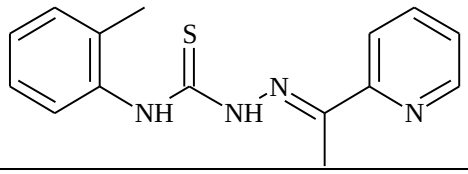	10.7 ± 0.5
674	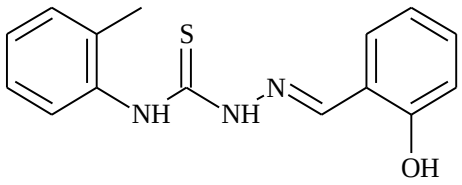	9.3 ± 0.1
675	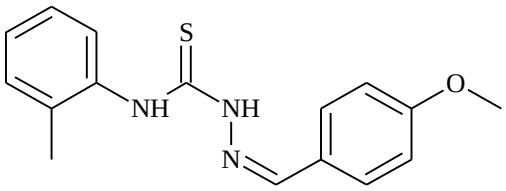	13.0 ± 0.1

Table 5.1. Continued

№	Formula	IC_{50} (μM)
676	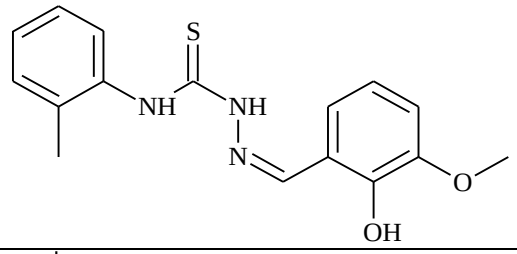	15.2 ± 0.3
677	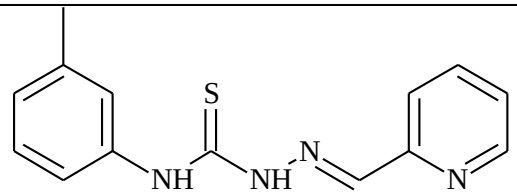	12.3 ± 0.8
678	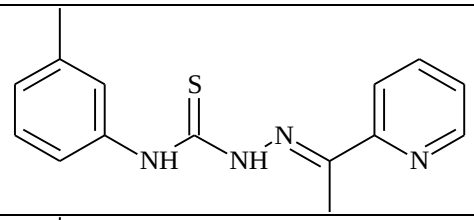	5.1 ± 0.1
679	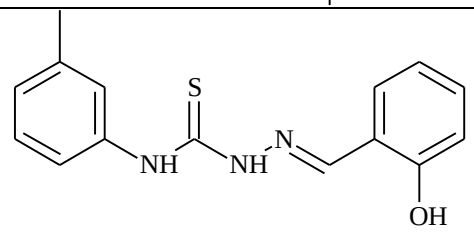	10.0 ± 0.4
680	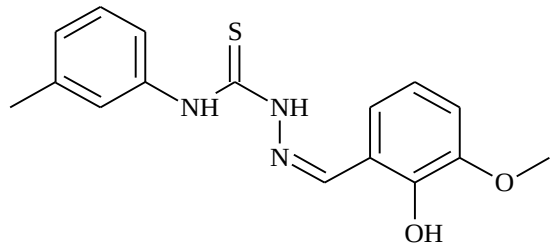	10.0 ± 0.7
681	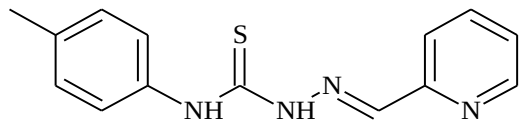	9.3 ± 0.1
682	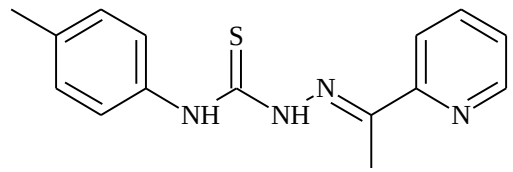	17.8 ± 0.5

Table 5.1. Continued

№	Formula	IC_{50} (μM)
683	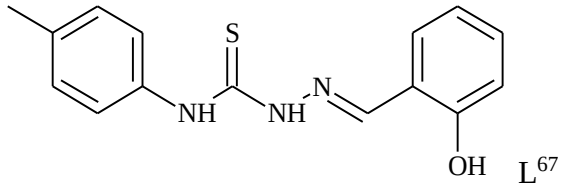 L^{67}	8.6 ± 0.2
684	Cu(1.10-Phen)(L^{67}-2H)	11.8 ± 0.2
685	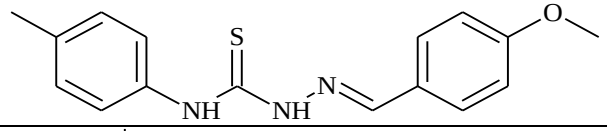	9.3 ± 0.2
686	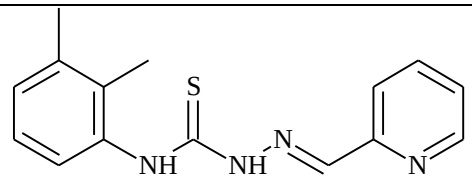	8.7 ± 0.1
687	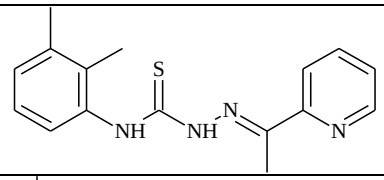	15.6 ± 0.2
688	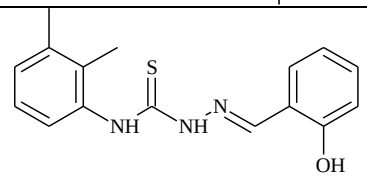 L^{68}	7.8 ± 0.4
689	Cu(L^{68}-H)(NO_3)	19.6 ± 0.5
690	Cu(L^{68}-H)Br	38.3 ± 0.8
691	Cu(L^{68}-H)Cl	27.2 ± 0.7
692	Cu_2(L^{68}-H)$_2SO_4$	13.2 ± 0.8
693	Ni(L^{68}-H)$_2$	7.2 ± 0.6
694	Co(L^{68}-H)$_2$(NO_3)	14.2 ± 0.2
695	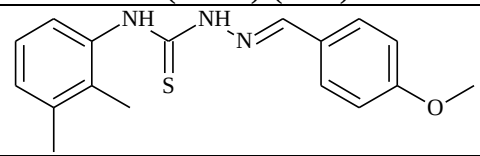	9.7 ± 0.2
696	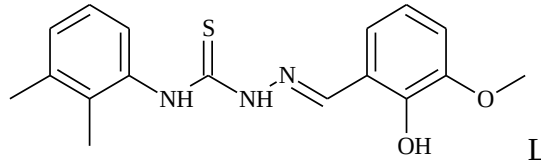 L^{69}	10.1 ± 0.4
697	Cu(2.2'-BPy)(L^{69}-2H)	9.9 ± 0.7
698	Cu(1.10-Phen)(L^{69}-2H)	2.7 ± 0.2

Table 5.1. Continued

№	Formula	IC_{50} (μM)
699	Cu(Im)(L^{69}-2H)	10.9 ± 0.1
700	Cu(3.5-Br_2Py)(L^{69}-2H)	5.7 ± 0.1
701	Cu(Str)(L^{69}-2H)	10.6 ± 0.3
702	Cu(L^{70}-2H) 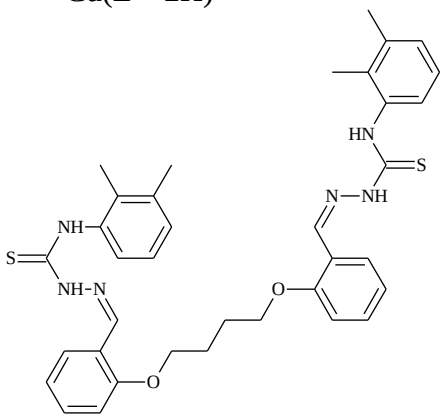 Where L^{70} is	≥100
703	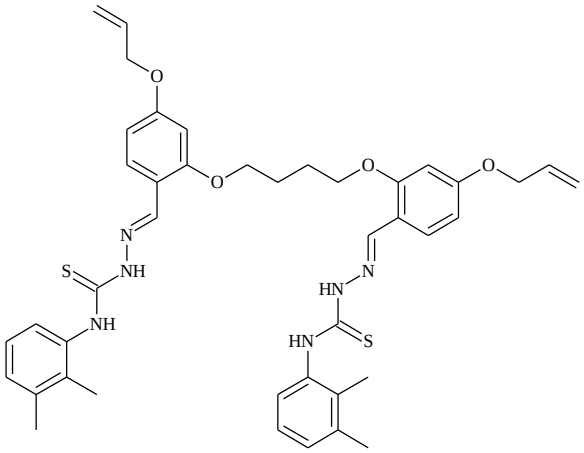 L^{71}	≥100
704	$Cu_2(L^{71}$-2H)$(OAc)_2 \cdot 2H_2O \cdot 4CH_3OH$	≥100
705	$Cu_2(L^{72}$-3H)$Cl \cdot H_2O$ 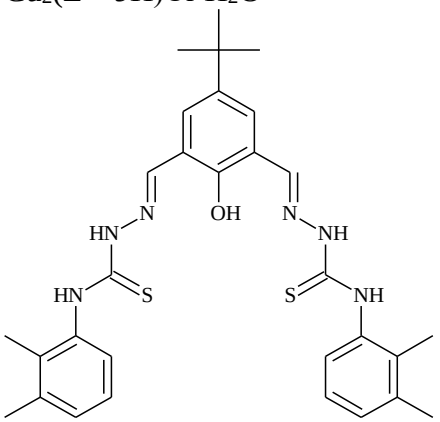 Where L^{72} is	≥100

Table 5.1. Continued

№	Formula	IC_{50} (μM)
706	$Cu_2(L^{72}\text{-}3H)NO_3$	≥100
707	$Cu_2(L^{72}\text{-}3H)Br\cdot 2H_2O$	≥100
708	$Cu_2(L^{72}\text{-}3H)ClO_4$	≥100
709	$Cu_2(L^{72}\text{-}3H)(OAc)$	≥100
710	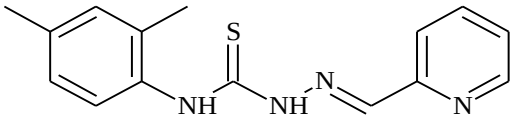	7.2 ± 0.2
711	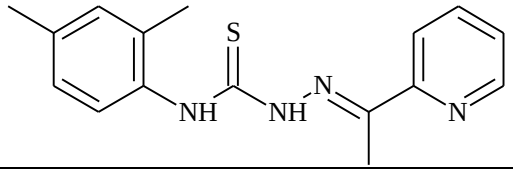	9.1 ± 0.2
712	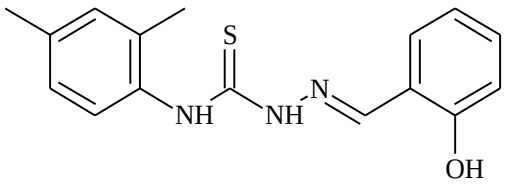	10.2 ± 0.5
713	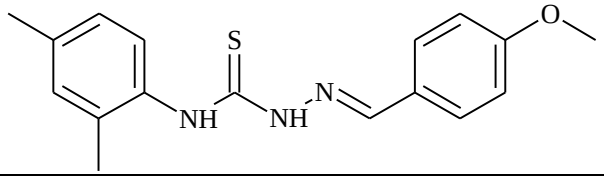	10.0 ± 0.2
714	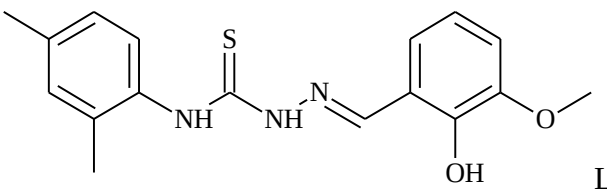 L^{73}	11.2 ± 0.3
715	$Cu(L^{73}\text{-}H)Br$	5.7 ± 0.4
716	$Cu(L^{73}\text{-}H)Cl$	15.7 ± 0.3
717	$Cu(L^{73}\text{-}H)NO_3\cdot H_2O$	9.5 ± 0.7
718	$Ni(L^{73}\text{-}H)_2$	2.9 ± 0.1
719	$Ni(L^{73}\text{-}2H)(H_2O)$	11.3 ± 0.6
720	$Co(L^{73}\text{-}H)_2Cl$	8.3 ± 0.1
721	$Co(L^{73}\text{-}H)_2(NO_3)$	12.0 ± 0.2
722	$Fe(L^{73}\text{-}H)_2Cl$	5.4 ± 0.5
723	$Fe(L^{73}\text{-}H)(NO_3)_2(H_2O)$	18.6 ± 0.4
724	$Fe(L^{73}\text{-}H)_2(NO_3)$	6.2 ± 0.6
725	$K_2Mn(L^{73}\text{-}2H)_2$	10.1 ± 0.3
726	$Cu(Im)(L^{73}\text{-}2H)$	10.0 ± 0.2

Table 5.1. Continued

№	Formula	IC_{50} (μM)
727	Cu(2.2'-BPy)(L^{73}-2H)	12.4 ± 0.1
728	Cu(1.10-Phen)(L^{73}-2H)	7.4 ± 0.1
729	Cu(3.5-Br_2Py)(L^{73}-2H)	3.3 ± 0.5
730	Cu(Str)(L^{73}-2H)	6.7 ± 0.6
731	Cu(L^{73}-2H)(H_2O)	6.9 ± 0.7
732	Cu(L^{73}-H)ClO_4	8.1 ± 0.8
733	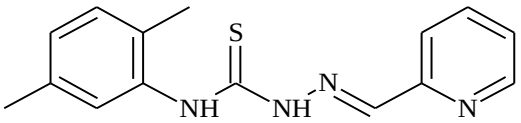	9.4 ± 0.5
734	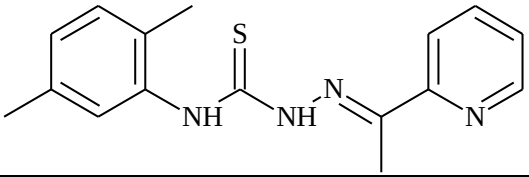	17.7 ± 0.3
735	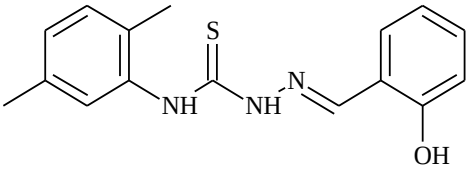	9.8 ± 0.9
736	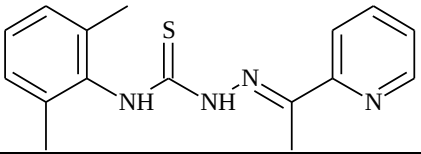	19.9 ± 0.6
737	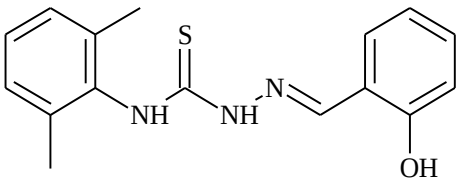 L^{74}	12.8 ± 0.1
738	$Cu_2(L^{74}\text{-H})_2SO_4$	≥100
739	Ni(L^{74}-H)Cl	9.6 ± 0.3
740	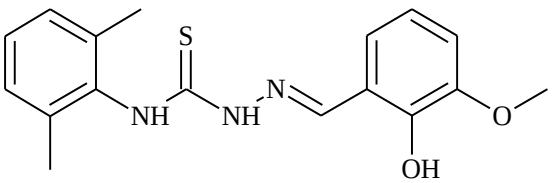	13.1 ± 0.8
741	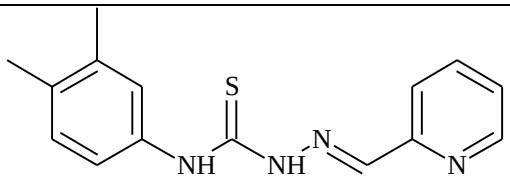	10.3 ± 0.3

Table 5.1. Continued

№	Formula	IC_{50} (μM)
742	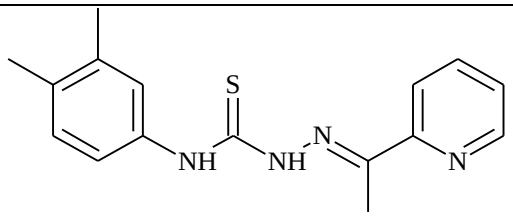	15.8 ± 0.2
743	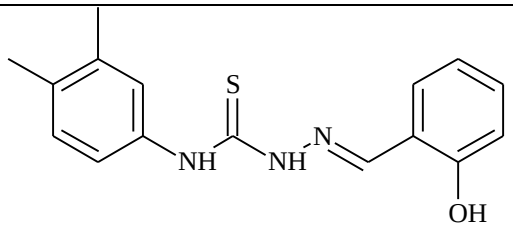	8.6 ± 0.2
744	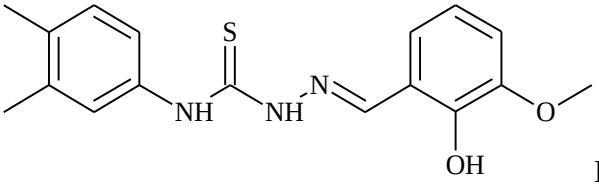 L^{75}	10.6 ± 0.5
745	$Cu(L^{75}\text{-}H)NO_3 \cdot H_2O$	15.7 ± 0.7
746	$Ni(L^{75}\text{-}H)Cl$	13.2 ± 0.4
747	$Cu(1.10\text{-}Phen)(L^{75}\text{-}2H)$	10.9 ± 0.1
748	$Cu(3.5\text{-}Br_2Py)(L^{75}\text{-}2H)$	6.3 ± 0.1
749	$Cu(2.2'\text{-}BPy)(L^{75}\text{-}2H)$	≥100
750	$Cu(L^{75}\text{-}H)Br$	9.3 ± 0.1
751	$Cu(L^{75}\text{-}H)ClO_4 \cdot 4H_2O$	30.8 ± 0.6
752	$Cu(L^{75}\text{-}H)Cl$	7.5 ± 0.3
753	$Co(L^{75}\text{-}H)_2Cl$	7.5 ± 0.5
754	$Co(L^{75}\text{-}H)_2(NO_3)$	11.1 ± 0.2
755	$Ni(L^{75}\text{-}2H)(H_2O)$	15.6 ± 0.3
756	$Cu(L^{75}\text{-}2H)(H_2O)$	8.5 ± 0.2
757	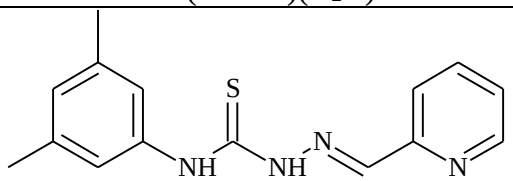	12.3 ± 0.9
758	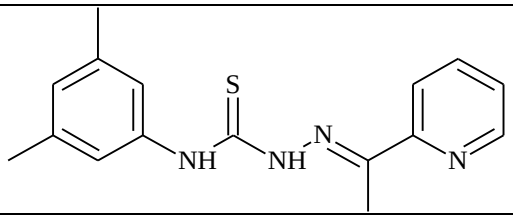	22.1 ± 0.5

Table 5.1. Continued

№	Formula	IC_{50} (μM)
759	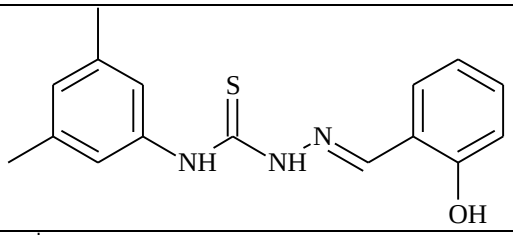	15.4 ± 0.6
760	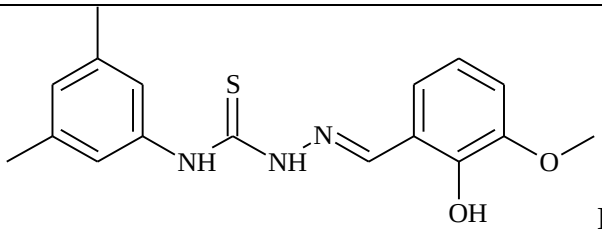 L^{76}	11.2 ± 0.1
761	$Ni(L^{76}\text{-}2H)(H_2O)$	17.6 ± 0.4
762	$Ni(L^{76}\text{-}H)_2$	12.7 ± 0.3
763	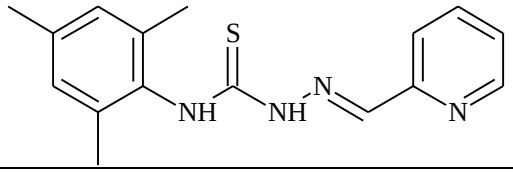	18.2 ± 0.2
764	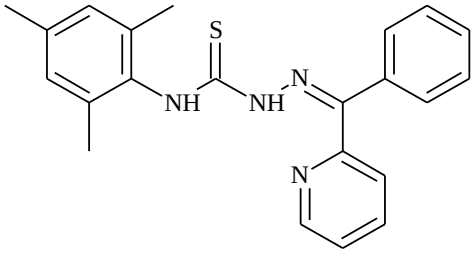	8.9 ± 0.1
765	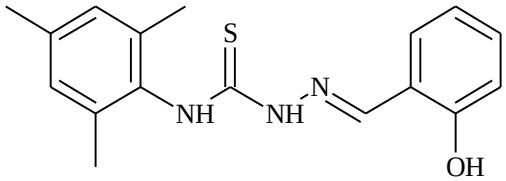 L^{77}	11.9 ± 0.8
766	$Cu(L^{77}\text{-}2H)(H_2O)$	≥100
767	$Cu(L^{77}\text{-}H)Cl$	76.5 ± 0.2
768	$Cu(L^{77}\text{-}H)(NO_3)$	91.9 ± 0.9
769	$Ni(L^{77}\text{-}2H)(H_2O)$	14.3 ± 0.2
770	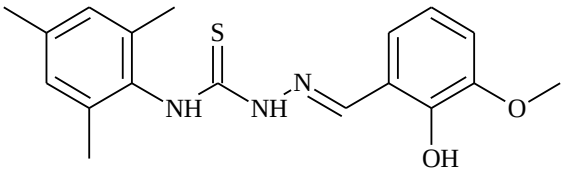	11.8 ± 0.4

Table 5.1. Continued

№	Formula	IC_{50} (μM)
771	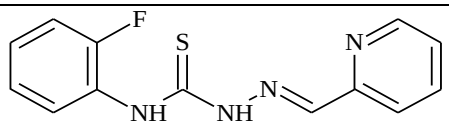 L^{78}	25.1 ± 1.7
772	$Cu(L^{78}\text{-}H)NO_3$	12.8 ± 0.9
773	$Cu(L^{78}\text{-}H)Br$	9.7 ± 0.8
774	$Cu(L^{78}\text{-}H)Cl$	9.1 ± 0.1
775	$Cu(L^{78}\text{-}H)(OAc)$	14.2 ± 0.9
776	$Ni(L^{78})_2(NO_3)_2$	83.0 ± 2.5
777	$Ni(L^{78}\text{-}H)_2$	≥100
778	$Fe(L^{78}\text{-}H)_2(NO_3)$	39.3 ± 0.7
779	$Fe(L^{78}\text{-}H)_2Cl$	105.3 ± 0.6
780	$Co(L^{78}\text{-}H)_2(NO_3)$	≥100
781	$Zn(L^{78}\text{-}H)_2$	60.6 ± 1.3
782	$Cu(L^{79}\text{-}H)NO_3$ 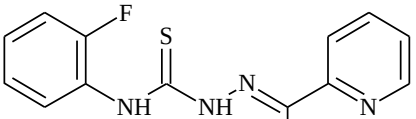 Where L^{79} is	55.2 ± 1.7
783	$Cu(L^{79}\text{-}H)Br$	56.3 ± 1.5
784	$Cu(L^{79}\text{-}H)Cl$	75.6 ± 1.4
785	$Cu(L^{79}\text{-}H)(OAc)$	44.9 ± 0.7
786	$Cu(L^{79}\text{-}H)(Cl_2CHCOO)$	84.9 ± 1.2
787	$Ni(L^{79})_2(NO_3)_2$	≥100
788	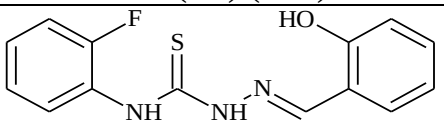 L^{80}	11.6 ± 0.9
789	$Cu(L^{80}\text{-}H)Cl$	169.3 ± 3.0
790	$Cu(L^{80}\text{-}H)Br$	≥100
791	$Cu(L^{80}\text{-}H)(NO_3)$	≥100
792	$Cu(L^{80}\text{-}H)(Cl_2CHCOO)$	100.8 ± 1.7
793	$Cu(L^{80}\text{-}H)(OAc)$	41.4 ± 1.9
794	$Cu(L^{80}\text{-}H)(ClO_4)$	88.8 ± 2.1
795	$Ni(L^{80}\text{-}H)_2$	8.1 ± 0.1
796	$Ni(L^{80}\text{-}H)Cl$	14.8 ± 0.9
797	$Ni(Im)_2(L^{80}\text{-}H)Cl$	133.6 ± 2.3
798	$Zn(L^{80}\text{-}H)_2$	1.8 ± 0.1
799	$Co(L^{80}\text{-}H)_2Br$	11.4 ± 0.2
800	$Co(L^{80}\text{-}H)_2(NO_3)$	1.9 ± 0.1
801	$Co(L^{80}\text{-}H)_2Cl$	2.1 ± 0.2

Table 5.1. Continued

№	Formula	IC_{50} (μM)
802	$Fe(L^{80}\text{-}H)_2(NO_3)$	10.2 ± 0.2
803	$Fe(L^{80}\text{-}H)_2Cl$	2.1 ± 0.2
804	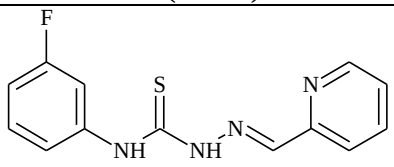 L^{81}	40.2 ± 1.4
805	$Cu(L^{81}\text{-}H)NO_3$	38.6 ± 1.3
806	$Cu(L^{81}\text{-}H)Br$	42.0 ± 1.9
807	$Cu(L^{81}\text{-}H)Cl$	54.7 ± 2.1
808	$Cu(L^{81}\text{-}H)(OAc)$	55.9 ± 0.2
809	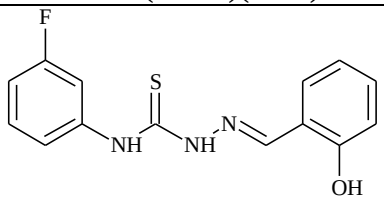 L^{82}	4.3 ± 0.3
810	$Cu(L^{82}\text{-}H)Cl$	12.1 ± 0.2
811	$Cu(L^{82}\text{-}H)NO_3$	≥100
812	$Ni(L^{82}\text{-}H)_2$	2.9 ± 0.5
813	$Fe(L^{82}\text{-}H)_2(NO_3)$	6.5 ± 0.1
814	$Co(L^{82}\text{-}H)_2(NO_3)$	4.6 ± 0.7
815	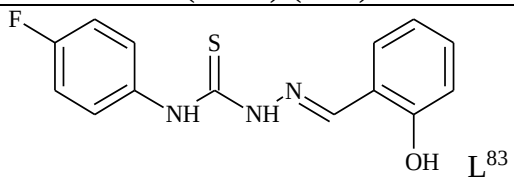 L^{83}	8.6 ± 0.8
816	$Cu(L^{83}\text{-}H)Cl$	13.2 ± 0.3
817	$Cu(L^{83}\text{-}H)NO_3$	24.3 ± 1.5
818	$Ni(L^{83}\text{-}H)_2$	1.5 ± 0.1
819	$Fe(L^{83}\text{-}H)_2(NO_3)$	3.8 ± 0.1
820	$Co(L^{83}\text{-}H)_2(NO_3)$	2.6 ± 0.6
821	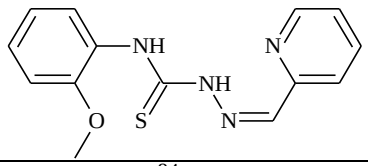	6.3 ± 0.1
822	$Cu(L^{84}\text{-}H)NO_3$ 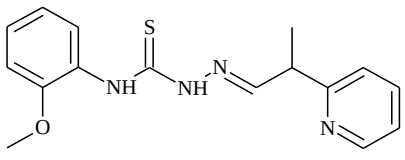 Where L^{84} is	19.9 ± 0.7

Table 5.1. Continued

№	Formula	IC_{50} (μM)
823	$Cu(L^{84}\text{-}H)Cl$	22.4 ± 0.2
824	$Cu(L^{85}\text{-}H)Cl$ 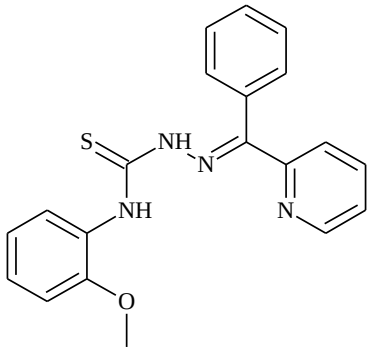 Where L^{85} is	82.5 ± 1.5
825	$Cu(L^{85}\text{-}H)NO_3$	23.0 ± 0.1
826	$Co(L^{85}\text{-}H)_2Cl$	18.7 ± 0.3
827	$Fe(L^{85}\text{-}H)_2NO_3$	≥100
828	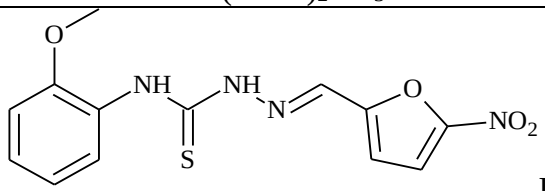 L^{86}	15.5 ± 0.1
829	$Cu(L^{86}\text{-}H)NO_3$	34.1 ± 0.8
830	$Co(L^{86}\text{-}H)_2Cl$	12.8 ± 0.4
831	$Fe(L^{86}\text{-}H)_2NO_3$	10.4 ± 0.1
832	$Cu(L^{87}\text{-}2H)(H_2O)$ 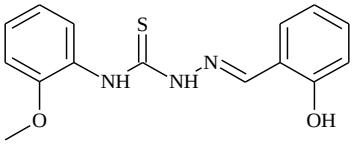 Where L^{87} is	12.3 ± 0.9
833	$Cu(L^{87}\text{-}H)Br$	15.9 ± 0.1
834	$Ni(L^{87}\text{-}H)_2$	12.2 ± 0.2
835	$Fe(L^{87}\text{-}H)_2NO_3$	20.4 ± 0.1
836	$Co(L^{87}\text{-}H)_2Cl$	9.7 ± 0.1
837	$Cu(L^{88}\text{-}H)Cl$ 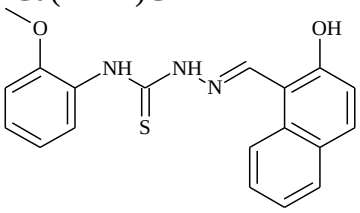 Where L^{88} is	27.5 ± 0.3

Table 5.1. Continued

№	Formula	IC_{50} (μM)
838	$Cu(L^{88}\text{-}H)NO_3$	18.8 ± 0.6
839	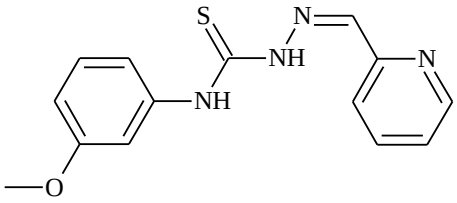 L^{89}	6.2 ± 0.2
840	$Cu(L^{89}\text{-}H)Cl$	11.4 ± 0.4
841	$Cu(L^{90}\text{-}H)NO_3$ 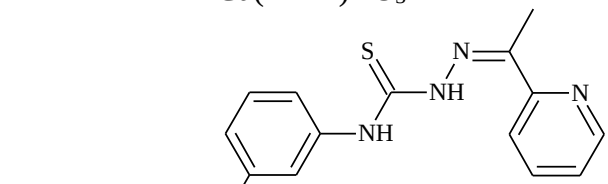 Where L^{90} is	14.6 ± 0.5
842	$Cu(L^{90}\text{-}H)Cl$	20.2 ± 0.2
843	$Cu(L^{91}\text{-}H)Cl$ 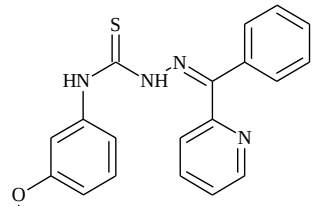 Where L^{91} is	≥100
844	$Cu(L^{91}\text{-}H)NO_3$	24.7 ± 0.3
845	$Co(L^{91}\text{-}H)_2Cl$	3.7 ± 0.5
846	$Co(L^{92}\text{-}H)_2Cl$ 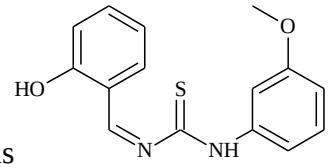 Where L^{92} is	9.0 ± 0.2
847	$Cu(L^{93}\text{-}H)NO_3$ 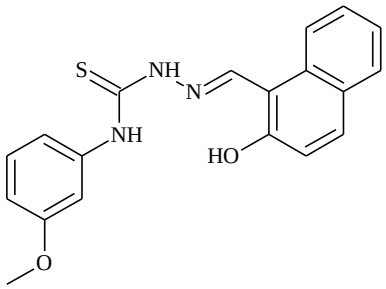 Where L^{93} is 	25.3 ± 0.9

Table 5.1. Continued

№	Formula	IC_{50} (μM)
848	$Cu(L^{93}\text{-}H)Cl$	40.5 ± 0.2
849	$Cu(L^{94}\text{-}H)NO_3$ Where L^{94} is 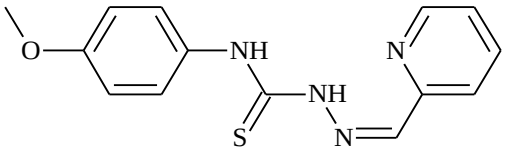	12.0 ± 0.5
850	$Co(L^{94}\text{-}H)_2Cl$	50.3 ± 0.5
851	$Cu(L^{95}\text{-}H)Cl$ Where L^{95} is 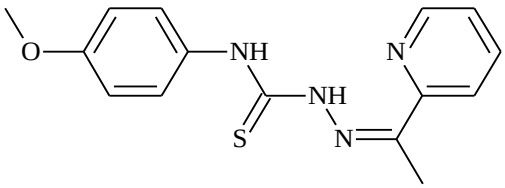	17.6 ± 0.1
852	$Cu(L^{96}\text{-}H)Cl$ Where L^{96} is 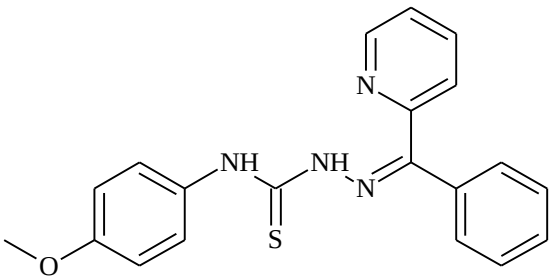	19.9 ± 0.3
853	$Cu(L^{96}\text{-}H)NO_3$	20.1 ± 0.2
854	$Co(L^{96}\text{-}H)_2Cl$	≥100
855	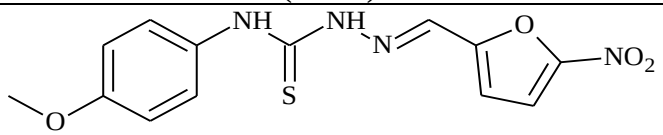	15.1 ± 0.2
856	$Co(L^{97}\text{-}H)_2Cl$ Where L^{97} is 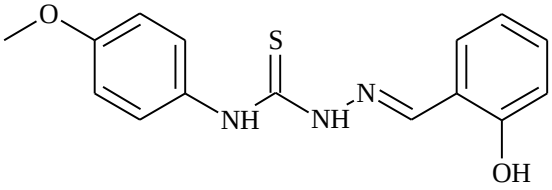	14.8 ± 0.7

Table 5.1. Continued

№	Formula	IC_{50} (μM)
857	$Cu(L^{98}\text{-}H)NO_3$ Where L^{98} is 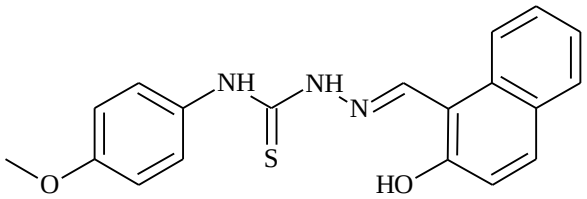	54.6 ± 0.4
858	$Cu(L^{98}\text{-}H)Cl$	38.5 ± 0.3
859	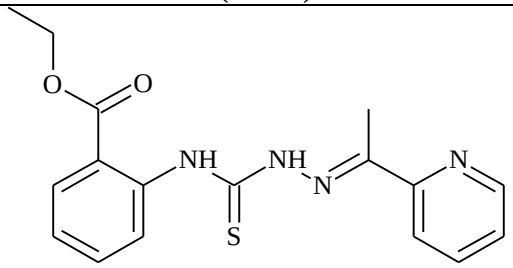	22.5 ± 0.4
860	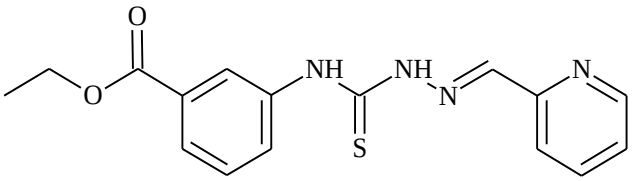 L^{99}	13.1 ± 0.1
861	$Cu(L^{99}\text{-}H)Cl$	90.6 ± 0.8
862	$Cu(L^{99}\text{-}H)NO_3$	119.8 ± 0.3
863	$Cu(L^{99}\text{-}H)ClO_4 \cdot H_2O$	138.3 ± 1.5
864	$Ni(L^{99}\text{-}H)Cl$	20.4 ± 0.9
865	$Zn(L^{99}\text{-}H)Cl \cdot H_2O$	11.5 ± 0.1
866	$Co(L^{99}\text{-}H)_2Cl$	≥100
867	$Fe(L^{99}\text{-}H)_2Cl$	48.8 ± 0.5
868	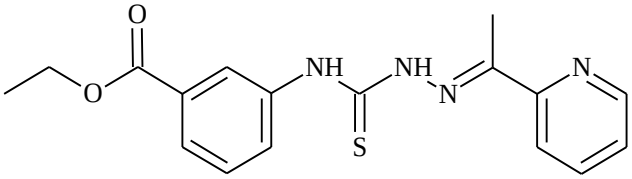 L^{100}	11.5 ± 0.4
869	$Cu(L^{100}\text{-}H)Cl$	114.7 ± 0.4
870	$Cu(L^{100}\text{-}H)NO_3$	114.6 ± 1.2
871	$Cu(L^{100}\text{-}H)Br$	116.6 ± 1.6
872	$Cu(L^{100}\text{-}H)(OAc)$	95.1 ± 0.4
873	$Cu(L^{100}\text{-}H)ClO_4 \cdot H_2O$	114.2 ± 0.8

Table 5.1. Continued

№	Formula	IC_{50} (μM)
874	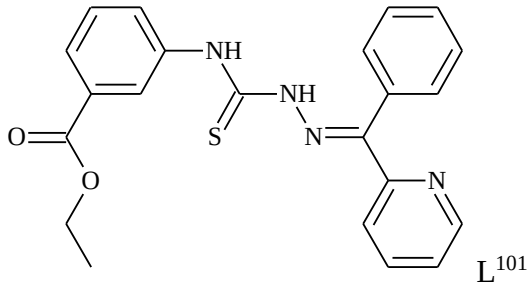 L^{101}	16.4 ± 0.8
875	$Cu(L^{101}\text{-}H)Cl$	≥100
876	$Cu(L^{101}\text{-}H)NO_3$	≥100
877	$Cu(L^{101}\text{-}H)Br$	≥100
878	$Cu(L^{101}\text{-}H)(OAc)$	100.3 ± 1.5
879	$Cu(L^{101}\text{-}H)ClO_4\cdot H_2O$	≥100
880	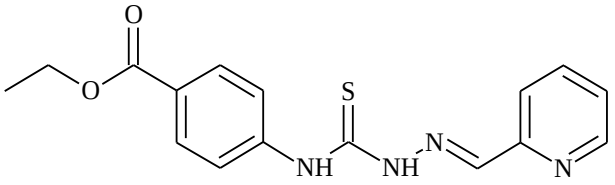 L^{102}	14.3 ± 0.6
881	$Cu(L^{102}\text{-}H)Cl$	6.6 ± 0.3
882	$Cu(L^{102}\text{-}H)Br$	9.1 ± 0.2
883	$Cu(L^{102}\text{-}H)NO_3\cdot H_2O$	8.0 ± 0.4
884	$Cu(L^{102}\text{-}H)(OAc)\cdot H_2O\cdot C_2H_5OH$	11.3 ± 0.3
885	$Cu(L^{102}\text{-}H)(ClO_4)\cdot C_2H_5OH$	13.3 ± 0.1
886	$Ni(L^{102}\text{-}H)Cl$	3.7 ± 0.6
887	$Ni(L^{102}\text{-}H)NO_3\cdot H_2O$	25.1 ± 0.7
888	$Ni(L^{102}\text{-}H)(OAc)\cdot H_2O$	61.3 ± 2.3
889	$Ni(L^{102}\text{-}H)Br\cdot H_2O$	48.2 ± 0.2
890	$Fe(L^{102}\text{-}H)_2Cl$	≥100
891	$Fe(L^{102}\text{-}H)_2NO_3$	83.2 ± 0.6
892	$Fe(L^{102}\text{-}H)_2Br$	≥100
893	$Zn(L^{102}\text{-}H)Cl\cdot H_2O$	23.4 ± 0.5
894	$Mn(L^{102}\text{-}H)_2$	14.0 ± 0.3
895	$Co(L^{102}\text{-}H)_2Cl$	≥100
896	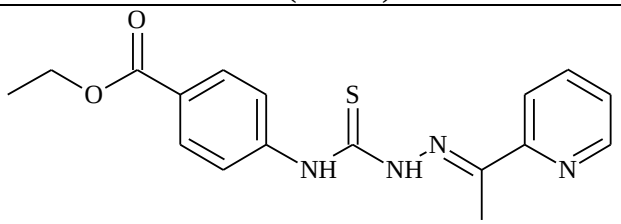 L^{103}	15.8 ± 0.4

Table 5.1. Continued

№	Formula	IC_{50} (μM)
897	$Cu(L^{103}\text{-}H)(OAc)\cdot H_2O$	95.1 ± 2.1
898	$Cu(L^{103}\text{-}H)Br\cdot H_2O$	33.5 ± 0.4
899	$Ni(L^{103}\text{-}H)Cl$	8.4 ± 0.1
900	$Ni(L^{103}\text{-}H)Br\cdot H_2O$	19.7 ± 0.8
901	$Fe(L^{103}\text{-}H)_2NO_3\cdot H_2O\cdot C_2H_5OH$	≥100
902	$Cu(L^{103}\text{-}H)(ClO_4)\cdot H_2O$	≥100
903	$Cu(L^{103}\text{-}H)NO_3$	83.3 ± 0.3
904	$Fe(L^{103}\text{-}H)_2Cl$	≥100
905	$Cu(L^{103}\text{-}H)Cl$	74.4 ± 0.7
906	$Fe(L^{103}\text{-}H)_2Br$	≥100
907	$Zn(L^{103}\text{-}H)Cl\cdot H_2O$	88.6 ± 1.4
908	$Co(L^{103}\text{-}H)_2Cl$	116.2 ± 1.9
909	$Mn(L^{103}\text{-}H)_2$	14.8 ± 0.8
910	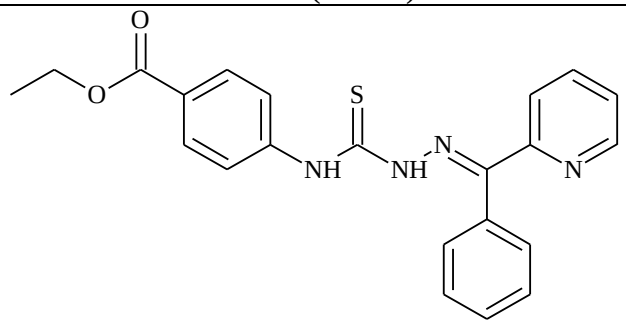 L^{104}	11.9 ± 0.2
911	$Cu(L^{104}\text{-}H)Cl$	≥100
912	$Cu(L^{104}\text{-}H)NO_3\cdot H_2O$	≥100
913	$Ni(L^{104}\text{-}H)Cl$	14.9 ± 0.1
914	$Ni(L^{104}\text{-}H)NO_3\cdot H_2O$	≥100
915	$Cu(L^{104}\text{-}H)(OAc)$	≥100
916	$Cu(L^{104}\text{-}H)Br$	≥100
917	$Cu(L^{104}\text{-}H)ClO_4\cdot H_2O$	≥100
918	$Fe(L^{104}\text{-}H)_2Cl$	≥100
919	$Fe(L^{104}\text{-}H)_2NO_3$	≥100
920	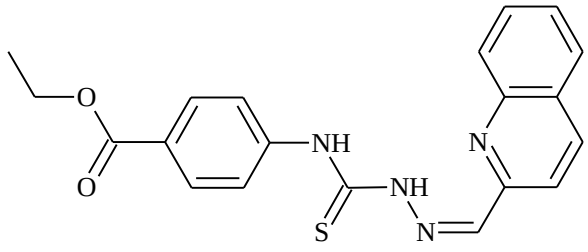 L^{105}	≥100
921	$Ni(L^{105}\text{-}H)Cl$	20.5 ± 0.1
922	$Cu(L^{105}\text{-}H)Cl$	65.3 ± 0.3

Table 5.1. Continued

№	Formula	IC_{50} (μM)
923	$Cu(L^{105}\text{-}H)(OAc)$	≥100
924	$Cu(L^{105}\text{-}H)(NO_3)$	≥100
925	$Cu(L^{105}\text{-}H)ClO_4 \cdot H_2O$	95.8 ± 3.5
926	$Cu(L^{105}\text{-}H)Br$	≥100
927	$Fe(L^{105}\text{-}H)_2NO_3$	≥100
928	$Fe(L^{105}\text{-}H)_2Br$	≥100
929	$Fe(L^{105}\text{-}H)_2Cl$	≥100
930	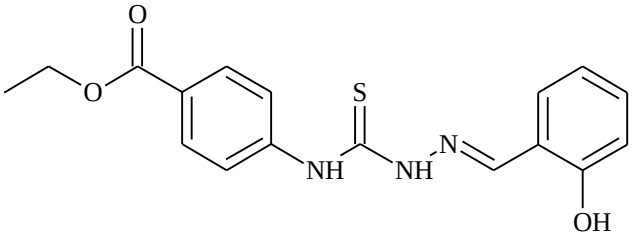 L^{106}	16.7 ± 0.8
931	$Cu(L^{106}\text{-}H)NO_3 \cdot H_2O$	35.8 ± 1.1
932	$Cu(L^{106}\text{-}H)OAc \cdot H_2O$	10.5 ± 0.4
933	$Co(L^{106}\text{-}H)_2NO_3$	10.7 ± 0.2
934	$Cu(L^{106}\text{-}H)ClO_4 \cdot H_2O$	11.5 ± 0.7
935	$Zn(L^{106}\text{-}2H) \cdot H_2O$	6.8 ± 0.9
936	$Fe(L^{106}\text{-}H)_2NO_3$	4.9 ± 0.2
937	$Fe(L^{106}\text{-}H)_2Br$	4.0 ± 0.4
938	$Ni(L^{106}\text{-}2H) \cdot H_2O$	6.7 ± 0.1
939	$Mn(L^{106}\text{-}2H)_2$	8.7 ± 0.2
940	$Cu(L^{106}\text{-}H)Br$	2.9 ± 0.7
941	$Cu(L^{106}\text{-}H)Cl$	32.5 ± 1.0
942	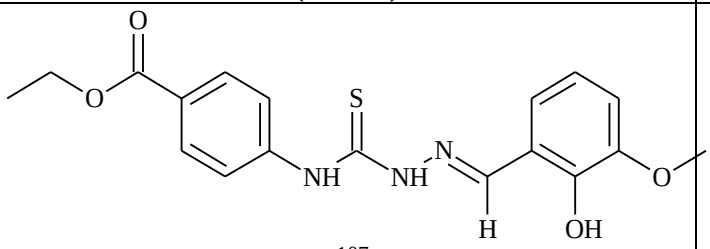 L^{107}	51.6 ± 0.2
943	$Cu(L^{107}\text{-}H)Cl \cdot H_2O$	13.1 ± 0.6
944	$Cu(L^{107}\text{-}2H) \cdot H_2O$	28.0 ± 0.3
945	$Cu(L^{107}\text{-}H)(NO_3) \cdot H_2O$	15.5 ± 0.9
946	$Cu(L^{107}\text{-}H)(ClO_4) \cdot H_2O$	8.7 ± 0.5
947	$Ni(L^{107}\text{-}H)Cl$	22.3 ± 0.1
948	$Ni(L^{107}\text{-}2H) \cdot H_2O$	25.9 ± 0.5
949	$Co(L^{107}\text{-}H)_2NO_3$	11.2 ± 0.6

Table 5.1. Continued

№	Formula	IC_{50} (μM)
950	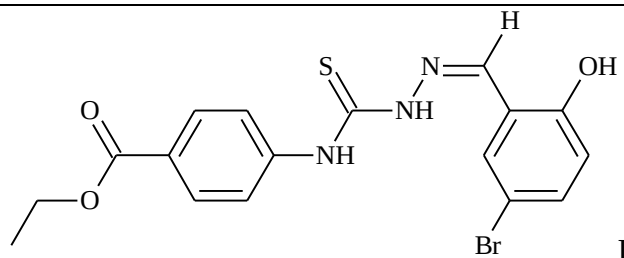 L^{108}	81.9 ± 0.6
951	$Cu(L^{108}\text{-}2H)\cdot H_2O$	≥100
952	$Cu(L^{108}\text{-}H)Br\cdot H_2O$	≥100
953	$Cu(L^{108}\text{-}H)Cl$	≥100
954	$Cu(L^{108}\text{-}H)(OAc)$	≥100
955	$Cu(L^{108}\text{-}H)(NO_3)$	≥100
956	$Ni(L^{108}\text{-}H)(NO_3)$	82.8 ± 1.6
957	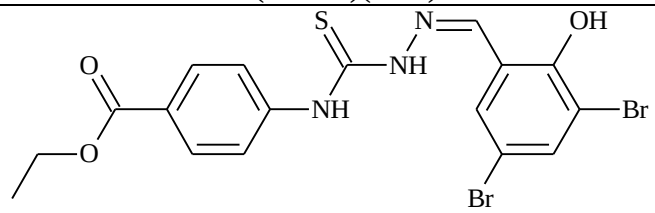 L^{109}	≥100
958	$Cu(L^{109}\text{-}2H)\cdot H_2O$	≥100
959	$Cu(L^{109}\text{-}H)Cl\cdot H_2O$	≥100
960	$Cu(L^{109}\text{-}H)(OAc)$	≥100
961	$Cu(L^{109}\text{-}H)(NO_3)$	≥100
962	$Cu(L^{109}\text{-}H)ClO_4\cdot H_2O$	≥100
963	$Ni(L^{109}\text{-}H)(NO_3)$	≥100
964	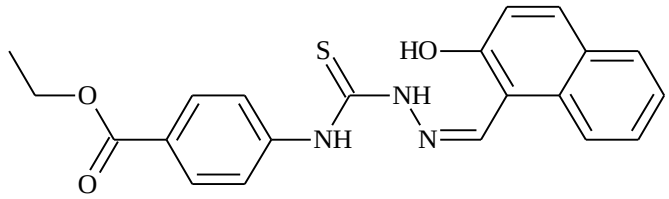 L^{110}	9.3 ± 0.1
965	$Cu(L^{110}\text{-}H)Cl\cdot H_2O$	95.1 ± 0.8
966	$Cu(L^{110}\text{-}2H)\cdot H_2O$	13.5 ± 0.2
967	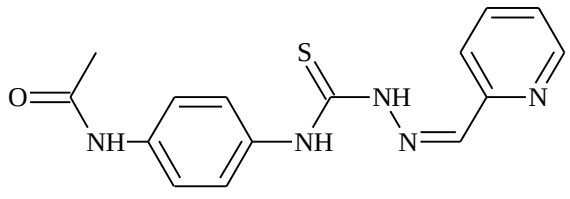 L^{111}	13.4 ± 0.3
968	$Ni(L^{111}\text{-}H)NO_3$	40.1 ± 0.4

Table 5.1. Continued

№	Formula	IC_{50} (μM)
969	$Ni(L^{111}\text{-}H)Cl$	29.7 ± 0.1
970	$Ni(L^{111}\text{-}H)(OAc)$	29.6 ± 0.7
971	$Ni(L^{111}\text{-}H)Br\cdot H_2O$	25.6 ± 0.2
972	$Cu(L^{111}\text{-}H)Cl\cdot H_2O$	9.2 ± 0.2
973	$Cu(L^{111}\text{-}H)Br\cdot H_2O$	43.3 ± 1.2
974	$Cu(L^{111}\text{-}H)HSO_4\cdot H_2O$	38.5 ± 1.4
975	$Cu(L^{111}\text{-}H)NO_3\cdot H_2O$	30.5 ± 0.6
976	$Cu(L^{111}\text{-}H)(OAc)\cdot H_2O$	21.3 ± 0.4
977	$Co(L^{111}\text{-}H)_2NO_3$	6.0 ± 0.2
978	$Co(L^{111}\text{-}H)_2Br$	6.1 ± 0.4
979	$Co(L^{111}\text{-}H)_2Cl$	6.2 ± 0.4
980	$Co(L^{111}\text{-}H)_2OAc$	7.7 ± 0.7
981	$Fe(L^{111}\text{-}H)_2Br$	8.8 ± 0.1
982	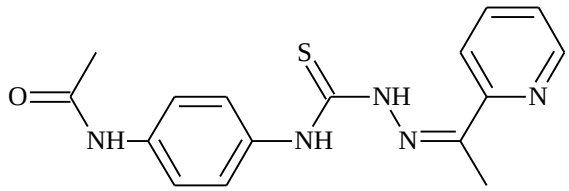 L^{112}	8.5 ± 0.4
983	$Cu(L^{112}\text{-}H)Cl$	24.3 ± 0.2
984	$Cu(L^{112}\text{-}H)NO_3$	23.3 ± 0.9
985	$Ni(L^{112}\text{-}H)Cl$	24.0 ± 0.1
986	$Cu(L^{112}\text{-}H)ClO_4\cdot H_2O$	10.1 ± 0.3
987	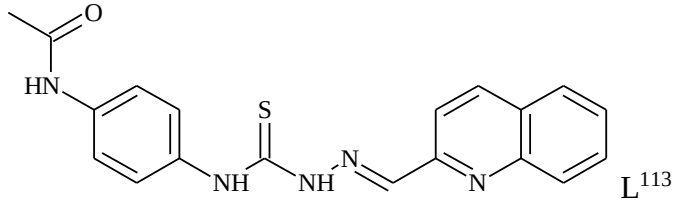 L^{113}	13.1 ± 0.5
988	$Cu(L^{113}\text{-}H)Br$	18.6 ± 0.3
989	$Cu(L^{113}\text{-}H)Cl$	14.3 ± 0.8
990	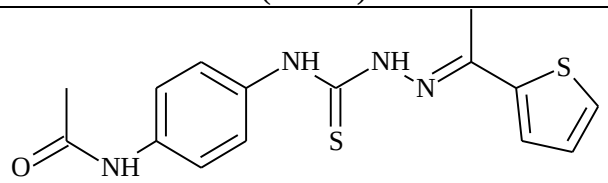	14.6 ± 0.1
991	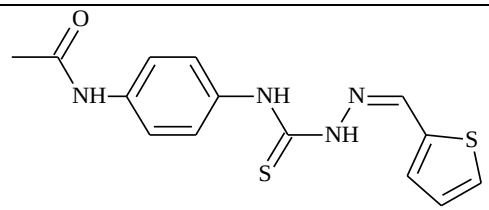	≥100

Table 5.1. Continued

№	Formula	IC_{50} (μM)
992	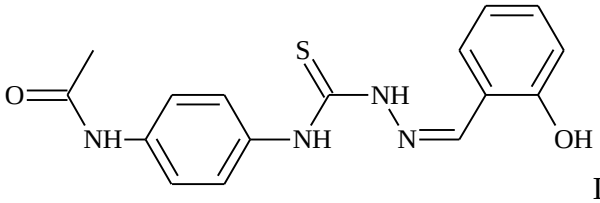 L^{114}	6.6 ± 0.1
993	$Co(L^{114}\text{-}H)_2NO_3 \cdot H_2O$	6.5 ± 0.1
994	$Ni(L^{114}\text{-}H)_2 \cdot H_2O$	14.3 ± 0.2
995	$Ni(L^{114}\text{-}H)Cl \cdot H_2O$	8.9 ± 0.5
996	$Ni(L^{114}\text{-}H)(OAc)$	2.8 ± 0.6
997	$Co(L^{114}\text{-}H)_2Br$	12.0 ± 0.1
998	$Co(L^{114}\text{-}H)_2Cl$	17.8 ± 0.2
999	$Co(L^{114}\text{-}H)_2(OAc)$	21.2 ± 0.7
1000	$Cu(L^{114}\text{-}H)ClO_4 \cdot H_2O$	28.5 ± 0.4
1001	$Cu(L^{114}\text{-}H)Br \cdot H_2O$	32.5 ± 0.7
1002	$Cu(L^{114}\text{-}2H)(H_2O)$	12.7 ± 0.4
1003	$Cu(L^{114}\text{-}H)Cl \cdot H_2O$	30.3 ± 0.6
1004	$Cu(L^{114}\text{-}H)(NO_3) \cdot H_2O$	10.9 ± 0.2
1005	$Co(L^{114}\text{-}H)_2Br \cdot H_2O$	17.1 ± 0.8
1006	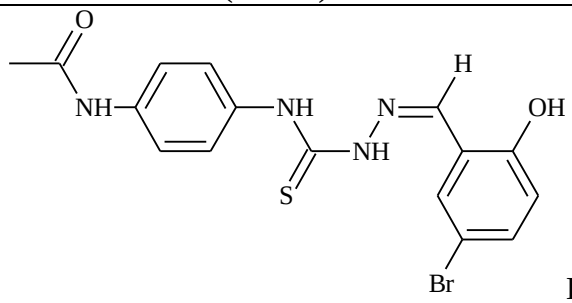 L^{115}	14.9 ± 0.1
1007	$Cu(L^{115}\text{-}2H)(H_2O)$	8.7 ± 0.5
1008	$Cu(L^{115}\text{-}H)(OAc) \cdot H_2O$	4.9 ± 0.3
1009	$Cu(L^{115}\text{-}H)(NO_3) \cdot H_2O$	6.6 ± 0.3
1010	$Cu(L^{115}\text{-}H)(ClO_4) \cdot H_2O$	2.4 ± 0.1
1011	$Ni(L^{115}\text{-}H)(NO_3) \cdot H_2O$	14.5 ± 0.6
1012	$Ni(L^{115}\text{-}H)(OAc)$	13.2 ± 0.3
1013	$Ni(L^{115}\text{-}H)_2 \cdot H_2O \cdot C_2H_5OH$	4.1 ± 0.4
1014	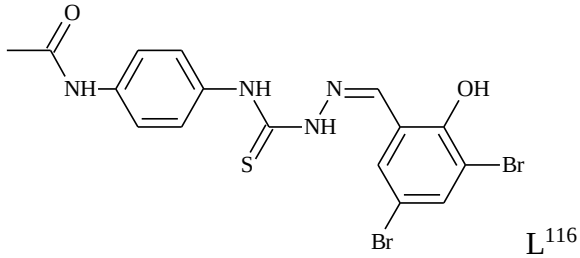 L^{116}	17.4 ± 0.7

Table 5.1. Continued

№	Formula	IC_{50} (μM)
1015	$Cu(L^{116}\text{-}H)Br\cdot H_2O$	27.2 ± 0.2
1016	$Cu(L^{116}\text{-}2H)(H_2O)$	31.9 ± 0.3
1017	$Cu(L^{116}\text{-}H)ClO_4\cdot C_2H_5OH$	38.9 ± 1.0
1018	$Cu(L^{116}\text{-}2H)\cdot H_2O\cdot C_2H_5OH$	15.0 ± 0.8
1019	$Ni(L^{116}\text{-}H)Cl$	28.8 ± 0.6
1020	$Ni(L^{116}\text{-}H)(OAc)\cdot H_2O$	22.3 ± 0.4
1021	$Ni(L^{116}\text{-}H)(NO_3)\cdot H_2O$	12.3 ± 0.3
1022	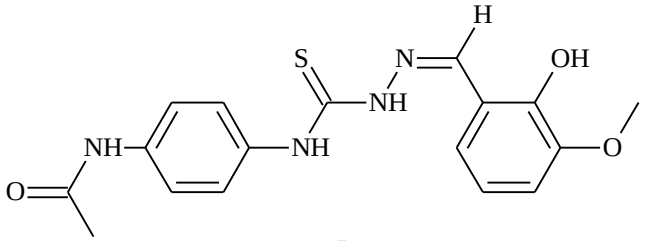 L^{117}	15.8 ± 0.2
1023	$Cu(L^{117}\text{-}2H)(H_2O)$	19.1 ± 0.2
1024	$Cu(L^{117}\text{-}H)NO_3\cdot H_2O$	15.1 ± 0.4
1025	$Ni(L^{117}\text{-}H)(OAc)\cdot H_2O$	6.9 ± 0.2
1026	$Cu(L^{117}\text{-}H)Cl\cdot H_2O$	15.6 ± 0.2
1027	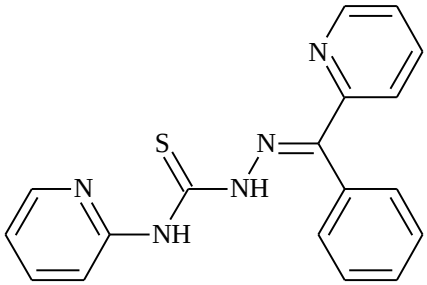 L^{118}	11.3 ± 0.4
1028	$Cu(L^{118}\text{-}H)Cl$	17.1 ± 0.6
1029	$Zn(L^{118}\text{-}H)Cl$	6.7 ± 0.1
1030	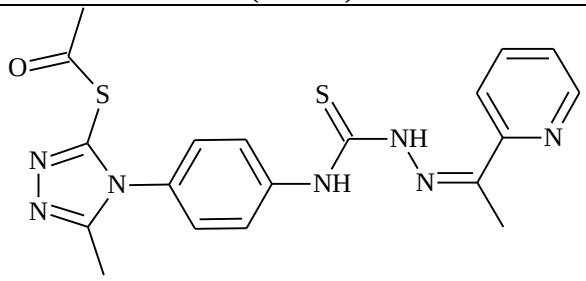	11.0 ± 0.4

Table 5.1. Continued

№	Formula	IC_{50} (μM)
1031	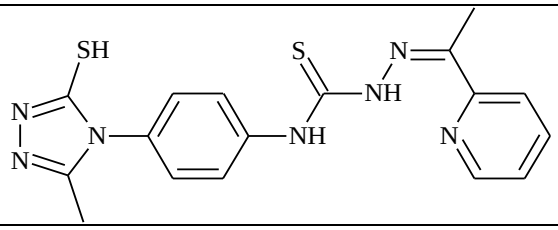	7.0 ± 0.3
1032	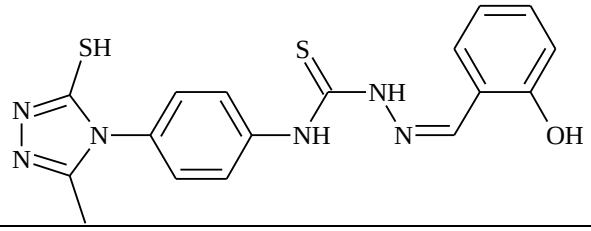	14.8 ± 0.5
1033	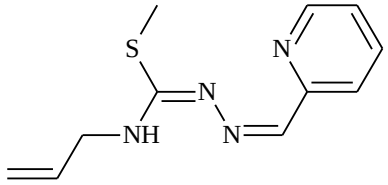 L^{119}	≥ 100
1034	L^{119}·HI	≥ 100
1035	$Cu(L^{119})(NO_3)_2$	≥ 100
1036	$Cu(L^{119})Cl_2$	≥ 100
1037	$Cu(L^{119})Br_2$	≥ 100
1038	$Cu(L^{119})(ClO_4)_2$	≥ 100
1039	$Co(L^{119}\text{-}H)_2I$	≥ 100
1040	$Co(L^{119}\text{-}H)_2(NO_3)$	≥ 100
1041	$Cu(Im)(L^{119})(NO_3)_2$	≥100
1042	$Cu(4\text{-}Pic)(L^{119})(NO_3)_2$	16.6 ± 0.1
1043	$Cu(3.4\text{-}Lut)(L^{119})(NO_3)_2$	10.1 ± 0.1
1044	$Cu(2.2'\text{-}BPy)(L^{119})(NO_3)_2$	≥ 100
1045	$Cu(1.10\text{-}Phen)(L^{119})(NO_3)_2$	≥ 100
1046	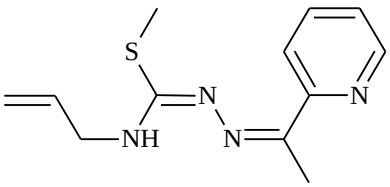 L^{120}	≥ 100
1047	$Cu(L^{120})SO_4$	≥100
1048	$Cu(L^{120})Cl_2$	≥100
1049	$Cu(L^{120})Br_2$	≥100
1050	$Ni(L^{120})_2(ClO_4)_2$	25.1 ± 0.1
1051	$Co(L^{120}\text{-}H)_2NO_3$	≥100
1052	$Co(L^{120}\text{-}H)_2I$	≥100

Table 5.1. Continued

№	Formula	IC_{50} (μM)
1053	$Cu(L^{120})(NO_3)_2$	≥ 100
1054	$Fe(L^{120}\text{-}H)_2Br$	≥ 100
1055	$Co(L^{120}\text{-}H)_2Cl$	≥ 100
1056	$Ni(L^{120})_2(NO_3)_2$	21.5 ± 0.4
1057	$Cu(L^{121})Br_2$ 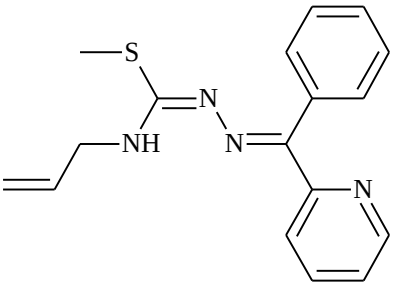 Where L^{121} is	45.9 ± 0.4
1058	$Cu(L^{121})(NO_3)_2$	104.4 ± 2.4
1059	$Cu(L^{121}\text{-}H)(OAc)$	≥100
1060	$Cu(L^{121})Cl_2$	≥100
1061	$Ni(L^{121})_2(NO_3)_2$	21.1 ± 0.4
1062	$Ni(L^{121})_2(ClO_4)_2$	22.0 ± 0.5
1063	$Co(L^{121}\text{-}H)_2(OAc)$	≥100
1064	$Co(L^{121}\text{-}H)_2NO_3$	≥100
1065	$Zn(L^{121})I_2$	55.7 ± 0.8
1066	$Fe(L^{122}\text{-}H)_2NO_3$ 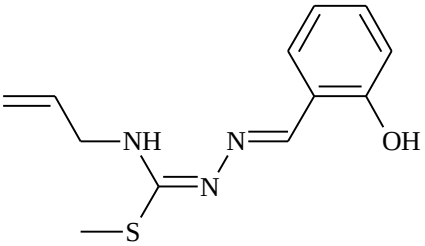 Where L^{122} is	10.0 ± 0.2
1067	$Fe(L^{122}\text{-}H)_2Cl$	9.4 ± 0.3
1068	$Co(L^{122}\text{-}H)_2NO_3$	7.1 ± 0.2
1069	$Co(L^{122}\text{-}H)_2Cl$	23.2 ± 0.6
1070	$Co(L^{122}\text{-}H)_2Br$	24.4 ± 0.7
1071	$Co(L^{122}\text{-}H)_2I$	21.7 ± 0.6
1072	$Cr(L^{122}\text{-}H)_2NO_3$	1.2 ± 0.1
1073	$Cu(Py)(L^{122}\text{-}H)NO_3$	46.6 ± 0.9
1074	$Cu(3\text{-}Pic)(L^{122}\text{-}H)NO_3$	53.1 ± 0.2
1075	$Cu(Im)(L^{122}\text{-}H)NO_3$	48.9 ± 0.7
1076	$Cu(3.4\text{-}Lut)(L^{122}\text{-}H)NO_3$	47.0 ± 0.1
1077	$Cu(1.10\text{-}Phen)(L^{122}\text{-}H)NO_3$	11.6 ± 0.5

Table 5.1. Continued

№	Formula	IC_{50} (μM)
1078	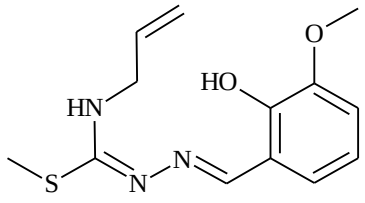 L^{123}	8.8 ± 0.3
1079	$L^{123}\cdot HI$	7.7 ± 0.4
1080	$Cu(L^{123}\text{-}H)Cl$	20.9 ± 0.3
1081	$Cu(L^{123}\text{-}H)NO_3$	38.9 ± 0.4
1082	$Ni(L^{123})(L^{123}\text{-}H)NO_3$	15.5 ± 0.1
1083	$Ni(L^{123})(L^{123}\text{-}H)I$	8.3 ± 0.3
1084	$Co(L^{123}\text{-}H)_2NO_3$	20.9 ± 0.7
1085	$Co(L^{123}\text{-}H)_2I$	19.2 ± 0.1
1086	$Co(L^{123}\text{-}H)_2Cl$	23.1 ± 0.4
1087	$Fe(L^{123}\text{-}H)_2NO_3$	9.6 ± 0.5
1088	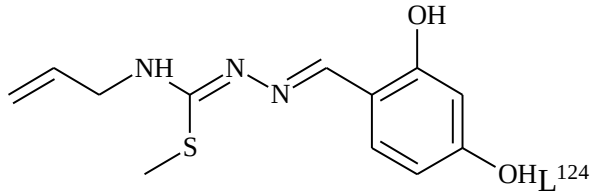 L^{124}	13.1 ± 0.8
1089	$Cu(L^{124}\text{-}H)Br$	26.2 ± 1.8
1090	$Fe(L^{124}\text{-}H)_2NO_3$	7.5 ± 0.6
1091	$Co(L^{124}\text{-}H)_2I$	10.3 ± 0.4
1092	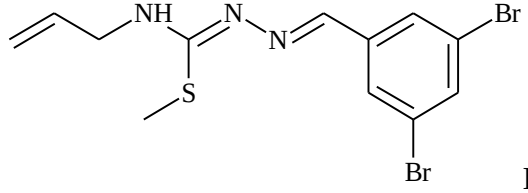 L^{125}	30.1 ± 0.5
1093	$Cu(L^{125}\text{-}H)Cl$	≥ 100
1094	$Cu(L^{125}\text{-}H)Br$	≥ 100
1095	$Cu(L^{125}\text{-}H)(OAc)$	≥ 100
1096	$Ni(L^{125})(L^{125}\text{-}H)I$	13.5 ± 0.2
1097	$Fe(L^{125}\text{-}H)_2NO_3$	97.9 ± 0.4
1098	$Co(L^{125}\text{-}H)_2I$	100.6 ± 1.8
1099	$Co(L^{125}\text{-}H)_2NO_3$	80.6 ± 2.2
1100	$L^{126}\cdot HI$ Where L^{126} is 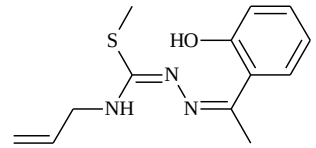	8.7 ± 0.5

Table 5.1. Continued

№	Formula	IC_{50} (μM)
1101	$Cu(L^{126}\text{-}H)Cl$	13.1 ± 0.5
1102	$Cu(L^{126}\text{-}H)NO_3$	12.2 ± 0.4
1103	$Cu(L^{126}\text{-}H)ClO_4$	16.3 ± 0.8
1104	$Cu(L^{126}\text{-}H)(OAc)$	19.8 ± 0.2
1105	$Ni(L^{126}\text{-}H)_2$	6.0 ± 0.4
1106	$Co(L^{126}\text{-}H)_2NO_3$	14.5 ± 0.5
1107	$Co(L^{126}\text{-}H)_2Br$	7.5 ± 0.3
1108	$Co(L^{126}\text{-}H)_2I$	15.3 ± 0.7
1109	$Fe(L^{126}\text{-}H)_2NO_3$	2.1 ± 0.1
1110	$Cu(L^{127}\text{-}H)ClO_4$ 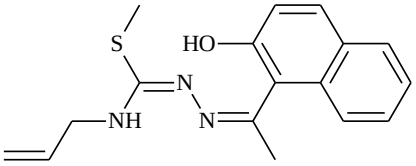 Where L^{127} is	11.9 ± 0.7
1111	$Ni(L^{127})(L^{127}\text{-}H)ClO_4$	5.2 ± 0.7
1112	$Co(L^{127}\text{-}H)_2NO_3$	16.5 ± 0.9
1113	$Cr(L^{127}\text{-}H)_2NO_3$	1.4 ± 0.3
1114	$Ni(L^{127}\text{-}H)_2$	8.6 ± 0.5
1115	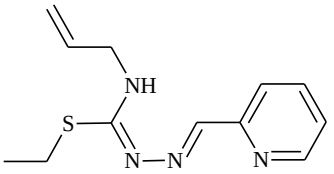 L^{128}	51.2 ± 0.5
1116	$Cu(L^{128}\text{-}H)Cl$	108.0 ± 1.5
1117	$Co(L^{128}\text{-}H)_2I$	≥100
1118	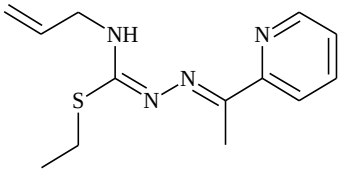 L^{129}	≥100
1119	$L^{129}\cdot HI$	41.2 ± 0.2
1120	$Co(L^{129}\text{-}H)_2I$	≥100
1121	$Ni(L^{129})_2I_2$	16.7 ± 0.2
1122	$L^{130}\cdot HI$ 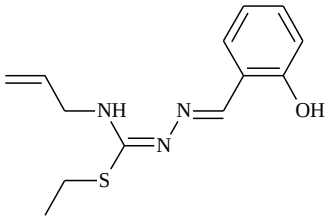 Where L^{130} is	13.7 ± 0.6

Table 5.1. Continued

№	Formula	IC_{50} (μM)
1123	$Cu(L^{130}\text{-}H)NO_3$	27.9 ± 0.4
1124	$Cu(L^{130}\text{-}H)Br$	38.6 ± 0.3
1125	$Ni(L^{130})(L^{130}\text{-}H)ClO_4$	8.0 ± 0.2
1126	$Fe(L^{130}\text{-}H)_2NO_3$	12.5 ± 0.1
1127	$Co(L^{130}\text{-}H)_2NO_3$	19.3 ± 0.3
1128	$Cu(L^{130}\text{-}H)Cl$	13.7 ± 0.1
1129	$Ni(L^{130})(L^{130}\text{-}H)I$	6.2 ± 0.6
1130	$Co(L^{130}\text{-}H)_2I$	30.1 ± 0.4
1131	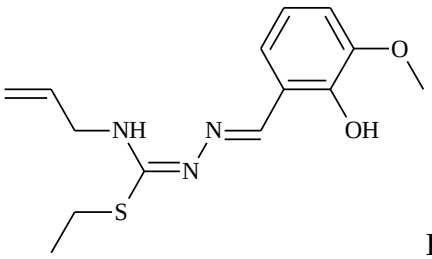 L^{131}	6.9 ± 0.4
1132	$L^{131}\cdot HI$	8.6 ± 0.4
1133	$Co(L^{131}\text{-}H)_2I$	19.0 ± 0.6
1134	$Ni(L^{131}\text{-}H)_2$	12.0 ± 0.6
1135	$Co(L^{131}\text{-}H)_2Br$	17.9 ± 0.1
1136	$Co(L^{131}\text{-}H)_2(OAc)$	23.2 ± 0.7
1137	$Co(L^{131}\text{-}H)_2NO_3$	21.7 ± 0.7
1138	$Fe(L^{131}\text{-}H)_2NO_3$	4.0 ± 0.1
1139	$L^{132}\cdot HI$ 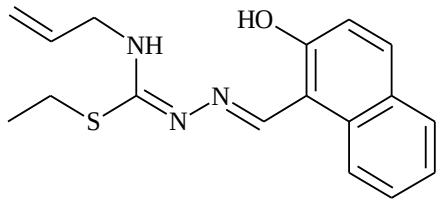 Where L^{132} is	6.2 ± 0.2
1140	$Co(L^{132}\text{-}H)_2I$	16.0 ± 0.4
1141	$L^{133}\cdot HI$ 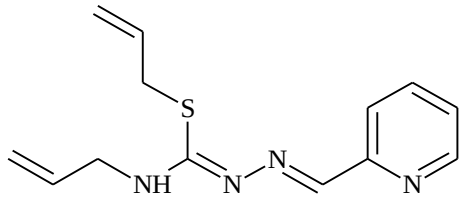 Where L^{133} is	28.5 ± 1.0
1142	$Cu(L^{133})Cl_2$	88.4 ± 0.5
1143	$Cu(L^{133})Br_2$	35.7 ± 1.1
1144	$Co(L^{133}\text{-}H)_2I$	25.7 ± 0.5

Table 5.1. Continued

№	Formula	IC_{50} (μM)
1145	$Co(L^{133}\text{-}H)_2NO_3$	19.9 ± 0.1
1146	$Co(L^{133}\text{-}H)_2Cl$	25.9 ± 0.4
1147	$Fe(L^{133}\text{-}H)_2NO_3$	27.4 ± 0.4
1148	$Fe(L^{133}\text{-}H)_2Br$	20.8 ± 1.0
1149	$Ni(L^{133})_2(NO_3)_2$	27.3 ± 0.7
1150	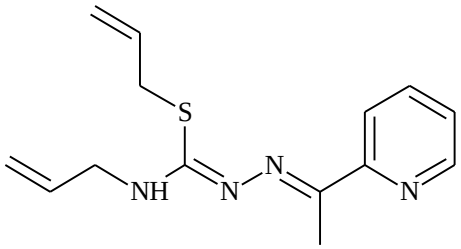 L^{134}	≥100
1151	$L^{134}\cdot HI$	49.9 ± 0.5
1152	$Cu(L^{134})Br_2$	65.6 ± 0.3
1153	$Cu(L^{134})(NO_3)_2$	25.1 ± 0.2
1154	$Cu(L^{134})Cl_2$	65.5 ± 0.5
1155	$Ni(L^{134})_2(NO_3)_2$	23.2 ± 0.4
1156	$Fe(L^{134}\text{-}H)_2NO_3$	69.4 ± 0.9
1157	$Ni(L^{134})_2I_2$	11.6 ± 0.3
1158	$Co(L^{134}\text{-}H)_2I$	72.4 ± 1.1
1159	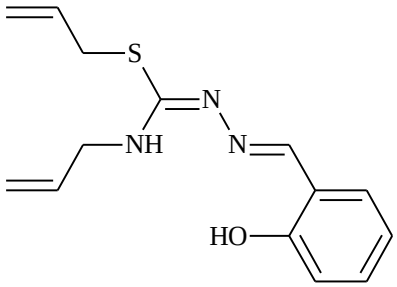 L^{135}	26.8 ± 0.2
1160	$L^{135}\cdot HI$	17.8 ± 0.1
1161	$Cu(L^{135}\text{-}H)Cl$	12.5 ± 0.4
1162	$Cu(L^{135}\text{-}H)NO_3$	10.3 ± 0.3
1163	$Cu(L^{135}\text{-}H)(Cl_2CHCOO)$	13.1 ± 0.4
1164	$Cu(L^{135}\text{-}H)(OAc)$	10.1 ± 0.1
1165	$Cu(1.10\text{-}Phen)(L^{135}\text{-}H)NO_3$	≥100
1166	$Cu(Im)(L^{135}\text{-}H)NO_3$	14.4 ± 0.1
1167	$Cu(3.4\text{-}Lut)(L^{135}\text{-}H)NO_3$	11.5 ± 0.2
1168	$Ni(L^{135}\text{-}H)(OAc)$	7.2 ± 0.5
1169	$Co(L^{135}\text{-}H)_2Cl$	9.3 ± 0.1
1170	$Fe(L^{135}\text{-}H)_2NO_3$	7.3 ± 0.1
1171	$Co(L^{135}\text{-}H)_2I$	7.5 ± 0.1

Table 5.1. Continued

№	Formula	IC_{50} (μM)
1172	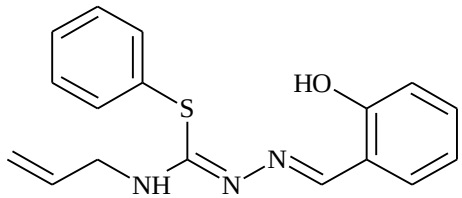 L^{136}	34.0 ± 1.9
1173	$Cu(L^{136}\text{-}H)Cl$	≥100
1174	$Cu(L^{136}\text{-}H)Br$	≥100
1175	$Cu(L^{136}\text{-}H)NO_3$	≥100
1176	$Cu(L^{136}\text{-}H)(OAc)$	≥100
1177	$Ni(L^{136}\text{-}H)_2$	≥100
1178	$Co(L^{136}\text{-}H)_2Cl$	≥100
1179	$Co(L^{136}\text{-}H)_2Br$	≥100
1180	$Fe(L^{136}\text{-}H)_2Cl$	22.3 ± 0.2
1181	$Fe(L^{136}\text{-}H)_2Br$	40.4 ± 1.3
1182	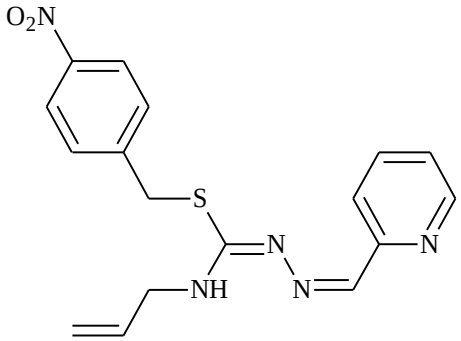 L^{137}	32.4 ± 0.4
1183	$L^{137}\cdot HBr$	23.9 ± 1.2
1184	$Cu(L^{137})Br_2$	25.7 ± 0.2
1185	$Cu(L^{137})Cl_2$	21.8 ± 0.4
1186	$Fe(L^{137}\text{-}H)_2Cl$	35.1 ± 0.3
1187	$Fe(L^{137}\text{-}H)_2Br$	66.0 ± 0.5
1188	$Co(L^{137}\text{-}H)_2Br$	≥100
1189	$Co(L^{137}\text{-}H)_2NO_3$	≥100
1190	$Co(L^{137}\text{-}H)_2Cl$	≥100
1191	$Ni(L^{137})_2(NO_3)_2$	≥100
1192	$Ni(L^{137})_2Br_2$	55.4 ± 2.5
1193	$Ni(L^{137})_2Cl_2$	55.9 ± 1.5
1194	$Ni(L^{137})Cl_2$	41.8 ± 1.0
1195	$Zn(L^{137}\text{-}H)Cl$	4.4 ± 0.1
1196	$Zn(L^{137}\text{-}H)Br$	26.6 ± 0.5

Table 5.1. Continued

№	Formula	IC_{50} (μM)
1197	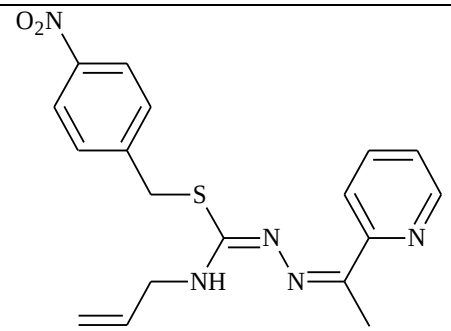 L^{138}	≥100
1198	$Cu(L^{138})Cl_2$	≥100
1199	$Cu(L^{138})Br_2$	≥100
1200	$Cu(L^{138})(NO_3)_2$	≥100
1201	$Cu(L^{138}\text{-}H)(OAc)$	≥100
1202	$Ni(L^{138})_2Br_2$	88.7 ± 1.6
1203	$Ni(L^{138})_2(NO_3)_2$	83.9 ± 1.5
1204	$Fe(L^{138}\text{-}H)_2Cl$	≥100
1205	$Fe(L^{138}\text{-}H)_2NO_3$	≥100
1206	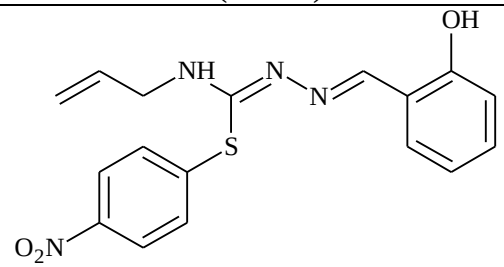 L^{139}	31.0 ± 1.3
1207	$Cu(L^{139}\text{-}H)Cl$	≥ 100
1208	$Ni(L^{139}\text{-}H)_2$	48.8 ± 0.1
1209	$Co(L^{139}\text{-}H)_2NO_3$	≥ 100
1210	$Fe(L^{139}\text{-}H)_2Br$	≥ 100
1211	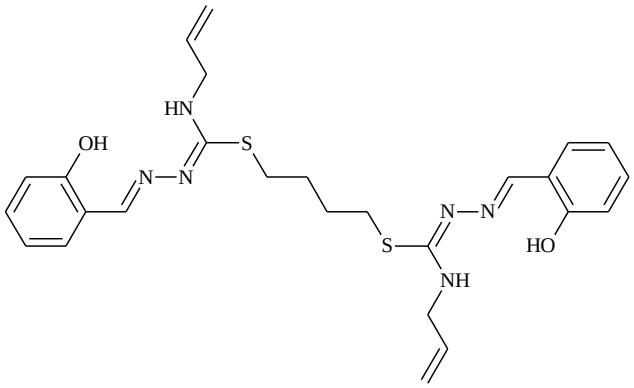 L^{140}	46.3 ± 0.6
1212	$Cu_2(L^{140}\text{-}2H)Cl_2$	8.8 ± 0.6

Table 5.1. Continued

№	Formula	IC_{50} (μM)
1213	$Cu_2(L^{140}\text{-}2H)Br_2$	9.7 ± 0.2
1214	$Cu_2(L^{140}\text{-}2H)(NO_3)_2$	31.9 ± 1.0
1215	$Ni_2(L^{140}\text{-}4H)(H_2O)_2$	42.9 ± 0.2
1216	$Ni_2(L^{140}\text{-}4H)(H_2O)_2$	73.8 ± 1.3
1217	$Ni_2(L^{140}\text{-}2H)(ClO_4)_2$	22.6 ± 0.3

Dose-response plots of percent inhibition versus concentration were obtained from triplicate samples and adjusted to sigmoidal curves, from which values of the 50% inhibitory concentration (IC_{50}) were calculated. $p < 0.05$, significantly different from the student's t-test.

It was found, that the reference compounds Trolox, Rutin, and DOXO exhibited antioxidant activity with IC_{50} values of 33.3±0.7 μM, 20.7±0.1 μM, 11.5±0.6 μM, respectively.

Annexes 1 and 2 provide the IC_{50} rate of compounds against $ABTS^{\bullet+}$ radical cation with a strong antioxidant activity, which exceeds the activity of Trolox. The $ABTS^{\bullet+}$ radical-scavenging measurement method, which is commonly used to evaluate antioxidant activity, takes advantage of the fact that $ABTS^{\bullet+}$ free radicals become stable by accepting a hydrogen ion from the antioxidant, losing their blue colors. Moreover, in the ABTS assay as well as in the DPPH assay, when antioxidant activity occurs, the ability to eliminate hydroxyl radicals or superoxide radicals through physiologic action or oxidation is evaluated with a high index indicating a strong antioxidant activity. ABTS radical-scavenging through antioxidant activity is well known to be attributable to their hydrogen-donating ability (Annexes 1 and 2). The concentration of these compounds required to inhibit 50% of the radical-scavenging effect (IC_{50}) has been determined by testing a series of concentrations. In particular, the azomethines, isothiocyanates, thioureas, hydrazones, triazoles, thiosemicarbazides substituted in the fourth position, and thiosemicarbazones showed the strongest antioxidant activity (Annex 1). The activity of the most widely represented thiosemicarbazones in annex 1 depends both on the nature of the substituent in the fourth position and on the residue of the carbonyl compound. In many cases, the presence in the fourth position of hydroxy-, dihydroxy-, trihydroxybenzylidene fragment is superior to the corresponding analogs with other substituents.

The most active coordination compounds are represented in annex 2. In addition to the nature of the ligand, the nature of the central atom greatly influences the activity of complexes. In many cases, nickel, zinc, and iron complexes significantly outperform the activity of copper and cobalt complexes. At the same

time, the presence of a 2-formylpyridine fragment in thiosemicarbazone often decreases the activity of the complexes formed by them.

In most cases, complexes exhibit less activity than ligands. Obviously, the coordination of organic molecules to the metal center leads to a marked decrease in their AOA.

In this study, 474 complexes and 248 ligands demonstrated to possess potential applications as antioxidants, demonstrating AOA higher than Trolox and Rutin (Annexes 1 and 2).

Many copper complexes with such thiosemicarbazones did not show antioxidant activity (IC_{50} >100), although it is known from the literature that these complexes often exhibit high antimicrobial, anticancer, and other activities.

Classical ligands such as oxalate (Ox), iminodiacetate (IDA), nitrilotriacetate (HNTA), or ethylenediaminetetraacetate (EDTA) does not exhibit any activity against radicals ABTS, while the corresponding Mo-complexes gives, for the best ones, moderate IC_{50} values. In contrast, when the Mo core is associated with L-Cysteine (L-Cys), which possesses intrinsic moderate antioxidative activity, the corresponding complexes appear highly efficient with IC_{50} up to ten times better than for Trolox and Rutin. The combination of the redox active cluster $[Mo_2O_2S_2]^{2+}$ and a redox-active ligand such as thiosemicarbazones leads to a new class of complexes of interest against free radicals [257, 258].

The experiment showed that the proligand 2-acetylpyridine N^4-allyl-*S*-methylisothiosemicarbazone (HL) and 3d metal coordination compounds zinc(II), copper(II), nickel(II), iron(III), and cobalt(III) coordination compounds, $[Zn(HL)I_2]$, $[Cu(HL)Cl_2]$, $[Cu(HL)Br_2]$ (3), {$[Cu(HL)NO_3]$ NO_3}n, $[Ni(HL)_2](NO3)_2$, $[Fe(L)_2]NO_3$, $[Co(L)_2]NO_3$, and [Co(L)2]Cl·H_2O do not manifest any significant antiradical activity against $ABTS^{\bullet+}$ as the obtained values of semimaximum inhibition $IC_{50} \geq 100$ μM [259].

The thiosemicarbazones 2-formylpyridine *N*4-allylthiosemicarbazone (HL) (3-formylpyridine N^4-allylthiosemicarbazone (HL^a) and 4formylpyridine *N*4-allylthiosemicarbazone (HL^b) manifest high antiradical activity toward $ABTS^{\bullet+}$ with IC_{50} values 14.2–20.6 μM comparing to the Trolox (IC_{50} value 33μM). Meanwhile complexes of copper(II) ([Cu(L)Cl], [Cu(L)Br], $[Cu_2(L)_2(CH_3COO)_2]\cdot 4H_2O$, and cobalt(III) $[Co(L)_2]Cl$ manifest much lower antiradical activity (IC_{50}>40μM). The nickel(II) complex $[Ni(HL)_2]Cl_2\cdot H_2O$ manifests the highest antiradical activity with IC_{50} value 8.6±0.1μM [260].

As a result of our investigations on the AOA of various compounds, six patents have been registered.

BOPI nr. 6/2019.MD 4636 [4-(2,4-Dimethylphenyl)-2-(2-hydroxy-3-methoxybenzylidene) hydrazinecarbothioamide-*S*][4-(2,4-dimethylphenyl)-2-(oxo-3-methoxybenzylidene) hydrazinecarbothioamido(2-)-*O,N,S*]-nickel(II) monoethanol solvate as an antioxidant.

The invention relates to chemistry and medicine, namely to a biologically active coordinative nickel compound from the class of transition metal thiosemicarbazones. The compound exhibits high antioxidant activity and can find application in medicine as a substance that inhibits the oxidation processes of organic molecules in the human body. Summary of the invention consists in producing a synthetic antioxidant based on [4- (2,4-dimethylphenyl)-2-(2-hydroxy-3-methoxybenzylidene)hydrazinecarbothioamide -*S*][4-(2,4-dimethylphenyl)-2-(oxo-3- methoxybenzylidene)hydrazinecarbothioamido (2-)-*O,N,S*]-nickel(II) monoethanol.The claimed compound expands the arsenal of synthetic antioxidants with high biological activity [261].

BOPI nr. 11/2017.MD 4527 Use of salicylidene-4-allyl-S-methylisothiosemicarbazidates of iron(III) and cobalt(III) as antioxidants.

The invention relates to chemistry and medicine, namely to the use as antioxidants of salicylidene-4-allyl-Smethylisothiosemicarbazidates of the iron(III) and cobalt(III). They can be used in medicine as substances that inhibit the oxidative processes of organic molecules in the human body, with a concentration of half-maximal inhibition IC50 of 0.5…0.7 μM [262].

BOPI nr. 3/2017.MD 4469 Use of di(μ-S)-bis{(4-aminobenzenesulphamide)-chloro-[2-picolidene-4- phenylthiosemicarbazidato-(1-)]-copper(II)} as an antioxidant.

The invention relates to chemistry and medicine, namely to the use of a coordinative compound from the class of thiosemicarbazones of biometals as an antioxidant and can be used in medicine as a substance that inhibits or substantially reduces the oxidation processes of organic molecules in the human body. Summary of the invention consists in the use as an antioxidant of di(μ-S)-bis{(4-aminobenzenesulphamide)-chloro-[2- picolidene-4-phenylthiosemicarbazidato-(1-)]- copper(II)}. The technical result of the invention is to establish in this compound the antioxidative activity, which 33.3 times exceeds the activity of Trolox and 1.6 times the analogous characteristics of the most active synthetic antioxidant containing a thioamidic fragment – the coumarylthiazole derivative [263].

BOPI nr. 5/2020.MD 4698 Catena-(μ-nitrato-O,O'-O''-{methyl-*N*-(prop-2-en-1-yl)-2-[1-(pyridine-2-

yl)ethylidene]hydrazinecarbimidothioate}copper(II) nitrate compound as superoxide radical inhibitors.

The invention relates to chemistry and medicine, namely to a biologically active coordination compound of copper from the class of transition metal isothiosemicarbazidates. This complex exhibits antiradical activity, inhibiting superoxide radicals in the body. Due to these properties, it can be used in medicine as a drug that prevents the development of cellular and tissue lesions, atherosclerosis, and carcinogenesis. According to the invention, claimed is catena-(μ-nitrato-O,O'-O"-{methyl-*N*-(prop-2- en-1-yl)-2-[1-(pyridine-2-yl)ethylidene]hydrazinecarbimidothioate}copp er(II) nitrate compound. The said compound expands the arsenal of synthetic superoxide radical inhibitors with high biological activity [264].

BOPI nr. 5/2021.MD 4755 Copper coordination compounds with 4-allylthiosemicarbazones of substituted 3-(phenyl)-1-(pyridin-2-yl)prop-2-en-1-ones as inhibitors of superoxide radicals.

The invention relates to chemistry and medicine, namely to a number of biologically active copper coordination compounds from the class of transition metal thiosemicarbazide. These complexes can be used in medicine as drugs that inhibit superoxide radicals, thus preventing multiple harmful effects on the body. Summary of the invention consists in producing several synthetic inhibitors of superoxide radicals based on copper coordination compounds with 4- allylthiosemicarbazones of substituted 3- (phenyl)-1-(pyridin-2-yl)prop-2-en-1-ones. The claimed compounds expand the arsenal of inhibitors of superoxide radicals with high biological activity [265].

BOPI nr. 3/2021.MD 4749 Use of coordination compounds of copper(II) salts with 2-(2- hydroxybenzylidene)-*N*-(prop-2-en-1-yl)-hydrazinecarbothioamide as inhibitors of superoxide radicals.

The invention relates to medicine, namely to the use of biologically active copper coordination compounds from the class of transition metal thiosemicarbazonates. These complexes can find application in medicine as drugs that inhibit superoxide radicals, thus preventing multiple harmful effects on the body. Summary of the invention consists in the use as synthetic inhibitors of superoxide radicals of chloro-2-{[2-(prop-2-en-1-ylcarbamothioyl)hydrazinylidene]methyl}phen olatocopper, bromo-2-{[2-(prop-2-en-1- ylcarbamothioyl)hydrazinylidene]methyl}phen olatocopper and nitrato-2-{[2-(prop-2-en-1- ylcarbamothioyl)hydrazinylidene]methyl}phen olatocopper. The said

compounds expand the arsenal of inhibitors of superoxide radicals with high biological activity [266].

5.2. DPPH• radical scavenging activity of the tested compounds

The DPPH assay is based on the measurement of the decrease in molar absorptivity of DPPH• at λ_{max} = 517±0.02 nm after reaction with the tested compounds. The effect of antioxidants on DPPH• radical scavenging is due to the hydrogen-donating ability or radical scavenging activity of the samples. The scavenging reaction between (DPPH•) and an antioxidant (AOH) can be written as scheme 5.2.

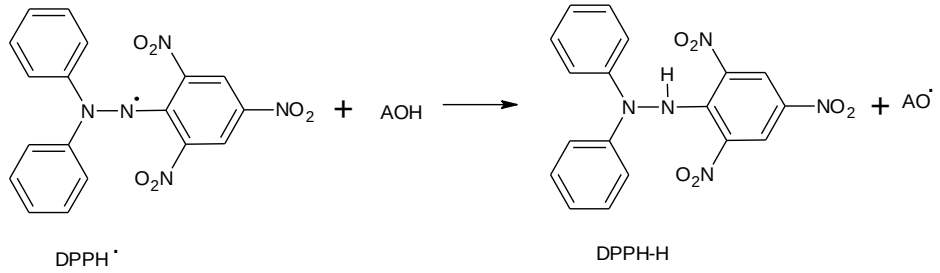

(Purple) (Yellow)

Scheme 5.2. **Reaction of stable radical DPPH• with an antiradical compound (AOH)**

The examined changes and comparisons in the DPPH• free radical scavenging ability of the tested compounds based on the IC_{50} values are represented in table 5.2. It was found, that the inhibitory effect of the compounds on percentage DPPH• scavenging activity was in a concentration-dependent manner.

Table 5.2. DPPH• radical scavenging activity of the tested compounds

№	Formula	IC_{50}±SD (μM)
1	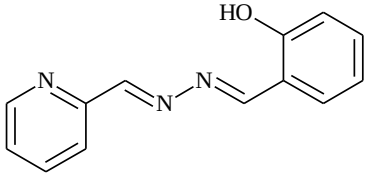	≥100
2	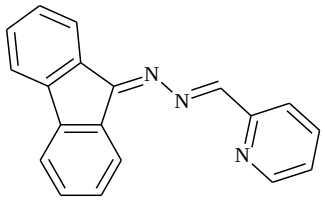	≥100

Table 5.2. Continued

№	Formula	IC_{50} (μM)
3	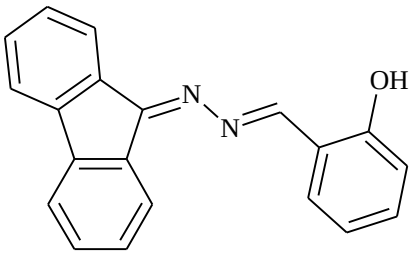	≥100
4	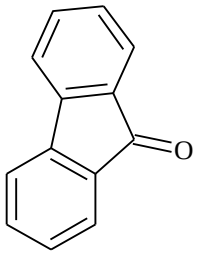	≥100
5	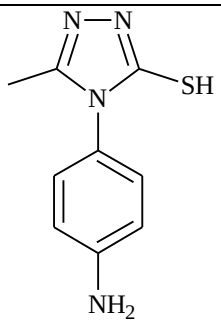	86.3 ± 2.4
6	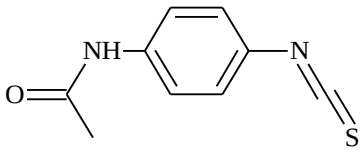	≥100
7	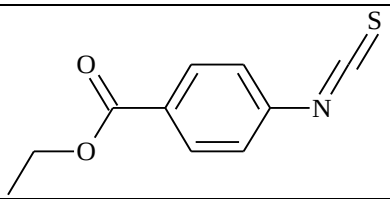	≥100
8	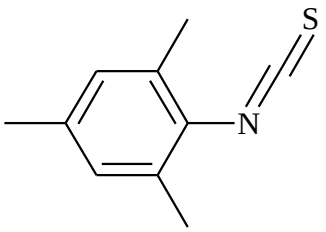	≥100

Table 5.2. Continued

№	Formula	IC_{50} (μM)
9	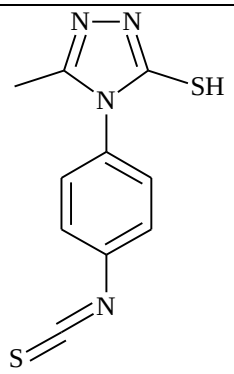	32.0 ± 1.9
10	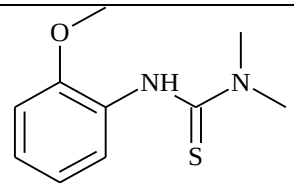	≥100
11	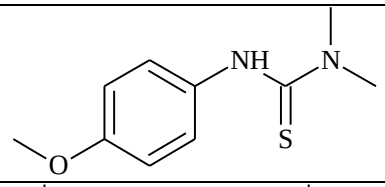	≥100
12	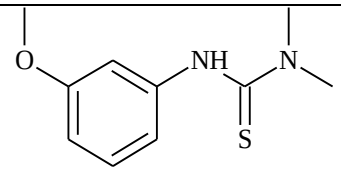	≥100
13	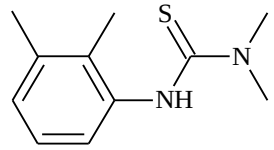	≥100
14	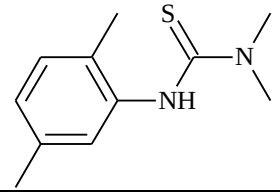	≥100
15	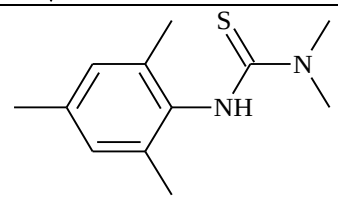	≥100

Table 5.2. Continued

№	Formula	IC_{50} (μM)
16	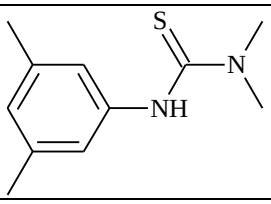	≥100
17	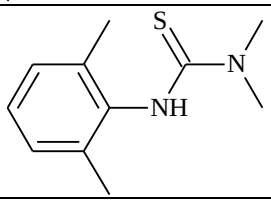	≥100
18	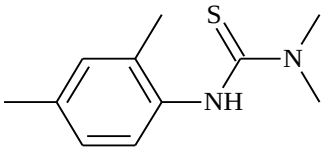	≥100
19	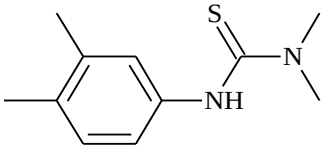	≥100
20	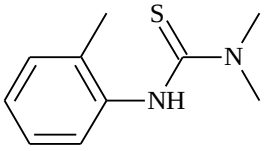	≥100
21	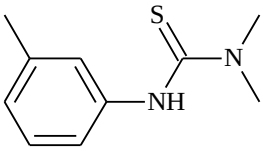	≥100
22	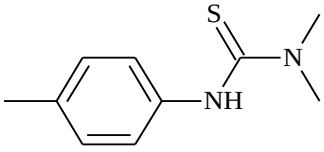	≥100
23	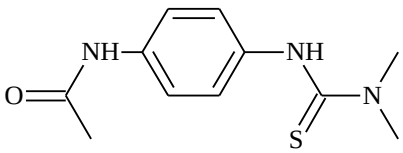	≥100

Table 5.2. Continued

№	Formula	IC_{50} (μM)
24	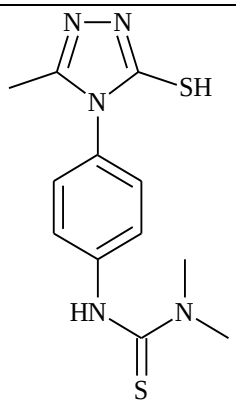	50.9 ± 2.2
25	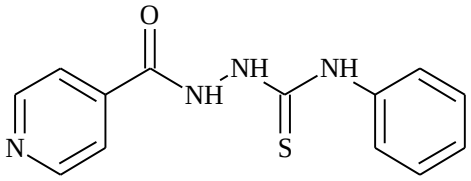	23.3 ± 1.7
26	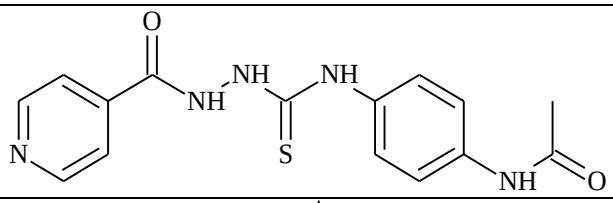	31.0 ± 0.6
27	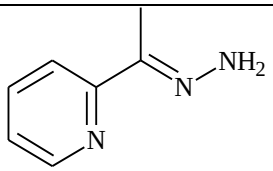	≥100
28	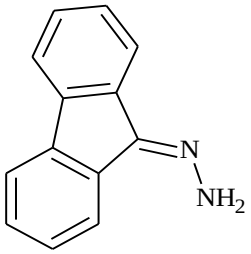	≥100
29	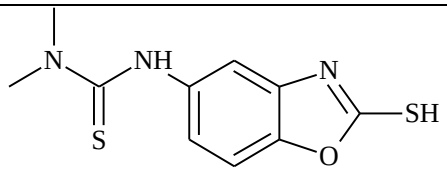	59.5 ± 2.5
30	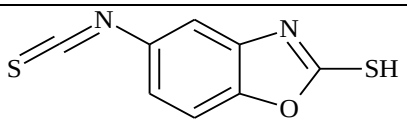	41.8 ± 1.6

Table 5.2. Continued

№	Formula	IC_{50} (μM)
31	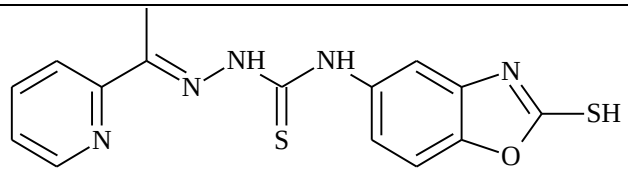	33.4 ± 0.6
32	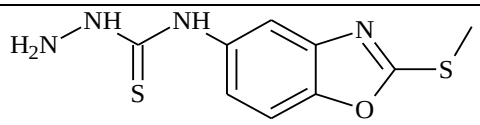	33.8 ± 0.6
33	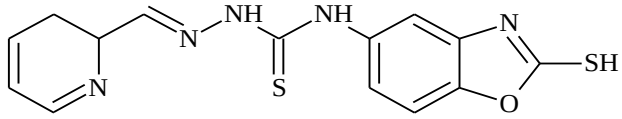	48.0 ± 1.5
34	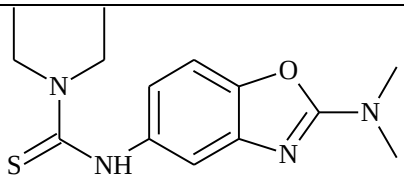	≥100
35	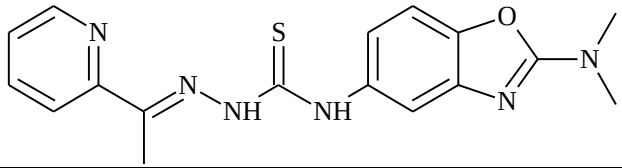	≥100
36	$Cu(L^3)Cl_2$ 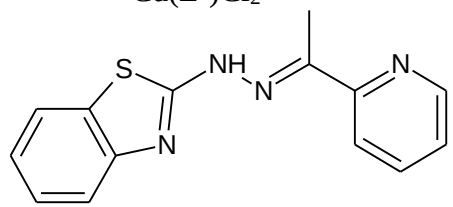 L^3 -	≥100
37	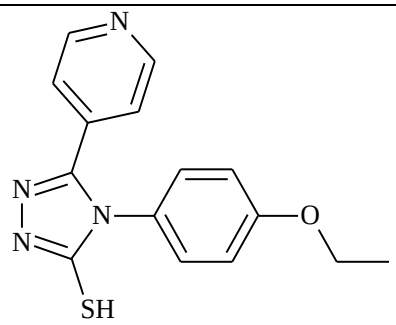	95.9 ± 5.1
38	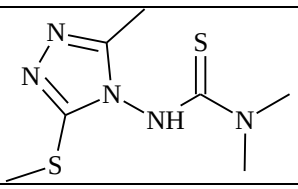	≥100

Table 5.2. Continued

№	Formula	IC_{50} (μM)
39	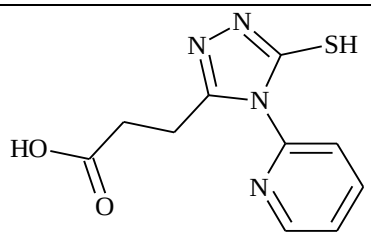	≥100
40	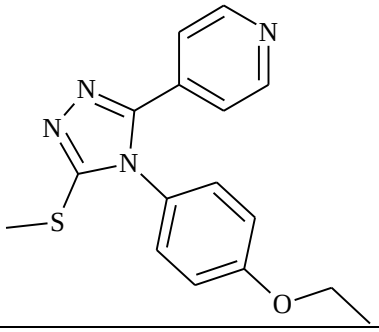	≥100
41	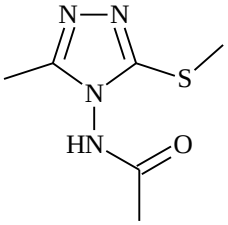	≥100
42	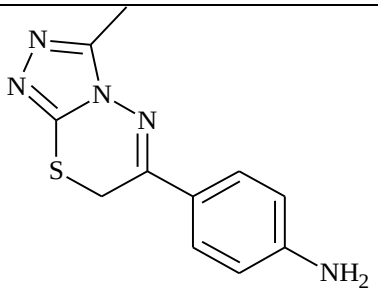	≥100
43	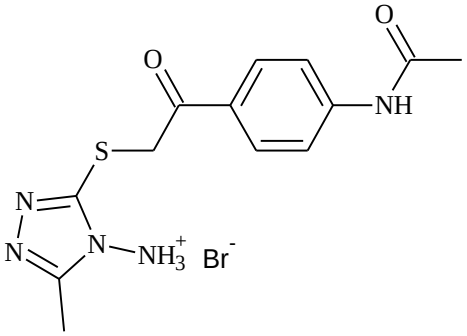	≥100

Table 5.2. Continued

№	Formula	IC_{50} (μM)
44	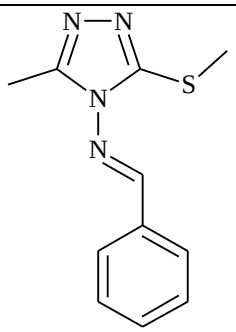	≥100
45	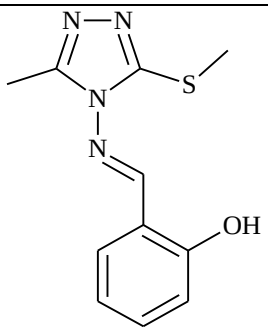	≥100
46	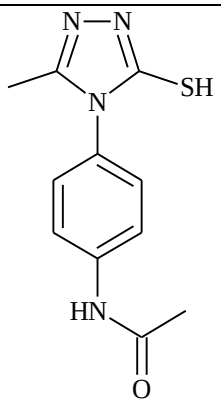	≥100
47	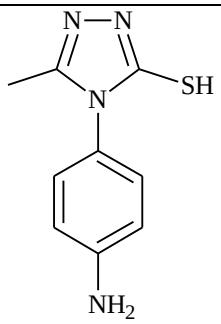	86.3 ± 0.4

Table 5.2. Continued

№	Formula	IC_{50} (μM)
48	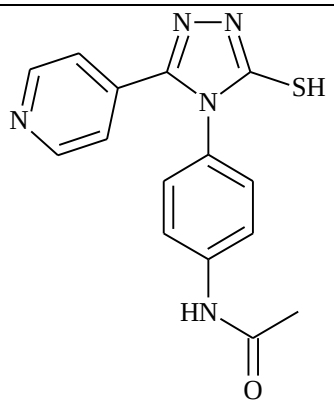	96.3 ± 1.7
49	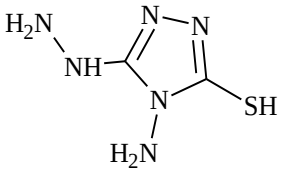	27.1 ± 0.9
50	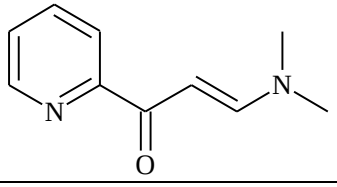	≥100
51	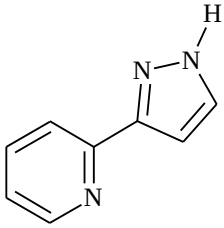	≥100
52	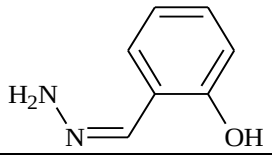	≥100
53	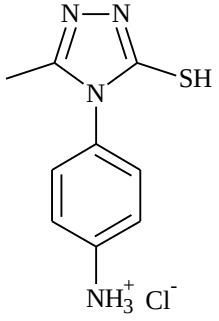	47.9 ± 1.2

Table 5.2. Continued

№	Formula	IC_{50} (μM)
54	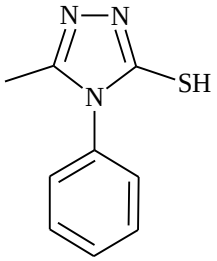	≥100
55	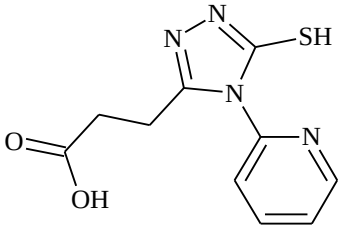	≥100
56	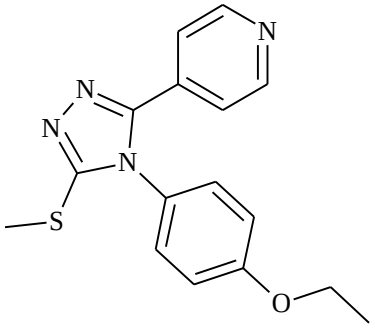	≥100
57	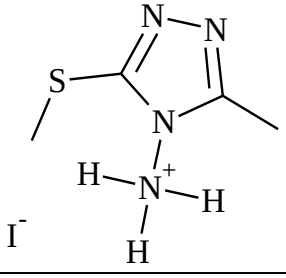	≥100
58	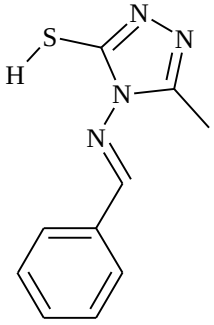	≥100

Table 5.2. Continued

№	Formula	IC_{50} (μM)
59	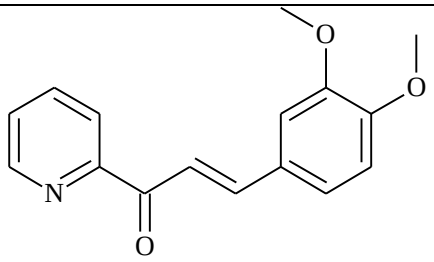	≥100
60	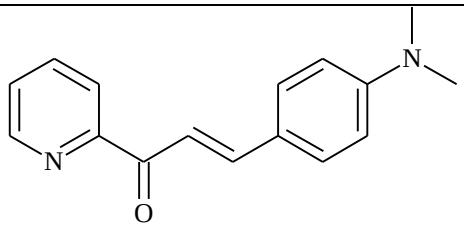	≥100
61	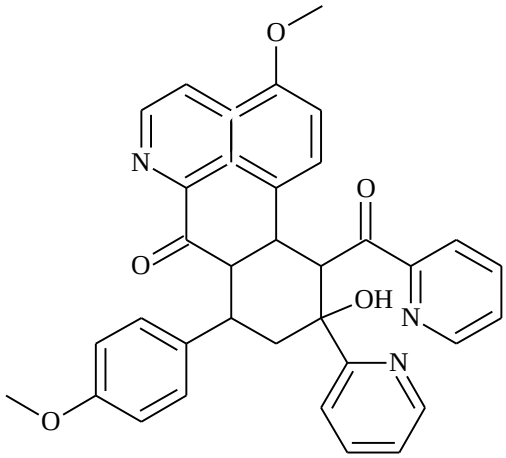	≥100
62	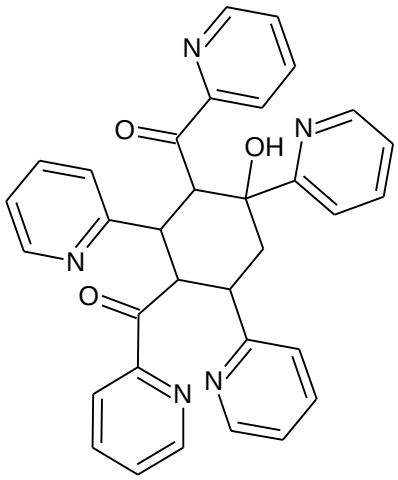	≥100

Table 5.2. Continued

№	Formula	IC_{50} (μM)
63	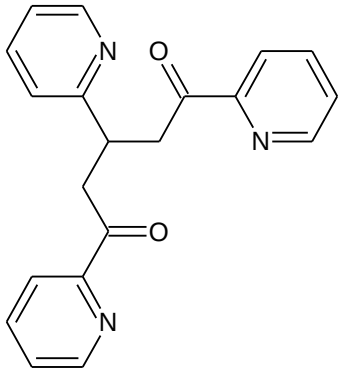	≥100
64	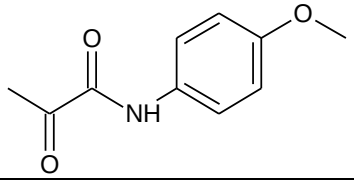	≥100
65	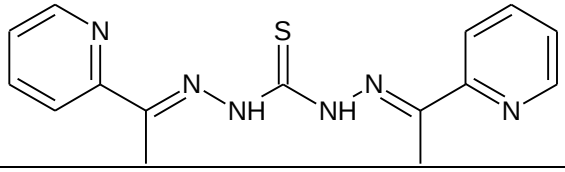	20.0 ± 0.4
66	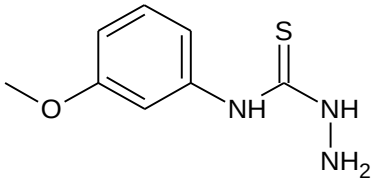 L^5	32.5 ± 1.3
67	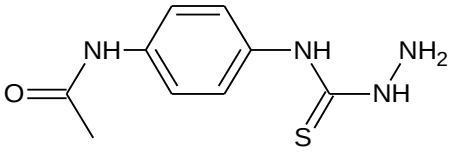	27.8 ± 1.0
68	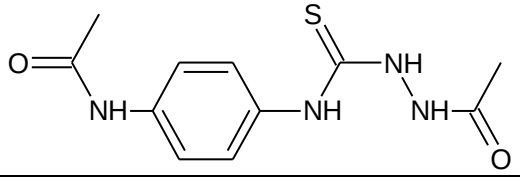	25.4 ± 0.2
69	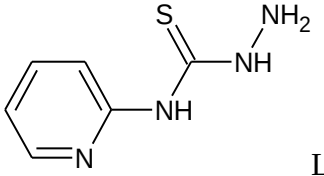 L^7	19.7 ± 0.3
70	$Cu(L^7)_2(NO_3)_2$	29.9 ± 0.5
71	$Cu(L^7)_2Cl_2$	27.9 ± 0.2

Table 5.2. Continued

№	Formula	IC_{50} (μM)
72	$Cu(L^7)_2SO_4$	5.5 ± 0.1
73	$Cu(L^7)_2(CH_3COO)_2$	45.6 ± 0.3
74	$Zn(L^7)_2Cl_2$	7.7 ± 0.1
75	$Ni(L^7)_2Cl_2$	8.8 ± 0.9
76	$Ni(L^7)_2(NO_3)_2$	14.9 ± 0.9
77	$Ni(L^7)_2SO_4$	7.8 ± 0.3
78	$Co(L^7)_2(ClO_4)_2$	≥100
79	$Co(L^7)_2Cl_2$	74.2 ± 1.2
80	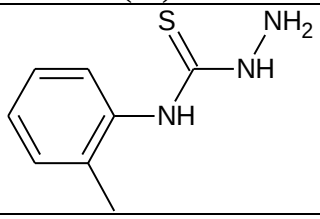	33.6 ± 0.1
81	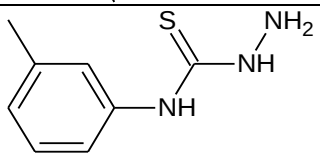	33.0 ± 0.7
82	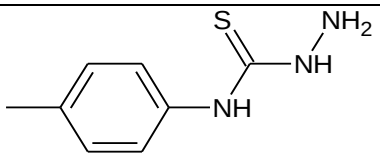	39.1 ± 0.8
83	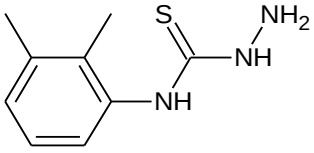	31.0 ± 0.7
84	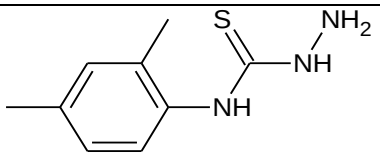	34.2 ± 0.5
85	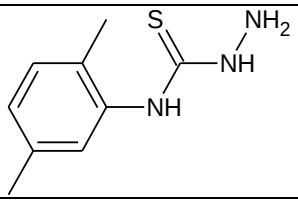	21.8 ± 0.6
86	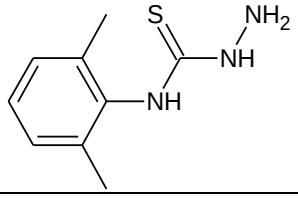	57.6 ± 0.6

Table 5.2. Continued

№	Formula	IC_{50} (μM)
87	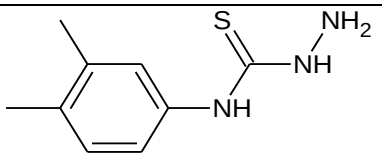	34.8 ± 3.2
88	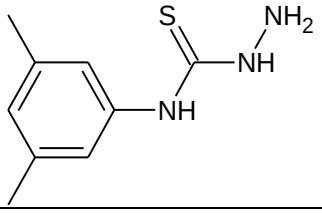	36.0 ± 2.5
89	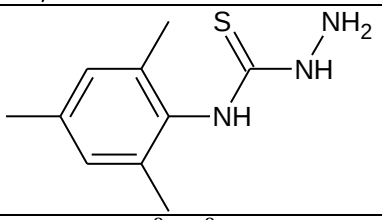	31.4 ± 0.8
90	$Cu(L^8)(L^8\text{-}H)Cl$ 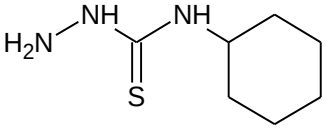 Where L^8 is	≥100
91	$Cu(L^8)(L^8\text{-}H)Br$	≥100
92	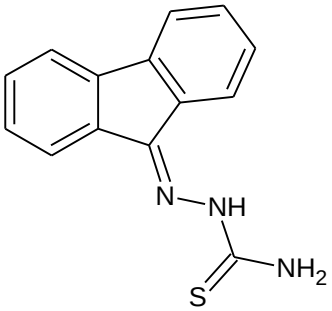	99.8 ± 0.2
93	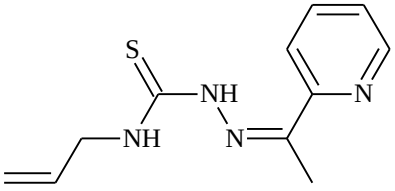 L^{36}	6.8 ± 0.9
94	$Cu(L^{36})(NO_3)_2$	≥100
95	$Cu(L^{36}\text{-}H)(OAc)$	≥100
96	$Cu(L^{36}\text{-}H)Cl$	≥100
97	$Cu(L^{36}\text{-}H)Br$	≥100
98	$(Cu(L^{36}\text{-}H))_2SO_4$	≥100

Table 5.2. Continued

№	Formula	IC_{50} (μM)
99	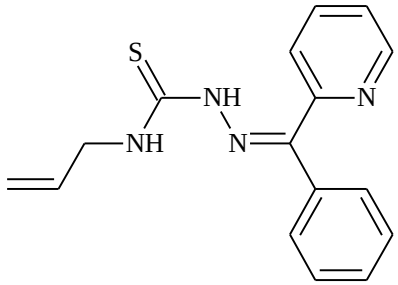 L^{37}	2.6 ± 0.2
100	$Cu(L^{37}\text{-}H)(NO_3)$	≥100
101	$Cu(L^{37}\text{-}H)Cl$	≥100
102	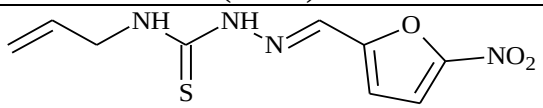	≥100
103	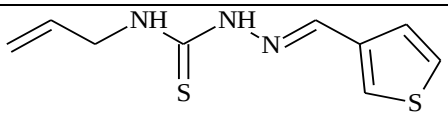	≥100
104	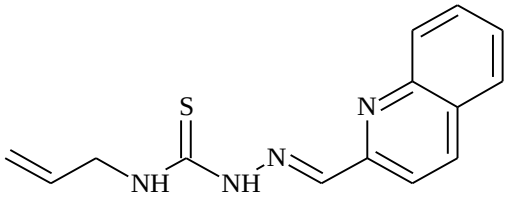	≥100
105	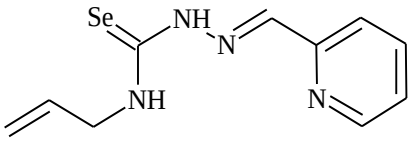	2.4 ± 0.1
106	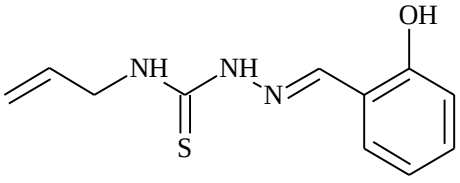 L^{38}	≥100
107	$Cu(L^{38}\text{-}H)Cl$	≥100
108	$Cu(L^{38}\text{-}H)Br$	≥100
109	$Cu(L^{38}\text{-}H)(NO_3)$	≥100
110	$Cu(L^{38}\text{-}2H)H_2O$	≥100
111	$Co(L^{38}\text{-}H)_2Cl$	≥100
112	$Co(L^{38}\text{-}H)_2(NO_3)$	82.5 ± 1.5
113	$Ni(L^{38})(L^{38}\text{-}H)Cl$	33.4 ± 0.7
114	$Zn(L^{38}\text{-}H)Cl$	≥100
115	$Fe(L^{38}\text{-}H)_2(NO_3)$	31.0

Table 5.2. Continued

№	Formula	IC_{50} (μM)
116	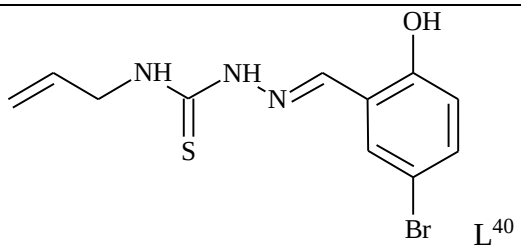 L^{40}	≥100
117	$Cu(L^{40}\text{-}H)Cl$	≥100
118	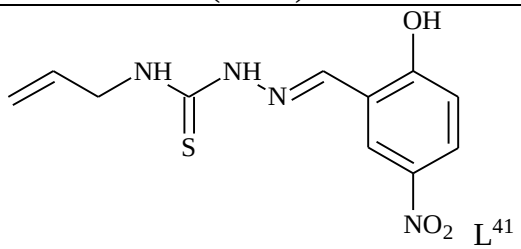 L^{41}	≥100
119	$Cu(L^{41}\text{-}H)Cl$	≥100
120	$Cu(L^{42}\text{-}H)Br$	≥100
121	$Co(L^{42}\text{-}H)_2NO_3$	≥100
122	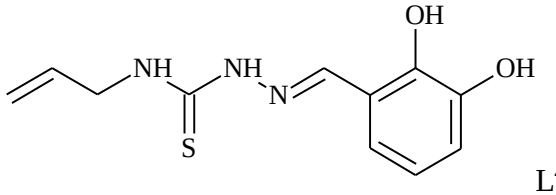 L^{43}	13.3 ± 0.2
123	$Cu(L^{43}\text{-}H)NO_3$	25.8 ± 0.3
124	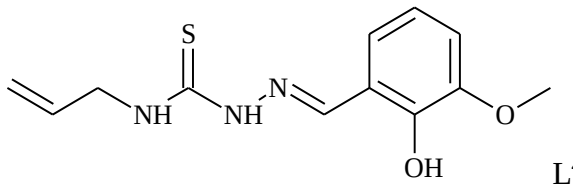 L^{44}	73.0 ± 0.8
125	$Cu(L^{44}\text{-}H)Cl$	≥100
126	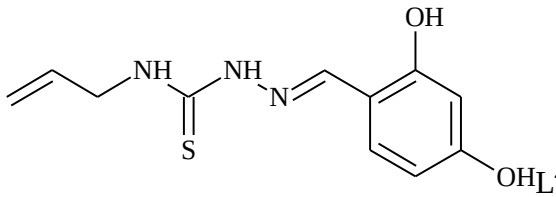 L^{45}	25.4 ± 0.2
127	$Cu(L^{45}\text{-}H)Cl$	35.1 ± 0.6
128	$Cu(L^{45}\text{-}H)NO_3$	27.7 ± 0.5

Table 5.2. Continued

№	Formula	IC_{50} (μM)
129	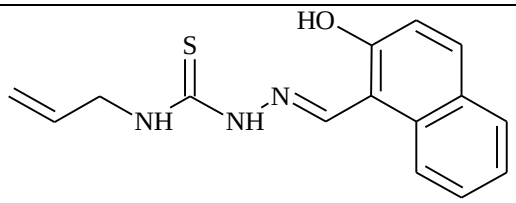 L^{47}	21.1 ± 0.4
130	$Cu(L^{47}\text{-}H)Cl$	≥100
131	$Cu(L^{47}\text{-}H)NO_3$	≥100
132	$Co(L^{47}\text{-}H)_2NO_3$	55.7 ± 1.2
133	$Ni(L^{47})(L^{47}\text{-}H)Cl$	16.4 ± 0.1
134	$Cr(L^{47}\text{-}H)_2NO_3$	6.6 ± 0.3
135	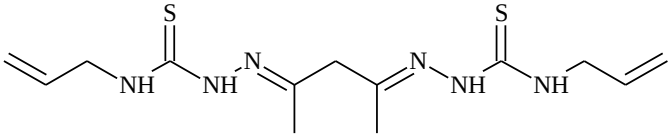	≥100
136	$Cu(L^{57})(ClO_4)_2$ Where L^{57} is 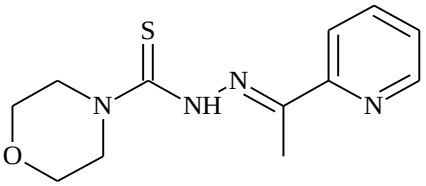	16.7 ± 0.3
137	$Co(L^{58})Cl_2$ Where L^{58} is 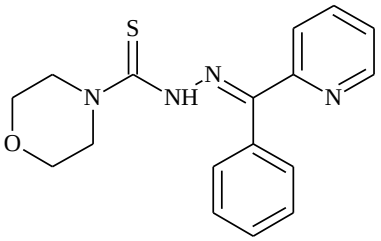	8.1 ± 0.3
138	$Co(L^{58})(NO_3)_2$	7.3 ± 0.1
139	$Ni(L^{58})Cl_2$	19.1 ± 0.2
140	$Cu(L^{58})Br_2$	20.9 ± 0.2
141	$Cu(L^{58})(NO_3)_2$	83.6 ± 0.5
142	$Cu(L^{59})(NO_3)_2$ Where L^{59} is 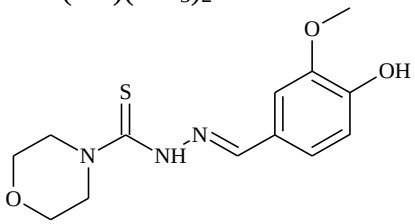	63.2 ± 0.1

Table 5.2. Continued

№	Formula	IC_{50} (μM)
143	$Cu(L^{59})Br_2$	38.5 ± 0.1
144	$Co(L^{59})(NO_3)_2$	18.0 ± 0.3
145	$Ni(L^{59})Cl_2$	15.2 ± 0.5
146	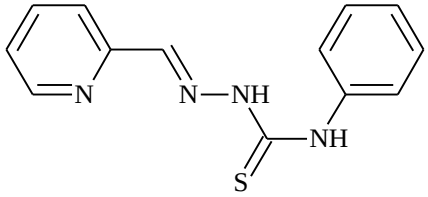 L^{62}	79.4 ± 0.2
147	$Cu(L^{62}\text{-}H)Cl$	≥100
148	$Cu(Str)(L^{62}\text{-}H)Cl$ 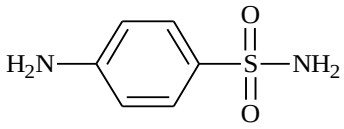 Where Str is	≥100
149	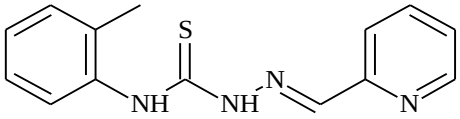	≥100
150	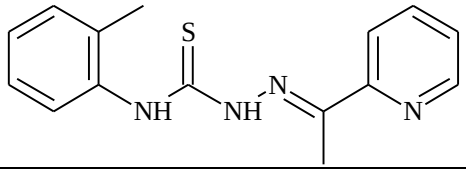	≥100
151	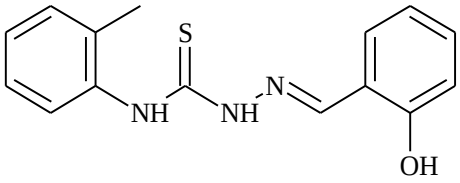	59.1 ± 0.5
152	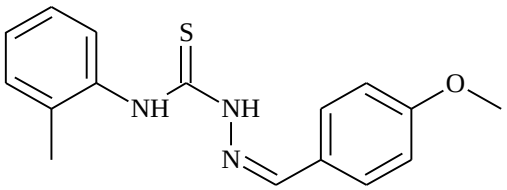	≥100
153	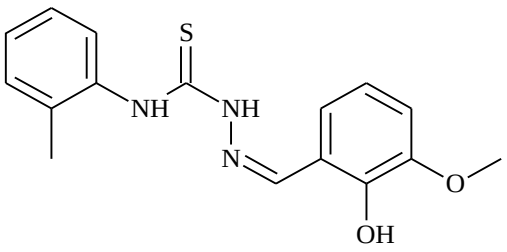	32.6 ± 0.5

Table 5.2. Continued

№	Formula	IC_{50} (μM)
154	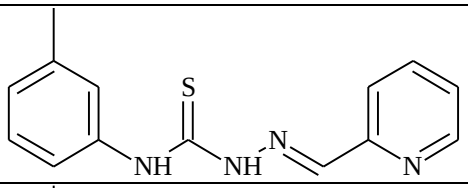	≥100
155	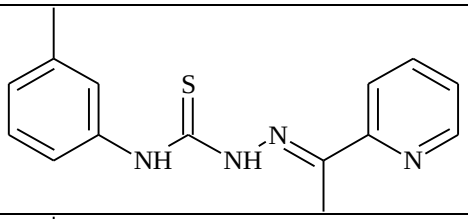	91.0 ± 0.6
156	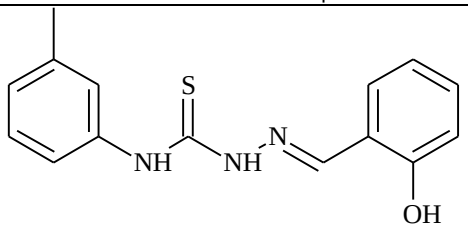	28.2 ± 0.6
157	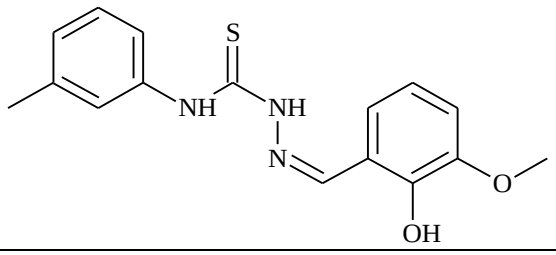	30.0 ± 0.4
158	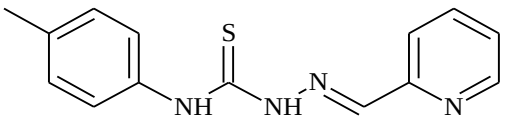	≥100
159	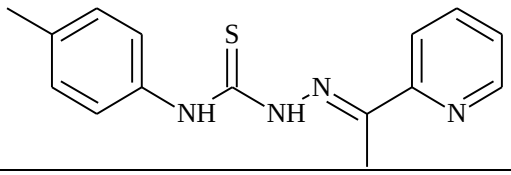	≥100
160	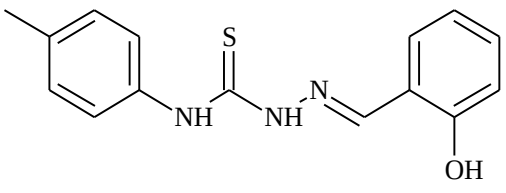 L^{67}	66.6 ± 1.4
161	Cu(1.10-Phen)(L^{67}-2H)	≥100
162	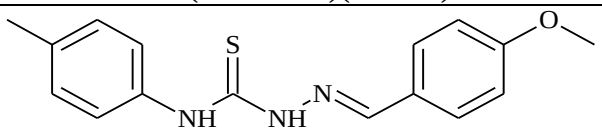	≥100

Table 5.2. Continued

№	Formula	IC_{50} (μM)
163	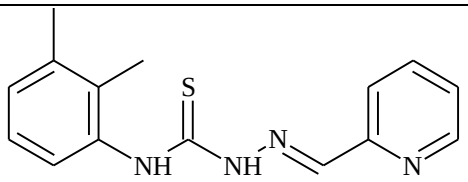	≥100
164	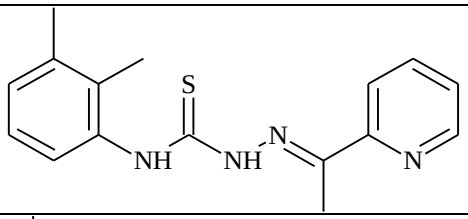	≥100
165	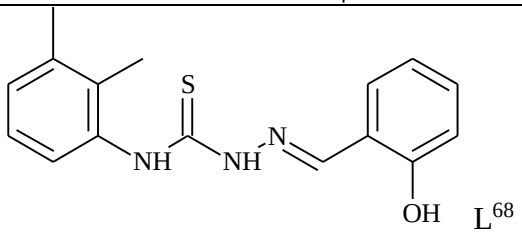 L^{68}	66.3 ± 1.9
166	$Cu(L^{68}\text{-}H)(NO_3)$	≥100
167	$Cu(L^{68}\text{-}H)Br$	≥100
168	$Cu(L^{68}\text{-}H)Cl$	≥100
169	$Cu_2(L^{68}\text{-}H)_2SO_4$	48.7 ± 0.1
170	$Ni(L^{68}\text{-}H)_2$	≥100
171	$Co(L^{68}\text{-}H)_2(NO_3)$	73.1 ± 2.0
172	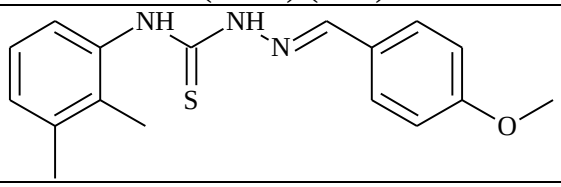	≥100
173	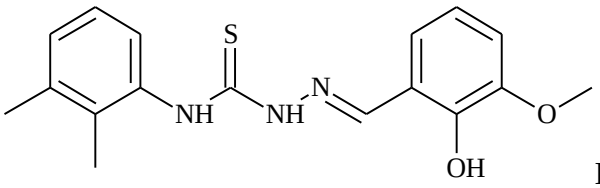 L^{69}	34.5 ± 0.5
174	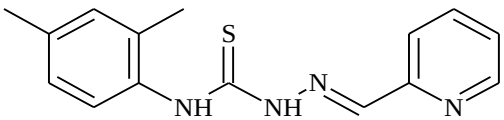	≥100
175	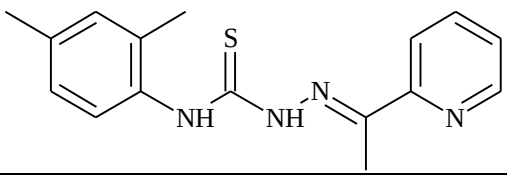	≥100

Table 5.2. Continued

№	Formula	IC_{50} (μM)
176	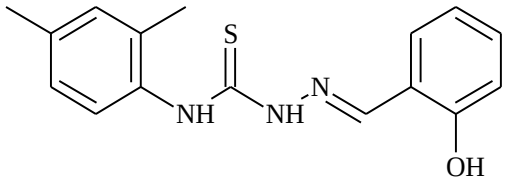	50.8 ± 1.6
177	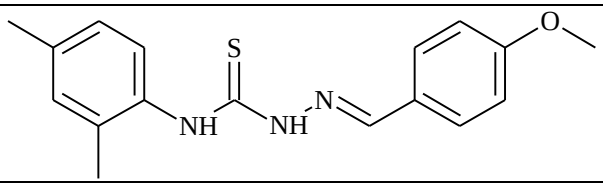	≥100
178	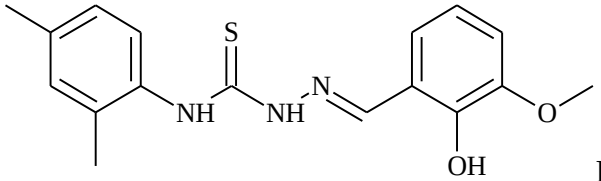 L^{73}	28.5 ± 1.9
179	$Cu(L^{73}\text{-}H)Cl$	≥100
180	$Cu(L^{73}\text{-}H)NO_3 \cdot H_2O$	79.6 ± 0.4
181	$Ni(L^{73}\text{-}H)_2$	32.8 ± 0.5
182	$Ni(L^{73}\text{-}2H)(H_2O)$	≥100
183	$Co(L^{73}\text{-}H)_2Cl$	35.5 ± 0.3
184	$Co(L^{73}\text{-}H)_2(NO_3)$	38.1 ± 0.1
185	$Fe(L^{73}\text{-}H)_2Cl$	58.0 ± 1.4
186	$Fe(L^{73}\text{-}H)(NO_3)_2(H_2O)$	100.3 ± 0.1
187	$Fe(L^{73}\text{-}H)_2(NO_3)$	25.0 ± 0.1
188	$K_2Mn(L^{73}\text{-}2H)_2$	≥100
189	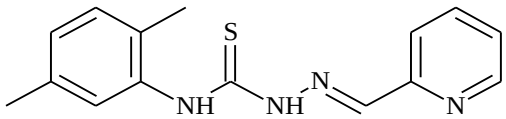	≥100
190	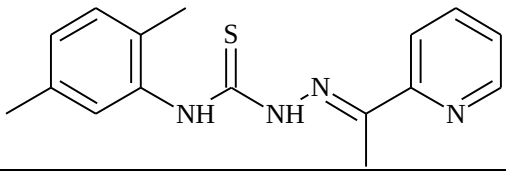	≥100
191	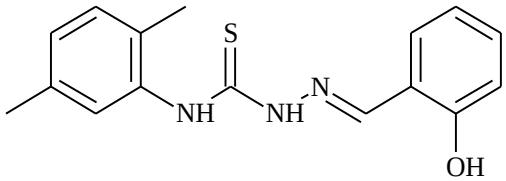	59.4 ± 1.2

Table 5.2. Continued

№	Formula	IC_{50} (μM)
192	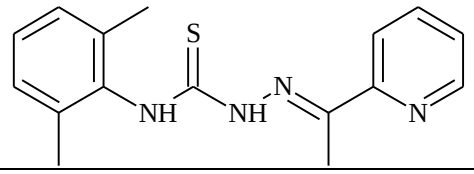	≥100
193	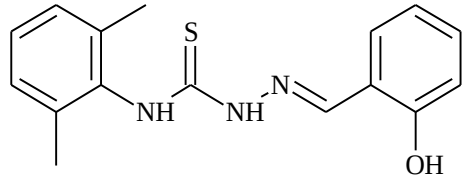 L^{74}	≥100
194	$Cu_2(L^{74}\text{-}H)_2SO_4$	≥100
195	$Ni(L^{74}\text{-}H)Cl$	71.5 ± 2.4
196	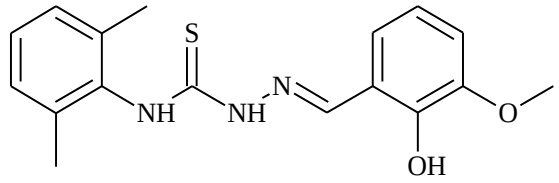	37.0 ± 0.9
197	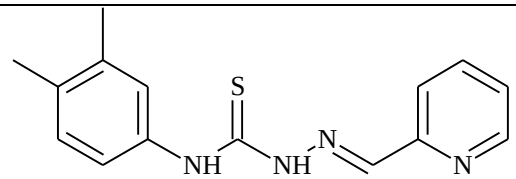	≥100
198	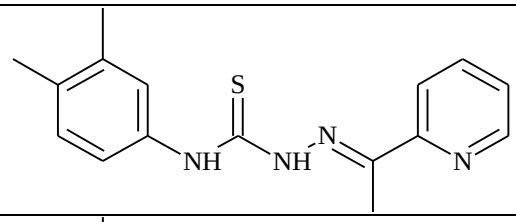	≥100
199	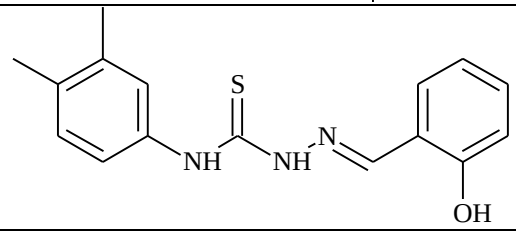	30.2 ± 0.1
200	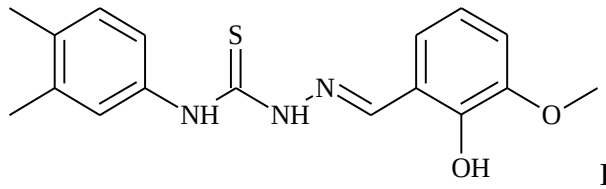 L^{75}	31.7 ± 0.8
201	$Cu(L^{75}\text{-}H)NO_3 \cdot H_2O$	≥100
202	$Ni(L^{75}\text{-}H)Cl$	≥100

Table 5.2. Continued

№	Formula	IC_{50} (μM)
203	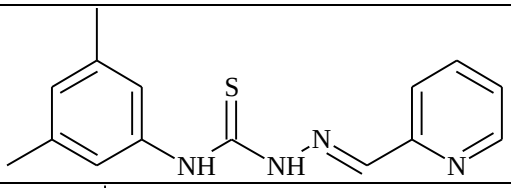	≥100
204	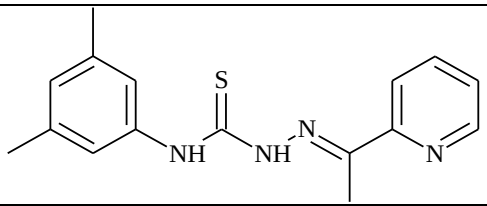	≥100
205	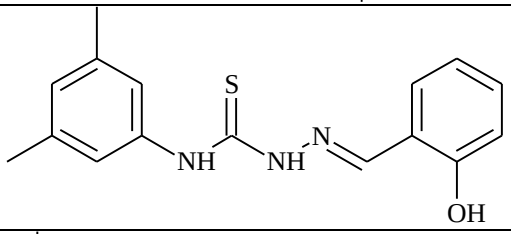	27.7 ± 0.9
206	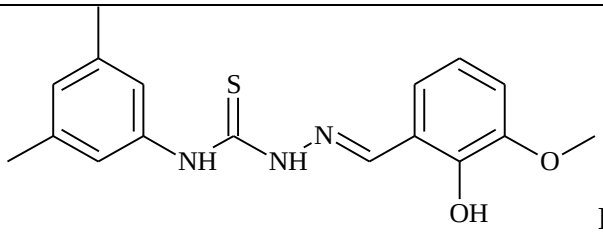 L^{76}	24.1 ± 0.2
207	$Ni(L^{76}\text{-}2H)(H_2O)$	≥100
208	$Ni(L^{76}\text{-}H)_2$	≥100
209	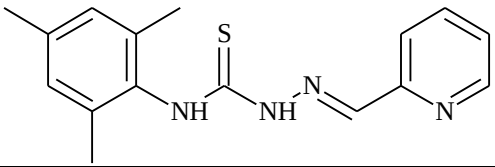	≥100
210	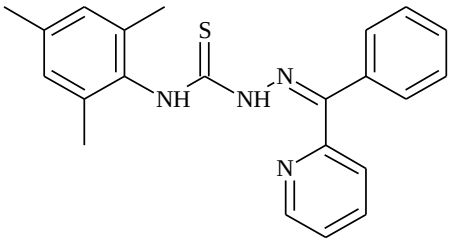	13.1 ± 0.8
211	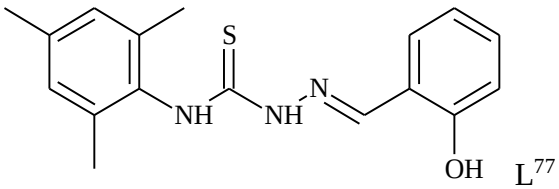 L^{77}	≥100

Table 5.2. Continued

№	Formula	IC_{50} (μM)
212	$Cu(L^{77}\text{-}2H)(H_2O)$	≥100
213	$Cu(L^{77}\text{-}H)Cl$	≥100
214	$Cu(L^{77}\text{-}H)(NO_3)$	≥100
215	$Ni(L^{77}\text{-}2H)(H_2O)$	88.2 ± 1.2
216	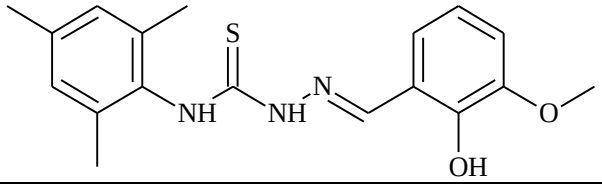	43.8 ± 1.3
217	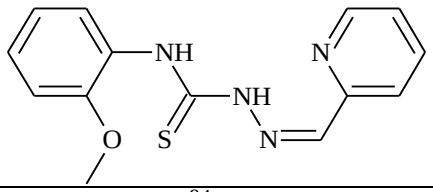	≥100
218	$Cu(L^{84}\text{-}H)NO_3$ Where L^{84} is 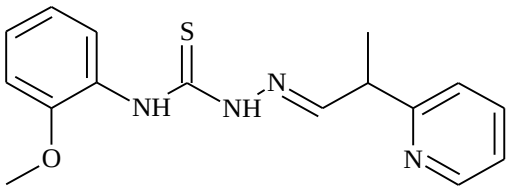	≥100
219	$Cu(L^{84}\text{-}H)Cl$	≥100
220	$Cu(L^{85}\text{-}H)Cl$ 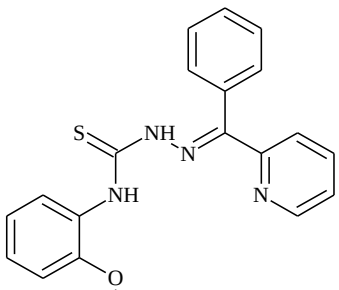 Where L^{85} is	≥100
221	$Cu(L^{85}\text{-}H)NO_3$	≥100
222	$Co(L^{85}\text{-}H)_2Cl$	81.3 ± 2.3
223	$Fe(L^{85}\text{-}H)_2NO_3$	≥100
224	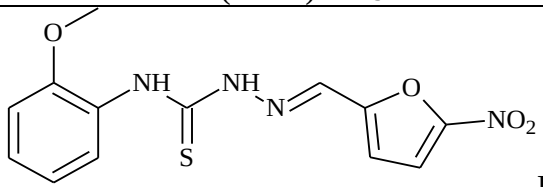 L^{86}	≥100

Table 5.2. Continued

№	Formula	IC_{50} (μM)
225	$Cu(L^{86}\text{-}H)NO_3$	≥100
226	$Co(L^{86}\text{-}H)_2Cl$	≥100
227	$Fe(L^{86}\text{-}H)_2NO_3$	≥100
228	$Cu(L^{87}\text{-}2H)(H_2O)$ 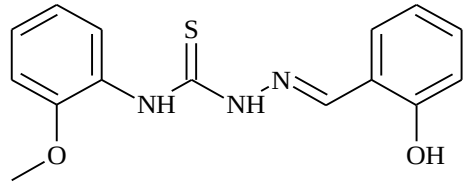 Where L^{87} is	≥100
229	$Cu(L^{87}\text{-}H)Br$	≥100
230	$Ni(L^{87}\text{-}H)_2$	≥100
231	$Fe(L^{87}\text{-}H)_2NO_3$	96.3 ± 0.3
232	$Co(L^{87}\text{-}H)_2Cl$	72.7 ± 3.0
233	$Cu(L^{88}\text{-}H)Cl$ 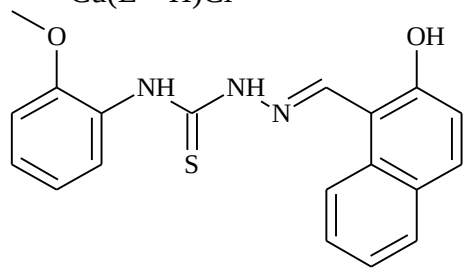 Where L^{88} is	≥100
234	$Cu(L^{88}\text{-}H)NO_3$	≥100
235	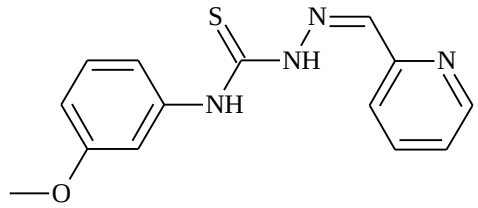 L^{89}	48.3 ± 1.0
236	$Cu(L^{89}\text{-}H)Cl$	≥100
237	$Cu(L^{90}\text{-}H)NO_3$ Where L^{90} is 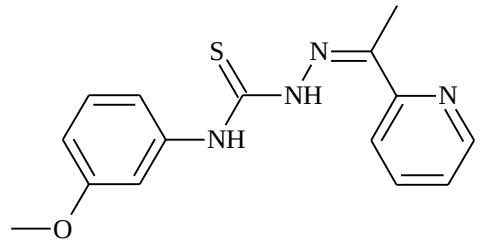	≥100
238	$Cu(L^{90}\text{-}H)Cl$	≥100

Table 5.2. Continued

№	Formula	IC_{50} (μM)
239	$Cu(L^{91}\text{-}H)Cl$ 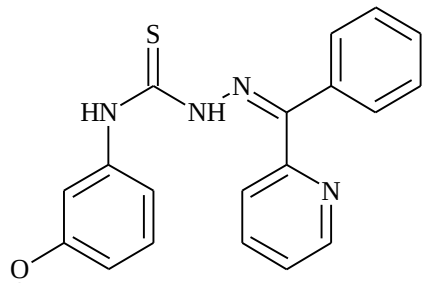 Where L^{91} is	≥100
240	$Cu(L^{91}\text{-}H)NO_3$	≥100
241	$Co(L^{91}\text{-}H)_2Cl$	47.6 ± 2.9
242	$Co(L^{92}\text{-}H)_2Cl$ 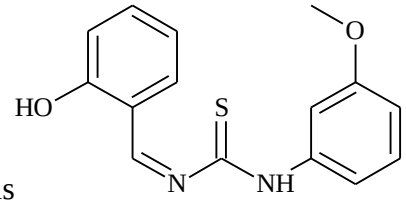 Where L^{92} is	91.3 ± 1.0
243	$Cu(L^{93}\text{-}H)NO_3$ 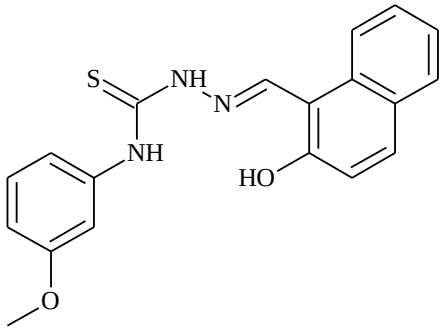 Where L^{93} is	60.3 ± 1.3
244	$Cu(L^{93}\text{-}H)Cl$	104.2 ± 3.2
245	$Cu(L^{94}\text{-}H)NO_3$ 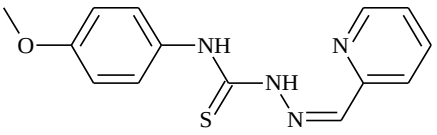 Where L^{94} is	≥100
246	$Co(L^{94}\text{-}H)_2Cl$	≥100
247	$Cu(L^{95}\text{-}H)Cl$ 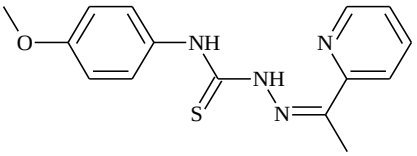 Where L^{95} is	≥100

Table 5.2. Continued

№	Formula	IC_{50} (μM)
248	$Cu(L^{96}\text{-}H)Cl$ Where L^{96} is 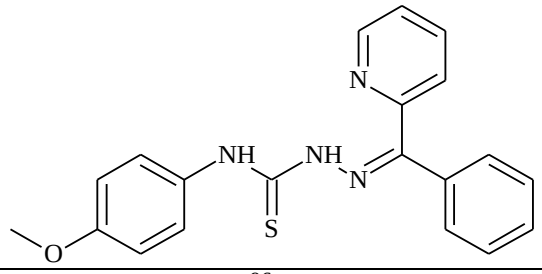	≥100
249	$Cu(L^{96}\text{-}H)NO_3$	≥100
250	$Co(L^{96}\text{-}H)_2Cl$	≥100
251	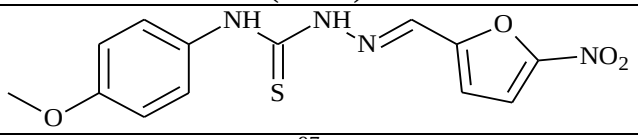	≥100
252	$Co(L^{97}\text{-}H)_2Cl$ Where L^{97} is 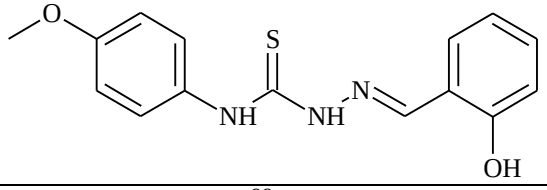	47.1 ± 2.4
253	$Cu(L^{98}\text{-}H)NO_3$ Where L^{98} is 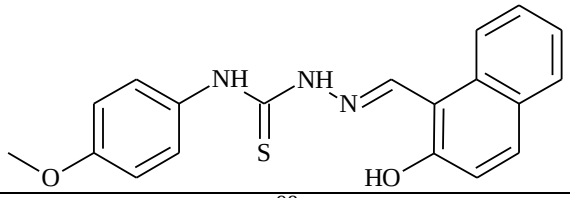	≥100
254	$Cu(L^{98}\text{-}H)Cl$	59.5 ± 0.7
255	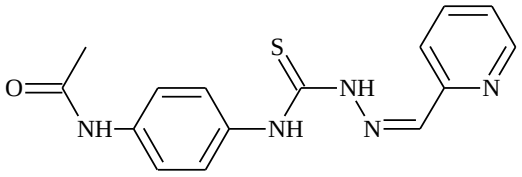 L^{111}	≥100
256	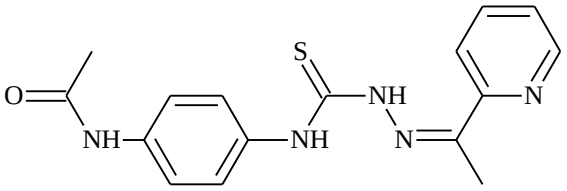 L^{112}	≥100

Table 5.2. Continued

№	Formula	IC_{50} (μM)
257	$Cu(L^{112}\text{-}H)Cl$	≥100
258	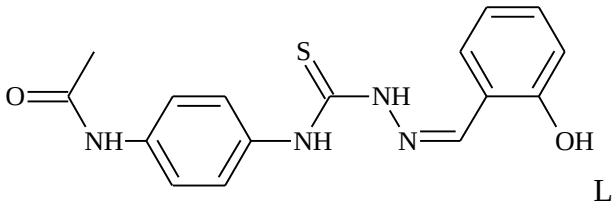 L^{114}	50.4 ± 1.5
259	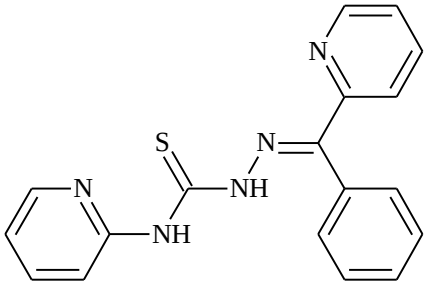 L^{118}	≥100
260	$Cu(L^{118}\text{-}H)Cl$	≥100
261	$Zn(L^{118}\text{-}H)Cl$	≥100
262	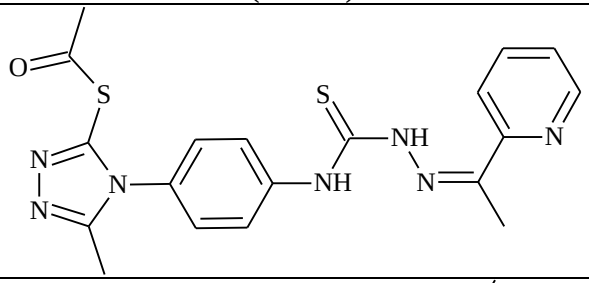	78.0 ± 0.8
263	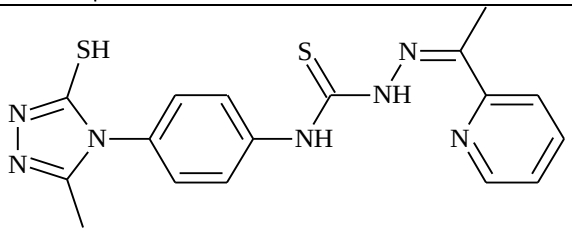	29.0 ± 0.5
264	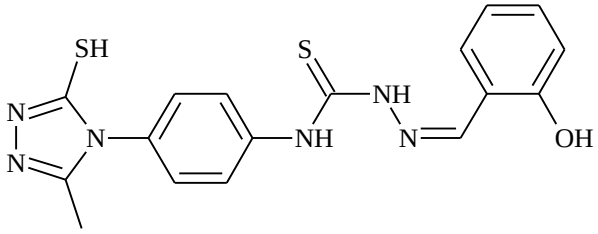	68.7 ± 0.2

Table 5.2. Continued

№	Formula	IC_{50} (μM)
265	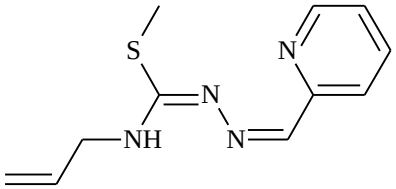 L^{119}	≥ 100
266	$L^{119}\cdot HI$	≥ 100
267	$Cu(L^{119})(NO_3)_2$	≥ 100
268	$Cu(L^{119})Cl_2$	≥ 100
269	$Cu(L^{119})Br_2$	≥ 100
270	$Cu(L^{119})(ClO_4)_2$	≥ 100
271	$Co(L^{119}\text{-}H)_2I$	≥ 100
272	$Co(L^{119}\text{-}H)_2(NO_3)$	≥ 100
273	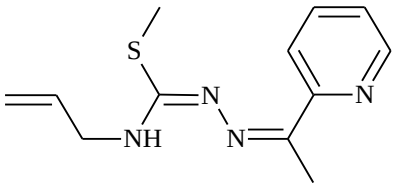 L^{120}	≥ 100
274	$Cu(L^{120})SO_4$	≥100
275	$Cu(L^{120})Cl_2$	≥100
276	$Cu(L^{120})Br_2$	≥100
277	$Ni(L^{120})_2(ClO_4)_2$	≥100
278	$Co(L^{120}\text{-}H)_2NO_3$	≥100
279	$Co(L^{120}\text{-}H)_2I$	≥100
280	$Cu(L^{120})(NO_3)_2$	≥ 100
281	$Fe(L^{120}\text{-}H)_2Br$	≥ 100
282	$Co(L^{120}\text{-}H)_2Cl$	≥ 100
283	$Ni(L^{120})_2(NO_3)_2$	≥ 100
284	$Cu(L^{121})Br_2$ 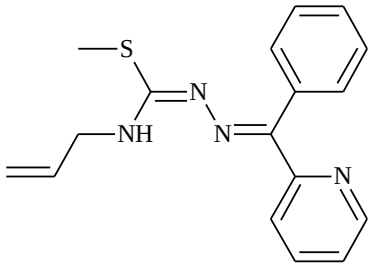 Where L^{121} is	≥100
285	$Cu(L^{121})(NO_3)_2$	≥100
286	$Cu(L^{121}\text{-}H)(OAc)$	≥100
287	$Cu(L^{121})Cl_2$	≥100
288	$Ni(L^{121})_2(NO_3)_2$	≥100

Table 5.2. Continued

№	Formula	IC_{50} (μM)
289	$Ni(L^{121})_2(ClO_4)_2$	≥100
290	$Co(L^{121}\text{-}H)_2(OAc)$	≥100
291	$Co(L^{121}\text{-}H)_2NO_3$	≥100
292	$Zn(L^{121})I_2$	≥100
293	$Fe(L^{122}\text{-}H)_2NO_3$ 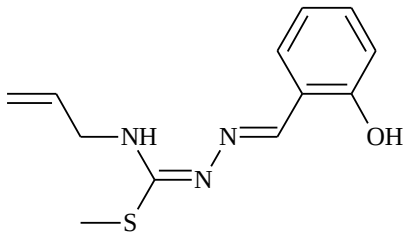 Where L^{122} is	≥100
294	$Fe(L^{122}\text{-}H)_2Cl$	≥100
295	$Co(L^{122}\text{-}H)_2NO_3$	≥100
296	$Co(L^{122}\text{-}H)_2Cl$	54.6 ± 0.4
297	$Co(L^{122}\text{-}H)_2Br$	62.8 ± 0.9
298	$Co(L^{122}\text{-}H)_2I$	48.6 ± 0.8
299	$Cr(L^{122}\text{-}H)_2NO_3$	37.7 ± 0.7
300	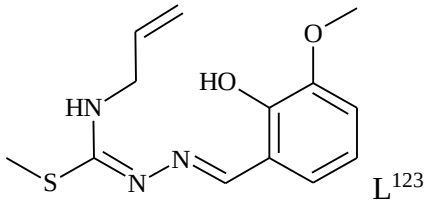 L^{123}	≥100
301	$L^{123}\cdot HI$	121.8 ± 3.0
302	$Cu(L^{123}\text{-}H)Cl$	≥100
303	$Cu(L^{123}\text{-}H)NO_3$	≥100
304	$Ni(L^{123})(L^{123}\text{-}H)NO_3$	≥100
305	$Ni(L^{123})(L^{123}\text{-}H)I$	≥100
306	$Co(L^{123}\text{-}H)_2NO_3$	16.1 ± 0.5
307	$Co(L^{123}\text{-}H)_2I$	17.2 ± 0.3
308	$Co(L^{123}\text{-}H)_2Cl$	≥100
309	$Fe(L^{123}\text{-}H)_2NO_3$	31.1 ± 0.3
310	$L^{126}\cdot HI$ 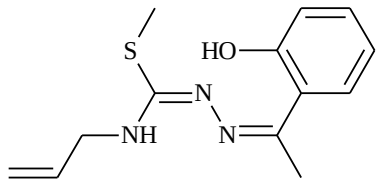 Where L^{126} is	≥100
311	$Cu(L^{126}\text{-}H)Cl$	25.0 ± 0.9
312	$Cu(L^{126}\text{-}H)NO_3$	21.3 ± 0.8

Table 5.2. Continued

№	Formula	IC_{50} (μM)
313	$Cu(L^{126}\text{-}H)ClO_4$	25.5 ± 0.1
314	$Cu(L^{126}\text{-}H)(OAc)$	32.2 ± 1.1
315	$Ni(L^{126}\text{-}H)_2$	≥100
316	$Co(L^{126}\text{-}H)_2NO_3$	35.5 ± 0.2
317	$Co(L^{126}\text{-}H)_2Br$	77.6 ± 0.1
318	$Co(L^{126}\text{-}H)_2I$	54.7 ± 1.1
319	$Fe(L^{126}\text{-}H)_2NO_3$	≥100
320	$Cu(L^{127}\text{-}H)ClO_4$ Where L^{127} is 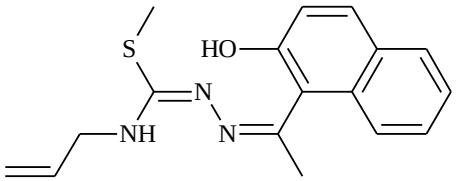	22.7 ± 0.4
321	$Ni(L^{127})(L^{127}\text{-}H)ClO_4$	101.8 ± 2.8
322	$Co(L^{127}\text{-}H)_2NO_3$	≥100
323	$Cr(L^{127}\text{-}H)_2NO_3$	52.6 ± 0.6
324	$Ni(L^{127}\text{-}H)_2$	≥100
325	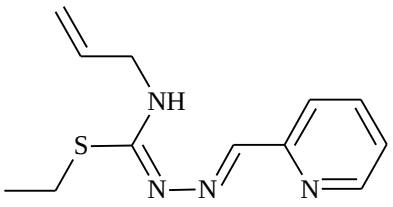 L^{128}	≥100
326	$Cu(L^{128}\text{-}H)Cl$	≥100
327	$Co(L^{128}\text{-}H)_2I$	≥100
328	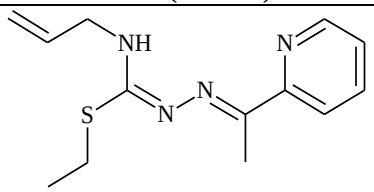 L^{129}	≥100
329	$L^{129}\cdot HI$	76.1 ± 0.4
330	$Co(L^{129}\text{-}H)_2I$	≥100
331	$Ni(L^{129})_2I_2$	≥100
332	$L^{130}\cdot HI$ Where L^{130} is 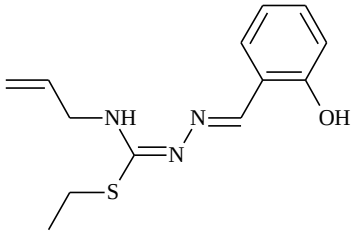	≥100

Table 5.2. Continued

№	Formula	IC_{50} (μM)
333	$Cu(L^{130}\text{-}H)NO_3$	27.0 ± 0.3
334	$Cu(L^{130}\text{-}H)Br$	≥100
335	$Ni(L^{130})(L^{130}\text{-}H)ClO_4$	≥100
336	$Fe(L^{130}\text{-}H)_2NO_3$	≥100
337	$Co(L^{130}\text{-}H)_2NO_3$	≥100
338	$Cu(L^{130}\text{-}H)Cl$	≥100
339	$Ni(L^{130})(L^{130}\text{-}H)I$	≥100
340	$Co(L^{130}\text{-}H)_2I$	≥100
341	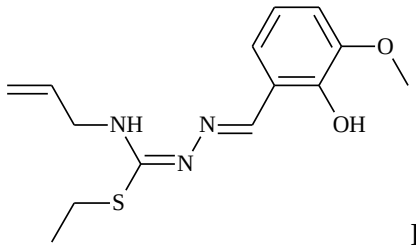 L^{131}	≥100
342	$L^{131}\cdot HI$	≥100
343	$Co(L^{131}\text{-}H)_2I$	26.1 ± 0.4
344	$Ni(L^{131}\text{-}H)_2$	≥100
345	$Co(L^{131}\text{-}H)_2Br$	34.5 ± 1.5
346	$Co(L^{131}\text{-}H)_2(OAc)$	32.8 ± 0.4
347	$Co(L^{131}\text{-}H)_2NO_3$	19.0 ± 0.6
348	$Fe(L^{131}\text{-}H)_2NO_3$	29.7 ± 0.3
349	$L^{132}\cdot HI$ 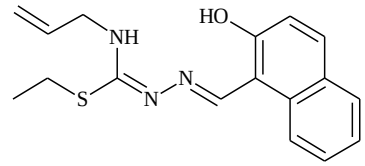 Where L^{132} is	38.2 ± 1.5
350	$Co(L^{132}\text{-}H)_2I$	≥100
351	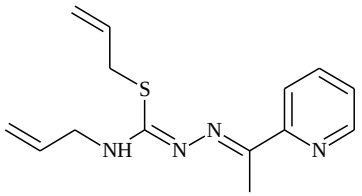 L^{134}	≥100
352	$L^{134}\cdot HI$	≥100
353	$Cu(L^{134})Br_2$	≥100
354	$Cu(L^{134})(NO_3)_2$	≥100
355	$Cu(L^{134})Cl_2$	≥100

Results were expressed as mean ± SD (number of experiments n=3) and considered to be statistically significant when P < 0.05.

The concentration of the tested compounds required to inhibit 50% of the radical-scavenging effect (IC_{50}) has been determined by testing a series of concentrations (0.1-100 μM).

For comparative analysis of the tested compounds, the reference antioxidant compounds Trolox, Rutin, and DOXO were determined with the IC_{50} values of 48.9±0.8 μM, 64.8±2.1μM, and ≥100 μM respectively.

The majority of thiosemicarbazides and thiosemicarbazones showed the strongest antioxidant activity (Table 5.2). In addition to the nature of the ligand, the nature of the central atom greatly influences the activity of complexes. In many cases, Zn(II), Cu(II), Ni(II), Co(III), Fe(III), and Cr(III) complexes significantly outperform the activity of Trolox and Rutin. The tested compounds (azomethines, hydrazones, isothiocyanates, thioureas, triazoles, and chalcones) showed inhibitory activity against $DPPH^{\bullet}$ radical with IC_{50} ≥100 μM.

In addition, the activity depends on the method used (ABTS or DPPH), the nature of the ligands and substituents in the ligands, the coordination mode of the ligands, the solvent, and the presence or not of protons in the ligands or complexes. In some series, the complexes have a lower IC_{50} than ligands, while the opposite is true in other series. Therefore, the tested compounds showed better inhibitory activity against $ABTS^{\bullet+}$ than the $DPPH^{\bullet}$ radical. That is, the ABTS assay is more sensitive in identifying antioxidant activity because of the faster reaction kinetics, and its response to antioxidants is higher.

The enhanced inhibition displayed on the $ABTS^{\bullet+}$ radical cation by the tested samples shows that the compounds can donate electrons to neutralize free radicals, indicating their potential as chemotherapeutic agents for radicals chain terminators.

5.3. Oxygen Radical Absorption Capacity (FL) activity of the tested compounds

The antioxidant capacity of the tested substances such as hydrazinecarbothioamide derivatives and their coordination compounds (Figure 5.1) was measured by ORAC assay, and their potency was compared with that of the reference antioxidant control Trolox. Anticancer drug DOXO was used as a control for comparative study because all tested compounds manifested high anticancer or antiproliferative properties.

L^1

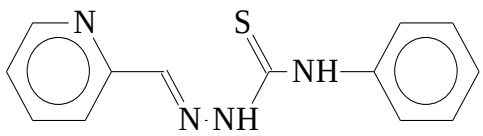

N-phenyl-2-(pyridin-2-ylmethylidene)hydrazinecarbothioamide

$[Cu(L^1\text{-}H)Cl]$

L^1-H=

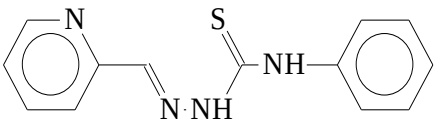

Chloro(*N*-phenyl-2-[pyridin-2-ylmethylidene] carbamohydrazonothioato)copper(II)

$[Cu(Str^1)(L^1\text{-}H)Cl]$

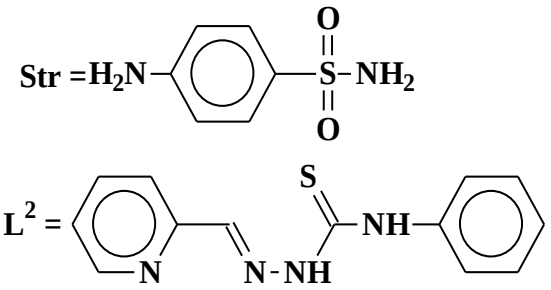

Chloro(*N*-phenyl-2-[pyridin-2-ylmethylidene]carbamohydrazonothioato) (4-aminobenzenesulfonamide)copper(II)

$[Cu(Str^2)\ (L^2\text{-}2H)]$

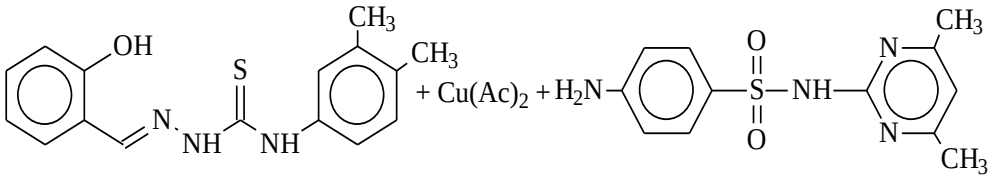

Hydrate (*N*-[3,4-dimethylphenyl]-2-[2-hydroxybenzylidene]carbamohydrazonothioato) (4-amino-*N*-(4,6-dimethylpyrimidin-2-yl)benzenesulfonamide)copper(II)

[Cu(Str^3) (L^3-2H)]

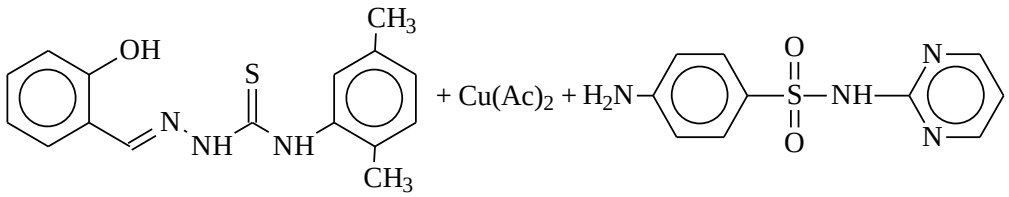

Hydrate *N*-(2,5-dimethylphenyl)-2-(2-hydroxybenzylidene)carbamohydrazonothioato(4-amino-*N*-(pyrimidin-2-yl)benzenesulfonamide)copper(II)

[CuL^{4}Cl$_2$],
L^4=

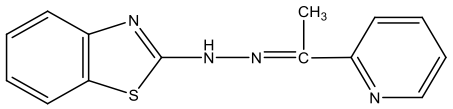

Chloro(2-{2-[1-(pyridin-2-yl)ethylidene]hydrazinyl}-1,3-benzothiazolo)copper(II)

L^5

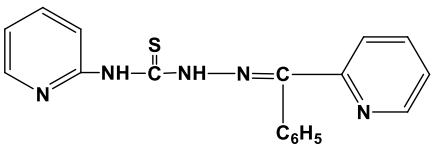

2-[phenyl(pyridin-2-yl)methylidene]-*N*-(pyridin-2-yl)hydrazinecarbothioamide

[Cu(L^5-H)Cl],
L^5-H=

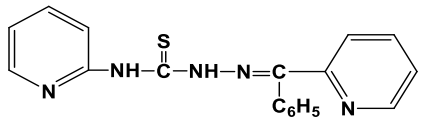

Chloro(2-[phenyl(pyridin-2-yl)methylidene]-*N*-(pyridin-2-yl)carbamohydrazonothioato)copper(II)

[Zn(L^5-H)Cl],
L^5-H =

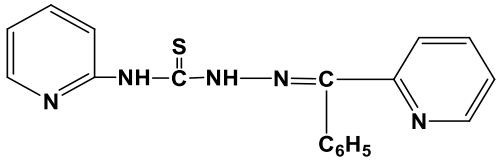

Chloro(2-[phenyl(pyridin-2-yl)methylidene]-*N*-(pyridin-2-yl)carbamohydrazonothioato)zinc

Fig. 5.1. **Hydrazinecarbothioamide derivatives and their coordination compounds**

The ORAC assay is based on *in situ* production of peroxyl free radicals generated via an azo-compound, 2,2,-azobis(2-methylpropionamidine) dihydrochloride (AAPH), according to the reaction presented in Scheme 5.3.

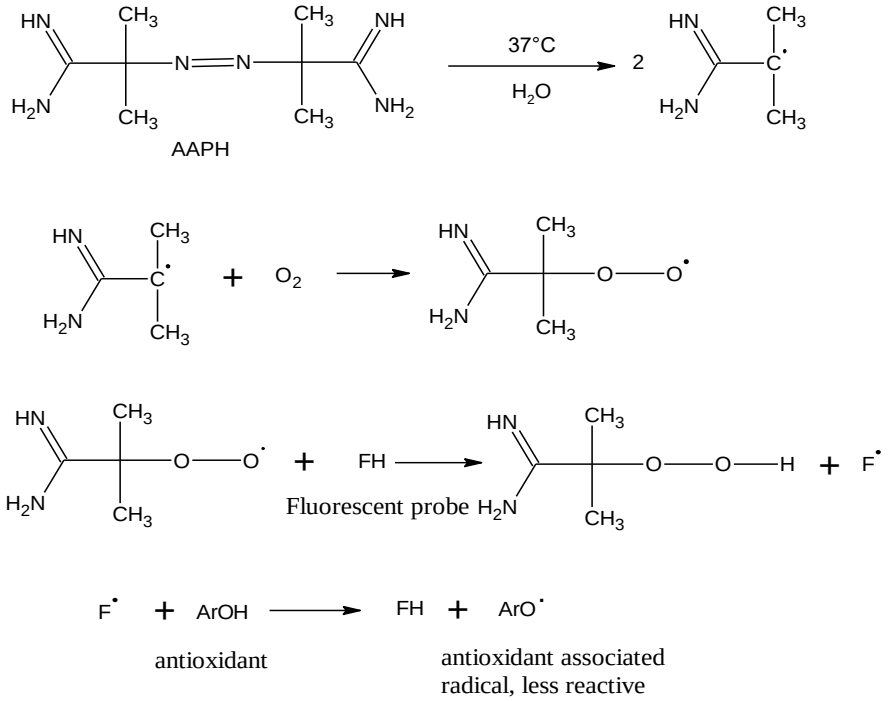

Scheme 5.3. **Oxygen Radical Absorption Capacity (ORAC) assay measuring principle**

An azo-compound, 2,2,-azobis(2-methylpropionamidine) dihydrochloride (AAPH), thermally generates C-centred free radicals, which in the presence of oxygen generate the peroxy free radicals interacting with the fluorescent probe.

The oxygen radical absorbance capacity assay measures the radical chain-breaking ability of antioxidants by monitoring the inhibition of peroxyl radical-induced oxidation. Peroxyl radicals are the predominant free radicals found in lipid oxidation in biological systems under physiological conditions.

Hence, ORAC values are considered by some to be of biological relevance as a reference for antioxidant effectiveness. In this assay, the peroxyl radical produced by a generator reacts with a fluorescent probe resulting in the loss of fluorescence, which is recorded with a fluorescence microplate reader. A set of fluorescence decay curves can be constructed in the absence or presence of antioxidants, and the net integrated area under the decay curves (area gain in the presence of antioxidants compared to that of a blank run without antioxidants) can be calculated as an indicator of the peroxyl radical scavenging capacity of the antioxidants.

A standard antioxidant Trolox was used as a reference, and ORAC values of the tested compounds are reported as Trolox equivalents. The ORAC method measures the hydrogen atom donating ability of antioxidants, and is, therefore, a hydrogen atom transfer (HAT) - based method.

The oxygen antioxidant capacity of the tested compounds hydrazinecarbothioamide derivatives and their coordination compounds was estimated by comparison to the standard curve of Trolox. Figure 5.2 depicting the kinetic curves of Trolox demonstrates the concentration-dependent protection of fluorescein against oxidative degradation by AAPH. The progress of each reaction was followed in real-time using the current state option [251].

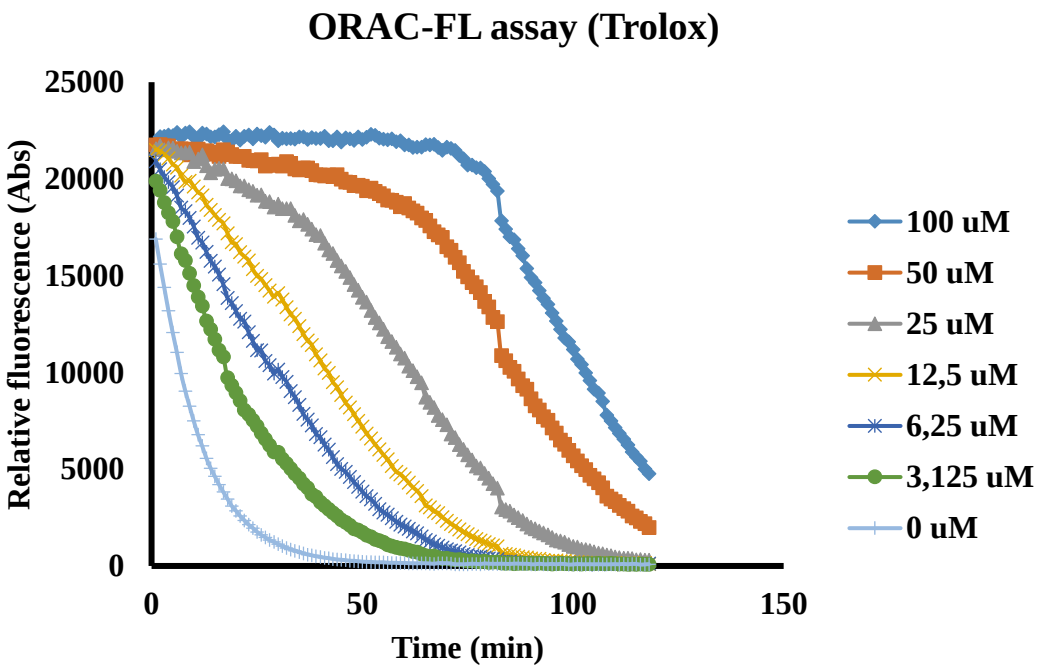

Fig. 5.2. **Plots of Trolox kinetic curves. The representative curves from the ORAC assay of varying concentrations of Trolox antioxidant standards ranged from 0 to 100 µM. The automated ORAC assay was performed on a microplate reader with fluorescence filters FP (485 nm / 528 nm). The experiment was conducted at 37^0 C under pH 7.4 conditions with a blank sample in parallel. The fluorescence was recorded every minute for 120 min.**

The Net AUC calculated by the equation is graphically indicated in Figures 5.3 and 5.4. The coefficient of determination values (R^2) are all fairly high: 0.99 for Trolox, 0.98 for DOXO, 0.88 for L^1, 0.87 for [Cu(L^1-H)Cl], 0.67 for [Cu(Str^1)(L^1-H)Cl], 0.98 for [Cu(Str^2) (L^2-2H)], 0.88 for [Cu(Str^3) (L^3-2H)], 0.79 for [CuL^4Cl_2], 0.73 for L^5, 0.93 for [Cu(L^5-H)Cl], and 0.87 for [Zn(L^5-H)Cl].

The antioxidant property for the tested compounds, anticancer drug DOXO, and the reference antioxidant control Trolox was determined by the ratio of the slope (m) of the linear regression curve. Slope (m) values are 1.2 for Trolox, 0.5 for DOXO, 3.4 for L^1, 3.5 for [Cu(L^1-H)Cl], 3.6 for [Cu(Str^1)(L^1-H)Cl], 2.7 for [Cu(Str^2)(L^2-2H)], 3.1 for [Cu(Str^3)(L^3-2H)], 3.6 for [CuL^4Cl_2], 3.5 for L^5, 2.8 for [Cu(L^5-H)Cl], and 3.2 for [Zn(L^5-H)Cl].

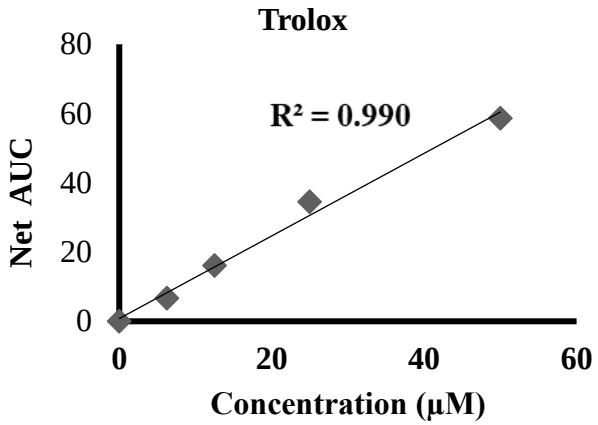

Fig. 5.3. **Trolox Standard Curve. The net AUC of varying concentrations of Trolox antioxidant standards ranging from 0 to 50 µM are plotted vs. concentration**

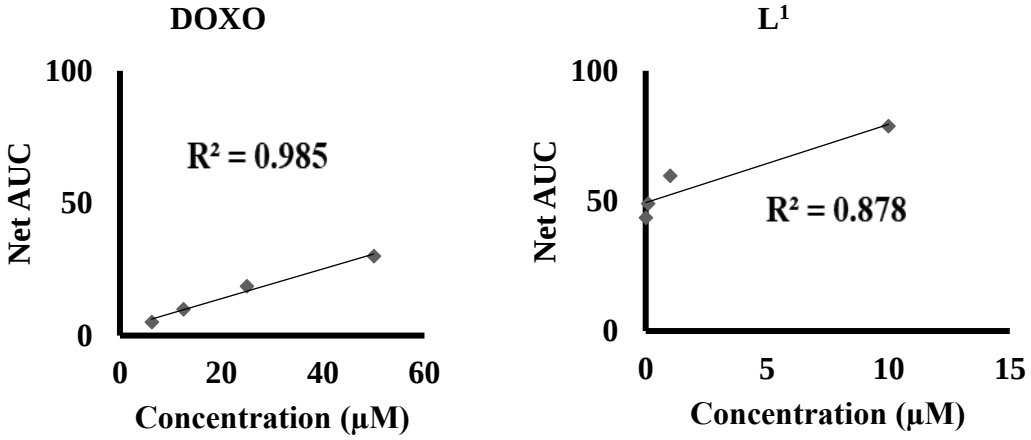

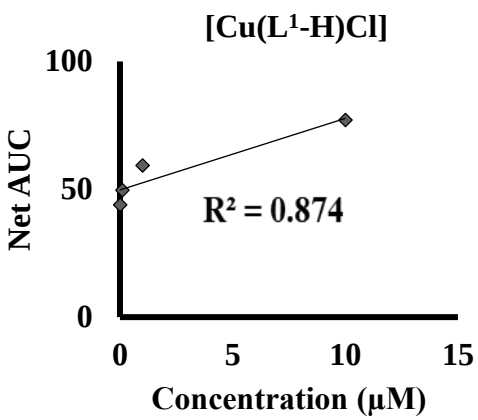
[Cu(L¹-H)Cl]
Net AUC
100
50
0
R² = 0.874
0
5
10
15
Concentration (µM)

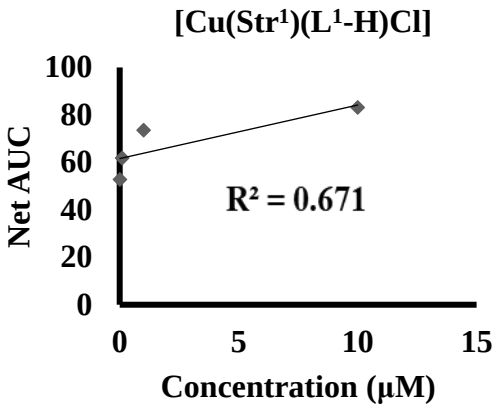
[Cu(Str¹)(L¹-H)Cl]
Net AUC
100
80
60
40
20
0
R² = 0.671
0
5
10
15
Concentration (µM)

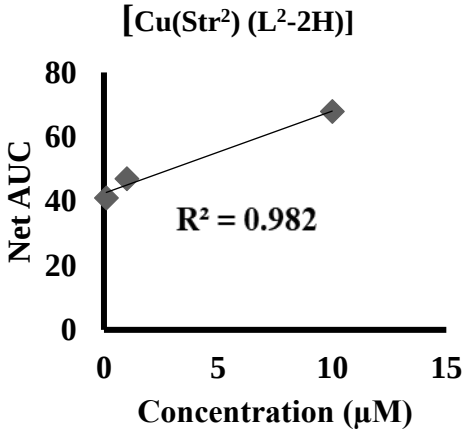
[Cu(Str²) (L²-2H)]
Net AUC
80
60
40
20
0
R² = 0.982
0
5
10
15
Concentration (µM)

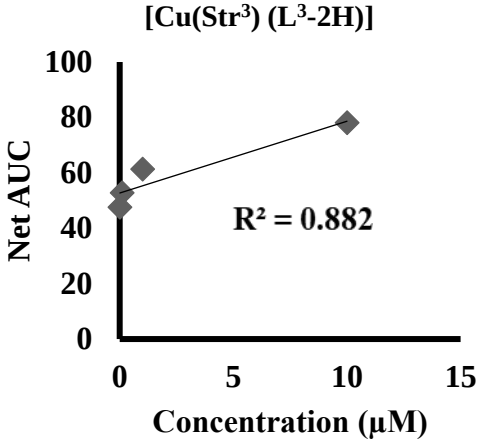
[Cu(Str³) (L³-2H)]
Net AUC
100
80
60
40
20
0
R² = 0.882
0
5
10
15
Concentration (µM)

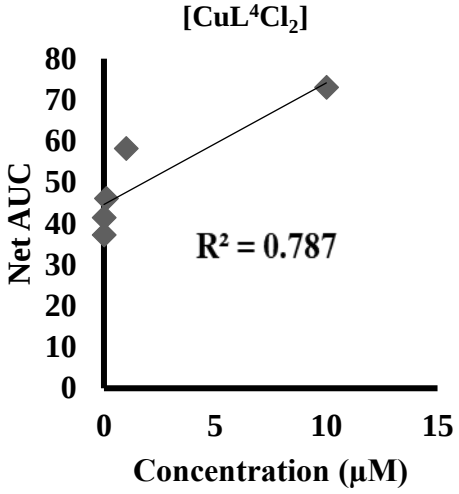
[CuL⁴Cl₂]
Net AUC
80
70
60
50
40
30
20
10
0
R² = 0.787
0
5
10
15
Concentration (µM)

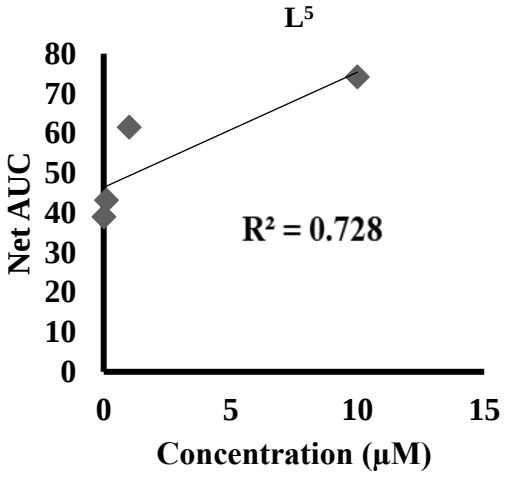
L⁵
Net AUC
80
70
60
50
40
30
20
10
0
R² = 0.728
0
5
10
15
Concentration (µM)

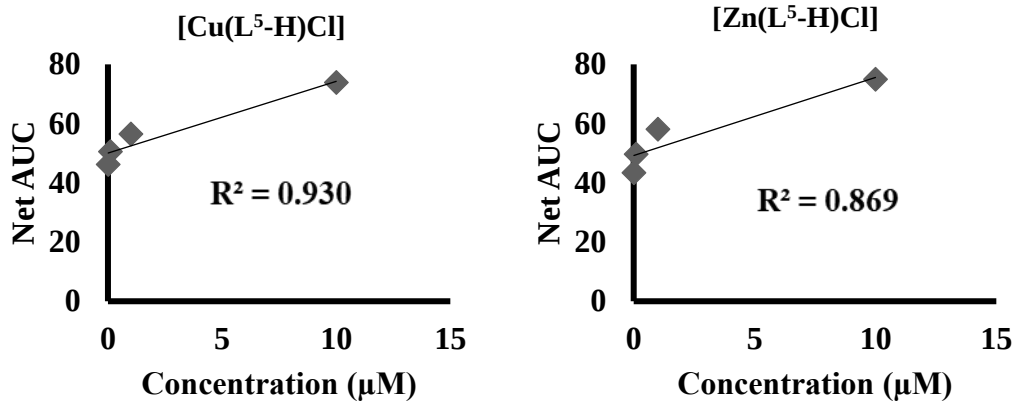

Fig. 5.4. **The Net AUC of varying concentrations of the reference antioxidant control Trolox, the anticancer drug doxorubicin, and the tested compounds. Values are represented as mean ± SD of 3 replicates.**

The calculated Trolox equivalents (TE) were used for comparative analysis of the antioxidant capacity of the tested compounds and anticancer drug DOXO (Table 5.3).

Table 5.3. Antioxidant activity of the tested compounds, reference antioxidant control Trolox and anticancer drug doxorubicin (DOXO)

Oxygen Radical Absorbance Capacity (ORAC-FR)		
Compound	**m**	**TE**
Trolox	1.2	-
DOXO	0.5	0.4
L^1	3.4	2.8
[Cu(L^1-H)Cl]	3.5	2.9
[Cu(Str^1)(L^1-H)Cl]	3.6	3.0
[Cu(Str^2) (L^2-2H)]	2.7	2.3
[Cu(Str^3) (L^3-2H)]	3.1	2.6
[CuL^4Cl_2]	3.6	3.0
L^5	3.5	2.9
[Cu(L^5-H)Cl]	2.8	2.3
[Zn(L^5-H)Cl]	3.2	2.7

Note: Trolox equivalent (TE), slope (m)

Analyzing the ORAC results, it was observed that TE (Trolox Equivalent) values are 0.4 for DOXO, 2.8 for L^1, 2.9 for **[**$Cu(L^1\text{-}H)Cl$**]**, 3.0 for **[**$Cu(Str^1)(L^1\text{-}H)Cl$**]**, 2.3 for **[**$Cu(Str^2)$ $(L^2\text{-}2H)$**]**, 2.6 for **[**$Cu(Str^3)$ $(L^3\text{-}2H)$**]**, 3.0 for **[**CuL^4Cl_2**]**, 2.9 for L^5, 2.3 for **[** $Cu(L^5\text{-}H)Cl$**]**, and 2.7 for **[**$Zn(L^5\text{-}H)Cl$**]**. The oxygen antioxidant capacity of the compounds can thus be ranked in the order **[**$Cu(Str^1)(L^1\text{-}H)Cl$**]** = $[CuL^4Cl_2]$ ≥ **[**$Cu(L^1\text{-}H)Cl$**]** = L^5 ≥ L^1≥ **[**$Zn(L^5\text{-}H)Cl$**]** ≥ **[**$Cu(Str^3)$ $(L^3\text{-}2H)$**]** ≥ **[**$Cu(Str^2)(L^2\text{-}2H)$**]** = **[**$Cu(L^5\text{-}H)Cl$**]** ≥ DOXO ≥ Trolox.

Thus, it was found that the tested compounds showed the highest oxygen radical absorbance capacity compared with DOXO and Trolox.

5.4. Antilipoxygenase activity of the tested compounds

Lipoxygenase constitutes a family of non-heme iron-containing enzymes, as versatile biocatalysts are capable of catalyzing many reactions involved in the xenobiotic metabolism. The lipoxygenase enzyme catalyzes the reaction: unsaturated fatty acid + O_2 = unsaturated fatty acid hydroperoxide. It is believed that only unsaturated fatty acids that contain a cis-cis-1,4-pentadiene group are exposed to the enzyme, as shown in Scheme 5.4.

Lipoxygenases (LOXs) enzymes are reported to convert the arachidonic, linoleic, and other polyunsaturated fatty acids into biologically active metabolites that are involved in inflammatory and immune responses. LOXs also play a significant role in cancer cell growth, metastasis, invasiveness, cell survival, and induction of cancer necrosis factor alpha (TNF-α) and start a cytokine storm [267] (Figure 5.5).

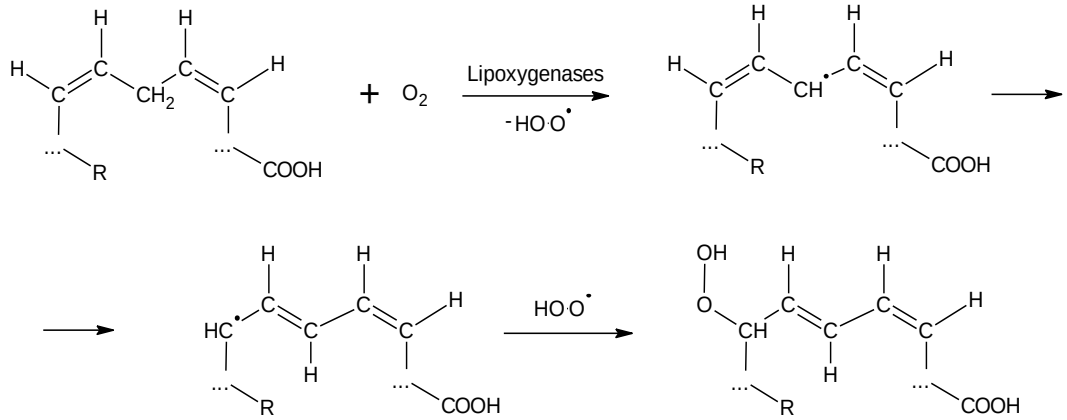

Scheme 5.4. **The oxidation reaction of polyunsaturated fatty acid by lipoxygenase enzyme**

The intermediate formation of radical results in peroxide, one double bond moves to the adjacent (conjugated) position, and the unsaturated fatty acid passe into the cis-trans isomer. Linoleic, linolenic, and arachidonic acids are oxidized by the

enzyme at the same rate. Fatty acids with trans-configuration of double bonds are not oxidized by the enzyme.

12/15-LOX is a member of the LOXs family which is widely distributed in different organizations. 12-LOX can be divided into three types, platelet-type 12-lipoxygenase (p12LOX), leukocyte-type 12-lipoxygenase (l12LOX), and epidermis-type 12-lipoxygenase (e12LOX) [268]. l12LOX deriving from rats, mice, cattle, and pigs is highly homologous to human 15-LOX-1 since both enzymes catalyze AA to produce 12-hydroxy dioctatetraenoic acid (12-HETE) and 15-hydroxy eicosatetraenoic acid (15-HETE) [269].

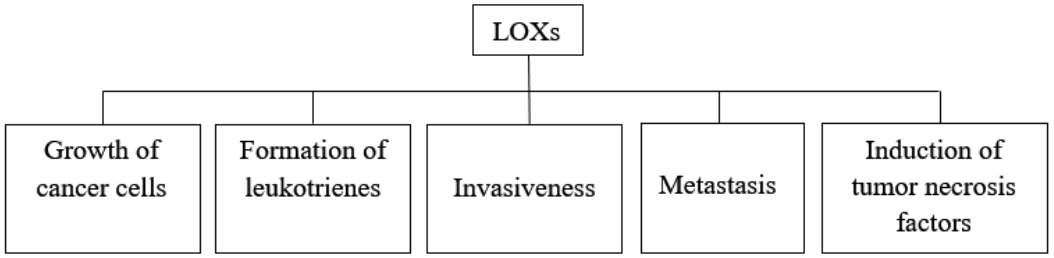

Fig. 5.5. **Significant role of LOXs in the organisms**

Apoptosis is a type of programmed cell death that was first proposed by Kerr in 1972. It has been reported that a variety of diseases are related to apoptosis including cancer, neurodegenerative disorders, autoimmune disease, virus infective disease, and so on [270]. In neuron cells, 12/15-LOX participated in apoptosis is mediated by the AIF (apoptosis-inducing factor) signal pathway which is implicated in caspase-independent forms of apoptosis. Glutathione peroxidase (GPX) which was later confirmed as GPX4 interacted with 12/15-LOX to regulate the redox state of the cells (Kuhn and Borchert). GPX4 could regulate 12/15-LOX to prevent the 12S-HPETE to shift to 12S-HETE and the isomerization to hepoxilins. Meanwhile, glutathione (GSH) was a cofactor for GPX4. GSH depletion has been shown to impair GPX4 function [271]. Correspondingly, the inactivation of GPX4 in mice and cells induced 12/15-LOX-derived lipid peroxidation and then triggered AIF-mediated cell death. Since oxidative stress is related to various human diseases, identifying the GPX4/12/15-LOX proapoptotic pathway provides promising targets for future therapies [272].

In addition, the glutamate toxicity cell model is the most commonly used model for studying oxidative stress. Studies have shown that 12/15-LOX are characterized by sequentially timed aggregation closing to the nucleus accompanied

by mitochondrial AIF translocating to the endoplasmic reticulum and nuclear in excessive glutamate-induced cell death in HT22 cell line.

In this regard, in this study, the ability of all tested compounds as well as the anticancer drug DOXO to inhibit the activity of lipoxygenases (LOX) [276] was evaluated (Table 5.4).

In some cell and animal models which caused apoptosis, regulating the expression of 12/15-LOX by long noncoding RNA and miRNA contributed to the pathological process.

In a cultured cardiac myocytes apoptosis cell model treated with stimulated ischemia/reperfusion, baicalein, a specific 12/15-LOX inhibitor significantly inhibited cardiomyocyte apoptosis through activation of ERK1/2 and AKT pathways and inhibition of activation of p38 MAPK, JNK1/2, and NF-KB/p65 pathways [273]. (Figure 5.6)

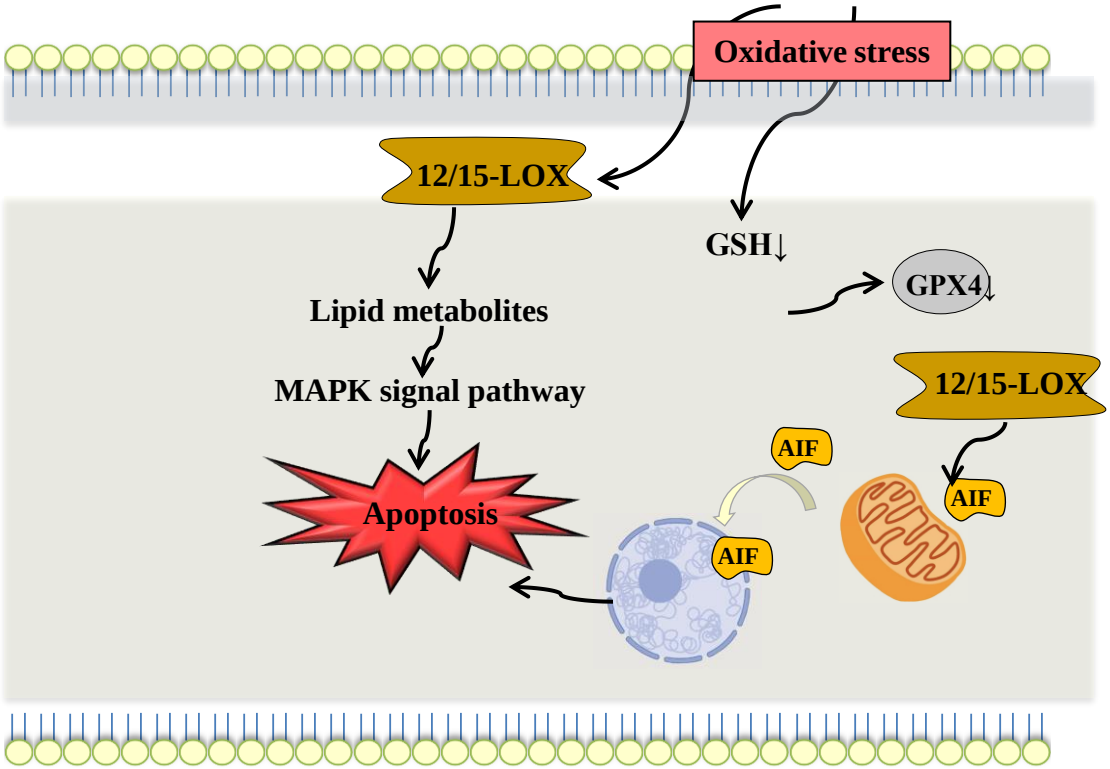

Fig. 5.6. **Cell death pathways of 12/15-LOX in apoptosis. Oxidative stress leads to the activation of 12/15-LOX coincided with the increasing metabolites which in turn activates the MAPK signal pathway and finally leads to apoptosis. On the other side, oxidative stress leads to a decrease in GSH coinciding with a decrease in the activity of GPX4 and activation of 12/15-LOX, resulting in the transfer of AIF from the mitochondria to the nucleus, eventually leading to apoptosis [275].**

LOXs are the key enzymes in the biosynthesis of leukotrienes (LTs) that play an important role in several inflammation-related diseases such as arthritis, asthma, cancer, and allergic diseases. High levels of LTs could be observed in the case of asthma, psoriasis, allergic rhinitis, rheumatoid arthritis, and ulcerative colitis. Therefore, it is of the view that the production of LTs can be prevented via inhibition of the LOX pathway, and targeting LOX with inhibitors is a promising therapeutic target for treating a wide spectrum of human diseases. Pidgeon et al., also suggested that LOX inhibitors may lead to the design of biologically and pharmacologically targeted therapeutic strategies inhibiting LOX isoforms and their biologically active metabolites which may be useful in cancer treatment. Many COX-2 or 5-LOX inhibitors have been developed as drugs to treat inflammation [274].

Table 5.4. The percentage of inhibition of the tested compounds and positive control Quercetin and anticancer drug DOXO on the inhibition of the lipoxygenase activity by FTC-based LOX activity method

Compound	% inhibition mean ± SD			R^2
	0.05 μM	0.50 μM	5.00 μM	
Quercetin	20.0±0.5	28.0±0.1	50.0±0.8	0.9
DOXO	34.5±0.5	37.0±1.0	40.0±1.0	0.9
L^1	48.5±0.5	52.5±2.5	61.0±1.0	0.9
[Cu(L^1-H)Cl]	44.2±1.5	53.1±0.5	77.6±1.9	0.9
[Cu(Str^1)(L^1-H)Cl]	48.4±0.5	53.1±0.4	58.1±0.9	0.9
[Cu(Str^2) (L^2-2H)]	40.1±0.5	54.0±0.6	61.1±1.2	0.9
[Cu(Str^3) (L^3-2H)]	44.6±0.4	57.2±1.2	66.3±0.6	0.9
[CuL^4Cl_2]	42.4±0.6	53.3±0.5	55.4±0.8	0.9
L^5	65.4±0.4	62.1±1.6	52.3±1.5	0.9
[Cu(L^5-H)Cl]	63.2±0.9	58.0±1.9	53.1±0.4	0.9
[Zn(L^5-H)Cl]	57.1±0.4	53.3±0.4	43.4±0.3	0.9

Note: Values are represented as mean ± SD of 3 replicates.

Inflammation is favorable in most cases because it is a kind of body`s defensive response to external stimuli; sometimes, inflammation is also harmful, such as attacks on the body's tissues. Inflammation is likely a unified process of injury and

resistance to injury. Inflammation brings extreme pain to patients, showing symptoms of rubor, swelling, fever, pain, and dysfunction. In these aspects, the medicinal properties of the tested compounds should be investigated on biological activities to counteract the inflammatory process, being with no side effects and with high economic viability.The antioxidant quercetin was used as a positive control. The tested hydrazinecarbothioamide derivatives and their coordination compounds were able to induce inhibition of soybean LOX in a dose-dependent manner with the IC_{50} values up 0.40 μM, to 0.03 μM. In contrast, the IC_{50} values for the assay positive control quercetin and anticancer drug DOXO reached values of 15.6±1.6 μM and 5.6±0.3 μM, respectively. Thus, these data demonstrate that the tested compounds are potent inhibitors of LOX activity (Table 5.5). The ligand 2-[phenyl(pyridin-2-yl)methylidene]-*N*-(pyridin-2-yl)hydrazinecarbothioamide and its complexes such as [Cu(L^5-H)Cl], [Zn(L^5-H)Cl] with IC_{50} of 0.03 μM show the highest activity in inhibiting LOX.

Table 5.5. The effects of IC_{50} of the positive control quercetin, anticancer drug DOXO and the tested compounds such as hydrazinecarbothioamide derivatives and their coordination compounds on the inhibition of the LOX activity

The effects of IC_{50} (μM) on the inhibition of the LOX activity		
Compound	**IC_{50} (μM)**	**SD (μM)**
Quercetin	15.6	0.5
DOXO	5.6	0.2
L^1	0.20	0.01
[Cu(L^1-H)Cl]	0.40	0.05
[Cu(Str^1)(L^1-H)Cl]	0.30	0.02
[Cu(Str^2) (L^2-2H)]	0.30	0.06
[Cu(Str^3) (L^3-2H)]	0.20	0.05
[CuL^4Cl_2]	0.20	0.03
L^5	0.030	0.004
[Cu(L^5-H)Cl]	0.030	0.003
[Zn(L^5-H)Cl]	0.030	0.004

Analyzing the antioxidant properties of the tested compounds by LOX assays, we can see that they are potent reductive inhibitors and showed good results, compared to DOXO and quercetin. Thus, they showed a strong potential to be developed as new anti-inflammatory drugs.

5.5. Impact of the tested compounds on methemoglobin formation

Studies on the mechanisms underlying the biochemical processes of disturbance of the oxygen transport function of the blood is an urgent task of modern biology and medicine.

One of the main links in the chain of metabolic disorders of the blood oxygen transport system is the reaction of the hemoglobin transformation into its inactive form - methemoglobin. In this regard, there is a need to search for methods and means of correcting such lesions that increase the efficiency of redox processes of methemoglobin reduction.

The spatial structure of the hemoglobin molecule was studied in detail by X-ray diffraction analysis as early as the end of the 1940s, mainly due to the works of the English biophysicist M. Perutz. Hemoglobin is a complex protein represented by two parts: a non-protein planar part — heme (4% of the hemoglobin molecule) and a protein oligomeric globule (96%).

Heme (protogem) is the tetrapyrrole aromatic structure of protoporphyrin IX, which necessarily contains the Fe^{2+} ion. The SP^2 hybrid atoms of the C and N π-electronic systems of the porphyrin oligand provide its planar structure [277]. Heme is a prosthetic group of heme-containing proteins that ensures their main functions: oxygen binding and transport, participation in the electron transfer chain, oxygen reduction to water, microsomal oxidation, decomposition of peroxides, etc. The presence of Fe^{2+} ion and the aromatic nature of the tetrapyrrole core provide intense heme color, which allows assigning of heme-containing proteins to the class of chromoproteins.

Globin, a protein component of hemoglobin, belongs to the group of histones. The number of amino acid residues in the polypeptide chain of different types ranges from 140 to 150, and numbers 141, 146, and 153 are more common. Human hemoglobin protomers contain either 141 (α-chain) or 146 (β-, γ-, δ -chains) of amino acid residues.

The secondary structure of hemoglobins is represented by an α-helix. Polypeptide chains in a hemoglobin molecule are represented by more than 70% twisted into α-helix spirals, fragments of which are separated by sections that form the bends of the secondary chain. Tertiary ovoid globules are formed as a result of this stacking. The number of helical regions varies in different Hb chains. The α-chain has 7 such domains and the β-chain - 8. Spiralized hemoglobin fragments are denoted in Latin letters, starting at the O end of the polypeptide chain (for example, in the α-subunit: A, B, C, D, E, F, H). The spatial layout of the tertiary structure of hemoglobin subunits corresponds to the principles of tertiary folding of most

globular proteins: maximum compactness, hydrophobic amino acid radicals are located inside the globule, and most hydrophilic amino acid residues are located on the surface of the protomer. The physiological form of the quaternary structure of human hemoglobins is tetrameric. All four hemoglobin protomers are spatially located in a certain ratio of "quaternary structure", forming a tetrahedral configuratconcerningt toconcerningach other. The hemoglobin tetramer is a spheroid 64A lon, 55A wide, and 50A high. Each Swedberg unit is in contact with three other Swedberg units, loosely linked by non-covalent bonds. Nonpolar hydrophobic bonds, being turned inside the protein, play a major role in stabilizing the quaternary hemoglobin structure.

O_2 addition is ensured by the content of the Fe^{2+} atom in the heme. This reaction is reversible and depends on the partial O_2 pressure. Besides transporting O_2 to tissues, Hb carries out the reverse transport of the main final gas metabolite of tissues - carbon dioxide. Approximately 15-20 % of carbon dioxide and H^+ ions present in the blood are carried by Hb molecules. Hemoglobin binds two protons for every four released oxygen molecules.

Typically, up to 1 % methemoglobin is accumulated in red blood cells per day, which is associated with the normal process of autooxidation of normal hemoglobin. Methemoglobin is formed as a result of iron oxidation in hemoglobin heme, i.e. methemoglobin formation occurs under the influence of any substances. This is facilitated by a change in the conformation of the protein part of the hemoglobin molecule due to the oxidatioseveraler of functional groups of the protein.

In the blood of a healthy person, the content of methemoglobin does not exceed 3-4%, which is achieved by the equilibrium between the reactions of its formation and the reactions of methemoglobin reduction. If the content of methemoglobin in the blood exceeds 3%, this is methemoglobinemia.

Many medicinal substances, especially with prolonged use in large doses, can cause methemoglobinemia. However, in most people metHb in Hb is restored after drug withdrawal under the influence of methemoglobin reductase [278].

Any methemoglobinemia is based on acute or chronic hypoxia due to a decrease in oxygen saturation of arterial blood. Moreover, methemoglobin not only does not participate in oxygen transport, but also worsens the transport function of the existing oxyhemoglobin. Toxic methemoglobinemia of exogenous origin is known to occur when exposed to chemical agents, such as analgesics (acetanilide, phenacetinitrobenzenes/nitrobenzoatesates, nitroglycerin, nitrofuragin, trinitrotoluene, hydroxylamine, dimethylamine, local anesthetics (lidocaine, prilocadone, prilocadone, prilocainum, prilocadone, dlocadone, dlocadone,

dlocadone, metoclopramide (Cerucal), sulfamethoxazole, sulfonamides, menadione (vitamin K3), naphthoquinophenazopyridinedine (Puridium), antibiotics (ampicillin, amikacin, gentamicin, carbenicillin). Some of them directly oxidize Hb, and others form intermediate aggressive forms. Acute poisoning poses a threat to life, therefore, those who exhibit atypical cyanosis or cyanosis, combined with a normal blood gas content, need to measure methemoglobin content.

The severity of symptoms depends on the content of methemoglobin in the blood (Table 5.6) [279]. Cyanosis occurs at around 15-30 % metHb and tissue hypoxia can occur as levels rise further - metHb levels of 70 % can be fatal [279].

Table 5.6. Relationship of clinical symptoms with the proportion of methemoglobin fraction in the blood

MetHb (%)	Symptomatology
<3	Lack of clinical manifestations
3—15	Grayish skin tone
15—30	Cyanosis, brown staining of blood
30—50	Dyspnea, headache, weakness, dizziness, fainting
50—70	Tachypnea, metabolic acidosis, arrhythmias, convulsions, coma
>70	Hypoxia, death

Erythrocytes contain endogenous enzymatic and non-enzymatic methemoglobin reductase systems. The main system of protection against oxidizing agents, which allows maintaining the hemoglobin fraction in healthy subjects at the level of 1.0-1.5%, includes three components: reduced nicotinamidine nucleotide (NAD-H), heme-containing hemoproteincytochrome b5 and the enzyme cytochrome b5 reductase. The electron donor is the glycolysis product NAD-H. An electron is transferred from NAD-H to cytochrome b5 and ultimately to methemoglobin. Electron transport is catalyzed by the enzyme cytochrome b5 reductase. This mechanism is responsible for the recovery of 99 % of hemoglobin from methemoglobin. Another way to restore hemoglobin, associated with the activity of NADP-methemoglobin reductase, under normal conditions, has little effect. Its role increases in the event of a deficiency of cytochrome b5 reductase.

However, in conditions of massive toxic methemoglobin formation, the enzymatic efficiency is sharply reduced. Therefore, this requires the presence of drugs in the cell that can activate endogenous methemoglobin reductase systems or restore methemoglobin directly. Substances with redox properties can be considered the most promising among the drugs studied to date. The most active antidote for toxic

methemoglobinemia is methylene blue, which has a high redox potential. However, methylene blue has negative properties. The most dangerous of them is intravascular hemolysis. Currently, methylene blue is not used in medical practice.

Hypoxia and methemoglobinemia are major concerns for patients undergoing anti-cancer therapies and who have compromised cardiopulmonary function [280]. The biomedical significance of metal-catalyzed HbO_2 oxidation is through acquired methemoglobinemia. There has been serious concern about hypoxia and methemoglobinemia side effects during anticancer therapies using the well-known iron chelator 3-aminopyridine-2-pyridinecarbaldehyde thiosemicarbazone (3-AP; Triapine), which is being examined in phase I, II and phase III clinical trials for the treatment of various cancers. 3-AP has been shown to induce the formation of metHb (methemoglobinemia) and hypoxia in patients, limiting its usefulness. The mechanism responsible was not known and considering the interest in the development of novel thiosemicarbazones as anti-cancer agents, it was crucial to investigate their effect on oxyHb, as this would facilitate the development of these compounds [280].

Patricia Quach demonstrated that the iron complexes of 3-AP and the lead DpT and BpT chelators, di-2-pyridylketone-4,4-dimethyl-3-thiosemicarbazone (Dp44mT) and 2-benzoylpyridine-4-ethyl-3-thiosemicarbazone (Bp4eT), induce metHb- and metmyoglobin (metMb)-formation, *invitro* and *in vivo* [281].

Considering this problem, we assessed the tested compounds with antioxidant and antiproliferative activities against cancer cells that were subjected to screening on methemoglobin formation in human RBCs, because it is a serious toxic effect. This study of the tested substances such as hydrazinecarbothioamide derivatives and their coordination compounds showed good results, which did not exceed the permissible values in the 1 - 10 μM concentration range (Figure 5.7).

Hence, no significant fluctuations in metHb formation were observed after exposure of RBCs to various concentrations of hydrazinecarbothioamide derivatives and their coordination compounds. Thus, the application of 10 μM of DOXO, L^1, **[**Cu(L^1-H)Cl**]**, **[**Cu(Str^1)(L^1-H)Cl**]**, **[**Cu(Str^2) (L^2-2H)**]**, **[**Cu(Str^3) (L^3-2H)**]** [Cu(L^5-H)Cl], and [Zn(L^5-H)Cl] induced the formation of metHb in 3.5%, 3.8%, 10.5%, 5.3%, 8.1%, 6.9%, 8.0%, 6.2% of cases, respectively. This study of the tested compounds showed results, which did not exceed the permissible values in the therapeutic concentration of range [282].

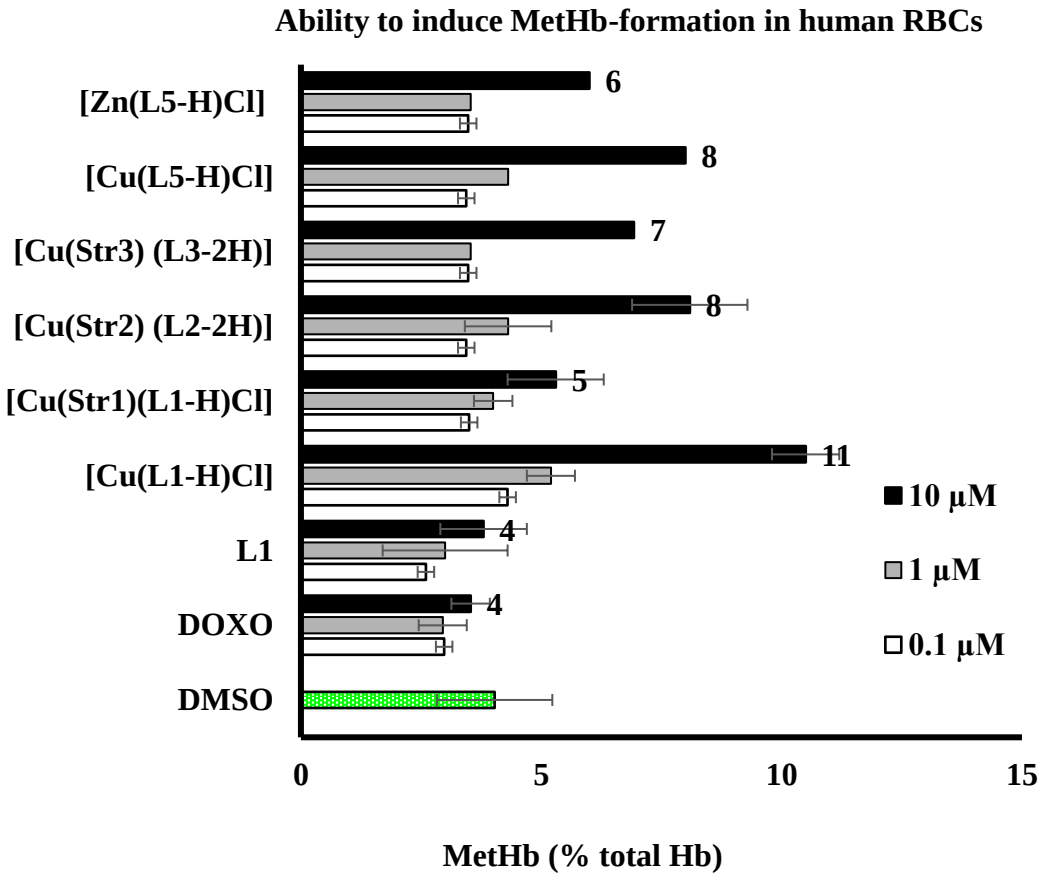

Fig. 5.7. **Effect of the tested compounds and the anticancer control DOXO on metHb formation *in vitro.* Dilutions of the tested compounds were prepared in DMSO at three concentrations (0.1, 1, 10 µM). Values are represented as mean ± SD of 3 replicates.**

5.6. Impact of the tested compounds on RBCs hemolysis

Toxic ROS constantly appear in small amounts from O_2. These compounds are strong oxidizing agents or extremely reactive free radicals that destroy cellular structures and functional molecules.

The oxygen molecule (O_2) contains two unpaired electrons and, therefore, is a biradical. However, unpaired electrons are arranged so that the O_2 molecule remains relatively stable. Nevertheless, if the molecule attaches an additional electron, a highly reactive superoxide radical ($^{\bullet}O_2^-$) is formed. The next stage of reduction leads to the peroxide anion ($^{\bullet}O_2^-$), which easily binds protons and, as a result, transfers to hydrogen peroxide (H_2O_2). The addition of the third electron leads to the splitting of the molecule into O_2^- and O^- ions. While O_2^- forms water by the addition of two protons, the protonation of O^- leads to a particularly dangerous hydroxyl radical. The

addition of the fourth electron and the final protonation of O^- end with the formation of water is depicted below (Scheme 5.5).

$$\begin{array}{l} Hb\left(Fe^{2+}\right) \\ \quad\downarrow \longrightarrow \bar{e} + O_2 \longrightarrow O_2^- \xrightarrow[\bar{e},2H^+]{} H_2O_2 \xrightarrow[\bar{e},H^+]{} H_2O + OH^{\bullet} \\ MetHb\left(Fe^{3+}\right) \end{array}$$

Scheme 5.5. **Formation of reactive oxygen forms and possible pathways for electron loss**

Red blood cells are especially susceptible to ROS damage, which, due to their transport function, is characterized by a high oxygen concentration. ROS can cause erythrocyte hemolysis. Red blood cells contain an enzyme system that prevents the toxic effects of oxygen radicals and the destruction of red blood cell membranes.

To protect against ROS and other radicals, all cells contain antioxidants. The latter are reducing agents that readily react with oxidizing substances and therefore protect the more important molecules from oxidation. Biological antioxidants include vitamins C and E, coenzyme Q, and some carotenoids. The bilirubin formed during the destruction of heme also serves as protection against oxidation.

Glutathione, the Glu-Cys-Gly tripeptide, which is found in almost all cells in high concentration, is especially important. The thiol group of the cysteine residue is the reducing agent here. Two molecules of the reduced form (GSH) develop a disulfide upon oxidation. Red blood cells also have a system (superoxide dismutase, catalase, GSH) that can inactivate ROS and repair the damage they cause. For this, substances are needed that ensure the maintenance of normal metabolism in red blood cells. The metabolism in red blood cells is, in essence, limited by anaerobic glycolysis and the pentose phosphate pathway.

The ATP formed during glycolysis serves primarily as a substrate of Na^+, K^+, and ATPase, which supports the membrane potential of red blood cells. NADPH + H^+ is formed in the pentose phosphate pathway, which supplies H^+ to regenerate reduced glutathione (GSH) from glutathione disulfide (GSSG) using glutathione reductase. Reduced glutathione is the most important red blood cell antioxidant; it serves as a coenzyme in the reduction of methemoglobin into functionally active hemoglobin. Selenium-containing glutathione peroxidase is also an important protective enzyme.

H_2O_2 detoxication occurs with the aid of reduced glutathione, which detoxifies, as well as hydroperoxides, which arise during the reaction of ROS with unsaturated fatty acids of the erythrocyte membrane.

When taking certain medicinal substances, which are strong oxidizing agents, the potential of glutathione protection may not be sufficient. This leads to an increase in the content of ROS in cells that cause the oxidation of SH groups of hemoglobin molecules. The formation of disulfide bonds between the hemoglobin and methemoglobin protomers results in their aggregation - the formation of Heinz bodies. The latter contributes to the destruction of red blood cells (hemolysis) when they penetrate small capillaries. The hemolysis process is characterized by a rupture or a sharp increase in the permeability of the erythrocyte membrane and the release of hemoglobin into the plasma [283].

Although the majority of normal individuals may suffer toxic hemolysis at sufficiently high concentrations of hemolytic drugs, for most drugs toxic hemolysis involves lower doses given to individuals who are genetically predisposed to hemolysis. It is strongly recommended for excipients intended for injectable use, that an *in vitro* hemolysis study should be performed at the intended concentration for administration to test for hemolytic potential. The *in vitro* hemolysis assay evaluates hemoglobin release in the plasma as an indicator of red blood cell lysis, following test agent exposure (tested compounds). Formulations with a hemolysis value of <20 % were considered nonhemolytic while values >25 % were considered for hemolysis.

One of the important criteria for the use of substances as anticancer drugs is the absence of a side effect associated with an increase in the formation of erythrocyte hemolysis caused by oxidative stress during chemotherapy.

In this regard, *in vitro* hemolysis testing of 5 experimental substances with anti-cancer properties and DOXO, was performed to screen for toxic hemolysis.

Additionally, hypotonic 0.1 % and isotonic 0.9 % solutions of NaCl were used as positive and negative controls, respectively. As expected, the application of negative and positive controls has induced 100% and < 10% of RBCs hemolysis [284].

In contrast, various concentrations of the tested compounds demonstrated low hemolytic activity reaching maximum values of 8.2%, 10.2%, 10.4%, 14.2%, 10.3%, 12.1%, 9.0% after exposure of RBCs to 10 μM of L^1, **[**$Cu(L^1\text{-}H)Cl$**]**, **[**$Cu(Str^1)(L^1\text{-}H)Cl$**]**, **[**$Cu(Str^2)$ $(L^2\text{-}2H)$**]**, **[**$Cu(Str^3)$ $(L^3\text{-}2H)$**]**, $[Cu(L^5\text{-}H)Cl]$, and $[Zn(L^5\text{-}H)Cl]$ respectively. Incubation of RBCs with DOXO drug promotes hemolysis of 17.0±0.2 % (Figure 5.8).

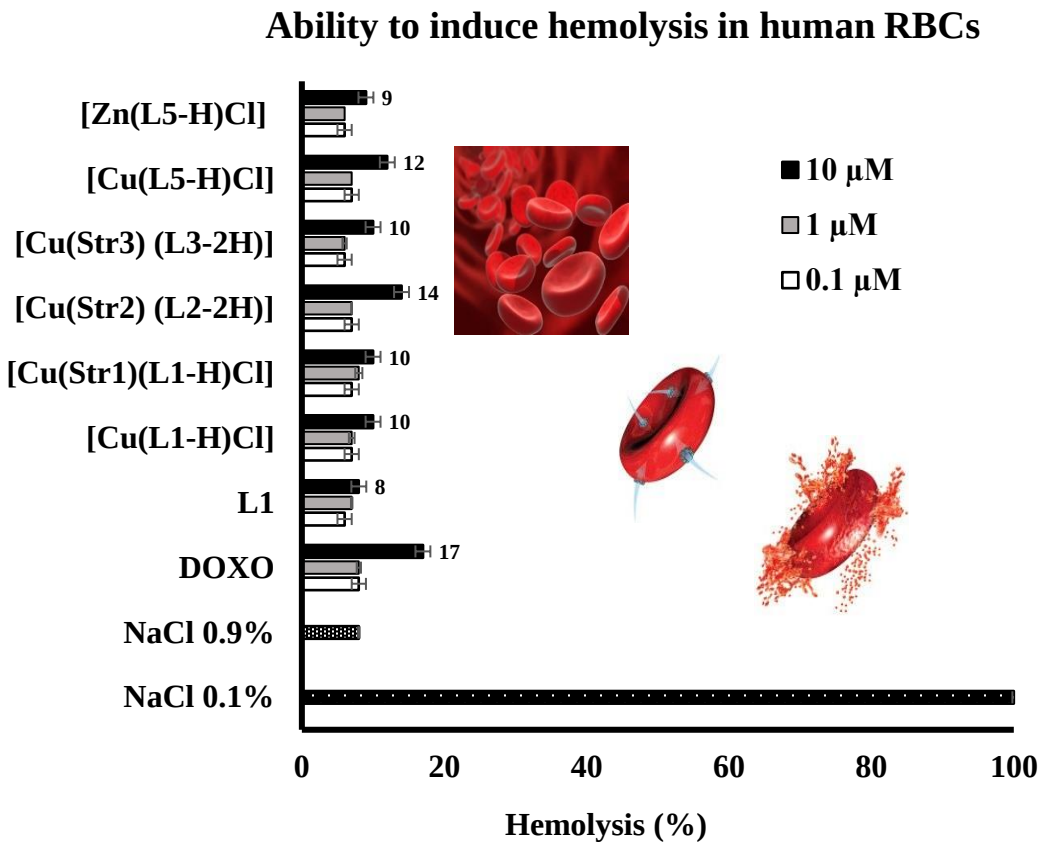

Fig. 5.8. **Percentage of hemolysis activity of the tested compounds and anticancer control DOXO as well as control (100 % lysis) NaCl 0.1 %. Hemolytic activity was evaluated by determining hemoglobin release from erythrocytes after incubation with compounds at three concentrations (0.1 µM, 1 µM, 10 µM). Values are represented as mean ± SD of 3 replicates.**

These results indicate, that the tested compounds have a low ability to induce RBCs hemolysis, as compared with DOXO. So, an induced hemolysis study of the tested compounds showed results, which did not exceed the permissible values in the therapeutic concentration range [282].

6. Antioxidant properties of natural products of honey bee *(Apis mellifera)*

Honey bee products have been known since ancient times and were used for both their nutritional value and a wide spectrum of therapeutic purposes. They are

considered a possible source of naturally-occurring antioxidants that can prevent the effects of oxidative stress responsible for the pathogenesis of many diseases.

The modulation of oxidative stress, for example, has been suggested as one of the mechanisms through which honey exercises chemopreventive effects against cancer. We have developed a method designed to enhance the antioxidant capacity of bee products *Apis mellifera* such as honey, pollen, propolis, and beeswax taking into account the growing interest in using bioactive naturally-occurring substances, possessing pronounced antioxidant properties, to promote health and reduce the risk of developing certain diseases.

We aimed to increase the antioxidant capacity of beehive products *(Apis mellifera)* with the help of biologically active compounds, which will increase their value. In this regard, biologically active coordination compounds $Na_2[Mo_2O_4EDTA]\cdot 5H_2O$ and $Li_2[Mo_2O_4EDTA]\cdot 5H_2O$ (Figure 6.1) have been synthesized to enhance the quality of beekeeping products.

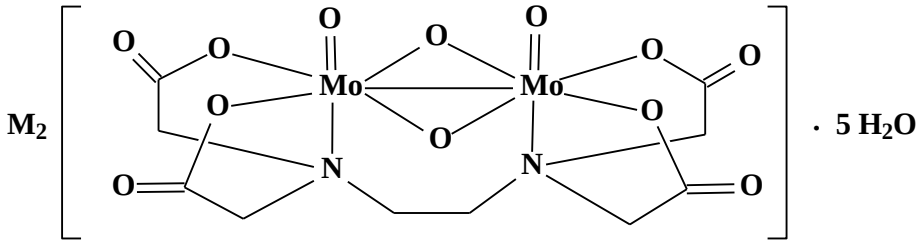

Fig. 6.1. **Sodium and lithium bis(μ$_2$-oxo)-dioxo(μ$_2$-ethylenediaminetetraacetato-N,O,O')-dimolybdates(V). M = Na^+, Li^+ (corresponding substances I and II). The synthesis procedure of compounds I–II, structure, and physicochemical properties are described in the literature [285]**

The essence of the process consists in adding a biologically active substance to 50% sugar syrup for feeding colonies of *Apis mellifera* bees in late winter or early spring. The bees are fed in the amount of 120 mL of the mixture placed on a bee frame every two days, for two weeks.

The result obtained is due to the fact that, after the first collection of honey, the biological material is sampled from 10 groups for the additional study of the total antioxidant status by $ABTS^{\bullet+}$ and $DPPH^{\bullet}$ radical scavenging assays.

6.1. The action of synthetic stimulators antioxidant capacity of honey bee products

After winter, solutions of the biologically active compounds $Na_2[Mo_2O_4EDTA]\cdot 5H_2O$, $Li_2[Mo_2O_4EDTA]\cdot 5H_2O$ and prototype $Na_2MoO_4\cdot 2H_2O$ were added to the first feeding for two weeks to 10 groups of *Apis mellifera*. For

quality control, subsequent feeding was performed without adding biologically active substances to 10 groups of *Apis mellifera*. The biological material was collected (honey, beeswax, royal jelly, bee uterus, propolis, and pollen) in late May. The samples were collected and registered at the apiary of the Republic of Moldova (Institute of Zoology, Ghidighici Forest District, no. 7; PhD. Cebotari V.).

Honey dissolved in a water-alcohol solution (1:1); beeswax, royal jelly, bee uterus, propolis, and pollen dissolved in 96% ethanol were incubated in a thermostat at 25°C for 2 days. The biological material is examined at least 3 times at different concentrations ranging from 0.01 to 100.00 μM. In this study, the two most frequently used methods for assessing free radical scavenging ability, $DPPH^{\bullet}$ and $ABTS^{\bullet+}$ assays, were performed, and Trolox was used as a reference (Table 6.1.)

Table 6.1. Antioxidant capacity (AOC) of Trolox

Trolox	**$ABTS^{\cdot+}$**			**$DPPH^{\cdot}$**		
C (uM)	**Abs (734 nm)**	**inh (%)**	**IC_{50} (uM)**	**Abs (517 nm)**	**inh (%)**	**IC_{50} (uM)**
100.0	0.153	81.73±0.25	**23.91±0.30**	0.218	73.99±1.26	**37.72±0.91**
10.0	0.600	28.57±0.17		0.679	19.11±0.42	
1.0	0.805	4.11±0.42		0.803	4.35±0.25	

The IC_{50} values of the bee products in control exhibiting the concentration that caused 50% scavenging of free radicals $DPPH^{\bullet}$ and $ABTS^{\bullet+}$ are presented in Table 6.2. These two free radical scavenging activities revealed that the IC_{50} values of the tested samples ranged from 0.13 -543.00 mg/mL for the $DPPH^{\bullet}$ assay and from 0.08 -159.40 mg/mL for the $ABTS^{\bullet+}$ assay. The Table data indicate that all honey bee products display a significant antioxidant capacity. The $ABTS^{\bullet+}$radical scavenging ability of the tested samples can be ranked in the following order: Propolis ≥ Bee Bread ≥ Royal Jelly ≥ Beeswax ≥ Bee Uterus ≥ Honey.

Of honey bee products, propolis seems to be the most powerful antioxidant as it contains the highest levels of phenols and flavonoids, followed by pollen and royal jelly, according to literature data [286]. Our AOC studies on bee products in the control group showed a level of activity consistent with data from literary sources. Propolis has demonstrated the highest radical scavenging activity, IC_{50} making 0.08 mg/mL for $ABTS^{\bullet+}$ and 0.13 mg/mL for $DPPH^{\bullet}$.

Propolis (bee glue) is not a food, unlike honey and pollen. Bees utilize it as both a building material and a protective substance. They use it to repair combs and strengthen thin honeycomb edges. Propolis is also employed for its biological activity as an insulating material to prevent microorganisms (fungi and bacteria)

from penetrating the hive and to build the most sterile environment known in nature [287]. It is also active against human pathogens. Generally, naturally-occurring propolis is composed of 50% resin and vegetable balsam (including phenolic compounds), 30–40% wax and fatty acids, 5–10% essential and aromatic oils, 5% pollen, and approximately 5% other substances, including micronutrients, amino acids, and vitamins (pyridoxine, thiamin, vitamins C and E and riboflavin,).

Table 6.2. AOC of the bee products of the control group

Control	ABTS$^{\bullet+}$					DPPH$^{\bullet}$			
	C (mg/mL)	Abs 734nm	Inh (%)	SD (%)	IC_{50} (mg/mL)	Abs 517nm	inh (%)	SD (%)	IC_{50} (mg/mL)
HONEY	100.00	0.506	39.76	0.51	159.40±8.91	0.561	33.15	0.08	543.00±38.18
	10.00	0.782	6.85	0.59		0.708	15.71	0.17	
	1.00	0.813	3.15	0.42		0.722	13.99	0.08	
	0.10	0.825	1.79	0.67		0.759	9.64	1.18	
BEE BREAD	50.00	0.054	93.57	0.34	2.43±0.01	0.026	96.85	0.08	1.45±0.04
	5.00	0.369	56.07	0.34		0.126	85.00	0.17	
	0.50	0.591	29.58	0.42		0.685	18.39	0.93	
	0.05	0.775	7.68	0.42		0.802	4.52	1.85	
BEESWAX	50.00	0.063	92.44	0.42	9.26±0.07	0.019	97.74	0.01	9.04±0.04
	5.00	0.597	28.93	0.67		0.644	23.33	0.51	
	0.50	0.770	8.33	0.17		0.753	10.30	1.26	
	0.05	0.838	0.24	0.17		0.800	4.70	0.25	
PROPOLIS	5.00	0.060	92.86	1.52	0.08±0.01	0.092	88.99	0.42	0.13±0.01
	0.50	0.291	65.30	0.08		0.145	82.74	1.52	
	0.05	0.404	51.90	0.17		0.633	24.64	0.51	
	0.01	0.735	12.44	0.25		0.772	8.04	1.43	
ROYAL JELLY	50.00	0.045	94.58	0.93	6.65±0.05	0.050	93.99	0.08	15.14±1.51
	5.00	0.512	39.05	0.34		0.755	10.12	0.84	
	0.50	0.732	12.86	0.34		0.761	9.35	0.59	
	0.05	0.827	1.55	0.17		0.796	5.24	1.01	
BEE UTERUS	50.00	0.060	92.86	1.68	9.11±0.24	0.061	92.74	2.69	12.54±0.89
	5.00	0.594	29.23	0.25		0.709	15.54	0.42	
	0.50	0.748	10.89	0.25		0.738	12.08	0.93	
	0.05	0.836	0.42	0.25		0.833	0.77	0.42	

Bee bread showed radical scavenging activity with IC_{50} values of 2.43 mg/mL for ABTS$^{\bullet+}$ assay and 1.45 mg/mL for DPPH$^{\bullet}$ assay. Bee bread is a part of the pollen stored by bees in their combs, sealed with a thin honey and beeswax layer, and

matured in a beehive. It is used by worker bees as food for larvae, and the production of royal jelly by young bees. Bee bread is processed by bees for storage by adding various enzymes and honey, leading to fermentation renders. The end product is enriched with new nutrients and becomes more digestible due to this type of lactic acid fermentation, as cell walls are partly destroyed during this process. Bee bread is more nutritious than pollen because of its higher free amino acid content and easily assimilated sugars. Its almost unlimited storage capacity as compared with dried or frozen pollen in which nutritional values rapidly vanish is one of the bee bread advantages [288, 289].

The royal jelly manifested high AOC, with IC_{50} values of 6.65 mg/mL and 15.14 mg/mL for $ABTS^{\bullet+}$ and $DPPH^{\bullet}$ radicals, respectively. Royal jelly is a compound that is secreted by the hypopharyngeal and mandibular glands of worker honeybees. It is a yellowish, creamy, acidic substance with a slightly acrid scent and taste constituted on a wet weight basis including water (60–70%), proteins (9–18%), sugars (7–18%) (mainly fructose, glucose, and sucrose), lipids (3–8%), minerals (0.8–3.0%), ash (0.8–3%), and traces of polyphenols and vitamins [290]. All bee larvae in the early stages of life and the queen bee until she dies are fed with royal jelly. It plays a decisive role in determining the class of honeybees because larvae fed with greater amounts of royal jelly for longer periods grow into large, fertile, long-living queens rather than smaller, infertile, short-living workers. Ramadan and Al-Ghamdi reported in their review that royal jelly possesses a large number of functional properties such as disinfectant action, antibacterial, vasodilative, hypotensive, anti-inflammatory, antihypercholesterolemic, antioxidant, and antitumor activity [291].

The antioxidant performance of royal jelly is attributed to its free amino acids, including essential ones; polyphenolic and flavonoid compounds; small peptides, such as di-peptides (Lys-Tyr, Arg-Tyr, and Tyr-Tyr) yielded from protease hydrolyzed royal jelly proteins; vitamins; fatty acids (the main being 10-hydroxydecanoic acid); and peptides and proteins [291]. The major flavonoids that occur in royal jelly include flavonols (e.g., kaempferol, quercetin, fisetin, and galangin), flavanones (e.g., pinocembrin, naringin, and hesperidin), and flavones (e.g., acacetin, apigenin, luteolin, and chrysin). A family of proteins secreted by honey bees comprises major royal jelly proteins (MRJPs). The family includes nine proteins, of which MRJP1 (also called royalactin), MRJP2, MRJP3, MRJP4, and MRJP5 are present in the royal jelly secreted by worker bees. MRJP1 is the amplest and largest in volume. The five proteins make 82–90% of the total proteins in royal jelly [291]. DPPH radical-scavenging assay carried out by Park et al. confirmed the

antioxidant capacity of MRJPs 1–7 of *Apis mellifera* at levels varying between approximately 30 and 80% of the residual radical.

Beeswax and Bee Uterus demonstrated relatively similar strong AOC, with IC_{50} values of 9.26 mg/mL ($ABTS^{\bullet+}$) – 9.04 mg/mL ($DPPH^{\bullet}$) and 9.11 mg/mL ($ABTS^{\bullet+}$) – 12.54 mg/mL ($DPPH^{\bullet}$), respectively. Beeswax is secreted by Beeswax Worker bees through wax glands located in the abdomen. The peaks of this substance production fall generally during the colony growth phase in late spring. Beeswax is used to make combs. The synthesis of beeswax starts from honey sugars, and it has a crystalline structure suitable for hive construction. Chemical composition depends on bee species and geographical zones and includes free fatty acids, free fatty alcohols, and hydrocarbons, linear wax monoesters, hydroxymonoesters deriving from palmitic, 15- hydroxypalmitic and oleic acids, and complex wax esters containing 15-hydroxypalmitic acid and diols.

The studies on the beeswax AOC involve the by-products of wax recycling and the associated cost-benefit tradeoff. Honey, propolis, pollen, and royal jelly are considered commodities, while honeycomb is discarded as a by-product in bee product processing and production. Beeswax recycling can transform it into compounds previously considered industrial waste, though they could be of great value in biomedicine. This issue needs further exploration. It has been demonstrated by Zhao et al. and Giampieri et al. that byproducts from beeswax recycling present a rich source of proteins, minerals, and polyphenols, conferring strong total antioxidant capacity and low toxin levels.

Honey, a sweet naturally-occurring product appreciated for its nutritive value and beneficial health effects, is produced by honeybees *Apis mellifera* that directly select nectar from plants or the excretions of plant-sucking insects. Honey is known for its high antibacterial activity; thus, its use in modern medicine represents an attractive alternative treatment to deal with multidrug-resistant pathogens. Different factors, including hydrogen peroxide, a low pH, and high osmolarity contribute to honey's antibacterial activity. The presence, among its various components, of natural antioxidants is the most important therapeutic property of honey. It contains about 200 compounds, which are mainly sugars (fructose 25–45% and glucose 20–40%), water, and other substances, such as protein, amino acids, vitamins, enzymes, ash, organic acids, minerals, and phenolic and flavonoid compounds, which greatly contribute to its biological activity. The therapeutic capacity of honey is linked to the presence, variety, and amounts of bioactive compounds. In its turn, this depends on the type of flora, climatic conditions, geographical location of production, soil composition, seasonal

factors, environmental conditions, botanical and entomological sources, as well as the production process. The enormous number of bioactive compounds in honey consists of molecules with phenolic structures, such as phenolic acids, flavonoids, anthocyanins, procyanidins, vitamin E, vitamin C (ascorbic acid), enzymes (e.g., catalase, peroxidase), carotenoids, Maillard reaction products, and trace elements. The principle composition of phenolic compounds in different honey varieties is relatively similar and includes phenolic acids, such as ellagic, caffeic, p-coumaric, and ferulic acids; flavonoids, including galangin, apigenin, chrysin, kaempferol, hesperetin, quercetin, and pinocembrin, and antioxidants, such as ascorbic acid, tocopherols, catalase (CAT), superoxide dismutase (SOD), and reduced glutathione (GSH) [292]. In our studies, the Honey displayed AOC in the IC_{50} values (159.40 mg/mL for $ABTS^{\bullet+}$ and 543.00 mg/mL for $DPPH^{\bullet}$).

All bee products have a high AOC, which is correlated with the content of antioxidant compounds such as flavonoids, phenolic acids, organic acids, amino acids, vitamins, enzymes, minerals, etc. The AOC of bee products in most cases exceeds the activity of a water-soluble analog of vitamin E - Trolox, which is a common standard antioxidant employed in biochemical techniques conducted to reduce oxidative stress. It has also been established that the tested biologically active substances I and II, added furthermore to the food of *Apis mellifera*, generally improved the AOC of bee products (Table 6.3).

Table 6.3. AOC of the bee products of the tested groups

C (mg/mL)		ABTS$^{\bullet+}$				DPPH$^{\bullet}$			
		Abs (734 nm)	**inh (%)**	**SD (%)**	**IC_{50} (mg/mL)**	**Abs (517 nm)**	**inh (%)**	**SD (%)**	**IC_{50} (mg/mL)**
$Na_2MoO_4 \cdot 2H_2O$									
HONEY	100.0	0.463	44.88	0.17	123.2±1.1	0.526	37.32	0.42	395.5±20.7
	10.00	0.783	6.73	0.08		0.705	16.01	0.42	
	1.00	0.809	3.63	0.08		0.773	7.98	1.01	
	0.10	0.827	1.55	0.34		0.782	6.85	0.93	
BEE BREAD	50.00	0.038	95.42	0.08	2.28±0.04	0.038	95.42	0.08	1.39±0.01
	5.00	0.359	57.26	0.17		0.114	86.43	0.01	
	0.50	0.593	29.40	0.51		0.683	18.63	0.42	
	0.05	0.768	8.51	0.59		0.788	6.13	0.08	

Table 6.3. Continued

BEES-WAX	50.00	0.050	93.99	0.25	9.12±0.06	0.020	97.56	2.95	9.13±1.14
	5.00	0.603	28.15	0.59		0.652	22.32	0.08	
	0.50	0.764	8.99	0.59		0.755	10.12	0.34	
	0.05	0.811	3.45	0.51		0.794	5.42	0.08	
PROPO-LIS	5.00	0.050	94.05	0.17	0.19±0.01	0.014	98.27	0.25	0.13±0.01
	0.50	0.357	57.44	0.25		0.138	83.51	0.08	
	0.05	0.542	35.42	0.59		0.636	24.23	0.08	
	0.01	0.771	8.21	0.34		0.756	10.00	0.17	
ROYAL JELLY	50.00	0.056	93.27	0.25	8.26±0.14	0.089	89.35	0.59	14.6±0.3
	5.00	0.565	32.68	0.42		0.727	13.39	0.25	
	0.50	0.747	11.07	0.67		0.776	7.62	0.17	
	0.05	0.821	2.26	0.34		0.817	2.68	0.59	
BEE UTERUS	50.00	0.089	89.40	0.17	12.89 ±0.05	0.023	97.26	0.34	2.44±0.01
	5.00	0.686	18.33	0.00		0.229	72.74	0.34	
	0.50	0.780	7.08	0.08		0.755	10.12	0.17	
	0.05	0.833	0.83	0.34		0.815	2.98	1.01	
$Na_2[Mo_2O_4EDTA]\cdot 5H_2O$									
HONEY	100.0	0.473	43.69	2.69	142.0±22.3	0.552	34.29	1.85	435.0±7.1
	10.00	0.753	10.36	0.17		0.714	14.94	0.59	
	1.00	0.813	3.15	0.25		0.722	14.05	0.17	
	0.10	0.789	6.07	0.34		0.740	11.90	0.67	
BEE BREAD	50.00	0.044	94.70	0.08	**0.79±0.02**	0.073	91.31	0.17	**1.03±0.01**
	5.00	0.356	57.56	0.08		0.127	84.82	0.08	
	0.50	0.408	51.37	0.42		0.580	30.95	0.00	
	0.05	0.655	21.96	0.42		0.754	10.24	0.17	
BEES-WAX	50.00	0.053	93.69	0.00	9.89±0.01	0.045	94.64	0.51	10.1±0.1
	5.00	0.631	24.82	0.08		0.646	23.04	0.08	
	0.50	0.774	7.80	0.59		0.738	12.14	0.00	

Table 6.3. Continued

	0.05	0.806	3.99	0.25		0.762	9.23	0.25	
PROPO-LIS	5.00	0.049	94.11	0.08	**0.08±0.01**	0.057	93.21	2.36	**0.06 ±0.01**
	0.50	0.354	57.80	0.25		0.139	83.45	0.34	
	0.05	0.369	56.01	0.25		0.421	49.88	0.00	
	0.01	0.691	17.74	0.34		0.743	11.55	0.17	
ROYAL JELLY	50.00	0.057	93.15	0.08	7.06±0.12	0.050	93.99	0.25	12.6±0.3
	5.00	0.525	37.44	0.42		0.724	13.81	0.51	
	0.50	0.728	13.27	0.25		0.746	11.19	0.34	
	0.05	0.815	2.98	0.17		0.787	6.25	0.08	
BEE UTERUS	50.00	0.057	93.21	0.34	12.15±0.03	0.077	90.83	1.18	36.65±0.40
	5.00	0.703	16.31	0.51		0.890	-6.01	0.93	
	0.50	0.776	7.56	0.25		0.748	10.89	0.08	
	0.05	0.826	1.61	0.25		0.784	6.61	0.25	
$Li_2[Mo_2O_4EDTA]\cdot 5H_2O$									
HONEY	100.0	0.344	58.99	0.25	**71.64±0.58**	0.224	72.00	1.41	**36.0±1.1**
	10.00	0.757	9.82	0.08		0.624	21.94	0.44	
	1.00	0.788	6.19	0.51		0.717	10.38	0.00	
	0.10	0.788	6.19	0.51		0.745	6.81	0.27	
BEE BREAD	50.00	0.039	95.30	0.08	**1.09±0.02**	0.070	91.25	5.13	**1.13±0.01**
	5.00	0.345	58.87	0.08		0.104	87.00	0.53	
	0.50	0.463	44.82	0.25		0.586	26.69	0.09	
	0.05	0.692	17.56	0.59		0.744	6.94	0.27	
BEES-WAX	50.00	0.065	92.26	3.03	8.24±0.35	0.036	95.50	0.18	10.0±0.1
	5.00	0.559	33.39	0.08		0.622	22.19	0.09	
	0.50	0.751	10.60	0.34		0.708	11.50	0.18	
	0.05	0.777	7.44	0.42		0.748	6.44	0.09	
PROPO-LIS	5.00	0.044	94.76	0.17	**0.11±0.01**	0.032	95.94	0.09	**0.12±0.01**
	0.50	0.346	58.81	0.00		0.136	82.94	0.27	

Table 6.3. Continued

	0.05	0.455	45.83	0.34		0.572	28.50	0.18	
	0.01	0.711	15.30	0.42		0.740	7.44	0.09	
ROYAL JELLY	50.00	0.048	94.23	0.08	6.87±0.06	0.067	91.63	1.41	14.5±1.0
	5.00	0.519	38.21	0.17		0.710	11.25	3.01	
	0.50	0.736	12.38	0.34		0.726	9.19	0.62	
	0.05	0.806	4.05	0.34		0.763	4.56	0.80	
BEE UTERUS	50.00	0.065	92.20	0.08	6.25±0.10	0.049	93.88	1.59	11.5±0.3
	5.00	0.487	41.96	0.42		0.657	17.81	0.97	
	0.50	0.745	11.31	0.34		0.707	11.56	0.62	
	0.05	0.811	3.39	0.59		0.768	3.94	0.27	

All tested complexes under study enhance the AOA of propolis and bee bread by up to 2 and 3 times, respectively. Additionally, all the compounds tested increased the antioxidant properties of honey by up to 2.2 times with regard to $ABTS^{\bullet+}$ radical cation and by up to 15 times with regard to $DPPH^{\bullet}$ radical. All tested groups of royal jelly and bee uterus exhibited high AOC, the IC_{50} ranging from 6 mg/mL to 16 mg/mL. The results of these studies can be useful in the development of biologically active substances that enhance the AOA of the main bee products.

6.2. Stimulation of the total antioxidant status of the hemolymph of honey bees *(Apis Mellifera)* and larvae

The metabolic processes of aerobes unceasingly generate reactive oxygen species. An organism tries to keep an equilibrium between the ROS amount and antioxidant processes. Oxidative stress is an important factor in the development of many diseases and pathological processes in insects. As a result of the activation of free radical processes, damage to basic molecules occurs through peroxidation of lipids, nucleic acid disruption, modification of amino acids in proteins, and altering their biological activity, which ultimately leads to damage and death of cells of individual tissues and organs of bees and their larvae.

It is known from the literature that low temperatures induce in honey bee broods gene expression in the antioxidant and heat shock responses [293]. Basic components of the antioxidant enzyme system have been detected in the genome of honey bees [294]. Organisms developed defensive mechanisms to prevent the undesired ROS impacts. They comprise both enzymatic and non-enzymatic components (Figure 6.2) [295]. To

assess the functional state of the antioxidant system of bees and their larvae, the Total Antioxidant Status (TAS) is used as an indicator. An efficacious antioxidative system is particularly essential for insects with a high metabolism rate and naturally produce large amounts of free radicals [296]. An efficient antioxidative system is of particular importance for insects, which have a high rate of metabolism, and naturally generate huge amounts of free radicals.

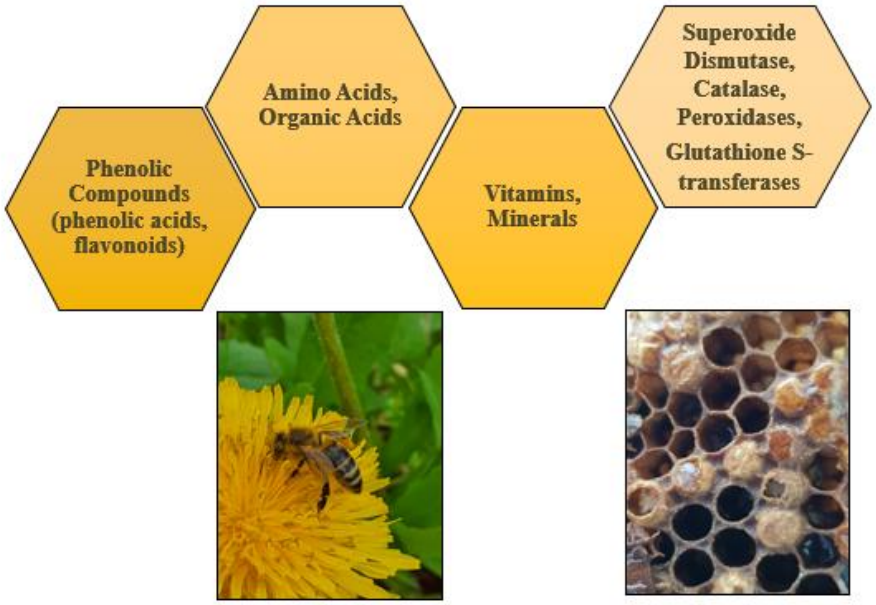

Fig. 6.2. **Enzymatic and non-enzymatic antioxidant components of the defensive antioxidant mechanisms of bees and bee brood**

Of the chemical compounds, described in the literature, which regulate the TAS of the hemolymph, the highest stimulatory effect was obtained (the prototype) [295] in the case of Vitamin C (lat: *Acidum ascorbinicum*). This compound is used in the biochemical analysis as a standard for the determination of the antioxidant activity of natural and synthetic products. This important antioxidant works in the organism's aqueous environments. Moreover, in the extracellular environment, ascorbic acid can be oxidized in the presence of metal ions to dehydroascorbic acid, which is transported into the cell through the glucose transporter (Figure 6.3). Vitamin E and carotenoids are their primary antioxidant partners working alone with the antioxidant enzymes. In membrane lipoproteins, Vitamin C cooperates with Vitamin E to regenerate α-tocopherol from α-tocopherol radicals. Being a reducing agent, Vitamin C can reduce and thereby neutralize ROS such as hydrogen peroxide [297].

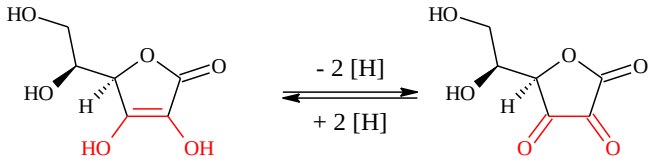

L-ascorbic acid L-dehydroascorbic acid

Fig. 6.3. **The redox reaction of vitamin C, molecular forms in equilibrium. L-dehydroascorbic acid also possesses biological activity and it is reduced to form ascorbic acid in the organism due to this quality**

Diet has a vital effect on the survival and condition of a honey bee *Apis mellifera* colony in the spring. Prevention methods attenuating the oxidative stress effects can be helpful for the protective forces of an organism of *Apis mellifera*. The introduction of exogenous compounds with antioxidative properties may be one of these methods. In this regard, we have developed a method for stimulating the status of the general antioxidant activity of the hemolymph of *Apis mellifera* bees and their larvae by new synthetic coordination compounds $Na_2[Mo_2O_4EDTA]\cdot 5H_2O$, $Li_2[Mo_2O_4EDTA]\cdot 5H_2O$.

Initially, investigated sodium and lithium bis(μ_2-oxo)-dioxo(μ_2-ethylenediaminetetraacetato-N,O,O')-dimolybdates(V) (corresponding substances I and II) were tested for toxicity using *Daphnia magna* (ISO 6341: 2012), which indicated the possibility of their use as bee development stimulators (Table 8.4).

Biologically active substances I and II were added furthermore to the food of 10 groups of *Apis mellifera* for 14 days. At the end of May, the samples of faunal material (hemolymph of bees and their larvae) were collected and registered at the apiary of the Republic of Moldova (Institute of Zoology, Ghidighici Forest District, no. 7; Dr Cebotari V.).

The hemolymph of bees and larvae in 96% ethanol were incubated in a thermostat at 25°C for two days. The biological material was studied in the concentration range from 0.01 to 100.00 µM in a triplet. Before starting the absorbance measurements, the samples were centrifuged for 5 min at 2000 r/min, then the supernatant was discarded, and 20 µL samples were added to 180 µL (0.02 M) $ABTS^{\bullet+}$ with ethanol in 96 wells ($ABTS^{\bullet+}$ free radicals must be added in 95% ethanol to avoid precipitation after the addition of tested samples). The samples were incubated in the dark at room temperature for 30 minutes.

The TAS results of the hemolymph of worker-bees and larvae without the presence of biologically active substances are presented in Table 6.4.

The AOC of hemolymph of worker-bees and larvae after exposure to the tested compounds I, and II are shown in Table 6.5. The tested complexes act on the organism of bees and larvae as antioxidants, inhibiting the activity of $ABTS^{\bullet+}$ and $DPPH^{\bullet}$ free radicals.

Table 6.4. TAS of hemolymph of worker-bees and larvae of the control group

Control group	C (mg/mL)	ABTS$^{\cdot+}$				
		Abs (734 nm)	% inh	SD (%)	IC_{50} (mg/mL)	SD (mg/mL)
Hemolymph of bees	100.00	0.156	81.43	2.02	13.56	0.37
	10.00	0.482	42.56	2.27		
	1.00	0.701	16.49	0.42		
	0.10	0.805	4.17	0.51		
Hemolymph of larvae	50.00	0.061	92.74	4.55	9.95	0.70
	5.00	0.627	25.36	1.68		
	0.50	0.755	10.06	0.08		
	0.05	0.835	0.54	0.08		

Table 6.5. SAT of hemolymph of worker-bees and larvae in the tested groups

Group I	C (mg/mL)	ABTS$^{\cdot+}$				
		Abs (734 nm)	% inh	SD (%)	IC_{50} (mg/mL)	SD (mg/mL)
Hemolymph of bees	100.00	0.197	76.55	0.01	**4.95**	0.11
	10.00	0.388	53.75	0.08		
	1.00	0.491	41.55	0.67		
	0.10	0.736	12.38	0.17		
Hemolymph of larvae	50.00	0.037	95.60	5.89	**4.93**	0.36
	5.00	0.462	45.00	1.01		
	0.50	0.692	17.62	0.17		
	0.05	0.794	5.42	0.42		
Group II						
Hemolymph of bees	100.00	0.187	77.68	0.76	**3.63**	0.01
	10.00	0.391	53.39	0.08		
	1.00	0.428	48.99	0.25		
	0.10	0.722	13.99	0.08		
Hemolymph of larvae	50.00	0.062	92.62	0.67	**3.65**	0.05
	5.00	0.394	53.04	0.08		
	0.50	0.679	19.11	0.25		
	0.05	0.784	6.67	0.34		

The results of the research showed that the case of the tested compounds I, II, increased SAT in the hemolymph of bees and larvae by up to 3.8 and 2.7 times, respectevly.

The effect of bis(μ_2-oxo)-dioxo(μ_2-ethylenediaminetetraacetato-*N*,O,O')-dimolybdate(V) sodium and lithium pentahydrate on hemolymph SAT exceeds the activity of vitamin C [295] by up to 3.5 times.

The detected properties of $Na_2[Mo_2O_4EDTA]\cdot 5H_2O$, $Li_2[Mo_2O_4EDTA]\cdot 5H_2O$ are of interest for biotechnology and beekeeping from the point of view of expanding the arsenal of stimulators of the total antioxidant status of the hemolymph of *Apis mellifera* bees and larvae.

7. Varroosis (*Varroa destructor*)

The gross loss rate of managed colonies of honey bees, *Apis mellifera*, exceeds 30% yearly in many areas of the world [298, 299]. Although the reasons for this decline are multifaceted, the parasite *Varroa destructor* is considered by many honey bee researchers as the greatest contributing biological factor to honey bee colony losses [300]. Varroa severely weakens or causes the collapse of most honey bee colonies if left unmanaged [301].

In this regard, this paper presents the results of epizootological monitoring of the obligate ectoparasite *V. destructor* at all stages of bee development *Apis mellifera*, in the summer-autumn period of 2020-2022. The biological samples and examples of faunistic material were collected and registered at the apiary of the Republic of Moldova (Institute of Zoology, Ocolul Silvic Ghidighici, nr. 7). *V. destructor* mites parasitize bees and their broods, feeding on fat bodies and hemolymph (Figure 7.1 A, B, C), causing varroatosis, an invasive disease. *V. destructor* is also the vector of natural infection with viruses and simultaneously activates their replication, causing an increase in titer in the hemolymph of the bees.

Thus, honey bees, like other representatives of the animal world, are susceptible to viral diseases. The danger of viruses is due to their long incubation period in the host organism without clinical symptoms, rapid distribution, the presence of ectoparasites-carriers, and the ability, when certain conditions, to cause significant economic damage to beekeeping.

Important factors in the distribution of a mite in a family are its morphological and physiological features that allow you to quickly move from bee to bee. From one family to another, the *Varroa destructor* mite is transmitted by visiting bees families;

drones during departure and mating flights; upon contact with the injured and healthy bees on honey plants; with a close location of the hives to each other; at the permutation of the affected brood into healthy colonies or replacement of the uterus without examining it for the presence of mites.

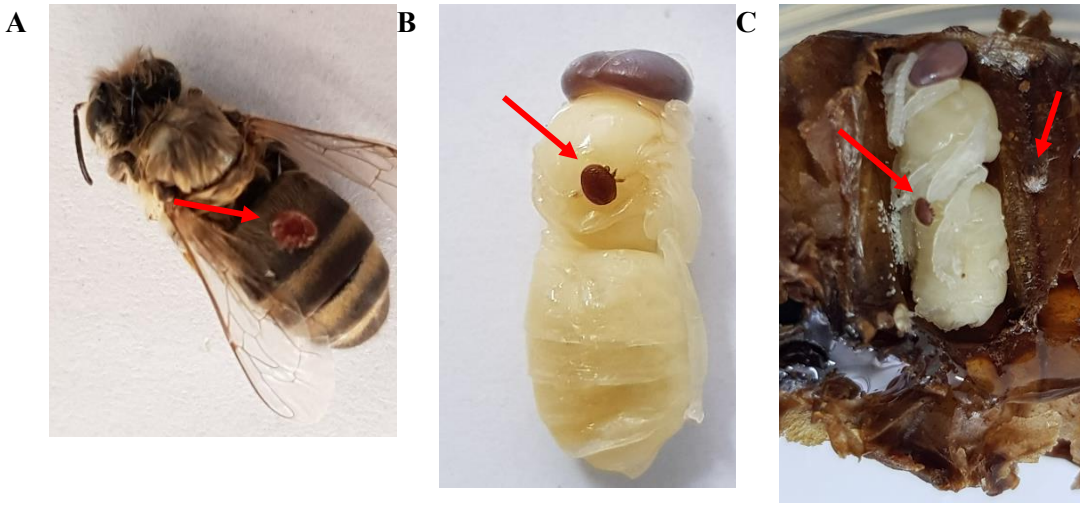

***Fig. 7.1. Varroa destructor* males on *Apis mellifera* honey bee (A) and chrysalis (B, C)**

The taxonomy of *Varroa* is summarized as follows (Lindquist et al., 2009):

Kingdom: Animalia
Phylum: Arthropoda
Class: Arachnida
Subclass: Acari
Superorder: Parasitiformes
Order: Mesostigmata
Family: Varroidae
Genus: Varroa

V. jacobsoni (Oudemans, 1904) - is a parasite of the Chinese wax bee (*Apis cerana*). It is now considered the main culprit of the decades-long ongoing planet panzootic varroatosis.

V. underwoodi (Delfinado-Baker and Aggarwal, 1987) – is a parasite of the Chinese wax bee (*Apis cerana*).

V. rindereri (De Guzman and Delfinado-Baker, 1996) - is a parasite of the Kochevnikov bee (*Apis koschevnikovi*).

V. destructor (Anderson and Trueman, 2000) - is a parasite that infects the honey bee (*Apis mellifera*). Mistakenly classified as *Varroa jacobsoni* for a long

time, until 2000 as a result of the study of mitochondrial DNA was not isolated in an independent view. It causes varroatosis in both the Chinese wax bee (*Apis cerana*) and the common honey bee (*Apis mellifera*). Previously, it only parasitized the Asian species *Apis cerana,* but subsequently switched to *Apis melífera* in its natural ranges.

Varroa males are haploid with seven chromosomes, while females are diploid with 14 chromosomes. However, the genetic mechanism is the same (for example, the existence and the identity of a single genetic sex determination locus) remains unknown.

It is known from the literature that initially the analysis of mtDNA variability was carried out using the RFLP method (restriction fragment length polymorphism, RFLP) and DNA sequence sequencing, then polymerase chain reaction (PCR) [302, 303]. The study of mtDNA variability made it possible to identify the evolutionary lines of varroa, characterize the genetic diversity, and identify differences in subspecies of different evolutionary lines, as well as develop diagnostic DNA markers. All sequences of the COI gene of mitochondrial DNA are different between species, while within species there are no or insignificant differences in the COI sequence. On average, sequences differ between species by 7.93%, and within a species by 0.43%.

Microscopy Varroa destructor

The transition of the *Varroa* mite from the Indian bee *Apis cerana* to the honeybee *Apis mellifera* seems to have been facilitated by active human activity. In the Indonesian islands, in India, and southern China, many beekeepers artificially breed Indian bees in order to obtain honey. Numerous experiments by beekeepers on the rearrangement of combs with brood from the nests of the Indian bee to the nests of the honey bee served as a factor in the introduction of the varroa mite into them. By switching to a honey bee, the mite received the best opportunities for reproduction and a sudden expansion of its range. The *Varroa destructor* mite is registered in almost all countries. In the Republic of Moldova, *Varroa destructor* has been present since 1964 in all bee colonies of all apiaries, previously erroneously identified as *Varroa Jacobsoni,* having a negative economic impact on beekeeping in the Republic of Moldova. Four species of *Varroa* are easily identified by morphological analysis (Figure 7.2. A, B, C, D, E, F.)

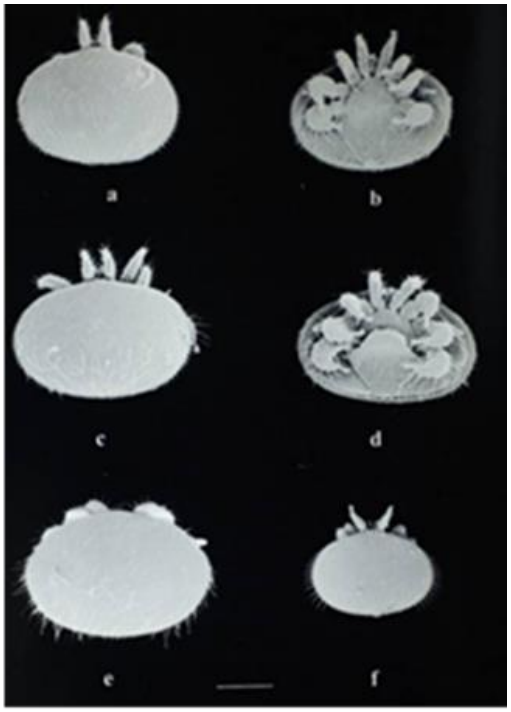

Fig. 7.2. Microimages of adult females (A, B) *Varroa jacobsoni*; (C, D) *Varroa destructor*; (E) *Varroa rindereri*; (F) *Varroa underwoodi (Photo: Denis Anderson).*

On the apiaries of the Republic of Moldova, we identified *Varroa destructor*, although there is a great similarity between the species *Varroa jacobsoni* and *Varroa destructor*, it is still phenotypically observed that the body size of adult *Varroa destructor* females is larger: 1.1-1.8 mm in length and 1.5-2 mm wide (Figure 7.3). The body of the female is strongly sclerotized, flattened in the dorsoventral direction, transversely oval in shape, and slightly convex from the side of the dorsal part. The dorsal scutellum is located along the entire length of the idiosome, and has dense pubescence in the form of thin, spirally curved setae, probably facilitating the movement of the mite in the sealed cell between the brood and the cocoon. The female has four pairs of strong six-segmented limbs ending with powerful suction cups.

The main role in the epizootiology of varroosis is played by female mites (Figure 7.4 D), which are able to exist outside the cell with brood and settle, as well as hibernate on bees. Immature individuals (Figure 7.4 A, B, C) and males (Figure 7.4 E, F) live only in sealed cells on the brood, where the reproduction and development of the mite take place. Varroosis strongly differs from other currently known infectious and invasive diseases of bees. All other diseases usually affect the brood or only adults in certain seasons of the year. The varroa mite harms the bee

family throughout the year, in all phases of its development. The damage caused to beekeeping by varroosis is high and consists of a decrease in the productivity of bee colonies, the high death of bees, and significant material and labor costs for anti-varroosis measures. This disease is one of the urgent problems of world beekeeping.

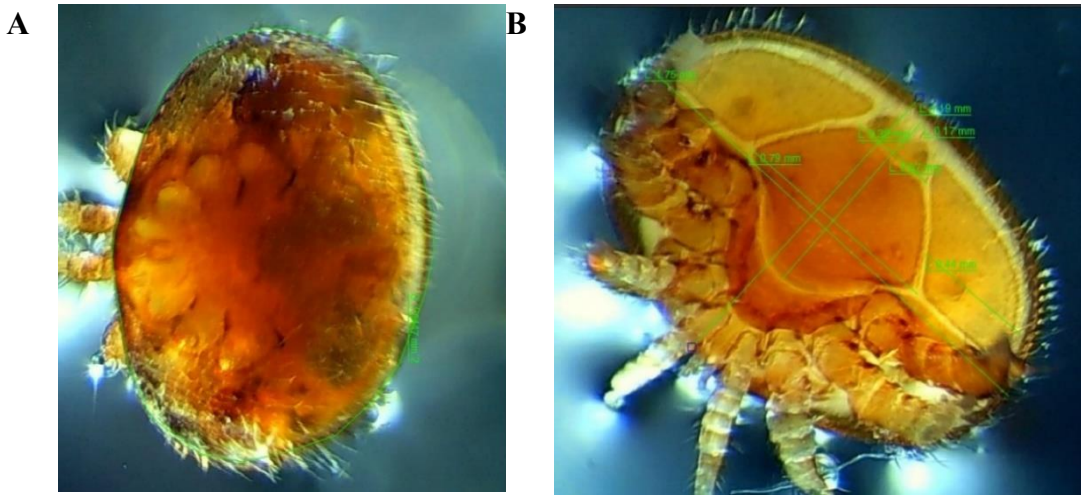

***Fig. 7.3. Varroa destructor* adult female: (A) dorsal view, (B) ventral view.**

Varroa females have a complex system of sensory organs that perceive chemical, mechanical, and hygrothermal stimuli. The main organs of the orientation of mites are the front paws, which have a set of special sense organs - sensilla, at the base of which there are nerve cells connected by processes with the central nervous system. Female mites have a developed system of respiratory tubes - tracheas, which open on the sides of the body with a pair of spiracles (stigma). ⅓ of the tubes are connected to the covers, the rest of them are free and mobile. This feature of the respiratory system is associated with the mite's life in different gas conditions: an excess of carbon dioxide in a sealed honeycomb cell and high aeration when flying on a bee. The oral apparatus of the females is piercing-sucking. The mite feeds with the chelicerae advanced forward and downward, cutting the soft intersegmental part of the bee cuticle and then swallowing the resulting drop of hemolymph. Thus, the mite leads to qualitative and quantitative changes in the uniform elements of the hemolymph of the bee. Pathological aging of the hemolymph occurs due to the accelerated transition of patterned elements from young to mature and aging stages.

As a result of mite parasitism, the total amount of hemolymph protein in affected bees decreases by 1.6–2.3 times, and residual nitrogen increases by 3.2–3.5 times. The degree of development of pharyngeal glands and fat body decreases by 1.3-1.4 and 1.2-2.2 times, respectively, compared to free of mites bees.

Underdevelopment of the pharyngeal glands and fat body, especially during the fall, indicates a sudden decrease in the reserves of reserve protein substances in the body of bees. These factors of the negative effect of the mite on bees lead to a sudden reduction in life expectancy.

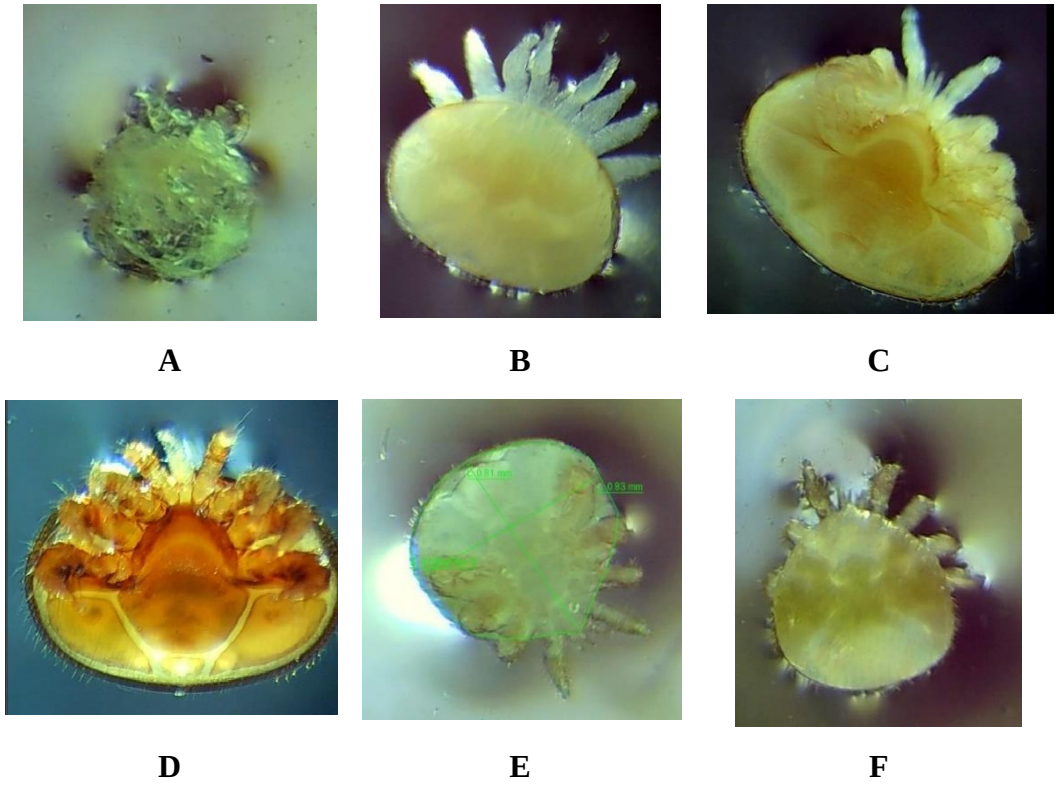

Fig. 7.4. **Microscoping *Varroa destructor*: protonymph (A), deutonymph (B), tritonymph (C), Varroa adult female (D), male ventral view (E) dorsal view (F) (оригинал). We carried out microscopy of *Varroa destructor* mites at different stages of their life cycle for identification of the species by morphological examination.**

The female reproductive system consists of paired ovaries, oviducts, uterus, and genital openings. The circulatory system is presented in the form of an ampoule-shaped expansion (heart). Among the specific morphological features of the female associated with parasitism, are the following characteristic: a particular body shape that provides a strong fixation between the rings of the bee's abdomen; a strongly pronounced chaetotaxy of the body with a springy cover that prevents the females from sticking during their life among the bee broods; the presence of a movable peritremal tube that regulates the mite's breathing in various conditions of its life; the presence of small, backward-directed teeth on the chelicerae, which keep mites from

falling out of the wound on the host's body; lack of anal valves associated with excretion in the tight space between brood and cocoon.

The development of the varroa mite is closely related to the biology of the bee colony. This relationship is due to both morphological and physiological characteristics of the developing brood. Mites accumulate in the brood when it reaches a certain biological state. In bee brood, this occurs a day, and in drone brood, three days before its sealing. The female mites in the cells of the combs are completely immersed in the gruel of food under the larvae, lying down with their ventral side to the surface of the body. After sealing the cells, the larvae start spinning a cocoon. At this time, the female mite passes to the active movement of the larva and repeated feeding. The stage of spinning a cocoon in a bee larva lasts two days, and in a drone - three, after which the prepupae stage begins. At this time, female mites begin to lay eggs. The localization of the laid eggs is due to the presence of free space in the cells. In the process of metamorphosis of the prepupa, such a space is first formed under the operculum, then in the upper and middle thirds of the cell. In the same sequence, females lay eggs in these places. During the cycle, the female can lay up to 5 eggs in the bee cell and up to 6 in the drone cell. The interval between the laying of the next egg varies within 1 day. Sclerotization of the chitinous cover of developing individuals of the bee family and a short period does not ensure the transformation of all the eggs laid by the female mite to adulthood. Full development is achieved only by those individuals that began their existence at the stage of the prepupae of the brood. The cycle of development of the female mite lasts 8-9 days and the male 6-7. Each female is capable of making up to three oviposition during the period of her life. Each time there is one male in the cell, which after mating with young females dies. Females live for 2-3 months in summer and 6-8 months in winter. In winter, when there is no brood in the colony, they penetrate deep between the sternites of the abdomen of the bee, more often between the first and second segments, and less often between the thoracic segments, in the joints of the chest and abdomen, chest and head. Females are also found on the combs, especially at the bottom of the cells after the brood has emerged. They can be found on the walls and bottom of the hive. The number of parasites in the nest of bees ranges from single specimens to 30 thousand or more. With the advent of the brood, females penetrate into it. The population of mites in the colony increases exponentially, however, the greatest damage to the brood is observed in spring and autumn when young bees build up to the main honey collection and the upcoming wintering. At that time the number of diseased pupae reaches more than 80%. For their development, females

prefer drone brood. Its prevalence in the middle geographical zone reaches its maximum in August.

In 2021 at the apiary of the Republic of Moldova (Institute of Zoology) it was revealed that at this time, the number of diseased pupae reached more than 80%. On drone pupae, we found up to 20 specimens of mites at different stages of development (Figure 7.5). On the pupae of bees, up to 12 specimens of mites at different stages of development were found (Figure 7.5). The greatest number of parasites is found on young bees and drones, relatively few of them occur on flying bees returning to the hive.

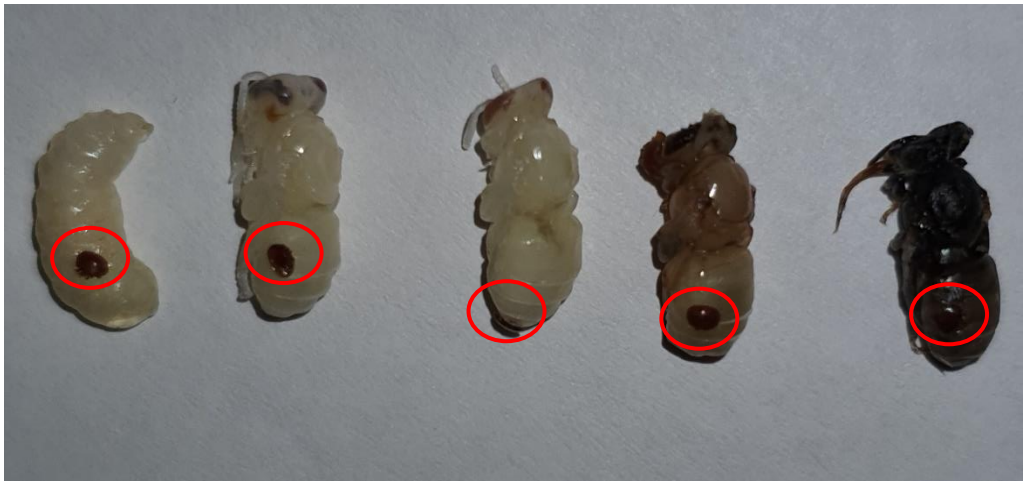

Fig. 7.5. **Mites on the larvae and pupae of drones at different stages of development. The spread of the *Varroa destructor* in the apiary was studied using samples of drone brood**

The spread of the *Varroa destructor* mite in the apiaries of the Republic of Moldova was studied by examining samples of drone brood. At least 110 cells of drone brood were selected. It was recorded the presence or absence of mites in the sample. As a result, *Varroa destructor* mites were found on larvae and pupae of drones at different stages of development. More than 180 mites were found in 110 cells of drone brood. Of the 110 cells, 45 were infected. Thus, to prevent the occurrence and spread of infectious diseases of bees, epizootological monitoring of varroa invasion is constantly carried out and, if necessary, preventive treatment of bee colonies is carried out.

The faunistic material discussed in this work was collected, studied, and registered in the apiaries of the Republic of Moldova, the coordinates are shown in Table 7.1. Scientific research and observations were carried out from August to September 2021, during the planned work in the apiary. Plastic and glass containers

were used to collect pests inside the hive. The pests were stored in 70% alcohol and a freezer. On the day of the research, photographs were taken to facilitate the identification of the pest species. To determine the species of mites, we used Varroa species identification keys (De-Guzman, Fernandez, and Coineau, 2007).

Table 7.1. Coordinates of the studied apiaries

Sampling date	The coordinates of the investigated apiary	Temperature °C, (on the day of collection)	Biological material	
04.08.2021	The Republic of Moldova, Rezina district, Tarasova village. Coordinates: 47°52′36″N 28°57′35″E47°52′36″N 28°57′35″E	+29°	*Apis mellifera* drone brood, infested with *Varroa destructor* mites.	
08.09.2021	The Republic of Moldova, Șoldănești district, Șipca village. Coordinates: 47°50′42″N 28°48′24″E47°50′42″N 28°48′24″E.	+25°		

For species identification of *Varroa destructor* mites, we produced morphometry of mites, collected from honey bee drone brood cells (Table 7.2). As a result of morphometry, the biometric parameters of indigo and *Varroa destructor* nymphs were calculated (Table 7.2). The average sizes of grayish-white males are L=0.91±0.15 mm and D=1.11±0.38 mm. The brown body of the female is strongly sclerotized, flattened in the dorsoventral direction, transversely oval in shape, slightly convex from the side of the dorsal part, and has dimensions L=1.15±0.05 mm and D=1.74±0.05 mm. Incompletely sclerotized tritonymphs have dimensions L=1.11±0.06 mm and D=1.55±0.12 mm. The parameters presented in Table 7.2 correspond to *Varroa* species identification keys (De-Guzman, Fernandez, and Coineau, 2007).

Table 7.2. Biometric parameters of *Varroa destructor*

	L,mm	D,mm	H,mm	S,mm^2	S=πab	L/D	L/H	D/L	S $_{body}$	V $_{body}$
Protonymph										
MEAN	0.60	0.66			0.32	0.91		1.11	-	-
SD	0.10	0.11			0.11	0.06		0.08		
Tritonymph										
MEAN	1.11	1.55	0.33		1.35	0.72	3.45	1.40	3.14	0.31
SD	0.06	0.12	0.06		0.16	0.05	0.71	0.08	0.37	0.07
Female										
MEAN	1.15	1.74	0.46	1.57	1.57	0.66	2.56	1.52	3.85	0.49
SD	0.05	0.05	0.08	0.12	0.10	0.03	0.41	0.07	0.28	0.09
Male										
MEAN	0.91	1.11	0.28	0.48	0.83	0.87	3.23	1.19	1.95	0.27
SD	0.15	0.38	0.03	0.04	0.41	0.17	0.34	0.24	0.89	0.26

Combating varroatosis

At present, the main methods of combating varroatosis are treated with chemicals, zootechnical measures, heat treatment, and combinations thereof. During the spring period of development of the bee colonies, a set of zootechnical and technological measures is being taken to prevent the spread of varroatosis, which provides for the systematic removal from the nest and the destruction of drone brood with ordinary and drone combs with mites. After pumping out marketable honey in August and reducing the nest, before the replenishment of fodder reserves, treatment against varroatosis with chemicals is carried out. The final treatment of bee colonies against varroatosis is carried out after the replenishment of food supplies and their sealing and the complete release of the brood. In this case, the air temperature should not be lower than 10°C.

For the treatment of varroatosis, chemical preparations are more often used. Recently, many substances that act on the *Varroa* mite have been developed, but derivatives have been recognized as the most effective: bromopropylate («Folbex», «Akarasan», «Polisan» preparations); organic carboxylic acids (oxalic, formic, lactic); amitraz («Bipin», «Bipin-T», «Apitak», «TEDA», «Amital», «Amicid», «Bivar», «Tanis», «Yantrin», «Tactics» preparations); fluvalinate («Apistan», «Bayvarol», «Fumisan», «Vetfor», «Barkas», «Akvo-flo», «API-star», «Apifit» preparations); phenotisine («Phenotiazine», «Varroxan», «Varrofen» preparations); coumaphos («Pericin», «Apiprotect», «Varrool» preparations); essential oils and medicinal plants. Physical control methods include: heat treatment of bees, pollination of bees' finely dispersed substances, ionizing radiation, ultraviolet and

infrared rays, ultrasound, polarization field, vacuum, electric current, etc. [304]. Biological control of Beauveria fungi, which are found naturally on Varroa, has not been widely adopted.

Despite collaborative efforts of insect pathologists, acarologists, and apiculturists, scientists have not produced long-term solutions for controlling *Varroa destructor* yet. As *Varroa destructor* continues to have a bad impact on honey bee populations worldwide, the development of new and innovative methods of mites combating should remain a priority among honey bee researchers [305]**.** Current research efforts aimed at controlling *Varroa* focus on developing efficacious acaricides, mechanical control, biological control, RNA interference, and breeding resistant bees [306, 307].

High populations of Varroa are needed in these studies. Presently, there is no other way to obtain *Varroa* for laboratory experiments other than collecting them from infested colonies [308]**.** The current process of obtaining Varroa for experimental purposes is dependent upon season and weather conditions, is time-consuming, and can be costly [308]. Additionally, researchers must leave their colonies untreated to obtain the number of mites necessary for experimentation, which can affect colony survival and pose a risk to nearby colonies [12].

The development of an *in vitro* rearing method for Varroa is quite challenging as *Varroa destructor* has very specific lifecycle requirements [309].

For the diagnosis, detection, and collection of mites, we used the following methodological approaches. A harmless diagnostic method is using powdered sugar (Figure 7.6). The principle of the method is based on the fact that when bees are dusted with powdered sugar, the mites lose their ability to stay on the bees and fall off. For research, a jar with a perforated lid (100-750 mL) was taken, bees were shaken off from a well-nurtured frame in it and the hole was closed with a perforated lid. Then, 10 grams of powdered sugar were added to 300 bees and placed in a jar. After 2 minutes of gentle shaking of the jar, the mites fell through the holes of the lid, and the bees remained in the jar; they were returned to the family, and the number of mites was counted on a light background. In order to quantify mites per 100 bees, the counted number was divided by 3.

The spread of the *Varroa destructor* mite in apiaries has also been studied by examining samples of drone brood. At least 50 cells of drone brood were selected. The presence or absence of mites in the sample was recorded. The degree of damage to bees by parasites was determined by the formula: $\mathbf{C=(K/P)\times 100,}$ where C is the degree of damage, the number of mites per 100 bees; K is the number of dead mites; P is the number of bees in the sample.

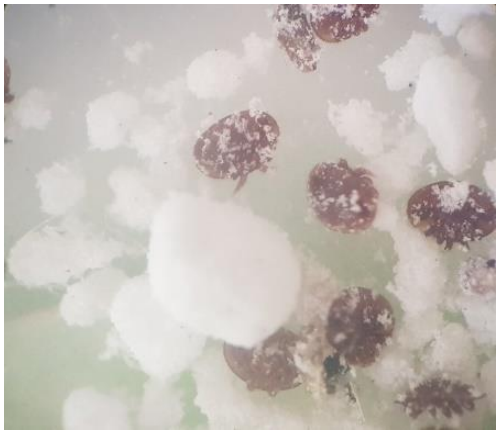

***Fig. 7.6. Varroa destructor* mites in powdered sugar**

The viability of bee families is predicted according to three degrees of damage: weak - up to two, medium - up to four, strong - more than four mites per 100 bees, and in 100 cells of drone or bee brood from the middle of the nest. In both studied apiaries, we found more than four mites per 100 bees, as well as in 100 cells of drone brood, to prevent the occurrence and spread of infectious diseases of bees, epizootological monitoring of varroa invasion is constantly carried out and, if necessary, preventive treatment of bee colonies is carried out.

In order to reduce the likelihood of death in bee colonies, it is necessary to control the population of the *Varroa* mite. In this regard, the coordination compounds $Na_2[Mo_2O_4EDTA]\cdot 5H_2O$ and $Li_2[Mo_2O_4EDTA]\cdot 5H_2O$ were synthesized.

To study the impact of substances on *Varroa*, we faced the task of determining the temperature and humidity regime, to ensure the viability of indigo varroa. Sexually mature females of Varroa were collected by the method of powdered sugar from honeycombs (Figure 7.7), placed in 2 mL biological test tubes (Figure 7.7), and planted one honey bee pupae. Biological tubes were placed vertically in a rack and incubated at a temperature of 34^0 C.

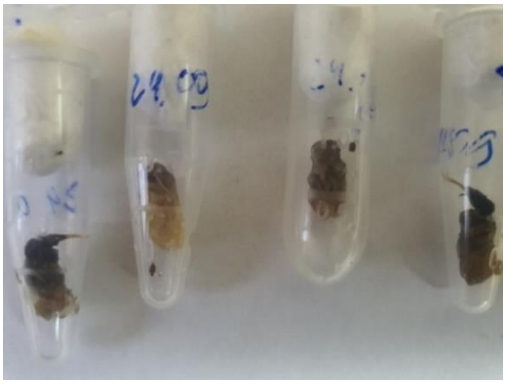

***Fig. 7.7.* Honey bee pupae with a varroa female placed in biological test tubes**

To study the effect of compounds on *Varroa*, we identified the optimal temperature-humidity regime for the viability of indigo *Varroa* in Eppendorf. Ten female *Varroa* were used to test one compound. The viability of the *Varroa* was investigated by microscopy after 24h of the incubation period by locomotor activity.

It is known from literary sources that female mites are not very resistant to external factors. The viability of *Varroa destructor* was significantly dependent on humidity, so the experiment was carried out at three levels of humidity. *Varroa destructor* survival was higher at relative humidity in the range of 65-75% than at 85% relative humidity. As a result, we adapted the method for studying acaricidal activity and determining the direct toxicity of the tested compounds [310].

As a negative control in an experiment with total longevity of *Varroa*, we used a single dose of lithium salt at a concentration of 25 mM. It is known from the literature that lithium salt has an acaricidal effect in the millimolar concentration range. As a result of the research, it was found that within 2-3 hours, the locomotor activity of mites slowed down, and they died in the interval of 24-48 hours while using a microscope, was visualized a specific increase of idiosomes. The shell between the genital and sternal shields was destroyed. Thus, the treatment of mites with lithium salt caused their 100% death.

This work represents a series of comparative biological studies of the complexes $Na_2[Mo_2O_4EDTA]\cdot 5H_2O$ and $Li_2[Mo_2O_4EDTA]\cdot 5H_2O$ in relation to anti-varroa activity (Table 7.3).

Table 7.3. LC_{50} (μM) values of test substances against mature female *Varroa destructor*

Compounds	LC_{50} (μM)
Control	≥100
Trilon B	≥100
$Na_2MoO_4\cdot 2H_2O$	**41.1**
$Na_2[Mo_2O_4EDTA]\cdot 5H_2O$	≥100
$Li_2[Mo_2O_4EDTA]\cdot 5H_2O$	**31.6**

The effect of the tested compounds on *Varroa destructor* exposed to concentrations of 1,10 and 100 μM. Control *Varroa* without treatment. Analyzing the results of the toxic bioassay it was observed that LC_{50} for $Li_2[Mo_2O_4EDTA]\cdot 5H_2O$ and $Na_2MoO_4\cdot 2H_2O$ are 32 and 41 μM, respectively. Thus, the test complex $Li_2[Mo_2O_4EDTA]\cdot 5H_2O$ showed significant inhibitory activity against *Varroa destructor*.

8. *In vivo* acute toxicity of the tested compounds against *Daphnia magna*

Toxicity studies are an important stage in the development of drugs, being a prerequisite before starting their use in preclinical and clinical trials.

Since the fundamental principle of toxicity studies is the protection of animals, including those participating in studies, it is currently recommended that in all possible cases, studies should be conducted on *in vivo* organisms at the lowest stage of evolutionary development, avoiding the inclusion of laboratory animals in studies.

In this work, *Daphnia magna* were used as test objects to detect the toxicity of active substances. Using *Daphnia* offers key advantages. First, they are simple to culture in the laboratory (or may be purchased from biological supply companies), and, thus, do not deplete field populations. Second, and perhaps most important, their biology and responses to a wide range of toxic substances are well documented (USEPA 2005) [311]. The survival percent of *Daphnia magna* and LC_{50} (lethal half-maximum concentration), which are quantitative indicators of the efficiency of the antagonist substance in choosing the optimal therapeutic dose, were used as indicators for a comparative evaluation of the results. In toxicology, the LC_{50} is a toxic unit that measures the lethal dose of a toxin. The value of LC_{50} for a substance is the dose required to kill half the members of a tested population after a specified test duration. LC_{50} figures are used as a general indicator of a substance's acute toxicity. A lower LC_{50} is indicative of increased toxicity.

The toxicity of the tested compounds was evaluated using the *Daphnia magna* bioassay by ISO 6341: 2012 (Figure 8.1).

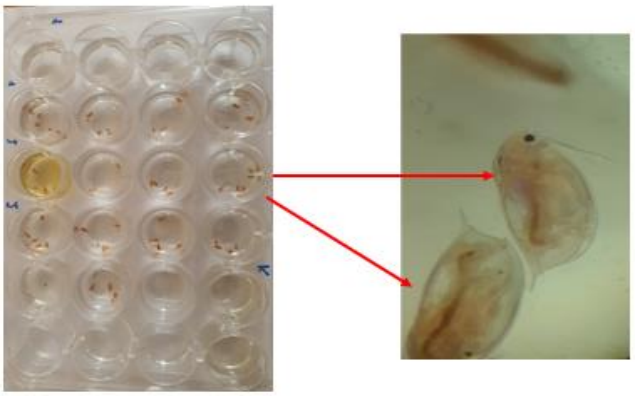

***Fig. 8.1. Daphnia magna* bioassay by (ISO 6341: 2012)**

In the paper (Gulea et al., 2022), we have evaluated the biological activities of the series of amine-containing mixed-ligand copper(II) coordination compounds

with 2-(2-hydroxybenzylidene)-N- (prop-2-en-1-yl)hydrazinecarbothioamide by quantitative and qualitative methods. The biological activities of the tested compounds were compared with the activity of reference compounds. DOXO doxorubicin ((7S,9S)-7-[(2R,4S,5S,6S)-4-amino-5-hydroxy-6-methyloxan-2-yl]oxy-6,9,11-trihydroxy-9-(2-hydroxyacetyl)-4-methoxy-8,10-dihydro-7H-tetracene-5,12-dione) was used as the reference anticancer compound.

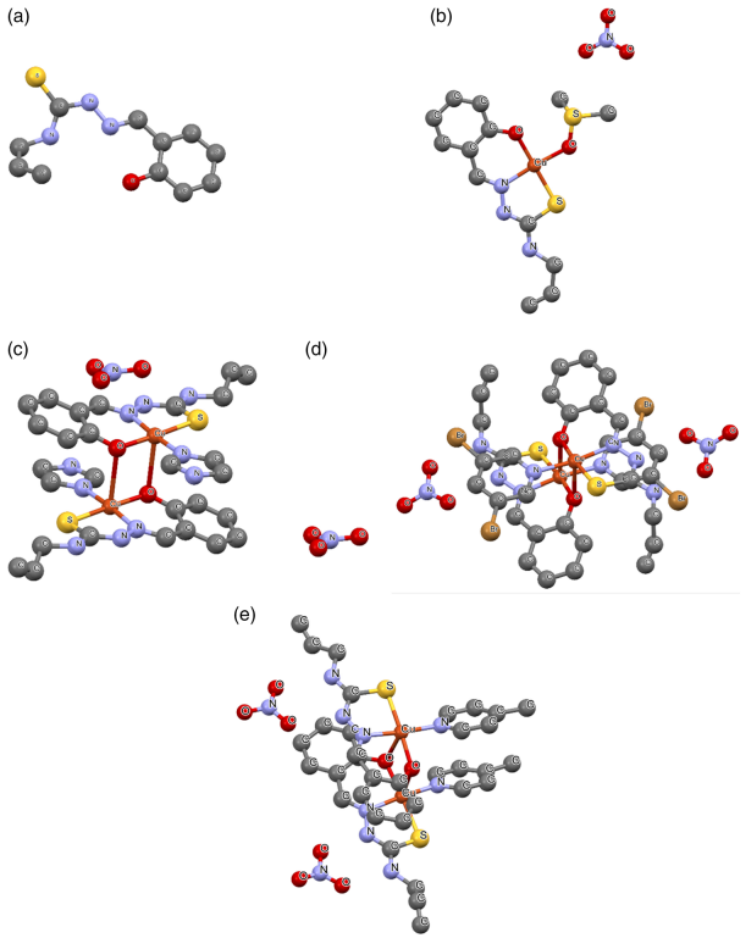

Fig. 8.2. **(A)Crystal structures of the tested compounds: 2-(2-hydroxybenzylidene)-N-(prop-2-en1-yl)hydrazinecarbothioamide H_2L, (B) bis[μ2-2-({2-[(prop-2-en-1-yl)carbamothioyl]hydrazinylidene}metphenolatelato-*S,N,O:O*]diaquadicopper(II) nitrate (1), (C) bis[μ2-2-({2-[(prop-2-en-1-yl)carbamothioyl]hydrazinylidene}metphenolatelato-*S,N,O:O*]diimidazoldicopper(II) nitrate (2), (D)bis[μ2-2-({2-[(prop-2-en-1-yl)carbamothioyl]-hydrazinylidene}metphenolatelato-*S,N,O:O*]bis-(3,5-dibromopyridine)dicopper(II) nitrate (3), (E) bis[μ2-2-({2-[(prop-2-en-1-yl)carbamothioyl]-hydrazinylidene}metphenolatelato-*S,N,O:O*]bis(4-methylpyridine)dicopper(II) nitrate hexahydrate (4)**

The 2-(2-Hydroxybenzylidene)-*N*-(prop-2-en1-yl)hydrazinecarbothioamide (H_2L), bis[μ_2-2-({2-[(prop-2-en-1-yl)carbamothioyl]-hydrazinylidene}methyl) phenolato-S,*N*,O:O]-diaquadicopper(II) nitrate (1), bis[μ_2-2-({2-[(prop-2-en-1-yl)carbamothioyl]hydrazinylidene}-methyl)phenolato-*S,N,O:O*]diimidazoledicopper(II) nitrate (2), bis[μ_2-2-({2-[(prop-2-en-1-yl)carbamothioyl]hydrazinylidene}methyl)phenolato-*S,N,O:O*]bis(3,5-dibromopyridine)-dicopper(II) nitrate (3), bis[μ_2-2-({2-[(prop-2-en-1-yl)carbamothioyl]-hydrazinylidene}methyl)phenolato-*S,N,O:O*]bis(4-methylpyridine)dicopper(II) nitrate hexahydrate (4) (Figure 8.2. A, B, C, D, E) were synthesized in Research Laboratory of Advanced Materials in Biopharmaceutics and Technics of the Moldova State University and are described in the literature (Gulea et al., 2021) [312].

The results of the *Daphnia magna* bioassay are given in Figures 8.3 and 8.4. The tested compounds manifest the general toxicity towards *Daphnia mana* after 24 h and 48 h of exposure. The general toxicity decreases in the following sequences: DOXO ≥ 2 ≥ 4 ≥ H_2L ≥ 1 ≥ 3 (24 h exposure) and DOXO ≥ 4 ≥ 2 ≥ 3 ≥ 1 ≥ H_2L (48 h exposure).

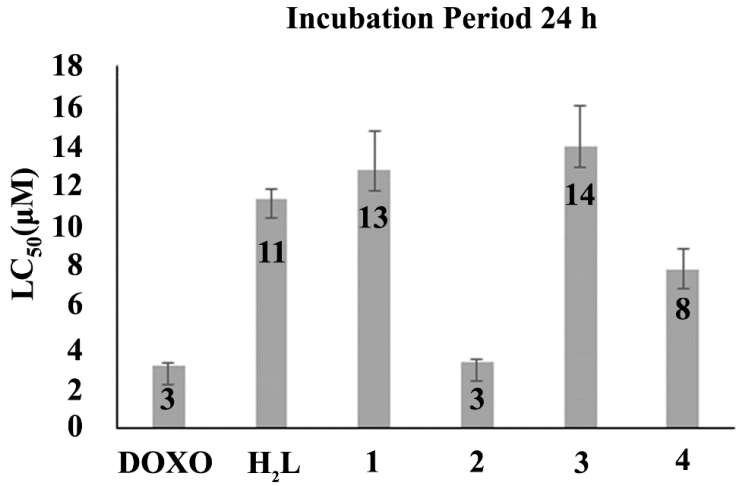

***Fig. 8.3. In vivo* toxicity of H_2L, complexes 1–4, and DOXO to *Daphnia magna* after 24-h incubation**

The intensity of the influence of compounds at the median lethal concentration (LC_{50}) on *Daphnia magna* was determined by microanalysis (Figure 8.5). As expected, the microscopy of *Daphnia magna* in control (without the tested compound) indicates the absence of pathological changes in the trunk of *Daphnia magna*. *Daphnia magna* were on the bottom of wells after incubation with the tested compounds. The light microscope revealed that most of the *Daphnia magna* were

slowly moving, while the rest of the crustaceans were motionless. The limbs and trunks of the *Daphnia magna* were deformed and their contents were mixed up with the growth media (Figure 8.5).

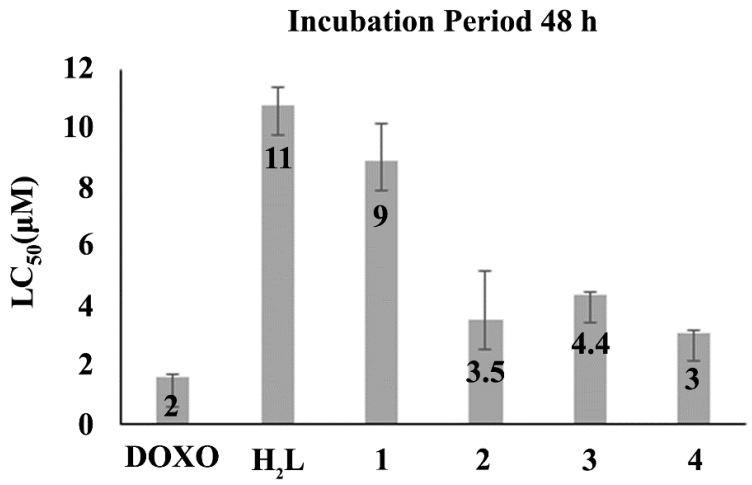

***Fig. 8.4. In vivo* toxicity of H_2L, complexes 1–4, and DOXO to *Daphnia magna* after 48-h incubation**

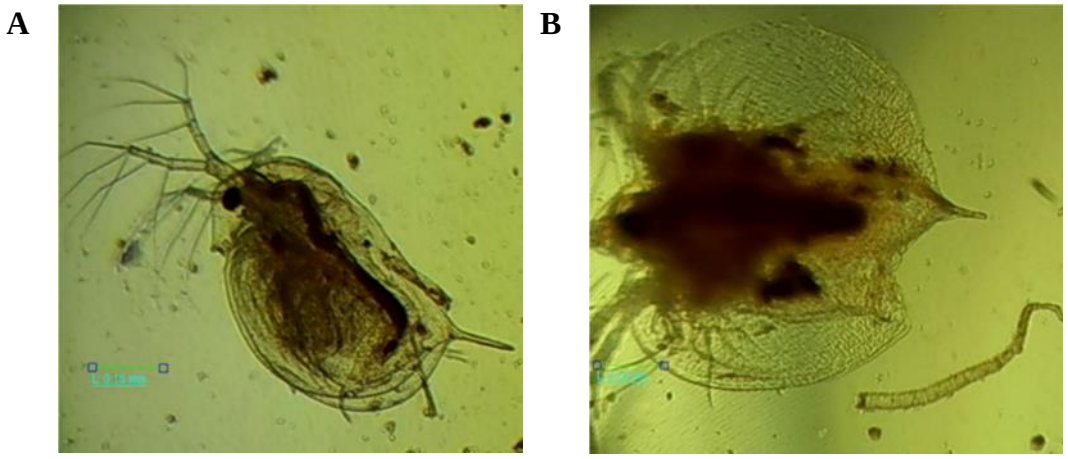

***Fig. 8.5.* Microscopy pictures of *Daphnia magna* in control (A) and afincubationtion with the tested compound (B)**

The ligand H_2L and complexes 1–4 have been screened for their *in vitro* antiproliferative activity. Inhibitors of cancer cell proliferation complexes 1–4 characterized by high selective activity, low toxicity, and higher efficiency compared to DOXO have been identified, which opens up the prospect of their employment as anticancer agents. Ligand H_2L at a concentration of 10 μM did not cause blebbing in cancer cells RD, Hela, while after exposure to complexes 1-4, pathological formation of microscopic cell vacuoles in cells was observed. In this way, the tested copper

complexes showed promising antiproliferative activity toward cancer cells and low toxicity on *Daphnia magna*. The above experimental data indicate the prospects for further search for selective anticancer substances with high antioxidant activity and low toxicity among copper mixed-ligand amino-containing coordination compounds.

In vitro biological evaluation, and *in vivo* toxicity of substances: Zn(II), Cu(II), Ni(II), and Co(III) complexes with 2-formylpyridine *N*4-allylthiosemicarbazone HL (Figure 8.6) has been described in the paper (Graur et al., 2022) [313].

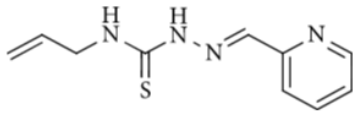

Fig. 8.6. **(HL) 2-Formylpyridine N^4-allylthiosemicarbazone**

As the obtained results of anticancer activity of the studied series of complexes and their selectivity are of both theoretical and practical interest, their toxicity has been studied *in vivo* on *Daphnia magna* (Table 8.1). The percentage of viability was measured after 24 h of staying in the environment with different concentrations of studied substances. As can be seen from Table 1, the nickel complex ($LC_{50} > 100\ \mu M$) practically does not affect *Daphnia magna*, while copper and zinc complexes as well as HL^1 are toxic at 10 and 100 μM concentrations and their LC_{50} values are in the range of 1.0–3.5 μM.

Table 8.1. The percentage of viability (V) of *Daphnia magna* in the presence of different concentrations of studied compounds and the corresponding LC_{50} values

Compound	V (%)				
	100 μM	**10 μM**	**1 μM**	**0.1 μM**	**LC_{50} (μM)**
HL	0.0	0.0	56.4±7.3	97±7.3	1.0±0.1
[Zn(H_2O)(L)Cl] (1)	0.0	0.0	56.4±7.3	102.6±0.0	1.0±0.1
[Cu(L)Cl] (2)	0.0	0.0	97.4±7.3	102.6±0.0	3.5±2.8
[Cu(L)Br] (3)	0.0	0.0	97.4±7.3	102.6±0.0	3.5±2.8
[$Cu_2L_2(CH_3COO_2]\cdot 4H_2O$ (4)	0.0	0.0	66.7±7.3	76.9±7.3	1.3±0.5
[Ni(*HL*)$_2$]$Cl_2\cdot H_2O$ (5)	87.2±7.3	97.4±7.3	102.6±0.0	102.6±0.0	≥100
[Co(L)$_2$]Cl (6)	35.9±7.3	92.3±0.0	97.4±7.3	97.4±7.3	65.4±11.8

The molecular electrostatic potential and the global reactivity indexes were calculated at the B3LYP level of theory and then discussed in terms of their

biological activities. It was found that the different reactivity descriptors of studied compounds strongly correlate with their biological activity and such dependences provide information for structure-activity study to design the biologically important molecules that can be applied in pharmacy and medicine.

In vitro biological evaluation, and *in vivo* toxicity of the *N*-phenyl-2-(pyridin-2-ylmethylidene)hydrazinecarbothioamide, cloro(*N*-phenyl-2-[pyridin-2-ylmethylidene]hydrazinecarbothioato)copper(II) and Cloro(*N*-phenyl-2-[pyridin-2-ylmethylidene]hydrazinecarbothioato) (4-aminobenzenesulfonamide) copper have been described in the paper (Garbuz et al., 2021) [314].

As the obtained results of anticancer, and antioxidant activities of the tested compounds are of both theoretical, and practical interest, their toxicity has been studied *in vivo* on *Daphnia magna*.

The results of the *Daphnia magna* bioassay are given in figure 8.7. The tested compounds have manifested general toxicity against *Daphnia magna* after 24h and 48h of exposure, according to the sequence: DOXO ≥ Cu(Str^1)(L^1-H)Cl ≥ Cu(L^1-H)Cl ≥ L^1 and DOXO ≥ Cu(Str^1)(L^1-H)Cl ≥ Cu(L^1-H)Cl ≥ L^1, respectively.

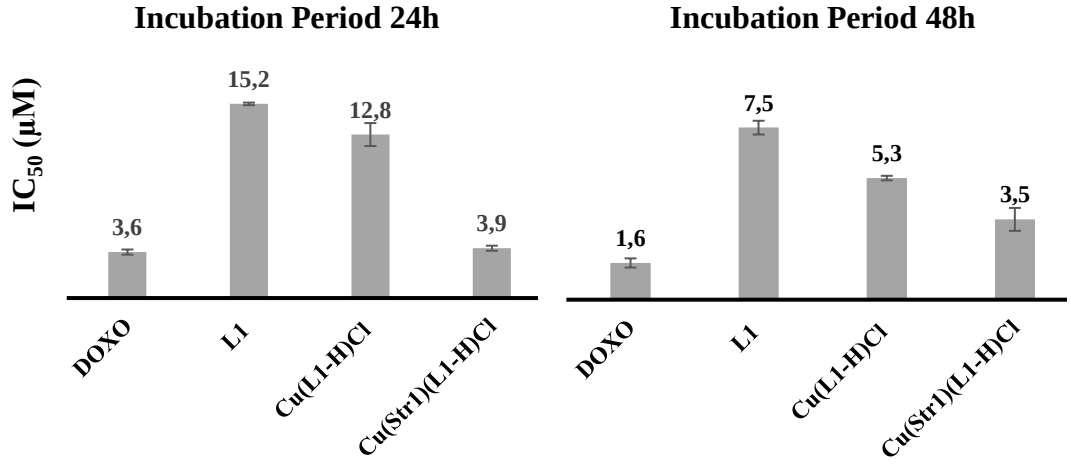

Fig. 8.7. **Toxicity on *Daphnia magna* of the the *N*-phenyl-2-(pyridin-2-ylmethylidene)hydrazinecarbothioamide, cloro(*N*-phenyl-2-[pyridin-2-ylmethylidene]hydrazinecarbothioato)copper(II) and Cloro(*N*-phenyl-2-[pyridin-2-ylmethylidene]hydrazinecarbothioato) (4-aminobenzenesulfonamide) copper**

The tested compounds are less toxic than DOXO for *Daphnia magna.* Thus, the tested compounds showed promising antiproliferative activity against cancer cells and low toxicity on *Daphnia magna.*

This research was focused on three new compounds: 2-acetylpyridine thiosemicarbazone as a ligand (H_2L^1) and two coordinating compounds of

copper(II): chloro(thiosemicarbazone-2- acetylpyridine)copper(II), nitrato(thiosemicarbazone-2-acetylpyridine)copper(II).

All tested compounds showed higher antioxidant activity than the compound de reference Trolox, which gave us the basis to continue the study of these compounds' toxicity.

The results of the *Daphnia magna* bioassay are presented in Table 8.2. The tested compounds have shown general toxicity to *Daphnia magna* after 24 hours of exposure. The general toxicity decreases in the following sequence: DOXO ≥ H_2L^1 ≥ $[Cu(H_2L^2)Cl]$ = $[Cu(H_2L^2)NO_3]$.

Table 8.2. *In vivo* toxicity of the tested compounds and DOXO on *Daphnia magna* after 24 hours incubation

LC_{50} ± SD (μM)	
H_2L^1	15.6±3.0
$[Cu(H_2L^2)Cl]$	≥100
$[Cu(H_2L^2)NO_3]$	≥100
DOXO	3.6±0.1

Complexes $[Cu(H_2L^2)Cl]$, $[Cu(H_2L^2)NO_3]$ showed toxicity to *Daphnia magna* with LC_{50} ≥100 μM. However, all tested compounds are less toxic than DOXO. Coordination of the H_2L^1 ligand with copper(II) ions leads to less toxicity than uncoordinated H_2L^1.

Research on the toxicity of the compounds tested on *Daphnia magna* showed that these compounds are less toxic than DOXO anticancer remedies.

The synthesized compounds thiosemicarbazone 2-acetylpyridine (H_2L), chloro(thiosemicarbazone-2-acetylpyridine)copper(II), and nitrato(thiosemicarbazone-2-acetylpyridine)copper(II) are perspective for further research in the field of anticancer activity.

It also studied the toxicity of a series of coordination compounds of some 3*d* metals with 2-formyl-, 2-acetyl, 2 benzoylpyridine *N*(4)-substituted thiosemicarbazones, which have biological activity, in particular antioxidant, which are of interest for further research. The vitality (%) and half-maximal concentration of substances regarding *Daphnia magna*, after 24h of incubation are presented in table 8.3.

Table 8.3. Toxicity on *Daphnia magna* of the tested coordination compounds

Coordination compounds of some 3*d* metals with 2-formyl-, 2-acetyl, 2-benzoylpyridine *N*(4)-substituted thiosemicarbazones	C μM	The incubation period (24h)			
		V (%)	SD	LC_{50} (μM)	SD
$[Cu(HL^2)Br_2]$ **HL^2**-CyTSC-2-Acpy	**100**	0.0	0.0	1.12	0.18
	10	0.0	0.0		
	1	56.4	7.3		
	0.1	87.2	7.3		
$[Cu(L^2)Cl]_2 \cdot (C_2H_5OH)_2$ **HL^2**-CyTSC-2-Acpy	**100**	0.0	0.0	0.46	0.23
	10	0.0	0.0		
	1	46.2	7.3		
	0.1	66.7	7.3		
$\{Cu(L^3)Cl\}$ **HL^3**-HexTSC-2-Acpy	**100**	0.0	0.0	3.49	2.80
	10	0.0	0.0		
	1	97.4	7.3		
	0.1	102.6	0.0		
$[Cu(L^4)Br]$ **HL^4**-CyTSC-2-Fopy	**100**	0.0	0.0	4.36	0.06
	10	25.6	7.3		
	1	87.2	7.3		
	0.1	92.3	0.0		
$[Cu(L^5)Br]_2$ **HL^5**-CyTSC-2-Bzpy	**100**	0.0	0.0	0.12	0.01
	10	0.0	0.0		
	1	0.0	0.0		
	0.1	87.2	7.3		
$\{Cu(L^4)NO_3\}$ **HL^4**-CyTSC-2-Fopy	**100**	0.0	0.0	2.60	0.85
	10	15.4	7.3		
	1	76.9	7.3		
	0.1	87.2	7.3		
$\{Zn(L^2)(H_2O)Cl\}$ **HL^2**-CyTSC-2-Acpy	**100**	0.0	0.0	0.29	0.24
	10	0.0	0.0		
	1	0.0	0.0		
	0.1	97.4	7.3		
$\{Cu(L^6)Br\}_2$ **HL^6**-t-But-TSC-2-Acpy	**100**	0.0	0.0	3.31	0.13
	10	25.6	7.3		
	1	76.9	7.3		
	0.1	97.4	7.3		
$[Cu(L^6)Cl]_2$ **HL^6**-t-But-TSC-2-Acpy	**100**	0.0	0.0	0.11	0.04
	10	0.0	0.0		

Table 8.3. Continued

	1	0.0	0.0		
	0.1	76.9	7.3		
[Cu(L^{7})Cl] **HL^{7}**-t-But-TSC-2-Bzpy	**100**	0.0	0.0	3.49	2.80
	10	0.0	0.0		
	1	97.4	7.3		
	0.1	102.6	0.0		
{Ni(L^{8})CH$_3$COO} **HL^{8}**-CyTSC-2-Fopy	**100**	35.9	7.3	**81.19**	10.44
	10	97.4	7.3		
	1	97.4	7.3		
	0.1	102.6	0.0		
{Cu(L^{9})Cl} **HL^{9}**-HexTSC-2-Fopy	**100**	0.0	0.0	1.57	0.09
	10	0.0	0.0		
	1	87.2	7.3		
	0.1	97.4	7.3		
{Cu(L^{4})Cl} **HL^{4}**-CyTSC-2-Fopy	**100**	0.0	0.0	3.49	2.80
	10	0.0	0.0		
	1	97.4	7.3		
	0.1	102.6	0.0		
{Cu(L^{4})H$_2$O} ClO$_4$ **HL^{4}**-CyTSC-2-Fopy	**100**	0.0	0.0	1.40	0.33
	10	0.0	0.0		
	1	76.9	7.3		
	0.1	97.4	7.3		
[Cu(L^{10})Cl]$_2$ **HL^{10}**-t-But-TSC-2-Fopy	**100**	0.0	0.0	3.62	2.61
	10	0.0	0.0		
	1	97.4	7.3		
	0.1	97.4	7.3		
[Mn(L^{6})$_2$] **HL^{6}**-t-But-TSC-2-Acpy	**100**	0.0	0.0	0.09	0.05
	10	0.0	0.0		
	1	25.6	7.3		
	0.1	46.2	7.3		
[Co(L^{5})$_2$]Br·H$_2$O **HL^{5}**-CyTSC-2-Bzpy	**100**	0.0	0.0	0.58	0.02
	10	0.0	0.0		
	1	35.9	7.3		
	0.1	87.2	7.3		
[Cu(L^{11})Cl] **HL^{11}**-Hex-TSC-2-Bzpy	**100**	0.0	0.0	0.11	0.04
	10	0.0	0.0		
	1	0.0	0.0		
	0.1	76.9	7.3		

Of all the tested complexes, acetato (*N*-cyclohexyl-2-(pyridine-2 ylmethylidene)carbamohydrazonothioato)nichel with LC_{50} 81.19±10.4 μM is non-toxic. Bis{N-tert-butyl-2-[1-(pyridin-2-yl)ethylidene]carbamohydrazonothioato} mangan proved to be the most toxic complex with LC_{50} of 0.09±0.05 μM. Whereas, the other tested complexes have toxicity against *Daphnia magna* with LC_{50} ranging from 0.09 to 4.40 μM.

In addition, the investigated biologically active compounds $Na_2[Mo_2O_4EDTA]\cdot 5H_2O$ and $Li_2[Mo_2O_4EDTA]\cdot 5H_2O$ were tested for toxicity using *Daphnia magna* (ISO 6341: 2012). Analyzing the results of the toxic bioassay it was observed, that both tested coordination compounds $Na_2[Mo_2O_4EDTA]\cdot 5H_2O$ and $Li_2[Mo_2O_4EDTA]\cdot 5H_2O$ are non-toxic and manifested the median lethal concentration LC_{50} ≥100 μM against *Daphnia magna* (Table 4).

Table 8.4. Effect of $Na_2[Mo_2O_4EDTA]\cdot 5H_2O$ and $Li_2[Mo_2O_4EDTA]\cdot 5H_2O$ on the viability of *Daphnia magna* exposed to concentrations (1-100 μM) after 24 h and 48 h of treatment

Compound	The incubation period (24h)	The incubation period (48h)
	LC_{50} (μM)	
$Na_2[Mo_2O_4EDTA]\cdot 5H_2O$	≥100	≥100
$Li_2[Mo_2O_4EDTA]\cdot 5H_2O$	≥100	≥100

As a result of the direct toxicity study of the test substances against *D. magna*, founding LC_{50} values indicate the possibility of their use as stimulants for the development of bees.

References

[1] Halliwell B., Gutteridge J.M.C. Free Radicals in Biology and Medicine, 3rd ed., Oxford University Press, 1999.

[2] Cadenas E. Biochemistry of oxygen toxicity. In: Ann. Rev. Biochem., vol. 58, pp.79-110, 1989.

[3] Valko M., Izakovic M., Mazur M., Rhodes C.J., Telser J. Role of oxygen radicals in DNA damage and cancer incidence. In: Mol. Cell. Biochem., vol. 266, pp. 37–56, 2004.

[4] Poli G., Leonarduzzi G., Biasi F., Chiarpotto E. Oxidative stress and cell signalling. In: Curr. Med. Chem., vol. 11, pp. 1163–118211, 2004.

[5] Halliwell B. Antioxidants in human health and disease. In: Ann. Rev. Nutr., vol 16, pp. 33–50, 1996.

[6] Saeed A., Khan SU., Mahesar PA., Channar PA., Shabir G., Iqbal J. «Substituted (E)-2-(2-benzylidenehydrazinyl)-4-methylthiazole-5-carboxylates as dual inhibitors of 15-lipoxygenase & carbonic anhydrase II: synthesis, biochemical evaluation and docking studies. In: Biochem Biophys Res Commun., т. 482, № 1, pp. 176-181, 2017 .

[7] Breitenbach M.; Eckl P. Introduction to Oxidative Stress in Biomedical and Biological Research. Biomolecules, vol. 5, pp. 1169–1170, 2015.

[8] Sies H. On the history of oxidative stress: Concept and some aspects of current development. In: Curr. Opin. Toxicol., vol 7, pp. 122–126, 2018.

[9] Ofosu F.K., Mensah D.-J.F., Daliri E.B.-M., Oh D.-H. ExploringMolecular Insights of Cereal PeptidicAntioxidants in Metabolic SyndromePrevention. Antioxidants, vol. 10, pp. 518, 2021.

[10] Sies H., (Ed.) Oxidative stress: Introductory remarks. In: Oxidative Stress, 1st ed., Academic Press: London, UK, pp. 1–8, 1985.

[11] Roede J.R., Stewart B.J., Petersen D.R. Hepatotoxicity of Reactive Aldehydes. In: Comprehensive Toxicology, 2nd ed.; McQueen C.A., Ed. Elsevier: Oxford, MA, USA, vol. 9, pp. 581–594, 2010.

[12] Lushchak V.I. Free radicals, reactive oxygen species, oxidative stress and its classification. In: Chem. Biol. Interact., vol. 244, pp. 164–175, 2014.

[13] El-Fawal H.A.N. Neurotoxicology. In: Encyclopedia of Environmental Health, 1st ed.; Nriagu J.O., Ed.; Elsevier: Burlington, MA, USA, vol. 4, pp. 87–106.

[14] Burton G.J., Jauniaux E. Oxidative stress. In: Best Pract. Res. Clin. Obs. Gynaecol., vol. 25, pp. 287-299, 2011.

[15] Jones D.P. Redefining oxidative stress. Antioxid Redox Signal., vol. 8, pp. 1865–1879, 2006.

[16] Калинченко С.Ю., Тюзиков И.А. Окислительный стресс и мужское бесплодие – взаимодействующие пандемии XXI века. Современные фармакотерапевтические возможности патогенетической коррекции нарушений сперматогенеза препаратами L-карнинита/ацетил-L-карнитина //, Эффективная фармакотерапия.. Вып. 22. Урология и нефрология. Спецвыпуск «Мужское здоровье». С. 6–19, 2017.

[17] Тюзиков И.А., Калинченко С.Ю. Окислительный стресс и ацидоз – просто диагностировать, просто лечить! Часть 1 // Эстетическая медицина. Том XVI. № 1,, С. 1–9, 2017.

[18] Тюзиков И.А., Калинченко С.Ю. Окислительный стресс и ацидоз – просто диагностировать, просто лечить! Часть 2 // Эстетическая медицина. Том XVI. № 2. 2017. С. 1–7.

[19] Zoja C., Benigni A., Remuzzi G. The Nrf2 pathway in the progression of renal disease. In: Nephrol. Dial. Transplant., vol. 29:I19–I24, 2014.

[20] Chen Z., Zhong C. Oxidative stress in Alzheimer's disease. In: Neurosci. Bull., vol. 30, pp. 271–281, 2014.

[21] Sureshbabu A., Ryter S.W., Choi M.E. Oxidative stress and autophagy: Crucial modulators of kidney injury. In: Redox Biol., vol. 4, pp. 208-214, 2015.

[22] Modlinger P.S., Wilcox C.S., Aslam S. Nitric oxide, oxidative stress, and progression of chronic renal failure. In: Semin. Nephrol., vol. 24, pp. 354–365, 2004.

[23] Lai E.Y., Wellstein A., Welch W.J., Wilcox C.S. Superoxide modulates myogenic contractions of mouse afferent arterioles. Hypertens., vol. 58, pp. 650–656, 2011.

[24] Li B., Haridas B., Jackson A.R., Cortado H., Mayne N., Kohnken R., Bolon B., McHugh K.M., Schwaderer A.L., Spencer J.D., et al. Inflammation drives renal scarring in experimental pyelonephritis. Am. J. Physiol. Ren. Physiol., vol. 312:F43–F53, 2017.

[25] Valko M., Rhodes C.J., Moncol J., Izakovic M., Mazur M. Free radicals, metals and antioxidants in oxidative stress-induced cancer. In: Chem. Biol. Interact., vol. 160, pp. 1-40, 2006.

[26] Sánchez-Moreno C. Review: Methods Used to Evaluate the Free Radical Scavenging Activity in Foods and Biological Systems, Food Science and Technology. International, (8)3, pp. 121-137, 2002.

[27] Morrison RT, Boyd RN. Organic chemistry, 6th edn. Prentice-Hall, Englewood Cliffs, 1992.

[28] Меньщикова Е.Б., Ланкин В.З., Зенков Н.К. и др. Окислительный стресс. Прооксиданты и антиоксиданты. М.: Фирма «Слово», 2006.

[29] Roediger B., Armati P.J. Oxidative stress induces axonal beading in cultured human brain tissue. In: Neurobiol. Dis., vol. 13, pp. 222-229, 2003.

[30] Young I.S., Woodside J.V. Antioxidants in health and disease. J. Clin. Pathol., vol. 54, pp. 176–186, 2001.

[31] Pisoschi A.M., Pop A. The role of antioxidants in the chemistry of oxidative stress: A review. Eur. J. Med. Chem., vol. 97, pp. 55–74, 2015.

[32] Kaminskyy V.O., Zhivotovsky B. Free radicals in cross talk between autophagy and apoptosis. Antioxid Redox Signal., vol. 1;21(1):86-102, 2014.

[33] Lobo V., Pati A., Phatak A., Chandra N. C. Free radicals, antioxidants and functional foods: Impact on human health. In: Pharmacogn Rev., vol. 4(8), pp. 118–126, 2010.

[34] Kurutas E.B. The importance of antioxidants which play the role in cellular response against oxidative/nitrosative stress: current state. Nutr J., vol. 15, pp. 71, 2015.

[35] Cheeseman K.H., Slater T.F. An introduction to free radicals chemistry. In: Br. Med. Bull., vol. 49, pp. 481–493, 1993.

[36] Panić M., Stojković M.R., Kraljić K., Škevin D., Redovniković I.R., Srček V.G., Radošević K. Ready-to-use green polyphenolic extracts from food by-products. In: Food Chem., vol. 283, pp. 628–636, 2019.

[37] Pruchniak Michał P., Araz´na Magdalena., Demkow Urszula. Biochemistry of Oxidative Stress. In: Advs Exp. Medicine, Biology - Neuroscience and Respiration, Springer International Publishing Switzerland, 2015.

[38] Graves D.B. The emerging role of reactive oxygen and nitrogen species in redox biology and some implications for plasma applications to medicine and biology. J. Phys. D Appl. Phys., vol. 45:263001, 2012.

[39] Fridovich I. Biological effects of the superoxide radical, Arch.Biochem. Biophys., vol. 247, pp. 1–11, (1986).

[40] Desideri A., Falconi M. Prokaryotic Cu, Zn superoxidies dismutases. In: Biochem. Soc. Trans., vol. 31, pp. 1322–1325, 2003..

[41] Michiels C., Raes M., Toussaint O., Remacle J. Importance of Se-glutathione peroxidase, catalase, and Cu/Zn-SOD for cell survival against oxidative stress. In: Free Rad. Biol. Med., vol. 17, pp. 235–248, 1994.

[42] Valko M., Morris H., Cronin M.T.D. Cronin, Metals, toxicity and oxidative stress, In: Curr. Med. Chem., vol. 12, pp. 1161–1208, 2005.

[43] Liochev S.I., Fridovich I. The Haber-Weiss cycle — 70 years later: an alternative view, Redox report., vol. 7, pp. 55–57, 2002.

[44] Valko M. et al. Free radicals, metals and antioxidants in oxidative. Chemico-Biological Interactions., vol.160, pp. 1–40, 2006.

[45] Archer S., Measurement of nitric-oxide in biological models,FASEB J., vol. 7, pp. 349–360, 1993.

[46] Birben E., Sahiner U.M., Sackesen C., Erzurum S., Kalayci O. Oxidative stress and antioxidant defense. World Allergy Organ. J., vol. 5, pp. 9–19, 2012.

[47] Dąbrowska N., Wiczkowski A. Analytics of oxidative stress markers in the early diagnosis of oxygen DNA damage. In: Adv. Clin. Exp. Med., vol. 26:155–166. doi: 10.17219/acem/43272, 2017.

[48] Marnett L.J. Lipid peroxidation-DNA damage by malondialdehyde. Mutat. Res. 1999;424:83–95.

[49] Dizdaroglu M., Jaruga P., Birincioglu M., Rodriguez H. Free radical-induced damage to DNA: Mechanisms and measurement. In: Free. Radic. Biol. Med., vol. 32, pp. 1102–1115. 2002.

[50] Chiorcea-Paquim A.-M., Oliveira-Brett A.M. Nanostructured material-based electrochemical sensing of oxidative DNA damage biomarkers 8-oxoguanine and 8-oxodeoxyguanosine. In: A comprehensive review. Mikrochim. Acta., vol. 188, pp. 58, 2021.

[51] Thannickal V.J., Fanburg B.L. Reactive oxygen species in cell signaling. In: Am. J. Physiol. Lung Cell. Mol. Physiol., vol. 279, pp. 1005-1028, 2000.

[52] Hensley K., Robinson K.A., Gabbita S.P., Salsman S., Floyd R.A. Reactive oxygen species, cell signaling, and cell injury. In: Free Rad. Biol. Med., vol. 28, pp.1456–1462, 2000.

[53] Sah V.P., Seasholtz T.M., Sagi S.A., Brown J.H. The role of Rho in G protein-coupled receptor signal transduction. In: Ann. Rev. Pharmacol. Toxicol., vol. 40. pp. 459–489, 2000.

[54] Storz P. Reactive oxygen species in tumor progression. In: Front. Biosci., vol. 10, pp. 1881–1896, 2005.

[55] Ogura S., Shimosawa T. Oxidative stress and organ damages. In: Curr. Hypertens. Rep., vol. 16, pp. 452, 2014.

[56] Efe U., Dede S., Yüksek V., Çetin S. Apoptotic and Oxidative Mechanisms in Liver and Kidney Tissues of Sheep with Fluorosis. In: Biol. Trace Elem. Res., vol. 199, pp. 136–141, 2021.

[57] La Russa D., Brunelli E., Pellegrino D. Oxidative imbalance and kidney damage in spontaneously hypertensive rats. Activation of extrinsic apoptotic pathways. Clin. Sci., vol. 131, pp. 1419–1428, 2017.

[58] Valko M., Leibfritz D., Moncol J., Cronin M.T.D., Telser J. Telser. Mutual effect of free radicals, redox metals and antioxidants, FEBS J., 2006.

[59] Siah C.W., Trinder D., Olynyk J.K., Iron overload. In: Clin. Chim. Acta., vol. 358, pp. 24-36, 2005.

[60] Liu K.J., Shi X.L. In vivo reduction of chromium(VI) and its related free radical generation. In: Mol. Cell. Biochem., vol. 222, pp. 41–47, 2001.

[61] Hanna P.M., Kadiiska M.B., Mason R.P. Oxygen-derived free radical and active oxygen complex-formation from cobalt(II) chelates in vitro. In: Chem. Res. Toxicol., vol. 5, pp. 109–115, 1992.

[62] Lee Y.W., Klein C.B., Kargacin B., Salnikow K., Kitahara J., K. Carcinogenic nickel silences gene-expression by chromatin condensation and DNA methylation — a new model for epigenetic carcinogens. In: Mol. Cell. Biol., vol. 15, pp. 2547–2557, 1995.

[63] Poljsak B., Šuput D., Milisav I. Achieving the Balance between ROS and Antioxidants: When to Use the Synthetic Antioxidants. In: Oxidative Med. Cell. Longev., vol. doi:10.1155/2013/956792, pp. 1–11, 2013.

[64] Lunec J., Griffits H.R. Measuring In Vivo Oxidative Damage; John Willey and Sons: New York, NY, USA, 2000.

[65] Poljsak B., Jamik P. Methodology for oxidative state detection in biological systems. In: Handbook of Free Radicals: Formation, Types and Effects; Cell Biology Research Progress Series; Kozyrev, D., Slutsky, V., Eds.; Nova Science: New York, NY,USA, 2010.

[66] Sahnoun Z., Jamoussi K., Zeghal K.M. Free radicals and antioxidants: Human physiology, pathology and therapeutic aspects. Therapie., vol. 52, pp. 251–270, 1997.

[67] Bunaciu A.A., Danet A.F., Fleschin Ş., Aboul-Enein H.Y. Recent Applications for in Vitro Antioxidant Activity Assay. In: Crit. Rev. Anal. Chem., vol. 46, pp. 389–399, 2016.

[68] Huang D., Ou B., Prior R.L. The chemistry behind antioxidant capacity assays. J. Agric. Food Chem., vol. 53, pp. 1841–1856, 2005.

[69] Pérez-Jiménez J., Arranz S., Tabernero M., Díaz- Rubio. Updated methodology to determine antioxidant capacity in plant foods, oils and beverages: Extraction, measurement and expression of results. In: Food Res. Int., vol. 41, pp. 274–285, 2008.

[70] Niki E., Noguchi N. Evaluation of antioxidant capacity. What capacity is being measured by which method? In: IUBMB Life., vol. 50, pp. 323–329, 2000.

[71] Bartosz G. Total antioxidant capacity. In Advances in Clinical Chemistry, 1st ed.; Spiegel, H.E., Ed.; Academic Press: New York., vol. 37, pp. 219−292, 2003.

[72] Magalhães L.M., Segundo M.A., Reis S., Lima J.L. Methodological aspects about in vitro evaluation of antioxidant properties. In: Anal. Chim. Acta ., vol. 613, pp. 1–19, 2008.

[73] Flieger J., Flieger W., Baj J., Maciejewski R. Antioxidants: Classification, Natural Sources, Activity/Capacity Measurements, and Usefulness for the Synthesis of Nanoparticles. Materials., vol. 14, pp. 4135, 2021.

[74] Ordoudi S.A., Tsimidou M.Z. Crocin bleaching assay step by step: Observations and suggestions for an alternative validated protocol. In: J. Agric. Food Chem., vol. 54, pp. 1663–1671, 2006.

[75] Prieto M.A., Vázquez J.A., Murado M.A. Crocin bleaching antioxidant assay revisited: Application to microplate to analyse antioxidant and pro-oxidant activities. In: Food Chem., vol. 167, pp. 299–310, 2015.

[76] Lussignoli S., Fraccaroli M., Andrioli G., Brocco G., Bellavite P. A microplate-based colorimetric assay of the total peroxyl radical trapping capability of human plasma. In: Anal. Biochem., vol. 269, pp. 38–44, 1999.

[77] Gupta D. Methods for Determination of Antioxidant Capacity. In: A Review. Int. J. Pharm. Sci. Res., vol. 6, pp. 546–566, 2015.

[78] Pisoschi A.M., Negulescu G.P. Methods for Total Antioxidant Activity Determination. In: A Review. Biochem. Anal. Biochem., vol. 1, pp. 106, 2011.

[79] Ndhlala A.R., Moyo M., Van Staden J. Natural antioxidants: Fascinating or mythical biomolecules? Molecules., vol. 15, pp. 6905–6930, 2010.

[80] Kaur I.P., Geetha T. Screening methods for antioxidants-a review. In: Mini Rev. Med. Chem., vol. 6, pp. 305–312, 2006.

[81] Christodouleas D., Fotakis C., Papadopoulos K., Dimotikali D, Calokerinos A.C. Luminescent Methods in the Analysis of Untreated Edible Oils. In: A Review. Anal. Lett., vol. 45, pp. 625–641, 2012.

[82] Popov I., Lewin G. Antioxidative homeostasis: Characterization by means of chemiluminescent technique. In: Methods Enzymol., vol. 300, pp. 437–456, 1999.

[83] Robak J., Gryglewski R.J. Flavonoids are scavengers of superoxide anions. In: Biochem. Pharmacol., vol. 37, pp. 837–841, 1988.

[84] Apak R., Güçlü K., Ozyürek M., Karademir S.E., Altun M. Total antioxidant capacity assay of human serum using copper(II)-neocuproine as chromogenic oxidant. In: The CUPRAC method. Free Radic. Res., vol. 39, pp. 949–961, 2005.

[85] Ozyurt D., Demirata B., Apak R. Determination of total antioxidant capacity by a new spectrophotometric method based on Ce(IV) reducing capacity measurement. Talanta. Vol. 71, pp. 1155–1165, 2007.

[86] Ozyurt D., Demirata B., Apak R. Modified cerium(IV)-based antioxidant capacity (CERAC) assay with selectivity over citric acid and simple sugars. In: J. Food Compos. Anal., vol. 23, pp. 282–288, 2010.

[87] Işık E., Şahin S., Demir C. Development of a new chromium reducing antioxidant capacity (CHROMAC) assay for plants and fruits. Talanta., vol. 111, pp. 119–124, 2013.

[88] Priya D., Rajaram K., Suresh-kumar P. In vitro antioxidant and preliminary phytochemical studies of Caralluma fimbriata wall. In: Int. J. Pharm. Res., vol. 4, 2012.

[89] Kumar C.S., Loh W.S., Ooi C.W., Quah C.K., Fun H.K. Structural correlation of some heterocyclic chalcone analogues and evaluation of their antioxidant potential. Molecules., vol. 18, pp. 11996–1201118, 2013,,

[90] Kikuzaki H., Nakatani N. Antioxidant Effects of Some Ginger Constituents. In: J. Food Sci.. vol. 58, pp. 1407–1410, 1993.

[91] Sharma B., Rout J. Biosynthesis of fluorescent gold nanoparticles using an edible freshwater red alga, Lemanea fluviatilis (L.) C.Ag. and antioxidant activity of biomatrix loaded nanoparticles. In: Bioprocess Biosyst. Eng., vol. 37, pp. 2559–2565, 2014.

[92] Friel J.K., Diehl-Jones W.L., Suh M., Tsopmo A., Shirwadkar V.P. Impact of iron and vitamin C-containing supplements on preterm human milk. In: In vitro. Free Radic. Biol. Med., vol. 42, pp. 1591–1598, 2007.

[93] Re R., Pellegrini N., Proteggente A., Pannala A. Yang M., Rice-Evans C. Antioxidant activity applying an improved ABTS radical cation decolorization assay. In: Free Radic. Biol. Med., vol. 26, pp. 1231–1237, 1999.

[94] Damien Dorman H.J., Shikov A.N., Pozharitskaya O.N., Hiltunen R. Antioxidant and pro-oxidant evaluation of a Potentilla alba L. rhizome extract. Chem. Biodivers., vol. 8, pp. 1344–1356, 2011.

[95] Fontana M., Mosca L., Rosei M.A. Interaction of enkephalins with oxyradicals. Biochem. Pharmacol. 2001, 61, 1253–1257.

[96] Habu, J.B.; Ibeh, B.O. In vitro antioxidant capacity and free radical scavenging evaluation of active metabolite constituents of Newbouldia laevis ethanolic leaf extract. In: Biol. Res., vol. 48, pp. 16, 2015.

[97] Bailly F., Zoete V., Vamecq J., Catteau J.P., Bernier J.L. Antioxidant actions of ovothiol-derived 4-mercaptoimidazoles: Glutathione peroxidase activity and protection against peroxynitrite-induced damage. In: FEBS Lett., vol. 486, pp. 19–22, 2000.

[98] Kunchandy E., Rao M.N.A. Oxygen radical scavenging activity of curcumin. In: Int. J. Pharm., vol. 58, pp. 237–240, 1990.

[99] Chu Y.H., Chang C.L., Hsu H.F. Flavonoid content of several vegetables and their antioxidant activity. In: J. Sci. Food Agric., vol. 80, pp. 561–566, 2000.

[100] Cheng Z., Zhou H., Yin J., Yu L. Electron spin resonance estimation of hydroxyl radical scavenging capacity for lipophilic antioxidants. In: J. Agric. Food Chem., vol. 55, pp. 3325–3333, 2007.

[101] Carini M., Aldini G., Piccone M., Facino R.M. Fluorescent probes as markers of oxidative stress in keratinocyte cell lines following UVB exposure. Farmaco., vol. 55, pp. 526–534, 2000.

[102] Nabavi S.M., Ebrahimzadeh M.A., Nabavi S.F., Hamidinia A., Bekhradnia A.R. Determination of antioxidant activity, phenol and flavonoids content of Parrotia persica Mey. Pharmacologyonline, vol. 2, pp. 560–567, 2008.

[103] Pedraza-Chaverri J., Barrera. Hernandez-Pando R. S-allylmercaptocysteine scavenges hydroxyl radical and singlet oxygen in vitro and attenuates gentamicin-induced oxidative and nitrosative stress and renal damage in vivo. In: BMC Clin. Pharmacol., vol. 4, pp. 5, 2004.

[104] Macku C., Shibamoto, T. Volatile antioxidants produced from heated corn oil/glycine model system. In: J. Agric. Food Chem., vol. 39, pp. 1990–1993, 1991.

[105] Sudan R., Bhagat M., Gupta S., Singh J., Koul A. Iron (FeII) Chelation, Ferric Reducing Antioxidant Power, and Immune Modulating Potential of Arisaema jacquemontii (Himalayan Cobra Lily). In: BioMed. Res. Int., 2014.

[106] Sousa S.J., Brizola V.R.A., Granato D. High-throughput assay comparison and standardization for metal chelating capacity screening: A proposal and application. In: Food Chem., vol. 214, pp. 515-522, 2017.

[107] Scampicchio M., Wang J., Blasco A.J., Sanchez Arribas A., Mannino S. Escarpa A. Nanoparticle-based assays of antioxidant activity. In: Anal. Chem., vol. 78, pp. 2060–2063, 2006.

[108] Özyürek M., Güngör N., Baki S., Güçlü K., Apak R. Development of a Silver Nanoparticle-Based Method for the Antioxidant Capacity Measurement of Polyphenols. In: Anal. Chem., vol. 84, pp. 8052–8059, 2012,.

[109] Niki E. Assessment of antioxidant capacity in vitro and in vivo. In: Free Radic Biol Med., Aug., 15;49(4):503-15, 2010.

[110] Niki E., Methods Enzymol., vol.186, pp. 100, 1990.

[111] Halliwell B., Murcia M.A., Chirico S., Aruoma O.I. In: Crit. Rev.Food Sci. Nutr., vol. 35, pp. 7, 1995.

[112] Huang D.J., Ou B.X., Prior R.L. In: J. Agric. Food Chem., vol. 53, pp. 1841, 2005.

[113] Glazer A.N., In: Methods Enzymol., vol. 186, pp. 161, 1990.

[114] Ou B.X., Hampsch-Woodill M., Prior R.L. In: J. Agric. Food Chem., vol. 49, pp. 4619, 2001.

[115] Huang D.J., Ou B.X., Hampsch-Woodill M., Flanagan J.A., Deemer E.K. In: J. Agric. Food Chem., vol. 50, pp. 1815, 2002.

[116] Naguib Y.M.A. In: Anal. Biochem., vol. 265,pp. 290, 1998.

[117] Huang D.J., Ou B.X., Hampsch-Woodill M., Flanagan J.A., Prior R.L. In: J. Agric. Food Chem., vol. 50, pp. 4437, 2002.

[118] Ou B., Hampsch-Woodill M., Flanagan J., Deemer E.K., Prior R.L., Huang D.J. In: J. Agric. Food Chem., vol. 50, pp. 2772, 2002.

[119] Wayner D.D.M., Burton G.W., Ingold K.U., Locke S. In: FEBS Lett., vol. 187, pp. 33, 1985.

[120] Valkonen M., Kuusi T. In: J. Lipid Res., vol. 38, pp. 823, 1997.

[121] Frankel E.N., Kanner J., German J.B., Parks E., Kinsella J.E., Lancet. vol. 341, pp. 454, 1993.

[122] Vinson J.A., Hontz B.A. In: J. Agric. Food Chem., vol. 43, pp. 401, 1995.

[123] Vinson J.A., Dabbagh Y.A., Serry M.M., Jang J.H., J. In: Agric.Food Chem., vol. 43, pp. 2800, 1995.

[124] Handelman G.J., Cao G., Walter M.F., Nightingale Z.D., Paul G.L., Prior R.L., Blumberg J.B. In: J. Agric. Food Chem., vol. 47, pp. 4888, 1999.

[125] Sanchez-Moreno C., Jimenez-Escrig A., Saura-Calixto F. In: Nutr. Res., vol. 20, pp. 941, 2000.

[126] Winston G.W., Regoli F., Dugas A.J., Fong J.H., Blanchard K.A. Free Radic. Biol. Med., vol. 24, pp. 480, 1998.

[127] Lichtenthaler R., Marx F., Kind O.M. In: Eur. Food Res. Technol., vol. 216, pp. 166, 2003.

[128] Alho H., Leinonen J. Methods Enzymol., vpl. 299, pp. 3, 1999.

[129] Lu C., Song G., Lin J.M., Trac-Trends Anal. Chem., vol. 25, pp. 985, 2006.

[130] Lissi E., Pascual C., Delcastillo M.D., Free Radic. Res.Commun., vol. 17, pp. 299, 1992.

[131] Lissi E., Salimhanna M., Pascual C., Delcastillo M.D., Free Radic. Biol. Med., vol.18, pp. 153, 1995.

[132] Hirayama O., Takagi M., Hukumoto K., Katoh S., In: Anal. Biochem., vol. 247, pp. 237, 1997.

[133] Aruoma O.I., Murcia A., Butler J., Halliwell B. J., Agric. Food Chem., vol. 41, pp. 1880, 1993.

[134] Quick K.L., Hardt J.I., Dugan L.L., J. Neurosci. Methods, vol. 97, pp.139, 2000.

[135] Wang S.Y., Jiao H.J., Agric J.. Food Chem., vol. 48, pp. 5677, 2000.

[136] Elstner E.F., Heupel A. Anal. Biochem., vol. 70, pp. 616, 1976.

[137] Vonkruedener S., Schempp H., Elstner E.F. Free Radic. Biol. Med., vol. 19, pp. 141, 1995.

[138] Lavelli V., Hippeli S., Peri C., Elstner E.F. J. Agric. Food Chem., vol. 47, pp. 3826, 1999.

[139] Calliste C.A., Trouillas P., Allais D.P., Simon A., Duroux J.L. J.Agric. Food Chem., vol. 49, pp. 3321, 2001.

[140] Li Y.B., Zhu H., Kuppusamy P., Roubaud V., Zweier J.L., Trush M.A. J. Biol. Chem., vol. 273, pp. 2015, 1998.

[141] Halliwell B. The antioxidant paradox. Lancet, vol. 355, pp. 1179–1180, doi:10.1016/S0140-6736(00)02075-4, 2000.

[142] Corbett J.T. J. Biochem. Biophys. Methods, vol. 18, pp. 297, 1989.

[143] Arnous A., Petrakis C., Makris D.P., Kefalas P. J. Pharmacol. Toxicol. Methods, vol. 48, pp. 171, 2002.

[144] Yildiz G., Demiryurek A.T., Sahin-Erdemli I., Kanzik I. Br. J. Pharmacol., vol. 124, pp. 905, 1998.

[145] Chang M.C., Uang B.J., Wu H.L., Lee J.J., Hahn L.J., Jeng J.H., Br. J. Pharmacol., vol 135, pp. 619, 2002.

[146] Halliwell B., Gutteridge J.M.C., Aruoma O.I. Anal. Biochem., vol. 165, pp. 215, 1987.

[147] Aruoma O.I., Grootveld M., Halliwell B. J. Inorg. Biochem., vol. 29, pp. 289, 1987.

[148] Hagerman A.E., Riedl K.M., Jones G.A., Sovik K.N., Ritchard N.T., Hartzfeld P.W., Riechel T.L. J. Agric. Food Chem., vol. 46, pp.1887, 1998.

[149] Zhu B.Z., Kitrossky N., Chevion M. Biochem. Biophys. Res.Commun., vol. 270, pp. 942, 2000.

[150] Hirayama O., Yida M. Anal. Biochem., vol. 251, pp. 297, (1997).

[151] Yildiz G., Demiryurek A.T. J. Pharmacol. Toxicol. Methods., vol. 39, pp. 179, 1998.

[152] Aruoma O.I. Gen. Pharmacol, vol. 28, pp. 269, 1997.

[153] Yan L.J., Traber M.G., Kobuchi H., Matsugo S., Tritschler H.J., Packer L. Arch. Biochem. Biophys., vol. 327, pp. 330, 1996.

[154] Gatto M.T., Firuzi O., Agostino R., Grippa E., Borso A. F. Biomed. Chromatogr., vol. 16, pp. 404, 2002.

[155] Mouithys-Mickalad A.M.L., Zheng S.X., Deby-Dupont G.P., Deby C.M.T., Lamy M.M., Reginster J.Y.Y., Henrotin Y.E. Free Radic. Res., vol. 33, pp. 607, 2000.

[156] Antwerpen Van Antwerpen P., Dubois J., Gelbcke M., Neve J. Free Radic. Res., vol. 38, pp. 251, 2004).

[157] Davies M.J. Photochem. Photobiol. Sci., vol. 3, pp. 17, 2004.

[158] Costa D., Fernandes E., Santos J.L.M., Pinto D.C.G.A., Silva A.M.S., Lima J.L.F.C. Anal. Bioanal. Chem., vol. 387, pp. 2071, 2007.

[159] Pacher P., Beckman J.S., Liaudet L. Physiol. Rev., vol. 87, pp. 315, 2007.

[160] Vriesman M.F., Haenen G.R.M.M., Westerveld G.J., Paquay J.B.G., Voss H.P., Bast A. Pharm. World Sci., vol. 19, pp. 283, 1997.

[161] Krol W., Czuba Z.P., Threadgill M.D., Cunningham B.D.M., Pietsz G. Biochem. Pharmacol., vol. 50, pp. 1031, 1995.

[162] Hevel J.M., Marletta M.A. Methods Enzymol., vol. 233, pp. 250, 1994.

[163] Perez C., Sanchez J., Marmol F., Puig-Parellada P., Pouplana R. QSAR Comb. Sci., vol. 26, pp. 368, 2007.

[164] Nagata N., Momose K., Ishida Y. J. Biochem., vol, 125, pp. 658, 1999.

[165] Zhang X., Kim W.S., Hatcher N., Potgieter K., Moroz L.L., Gillette R., Sweedler J.V. J. Biol. Chem., vol. 277, pp. 48472, 2002.

[166] Whiteman M., Halliwell B. Free Radic. Res., vol. 25, pp. 275, 1996.

[167] Kooy N.W., Royall J.A., Ischiropoulos H., Beckman J.S. Free Radic. Biol. Med., vol. 16, pp. 149, 1994.

[168] Radi R., Cosgrove T.P., Beckman J.S., Freeman B.A. Biochem.J., vol. 290, pp. 51, 1993.

[169] Miller N.J., Rice-Evans C., Davies M.J., Gopinathan V., Milner A. Clin. Sci., vol. 84, pp. 407, 1993.

[170] Strube M., Haenen G.R.M.M., Van den Berg H., Bast A., Free Radic. Res., vol. 26, pp. 515, 1997.

[171] Re R., Pellegrini N., Proteggente A., Pannala A., Yang M., Rice-Evans C. Free Radic. Biol. Med., vol. 26, pp. 1231, 1999.

[172] Miller N.J., Sampson J., Candeias L.P., Bramley P.M., Rice-Evans C.A. FEBS Lett., vol. 384, pp. 240, 1996.

[173] Van den Berg R., Haenen G.R.M.M., Van den Berg H., Bast A. Food Chem., vol. 66, pp. 511, 1999.

[174] Cano A., Hernandez-Ruiz J., Garcia-Canovas F., Acosta M., Arnao M.B. Phytochem. Anal., vol. 9, pp. 196, 1998.

[175] Alonso A.M., Dominguez C., Guillen D.A., Barroso C.G. J. Agric. Food Chem., vol. 50, pp. 3112, 2002.

[176] Blois M.S. Nature., vol. 181,pp. 1199, 1958.

[177] Brand-Williams W., Cuvelier M.E., Berset C. LWT-Food Sci. Technol., vol. 28, pp. 25, 1995.

[178] Milardovic S., Ivekovic D., Grabaric B.S. Bioelectrochemistry., vol. 68, pp.175, 2006.

[179] Milardovic S., Ivekovic D., Ruwenjak V., Grabaric B.S. Electroanalysis., vol. 17, pp. 1847, 2005.

[180] Stasko A., Brezova V., Biskupic S., Misik V. Free Radic. Res., vol. 41, pp. 379, 2007.

[181] Benzie I.F.F., Strain J.J. Anal. Biochem., vol. 239, pp. 70, 1996.

[182] Tsao R., Yang R., Young J.C. J. Agric. Food Chem., vol. 51, pp. 6445, 2003.

[183] Ou B.X., Huang D.J., Hampsch-Woodill M., Flanagan J.A., Deemer E.K. J. Agric. Food Chem., vol. 50, pp. 3122 , 2002.

[184] Singleton V.L., Singleton R., Lamuela-Raventos R.M. Methods Enzymol., vol. 299, pp. 152, 1999.

[185] Chevion S., Roberts M.A., Chevion M. Free Radic. Biol. Med., vol. 28, pp. 860, 2000.

[186] Piga R., Saito Y., Yoshida Y., Niki E. Cytotoxic effects of various stressors on PC12 cells: Involvement of oxidative stress and effect of antioxidants. NeuroToxicology., vol. 28, pp. 67–75, 2007.

[187] Terao J. Dietary flavonoids as antioxidants. In: Forum Nutr., vol. 61., vol. 87–94, 2009.

[188] Voss P., Siems W. Clinical oxidation parameters of aging. In: Free Radic. Res., vol. 40, pp. 1339–1349, 2006.

[189] Niki E. Lipid peroxidation products as oxidative stress biomarkers. BioFactors., vol. 34, pp. 171–180, 2008.

[190] Dizdaroglu M., Jaruga P., Birincioglu M., Rodriguez H. Free radical-induced damage to DNA: Mechanisms and measurement. In: Free Radic. Biol. Med., vol, 32, pp. 1102–1115, 2002.

[191] Etsuo Niki. Assessment of Antioxidant Capacity in vitro and in vivo. In: Free Radical Biology & Medicine., vol. 49, pp. 503–515, 2010.

[192] Tejchman K, Kotfis K, Sieńko J. Biomarkers and Mechanisms of Oxidative Stress-Last 20 Years of Research with an Emphasis on Kidney Damage and Renal Transplantation. In: Int J Mol Sci., Jul 27;22(15):8010, 2021.

[193] Bartz R.R., Piantadosi C.A. Clinical review: oxygen as a signaling molecule. In: Crit. Care., vol. 14. 5. 234, 2010.

[194] Rahal A., Kumar A., Singh V. et al. Oxidative stress, prooxidants, and antioxidants: the interplay. In: Biomed. Res. Int., 2014. 761264, 2014.

[195] Меньщикова Е.Б., Ланкин В.З., Зенков Н.К. и др. Окислительный стресс. Прооксиданты и антиоксиданты. М.: Фирма «Слово», 2006.

[196] Moharram H.A. & Youssef M.M. Methods for Determining the Antioxidant Activity. In: A Review. Alex. J. Fd. Sci. & Technol., vol. 11, 1., pp. 31-42, 2014.

[197] Campbell Michel J.M. Transition metal complexes of thiosemicarbazide and thiosemicarbazones, Coordination Chemistry Reviews., vol. 15, issues 2–3, pp. 279-319, 1975.

[198] Fuior A., Cebotari D., Haouas M., Marrot J., Espallargas GM., Guérineau V, Touboul David, Rusnac V Roman, Gulea Aurelian, Floquet Sébastien. Synthesis, Structures, and Solution Studies of a New Class of [Mo2O2S2]-Based Thiosemicarbazone Coordination Complexes, ACS Omega., vol. 7, 19, pp. 16547–16560, 2022.

[199] Reszka KJ., Britigan BE., «Doxorubicin inhibits oxidation of 2,2'-azino-bis(3-ethylbenzothiazoline-6-sulfonate) (ABTS) by a lactoperoxidase/H(2)O(2) system by reacting with ABTS-derived radical.,» Arch Biochem Biophys, т. 466, № 2, pp. 164-71, 2007.

[200] Gille L., Nohl H., «Analyses of the molecular mechanism of adriamycin-induced cardiotoxicity.,» Free Radic Biol Med., т. 23, № 5, pp. 775-782, 1997.

[201] Anwar H. et al. Effect of protein, probiotic, and symbiotic supplementation on serum biological health markers of molted layers. In: Poultry Science., 91(10), pp. 2606-2613, 2012.

[202] Carocho M., Ferreira IC. A review on antioxidants, prooxidants and related controversy: Natural and synthetic compounds, screening and analysis methodologies and future perspectives. Food and Chemical Toxicology., vol. 51, pp. 15-25, 2013.

[203] Crane E. Bees and Beekeeping—Science, Practice and World Resources; Heinemann Newnes: Oxford, UK., pp. 614, 1990.

[204] Bogdanov S. Honey in medicine: A review. Bee Prod. Sci., pp. 28, 2017.

[205] Kieliszek M., Piwowarek K., Kot A.M., Błażejak S., Chlebowska-Śmigiel A., Wolska I. Pollen and bee bread as new health-oriented products. In: A review. Trends Food Sci. Tech., vol. 71, pp. 170–180, 2018.

[206] Kocot J., Kiełczykowska M., Luchowska-Kocot D., Kurzepa J., Musik I. Antioxidant potential of propolis, bee pollen, and royal jelly. In: Possible medical application. Oxid. Med. Cell. Longev., pp. 2, 7074209, 2018.

[207] Badolato M., Carullo G., Cione E., Aiello F., Caroleo M.C. From the hive: Honey, a novel weapon against cancer. Eur. J. Med. Chem., vol. 147, pp. 290–299, 2017.

[208] Di Marco G., Manfredini A., Leonardi D., Canuti L., Impei S., Gismondi A., Canini A. Geographical, botanical and chemical profile of monofloral Italian honeys as food quality guarantee and territory brand. Plant Biosyst., vol 151, pp. 450–463, 2016.

[209] Biluca F.C., de Gois J.S., Schulz M., Braghini F., Gonzaga L.V., Maltez H.F., Rodrigues E., Vitali L., Micke G.A., Borges D.L.G. et al., Phenolic

compounds, antioxidant capacity and bioaccessibility of minerals of stingless bee honey (Meliponinae). J. Food Comp. Anal., vol. 63. pp. 89–97, 2017.

[210] Beretta G., Orioli M., Maffei Facino R. Antioxidant and radical scavenging activity of honey in endothelial cell cultures (EA.hy926). Planta Med., vol. 73, pp. 1182–1189, 2007.

[211] Deng J., Liu R., Lu Q., Hao P., Xu A., Zhang J., Tan J. Biochemical properties, antibacterial and cellular antioxidant activities of buckwheat honey in comparison to manuka honey. Food Chem., vol. 252, pp. 243–249, 2018.

[212] Hazirah H., Yasmin Anum M.Y., Norwahidah A.K. Antioxidant properties of stingless bee honey and its effect on the viability of lymphoblastoid cell line. Med. Health., vol. 14, pp. 91–105, 2019.

[213] Nakajima Y., Tsuruma K., Shimazawa M., Mishima S., Hara H. Comparison of bee products based on assays of antioxidant capacities. BMC Complement. Altern. Med., vol. 26, pp. 1–9, 2009.

[214] Gülçin I. Antioxidants and antioxidant methods: An updated overview. Arch. Toxicol., vol. 94, pp. 651–715, 2020.

[215] Park M.J., Kim B.Y., Deng Y., Park H.G., Choi Y.S., Lee K.S., Jin B.R. Antioxidant capacity of major royal jelly proteins of honeybee (Apis mellifera) royal jelly. J. Asia. Pac. Entomol., vol. 23, pp. 445–448, 2020.

[216] Jin T.Y., Saravanakumar K., Wang M.H. In vitro and in vivo antioxidant properties of water and methanol extracts of linden bee pollen. Biocatal. Agric. Biotechnol., vol. 13, pp. 13, 2018.

[217] Prior R.L., Wu X.L., Schaich K. Standardized methods for the determination of antioxidant capacity and phenolics in foods and.

[218] BRODSCHNEIDER R., MOOSBECKHOFER R., CRAILSHEIM K. Surveys as a tool to record winter losses of honey bee colonies: a two year case study in Austria and South Tyrol. Journal of Apicultural Research., vol. 49, pp. 23-30, 2010.

[219] ANDY D J., BECKER A., WEGENER B. Coordination and integration of metabolism in insect flight. Comparative Biochemistry and Physiology., vol. 117B, pp. 497-512, 1997.

[220] CORONA M., ROBINSON G E. Genes of the antioxidant system of the honey bee: annotation and phylogeny. Insect Molecular Biology, vol. 15, pp. 687-701, 2006.

[221] COLVEN R M., PINNELL S R. Topical Vitamin C in aging. Clinical Dermatology., vol. 14, pp. 227-234, 1996.

[222] Prior Rl., Hoang H., et al. Assays for hydrophilic and lipophilic antioxidant capacity (oxygen radical absorbance capacity (ORAC(FL))) of plasma and

other biological and food samples. In: Agric Food Chem., vol. 51, № 11, pp. 3273-9, 2003.

[223] Khan I., Nisar M., Ebad F., Nadeem S., Saeed M., et al. Anti-inflammatory activities of Sieboldogenin from Smilax china Linn.: experimental and computational studies. In: Ethnopharmacol., № 121, pp. 175-7, 2009.

[224] Gulea A., Toderas I., Garbuz O., Ulchina I., Graur V., & Railean, N. Biological Evaluation of a Series of Amine-Containing Mixed-Ligand Copper(II) Coordination Compounds with 2-(2-hydroxybenzylidene)-N-(prop-2-en-1-yl)hydrazinecarbothioamide., Microscopy and Microanalysis., vol. 28(5), pp. 1696-1702, 2022.

[225] Garbuz Olga, Railean Nadejda, Gostev Igor, Rusnac Anna, Toderaş Ion, Gulea Aurelian. Evaluarea biologică a compuși lor coordinativi ai cuprului(II) cu unele tiosemicarbazone heterociclice. In: Studia Universitatis Moldaviae, vol 6(156), pp. 144-149, 2022.

[226] Graur Vasilii O., Chumakov Yurii, Garbuz Olga, Hureau Christelle, Tsapkov Victor I., Gulea Aurelian. Synthesis, Structure, and Biologic Activity of Some Copper, Nickel, Cobalt, and Zinc Complexes with 2-Formylpyridine N4-Allylthiosemicarbazone., Bioinorganic Chemistry and Applications., nr. 1, pp. 1-18, 2022.

[227] GARBUZ O. Activitatea antioxidantă a unor noi compuşi coordinativi bioactivi in vitro. Culegere de rezumate ştiinţifice. Conferinţa ştiinţifică anuală a colaboratorilor şi studenţilor. Chişinău, Moldova, 2015.

[228] Gulea A., Gudumac V., Garbuz O., Cebotari D., Spinu I., Pirvu O., Sardari V., Tagadiuc O., Gostev I., Spinu C., Scoferta P. Antiproliferative and antioxidant activity of nitrato-[4-(3,4-dimethylphenyl)-2-(2-oxo-3-methoxybenzylidene) hydrazinecarbothioamido]copper. International research journal., т. 2, № 68, pp. 19-22, 2018.

[229] Fuior Arcadie, Cebotari Diana, Garbuz Olga, Calancea Sergiu, Gulea Aurelian, Floquet Sebastian. Biological properties of a new class of [Mo2O2S2]-based thiosemicarbazone coordination complexes. In: Inorganica Chimica Acta., nr. 548, 2023.

[230] Rusnac A., Garbuz O., Shova S., Gulea A. Copper complexes with N4(2-ethyl benzoate) thiosemicarbazone of 2-acetylpyridine. In: Life sciences in the dialogue of generations: connections between universities, academia and business community, 2022, Chişinău. Chișinău, Republica Moldova: Moldova State University, pp. 223, 2022.

[231] Chumakov Yurii, Graur Vasilii O., Ulchina Ianina, Smaglii Vadim, Gulea Aurelian, Garbuz Olga, Tsapkov Victor I. -N-(prop-2-en-1-yl)-carbamohydrazonothioato(2-)](2,2′- bipyridine)copper hemihydrates. In: Journal of Structural Chemistry. nr. 6(63), pp. 905-913, 2022. Crystal structures of [N′-(2- oxidobenzylidene)-N-(prop-2-en-1-yl)-

carbamohydrazonothioato(2-)](1,10- phenanthroline)copper and [N′-(2-oxidobenzylidene)-N-(prop-2-en-1-yl)- carbamohydrazonothioato(2-)](2,2′-bipyridine)copper hemihydrates. .

[232] Ulchina Ianina, Graur Vasilii O., Tsapkov Victor I., Celac Marina, Garbuz Olga, Gulea Aurelian. Cu(II) complexes with 4-allylthiosemicarbazone as possible antioxidant agents, In: Life sciences in the dialogue of generations: connections between universities, academia and business community. R, 29-30 septembrie, 2022, Chişinău. Chișinău, Republica Moldova: Moldova State University, p. 227, 2022.

[233] Rusnac A., Garbuz O., Shova S., Gulea A. Synthesis, characterization, antioxidant activity evaluation of 3d metals complexes with N(4)-((3)-ethyl benzoate) thiosemicarbazones of 2-formyl(2-acetyl, 2-benzoil)pyridine. In: Studia Universitatis Moldaviae, Seria Ştiinţe Reale şi ale Naturii, nr. 6(156), pp. 150-158, 2022.

[234] Rusnac A., Țurcanu N., Burduniuc (Popa) O., Balan G., Garbuz O., Gulea Aurelian. Sinteza combinațiilor coordinative cu unele metale 3d în baza N(4)-(4-benzoat de etil) tiosemicarbazone ale derivaților aldehidei salicilice proprietăți antimicrobiene, antifungice și antioxidative. In: Studia Universitatis Moldaviae. Seria Ştiinţe Reale şi ale Naturii, nr. 6(146), pp. 141-148, 2021.

[235] Graur Vasilii O., Usataia Irina, Bourosh Pavlina, Kravtsov Victor, Garbuz Olga, Hureau Christelle, Gulea Aurelian. Synthesis, characterization, and biological activity of novel 3d metal coordination compounds with 2-acetylpyridine N4-allyl-S-, methylisothiosemicarbazone. In: Applied Organometallic Chemistry., nr. 4(35), 2021.

[236] Gulea Aurelian, Gudumac Valentin, Garbuz Olga, Andronache Lilia. In vitro antiproliferative activity and antioxidant capacity of new organometallic coordination compounds, results correlation analysis, In: Buletinul Academiei de Ştiinţe a Moldovei. Ştiinţele vieţii., nr. 3(330), pp. 65-72, 2021.

[237] Rusnac Anna, Rusnac Roman, Garbuz Olga, Barbă Nicanor. Gulea Aurelian. Sinteza și studiul proprietăților antioxidative ale unor noi derivați ai benzoxazolilor. In: Studia Universitatis Moldaviae. Seria Ştiinţe Reale şi ale Naturii., nr. 1(111), pp. 133-143, 2018.

[238] Ulchina Ianina, Graur Vasilii O., Tsapkov Victor I., Chumakov Yurii, Garbuz Olga, Burduniuc (Popa) Olga., Ceban Emil., Gulea Aurelian. Introducing N-Heteroaromatic Bases into Copper(II) Thiosemicarbazon Complexes:, A Way to Change their Biological Activity. In: ChemistryOpen., nr. 12(11), pp. 1-7, 2018.

[239] Fuior Arcadie, Hijazi Akram, Garbuz Olga, Bulimaga Valentina, Zosim Liliana, Cebotari Diana, Haouas Mohamed, Toderash Ion, Gulea Aurelian, Floquet Sebastian. Screening of biological properties of MoV 2O2S2- and

MoV 2O4-based coordination complexes: Investigation of antibacterial, antifungal, antioxidative and antitumoral activities versus growing of Spirulina platensis biomass. In: Journal of Inorganic Biochemistry., nr. 226, 2022.

[240] Gulea Aurelian, Graur Vasilii O., Ulchina Ianina, Bourosh Pavlina, Smaglii Vadim, Garbuz Olga, Tsapkov Victor I. Synthesis, Structure, and Biological Activity of Mixed-Ligand Amine-Containing Copper(II) Coordination Compounds with 2-(2-, Hydroxybenzylidene)-N-(prop-2-en-1-yl)hydrazinecarbothioamide. In: Russian Journal of General Chemistry., nr. 1(91), pp. 98-107, 2021.

[241] Gulea Aurelian, Graur Vasilii O., Chumakov Yurii, Petrenko Peter A., Garbuz Olga, Tsapkov Victor I., Gudumac Valentin. Nickel(II) Complexes with Pentane-2,4-dione Bis(4-allylthiosemicarbazone). In: Russian Journal of General Chemistry., nr. 1(90), pp. 111-117, 2020.

[242] Bîrcă Maria, Cotovaia Aliona, Ţapcov Victor, Garbuz Olga, Crudu Valeriu, Gulea Aurelian. Sinteza, proprietăţile fizico-chimice, antioxidative și antituberculoase ale compușilor coordinativi ai unor metale 3d cu izonicotinoilhidrazona 2-hidroxi-3-, metoxibenzaldehida. In: Studia Universitatis Moldaviae. Seria Ştiinţe Reale şi ale Naturii., nr. 6(136), pp. 119-126, 2020.

[243] Graur Vasilii O., Garbuz Olga, Zariciuc Elena, Gudumac Valentin, Gulea Aurelian. Synthesis and biological activity of 2-formylpyridine n(4)-allyl-3-seleno-semicarbazone and its copper coordination compound, In: Buletinul Academiei de Ştiinţe a Moldovei. Ştiinţele vieţii., nr. 3(327), pp. 135-142, 2015.

[244] Rusnac Anna, Rusnac Roman, Garbuz Olga, Barbă Nicanor, Gulea Aurelian. Sinteza și cercetarea proprietăților biologice ale unor derivați ai 4-amino-5-metil-4h-1,2,4-triazolului-3-tiol, In: Studia Universitatis Moldaviae. Seria Ştiinţe Reale şi ale Naturii., nr. 6(96), pp. 195-203, 2016.

[245] Erhan Tatiana, Garbuz Olga, Gulea Aurelian. Sinteza și studiul unor N'-(N-dimetilfenil)-N,N-dimetiltiourei și N(4)-N-dimetilfenil-tiosemicarbazide. In: Studia Universitatis Moldaviae. Seria Ştiinţe Reale şi ale Naturii., nr. 1(101), pp. 89-95, 2017.

[246] Usataia Irina, Graur Vasilii O., Zariciuc Elena, Garbuz Olga, Gulea Aurelian. Synthesis and biological activity of copper(II), nickel(II) and cobalt(III) coordination compounds with 2-benzoylpyridine N(4)-allyl-S-methylisothiosemicarbazone, In: Buletinul Academiei de Ştiinţe a Moldovei. Ştiinţele vieţii., nr. 2(335), pp. 103-112, 2018.

[247] Rusnac R., Garbuz O., Barbă N., Gulea A., Balan G., Bruduniuc O. Sinteza unor derivați ai 1,2,4-triazolului în baza n-[4-(3-metil-5-sulfanil-4h-1,2,4-

triazol-4-il)fenil]acetamidei. In: Studia Universitatis Moldaviae, Seria Ştiinţe Reale şi ale Naturii., nr. 1(111), pp. 133-143, 2018.

[248] Ştîrba O., Garbuz O., Sardari V., Gudumac V. Metoda de determinare a capacității antioxidante în probele biologice. Certificat de inovator., nr. 5389. 2014.

[249] Garbuz O., Gulea A., Dyniewicz J., Zablocka B., Lipkowski AW. «The non-opioid receptor, antioxidant properties of morphine and the opioid peptide analog biphalin,» Peptides, т. 63, pp. 1-3, 2015.

[250] Chatterjee K., Zhang J., Honbo N., Karliner JS. Doxorubicin cardiomyopathy. Cardiology, т. 115, № 2, pp. 155-62, 2010.

[251] Gulea A., Gudumac V., Garbuz O., Andronache L. «In vitro antiproliferative activity and antioxidant capacity of new organometallic coordination compounds, rezults correlation analysis.,» Buletinul AȘM. Științele vieții., т. 3, № 330, pp. 65-72, 2016.

[252] Toderaş I., Gulea A., Roşcov E., Garbuz O. Influenţa substanţelor coordinative metaloorganice asupra viabilității populaţiei de Paramecium caudatum. Buletinul AŞM. Ştiinţele vieţii., т. 3, № 330, pp. 109-115, 2016.

[253] Brevet de invenție. 4644 C1, MD, C07F 11/00 . Ansamblu supramolecular (NMe4)(C42 H70O35)[Mo10 O10 S10 (OH)11 (H2O)4]·27H2O care manifestă activitate antioxidantă /, Arcadie Fuior, Sébastien Floquet, Emmanuel Cadot, Olga Garbuz, Victor Ţapcov, Ion Toderaş, Aurelian Gulea. Cererea depusă 22.03.2018, BOPI nr. 8/2019..

[254] Garbuz O., Graur V., Tagadiuc O., Andronache L., Sardari V., Gulea A., Gudumac V. In vitro antiproliferative potential and antioxidant capacity of new coordination compounds. International research journal., т. 5, № 59, pp. 122-125, 2017.

[255] Re R., Pellegrini N., Proteggente A., Pannala A., Yang M., Rice-Evans C. Antioxidant activity applying an improved ABTS radical cation decolorization assay. Free Radic Biol Med., т. 26, № 9-10, pp. 1231-7, 1999.

[256] Jian-Ming Lü Peter H. Lin Qizhi Yao Changyi Chen, «Chemical and molecular mechanisms of antioxidants: experimental approaches and model systems,» Journal of Cellular and Molecular Medicine, т. 14, № 4, pp. 840-860, 2010.

[257] Fuior Arcadie, Cebotari Diana, Garbuz Olga., Calancea Sergiu, Gulea Aurelian, Floquet Sebastian. Biological properties of a new class of [Mo2O2S2]-based thiosemicarbazone coordination complexes. In: Inorganica Chimica Acta., nr. 548, 2023.

[258] Fuior Arcadie, Hijazi Akram, Garbuz Olga, Bulimaga Valentina, Zosim Liliana, Cebotari Diana, Haouas Mohamed, Toderash Ion, Gulea Aurelian, Floquet Sebastian. Screening of biological properties of MoV 2O2S2- and

MoV 2O4-based coordination complex, Investigation of antibacterial, antifungal, antioxidative and antitumoral activities versus growing of Spirulina platensis biomass. In: Journal of Inorganic Biochemistry., nr. 226, 2022.

[259] Graur Vasilii O., Usataia Irina, Bourosh Pavlina, Kravtsov Victor, Garbuz Olga, Hureau Christelle, Gulea Aurelian. Synthesis, characterization, and biological activity of novel 3d metal coordination compounds with 2-acetylpyridine N4-allyl-S-, acetylpyridine N4-allyl-S-methylisothiosemicarbazone. In: Applied Organometallic Chemistry., nr. 4(35), p. 0, 2021.

[260] Graur Vasilii O., Chumakov Yurii, Garbuz Olga, Hureau Christelle, Tsapkov Victor I., Gulea Aurelian. Synthesis, Structure, and Biologic Activity of Some Copper, Nickel, Cobalt, and Zinc Complexes with 2-Formylpyridine N4-Allylthiosemicarbazone., Bioinorganic Chemistry and Applications., nr. 1, pp. 1-18, 2022.

[261] Gulea Aurelian, Md., Ţapcov Victor, Md., Cebotari Diana, Md., Guţu Tatiana, Md., Istrati Dorin, Md., Gudumac Valentin, Md. [4-(2,4-Dimethylphenyl)-2-(2-hydroxy-3-methoxybenzylidene)hydrazinecarbothioamide-S][4-(2,4-dimethylphenyl)-2-, (oxo-3-methoxybenzylidene)hydrazinecarbothioamido(2-)-O,N,S]-nickel(II) monoethanol solvate as an antioxidant. 2019.06.30, BOPI nr. 6/2019.

[262] Gulea Aurelian, Md., Usataia Irina, Md., Garbuz Olga, Md., Graur Vasilii, Md., Ţapcov Victor, Md., Gudumac Valentin, Md. Use of salicylidene-4-allyl-S-methylisothiosemicarbazidates of iron(III) and cobalt(III) as antioxidants. 2017.11.30, BOPI nr. 11/2017.

[263] Gulea Aurelian, Md., Gudumac Valentin, Md., Garbuz Olga, Md., Ţapcov Victor, Md., Pahonţu Elena-Mihaela, Ro. Use of di(μ-S)-bis{(4-aminobenzenesulphamide)-chloro-[2-picolidene-4-phenylthiosemicarbazidato-(1-)]-copper(II)} as an antioxidant. 2017.03.31,, BOPI nr. 3/2017.

[264] Gulea Aurelian, Md., Gudumac Valentin, Md., Istrati Dorin, Md., Usataia Irina, Md; Graur Vasilii, Md; Ţapcov Victor, Md; Şveţ Inna, Md; Pantea Valeriana, Md. Catena-(μ-nitrato-O,O'-O''-{methyl-N-(prop-2-en-1-yl)-2-[1-(pyridine-2- yl), ethylidene]hydrazinecarbimidothioate}copper(II) nitrate compound as superoxide radical inhibitors. 2020.05.31, BOPI nr. 5/2020.

[265] Gulea Aurelian, Md., Gudumac Valentin, Md., Ţapcov Victor, Md., Pantea Valeriana, Md., Graur Vasilii, Md., Andronache Lilia, Md., Şveţ Inna, Md., Botnaru Maria, Md. Copper coordination compounds with 4-allylthiosemicarbazones of substituted 3-(phenyl)-1-, (pyridin-2-yl)prop-2-en-1-ones as inhibitors of superoxide radicals. 2021.05.31, BOPI nr. 5/2021.

[266] Gulea Aurelian, Md., Gudumac Valentin, Md., Istrati Dorin, Md., Graur Vasilii, Md., Ţapcov Victor, Md., Pantea Valeriana, Md., Andronache Lilia, Md., Şveţ Inna, Md. Use of coordination compounds of copper(II) salts with 2-(2- hydroxybenzylidene)-N-, (prop-2-en-1-yl)-hydrazinecarbothioamide as inhibitors of superoxide radicals. 2021.03.31, BOPI nr. 3/2021.

[267] Rioux N., Castonguay A., «Inhibitors of lipoxygenase: a new class of cancer chemopreventive agents,» Carcinogenesis, № 19, p. 1393–400, 1998.

[268] Kuhn H., Thiele B.J., 1999. The diversity of the lipoxygenase family. Many sequence data but little information on biological significance. FEBS Lett 449, 7-11.

[269] Berger M., Schwarz K., Thiele H., Reimann,. I., Huth A., Borngräber S., Kühn H., Thiele B.-J. Simultaneous expression of leukocyte-type 12-lipoxygenase and reticulocyte-type15-lipoxygenase in rabbits. Molecular Biology 278, pp. 935-948, 1998.

[270] Geisbert T.W., Hensley L.E., Gibb T.R., Steele K.E., Jaax N.K., Jahrling P.B. Apoptosis induced in vitro and in vivo during infection by Ebola and Marburg viruses. Lab Invest 80, pp.171-186, 2000.

[271] Hangauer M.J., Viswanathan V.S., Ryan M.J., Bole D., Eaton J.K., Matov A., Galeas J., Dhruv H.D., Berens M.E., Schreiber S.L., McCormick F., McManus M.T. Drug-tolerantpersister cancer cells are vulnerable to GPX4 inhibition. Nature 551, 247-250, 2000.

[272] Seiler A., Schneider M., Forster H., Roth S., Wirth E.K., Culmsee C., Plesnila N., Kremmer E., Radmark O., Wurst W., Bornkamm G.W., Schweizer U., Conrad M. Glutathione peroxidase 4 senses and translates oxidative stress into 12/15-lipoxygenase dependent- and AIF-mediated cell death. Cell Metab 8, 237-248, 2008.

[273] Song L., Yang H., Wang H.X., Tian C., Liu Y., Zeng X.J., Gao E., Kang Y.M., Du J., Li H.H. Inhibition of 12/15 lipoxygenase by baicalein reduces myocardial ischemia/reperfusion injury via modulation of multiple signaling pathways., Apoptosis 19, 567-580, 2014.

[274] Muhammad Nisar, Waqar Ahmad Kaleem,Inamullah Khan et al. Molecular simulations probing Kushecarpin A as a new lipoxygenase inhibitor. Fitoterapia., № 82, pp. 1008-11, 2011.

[275] Qiu-Qi Li, Qin Li, Ji-Ning Jia, Zhao-Qian Liu, Hong-Hao Zhou, Xiao-Yuan Mao, 12/15 lipoxygenase: A crucial enzyme in diverse types of cell death, Neurochemistry International,V., № 118, pp. 34-41, 2018.

[276] Ştîrba O., Andronache L., Garbuz O. Metodă de determinare a activității lipoxigenazei. Certificat de inovator nr. 5319. 2014.

[277] PERUTZ MF., ROSSMANN MG., CULLIS AF., MUIRHEAD H., WILL G., NORTH AC. Structure of haemoglobin: a three-dimensional Fourier

synthesis at 5.5-A. resolution, obtained by X-ray analysis. Nature, т. 185, № 4711, pp. 416-22, 1960.

[278] Pantea V.,Tagadiuc O., Andronache L., Ştîrba O., Garbuz O., Gudumac V. Procedeu de dozare a niveluluide oxihemoglabina methemoglobina si sulfohemoglobina in aceiasi proba nr.5465. 2015.

[279] El-Husseini A., Azarov N. Is threshold for treatment of methemoglobinemia the same for all? A case report and literature review. Am J Emerg Med, т. 28, № 6, pp. 748.e5-748.e10, 2010.

[280] Chen J., Odenike O., Rowley JD. Leukaemogenesis: more than mutant genes. Nat Rev Cancer. 2010 Jan;10(1), pp. 23-36, 2010.

[281] Patricia Quach, Elaine Gutierrez, Maram Talal Basha, Danuta S. Kalinowski, Philip C. Iron Metabolism and Chelation Program, Department of Pathology and Bosch Institute,University of Sydney, Sydney, New South Wales, Australia, , 2006.

[282] GARBUZ O., SPINU I., PIRVU O., PINZARU I., APOSTOL M., GUDUMAC V., GULEA A., Anticancer, antioxidant and toxicity activities of new compounds along with their ability to include hemolysis and methemoglobin formation in human RBCs. 4th French-Romanian Colloquium on Medicinal Chemistry, Iasi, Romania., 2017.

[283] Yen Y., Margolin K., Doroshow J., Fishman M., Johnson B., Clairmont C., Sullivan D., Sznol M. A phase I trial of 3-aminopyridine-2-carboxaldehyde thiosemicarbazone in combination with gemcitabine for patients with advanced cancer., т. 54, № 4, pp. 331-42, Cancer Chemother Pharmacol. 2004.

[284] Andronache L., Garbuz O., Sardari V.,Svet I. . Procedeu de determinare a capacitatii de inducere a hemolizei nr.5464., 2015.

[285] Fuior A., Hijazi A., Garbuz O., Bulimaga V., Zosim L., Cebotari D., Haouas M., Toderas I., Gulea A., Floquet S. Screening of biological properties of MoV2O2S2- and MoV2O4-based coordination complexes : Investigation of antibacterial, antifungal,, antioxidative and antitumoral activities versus growing of Spirulina platensis biomass. J. of Inorganic Biochemistry., 226, 2022.

[286] Kocot J., Kiełczykowska M., Luchowska-Kocot D., Kurzepa J., Musik I. Antioxidant potential of propolis, bee pollen, and royal jelly: Possible medical application. Oxid. Med. Cell. Longev, 2. 2018.

[287] Borycka K., Grabek-Lejko D., Kasprzyk I. Antioxidant and antibacterial properties of commercial bee pollen products. J. Apic. Res., 54, 491–502, 2015.

[288] Kaškoniene V… Antimicrobial and antioxidant activities of natural and ˙, fermented bee pollen. Food Biosci, 34, 100532, 2020.

[289] Atsalakis E., Chinou I., Makropoulou M., Karabournioti S., Graikou K. Evaluation of phenolic compounds in Cistus creticus bee pollen from Greece. Antioxidant and antimicrobial properties. Nat. Prod. Comm., 12, 1813–1816, 2017.

[290] Pavel C.I., Mărghita L.A., Dezmirean D.S., Tomos L.I., Bonta V., ¸Sapcaliu A., Buttstedt A. Comparison between local and commercial royal jelly—Use of antioxidant activity and 10-hydroxy-2-decenoic acid as quality parameter. J. Apic. Res., 53. 116-123, 2014.

[291] Ramanathan A.N.K.G., Nair A.J., Sugunan V.S. A review on royal jelly proteins and peptides. J. Func. Foods, 44, 255–264, 2018.

[292] Mracevi´c S.Đ., Krsti´c M., Loli´c A., Raži´c S. Comparative study of the chemical composition and biological potential of honey from different regions of Serbia. Microchem. J., 152, 104420, 2020.

[293] Ramirez L., Negri P., Sturla L., et al. Abscisic acid enhances cold tolerance in honeybee larvae. Proc. R. Soc. B Biol. Sci. 284:20162140, 2017.

[294] Corona M., Robinson GE. Genes of the antioxidant system of the honey bee: Annotation and phylogeny.Insect Mol. Biol. 15, pp. 687–701, 2006.

[295] Farjan M., Dmitryjuk M., Lipiński Z., et al., Supplementation of the honey bee diet with vitamin C: The effect on the antioxidative system of Apismelliferacarnica brood at different stages. Journal of Apicultural Research,. 51:3, pp. 263-270, 2012.

[296] Candy D J., Becker A., Wegener B. Coordination and integration of metabolism in insect flight. Comparative Biochemistry and Physiology., 117B, pp. 497-512, 1997.

[297] Birk J., Meyer M., Aller I., Hansen HG., Odermatt A., Dick TP., Meyer AJ., Appenzeller-Herzog C. Endoplasmic reticulum: reduced and oxidized glutathione revisited. J Cell Sci. 126:1604–17, 2013.

[298] Brodschneider R, Brus J, Danihlík J. Comparison of apiculture and winter mortality of honey bee colonies (Apis mellifera) in Austria and Czechia. Agric Ecosyst Environ 274, pp. 24–32, 2019.

[299] Morawetz L., Köglberger H., Griesbacher A., Derakhshifar I., Crailsheim K., Brodschneider R. et al Health status of honey bee colonies (Apis mellifera) and disease-related risk factors for colony losses in Austria. PLoS ONE 14(7):e0219293, 2019.

[300] Dietemann V., Nazzi F,, Martin SJ., Anderson DL., Locke B., Delaplane KS et al Standard methods for Varroa research. J Apic Res 52:1–54, 2013.

[301] Thompson CE., Biesmeijer JC., Allnutt TR., Pietravalle S., Budge GE Parasite pressures on feral honey bees (Apis mellifera sp.). PLoS ONE 9:e105164, 2014.

[302] Duncan J. Clarke, Guillaume Mondesert, Marisa Segal, Bonnie L. Bertolaet, Sanne Jensen, Meira Wolff, Martha Henze, Steven I. Reed. Dosage Suppressors of pds1 Implicate Ubiquitin-Associated Domains in Checkpoint Control. 1997-2007.2001.

[303] Maeva A. Techer, Rahul V. Rane. Divergent evolutionary trajectories following speciation in two ectoparasitic honey bee mites. Communications Biology volume 2, Article number: 357, 2019.

[304] Ziegelmann B., Abele E., Hannus S. et al. Lithium chloride effectively kills the honey bee parasite Varroa destructor by a systemic mode of action. Sci Rep 8, 683, 2018.

[305] Dietemann V., Nazzi F., Martin SJ., Anderson DL., Locke B., Delaplane KS et al Standard methods for Varroa research. J Apic Res 52:1–54, 2013.

[306] Gregorc A., Adamczyk J., Kapun S., Planinc I Integrated Varroa control in honey bee (Apis mellifera carnica) colonies with or without brood. J Apic Res 55:253–258, 2016.

[307] Meikle WG., Sammataro D., Neumann P., Pfugfelder J Challenges for developing pathogen-based biopesticides against Varroa. Apidologie 43:501–514, 2012.

[308] Dietemann V., Pfugfelder J., Anderson D., Charriere JD., Chejanovsky N., Dainat B et. al Varroa destructor: research avenues towards sustainable control. J Apic Res 51:125–132, 2012.

[309] Rosenkranz P., Aumeier P., Ziegelmann B Biology and control of Varroa destructor. J Insect Pathol 103:S96–S119, 2010.

[310] Jack C.J., Dai PL., van Santen, E. et al. Comparing four methods of rearing Varroa destructor in vitro. Exp Appl Acarol 80, 463–476, 2020.

[311] Joseph M. Culp, Donald J. Baird, Establishing Cause-Effect Relationships in Multi-Stressor Environments, Methods in Stream Ecology (Second Edition), Academic Press, pp. 835-854, 2007.

[312] Gulea A., Graur V., Ulchina Ia., Bourosh P., Smaglii V., Garbuz O., Tsapkov V. Synthesis, Structure, and Biological Activity of Mixed-Ligand Amine-Containing Copper(II) Coordination Compounds with 2-(2-Hydroxybenzylidene)-N-(prop-2-en-1-yl), hydrazinecarbothioamide. Russian Journal of General Chemistry, 91 (1), pp. 98–107, 2021.

[313] Graur V., Chumakov Y., Garbuz O., Hureau C., Tsapkov V., GuleaA. Synthesis, Structure, and Biologic Activity of Some Copper, Nickel, Cobalt, and Zinc Complexes with 2-Formylpyridine N4-Allylthiosemicarbazone. Bioinorganic Chemistry and Applications, 2022. https://doi.org/10.1155/2022/2705332.

[314] Garbuz O., Toderas I., Railean N., Tapcov V., & Gulea A. Some inorganic and organic biological agents. Studia universitatis moldaviae. Științe Reale și ale Naturii 6(146), pp. 132–140, 2021.

Annexe

Annexe 1. The influence of the most active tested ligands on $ABTS^{\bullet+}$.

№	Formula	$IC_{50} \pm SD$ (μM)
1	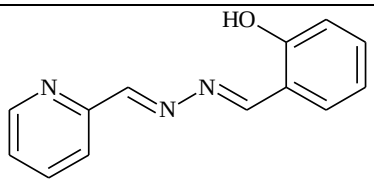	21.0 ± 0.4
2	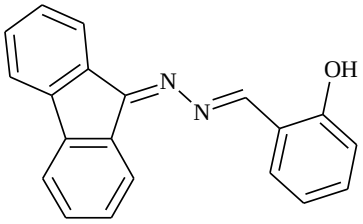	27.9 ± 0.9
3	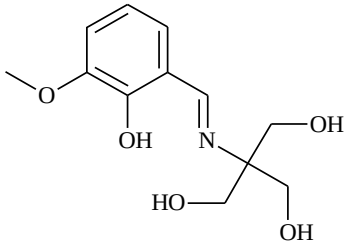 L^1	17.2 ± 0.2
4	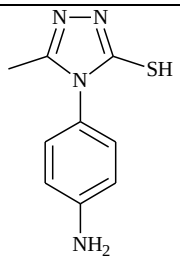	14.1 ± 0.2
5	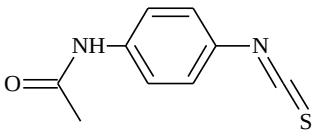	19.2 ± 1.1
6	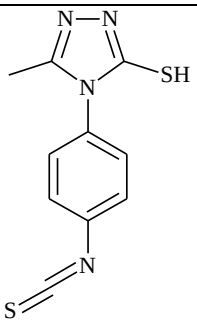	14.1 ± 0.2

Annexe 1. Continued

№	Formula	$IC_{50} \pm SD$ (μM)
7	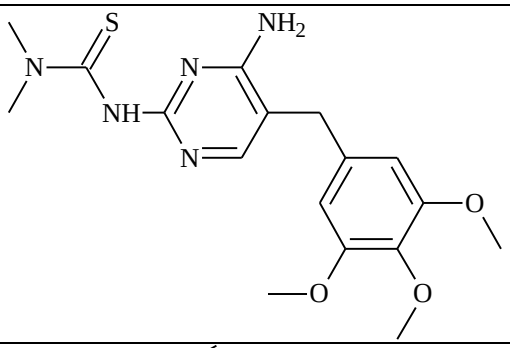	3.2 ± 0.3
8	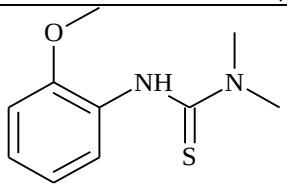	19.5 ± 0.2
9	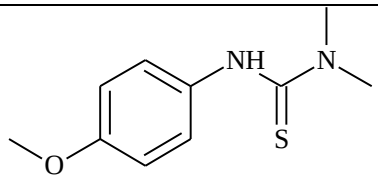	18.3 ± 1.1
10	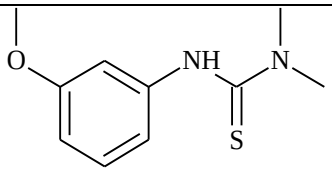	24.6 ± 0.3
11	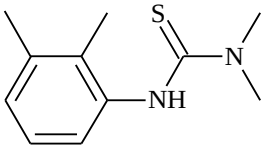	17.1 ± 0.1
12	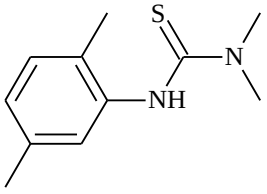	26.9 ± 0.1
13	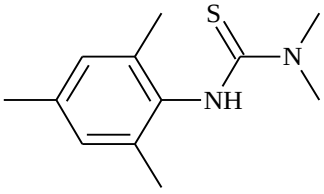	12.2 ± 0.2

Annexe 1. Continued

№	Formula	$IC_{50} \pm SD$ (μM)
14	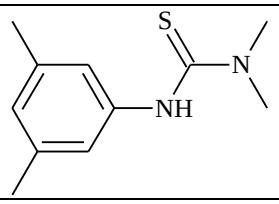	20.3 ± 0.8
15	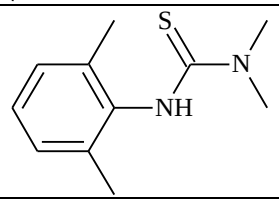	17.8 ± 0.4
16	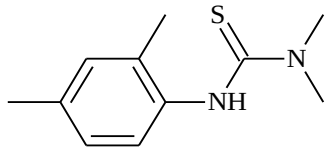	19.0 ± 0.3
17	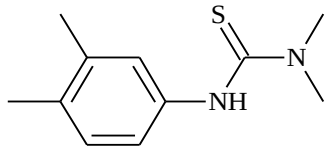	19.3 ± 1.0
18	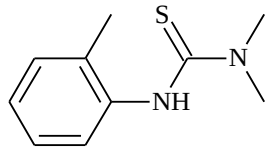	15.0 ± 0.1
19	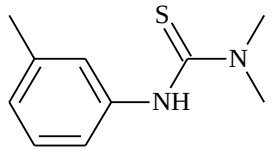	21.8 ± 0.8
20	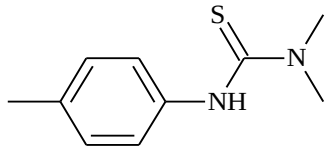	17.3 ± 0.5
21	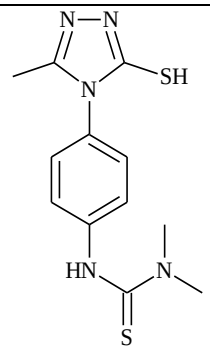	13.6 ± 0.3

Annexe 1. Continued

№	Formula	$IC_{50} \pm SD$ (μM)
22	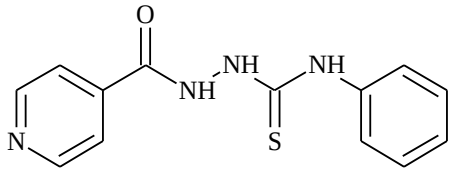	7.8 ± 0.6
23	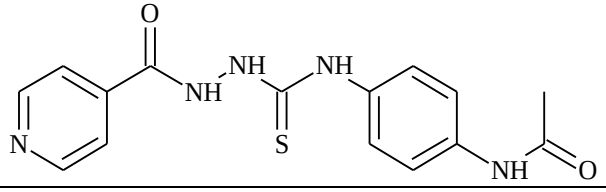	11.0 ± 0.3
24	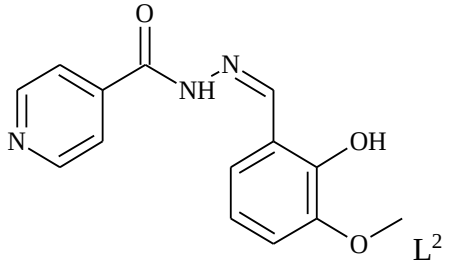 L^2	11.0 ± 0.7
25	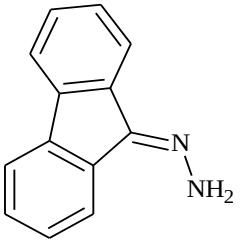	22.3 ± 0.4
26	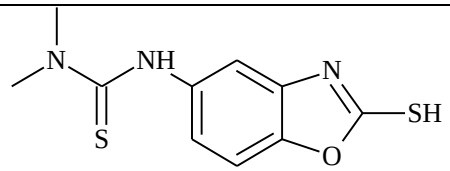	13.8 ± 0.7
27	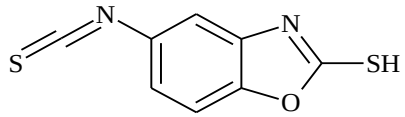	23.5 ± 0.1
28	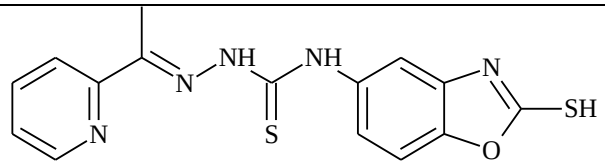	17.1 ± 0.7
29	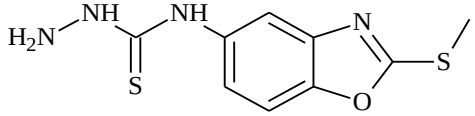	13.5 ± 0.5

Annexe 1. Continued

№	Formula	$IC_{50} \pm SD$ (μM)
30	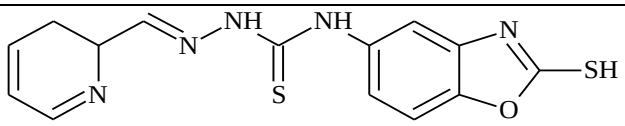	16.9 ± 0.6
31	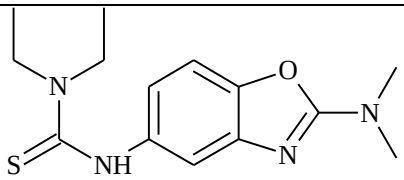	23.8 ± 0.7
32	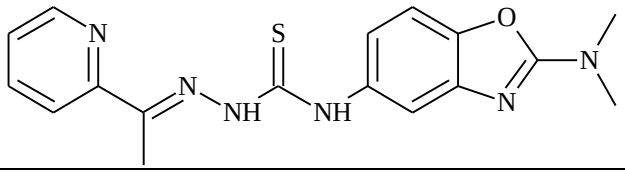	20.1 ± 0.9
33	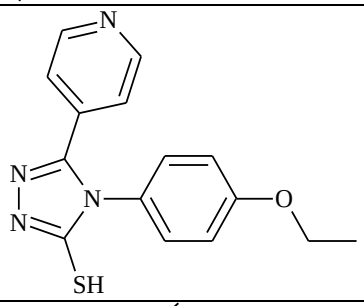	16.4 ± 0.2
34	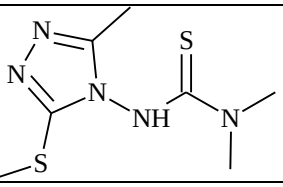	9.6 ± 0.2
35	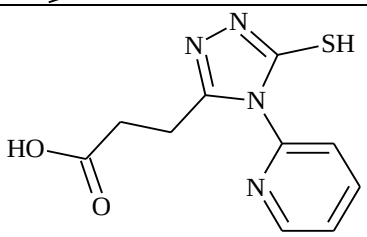	10.3 ± 0.1
36	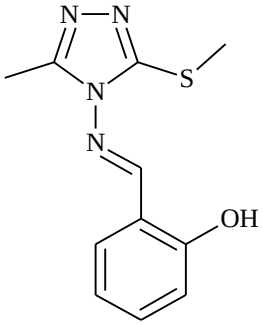	25.6 ± 0.6

Annexe 1. Continued

№	Formula	$IC_{50} \pm SD$ (μM)
37	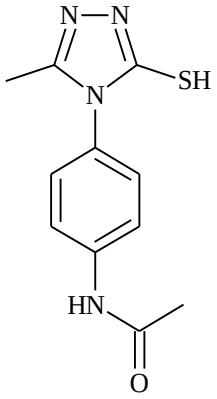	17.4 ± 0.5
38	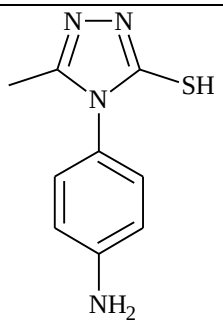	14.1 ± 0.1
39	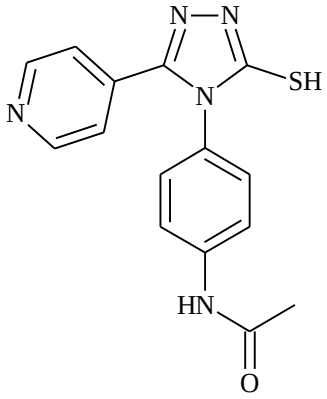	11.5 ± 0.5
40	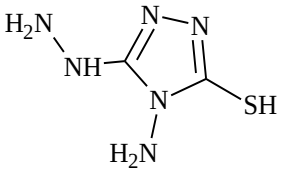	7.6 ± 0.3
41	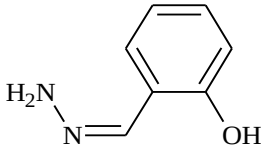	8.6 ± 0.3

Annexe 1. Continued

№	Formula	$IC_{50} \pm SD$ (μM)
42	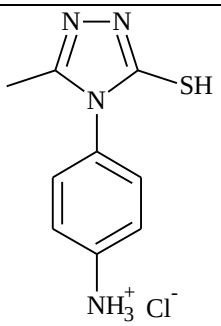	19.0 ± 0.6
43	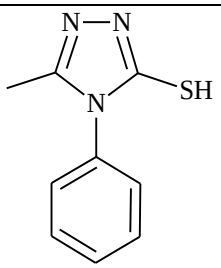	12.3 ± 0.2
44	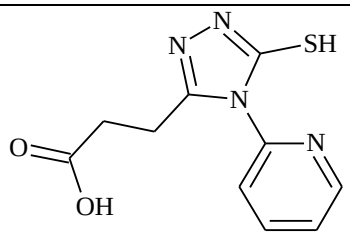	10.3 ± 0.1
45	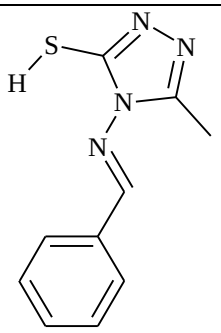	9.3 ± 0.5
46	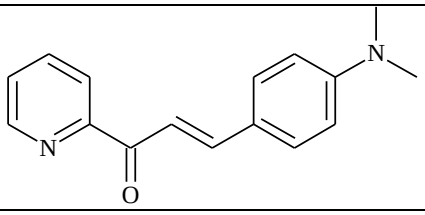	9.3 ± 0.8
47	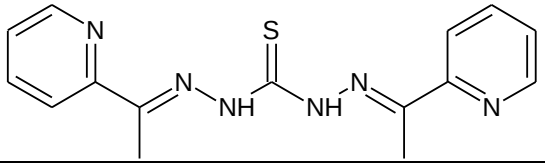	7.1 ± 0.1

Annexe 1. Continued

№	Formula	$IC_{50} \pm SD$ (μM)
48	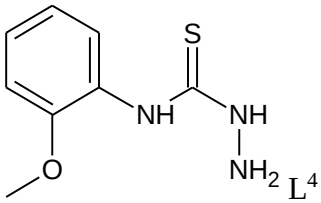 L^4	6.3 ± 0.1
49	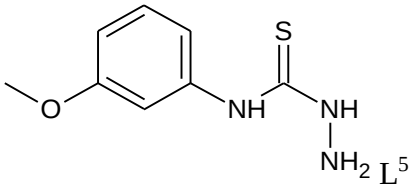 L^5	6.2 ± 0.4
50	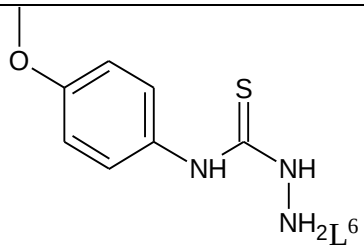 L^6	2.2 ± 0.2
51	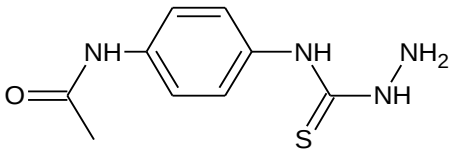	15.3 ± 0.6
52	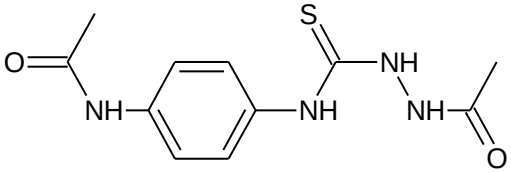	10.3 ± 0.8
53	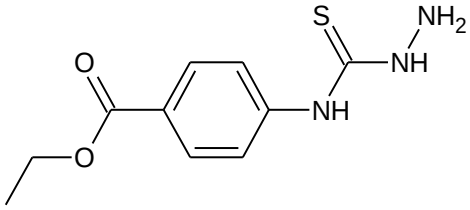	11.5 ± 0.6
54	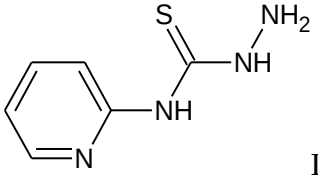 L^7	8.6 ± 0.9

Annexe 1. Continued

№	Formula	$IC_{50} \pm SD$ (μM)
55	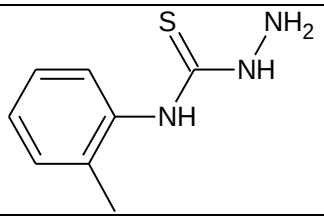	16.2 ± 0.1
56	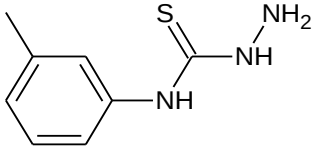	13.2 ± 0.2
57	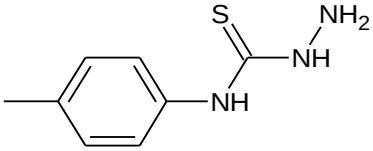	18.1 ± 0.6
58	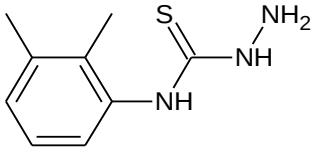	14.5 ± 0.1
59	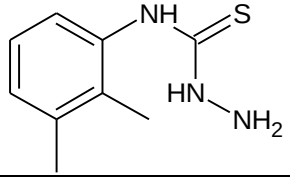	6.9 ± 0.9
60	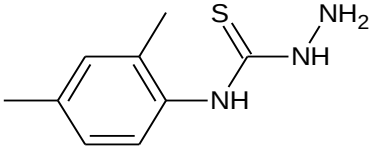	15.3 ± 0.8
61	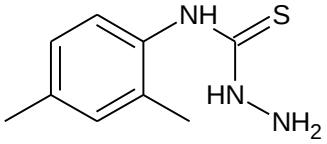	3.9 ± 0.1
62	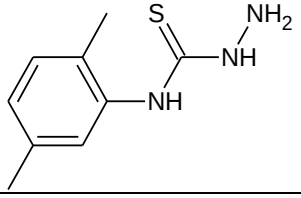	6.9 ± 0.2
63	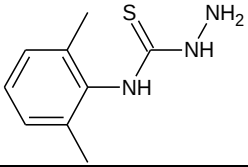	15.5 ± 0.2

Annexe 1. Continued

№	Formula	$IC_{50} \pm SD$ (μM)
64	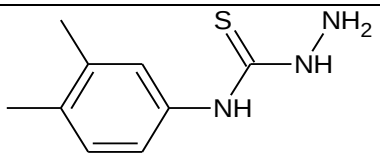	13.6 ± 0.5
65	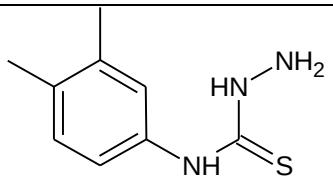	5.5 ± 0.1
66	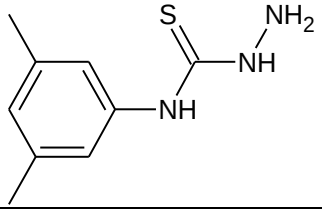	14.2 ± 0.2
67	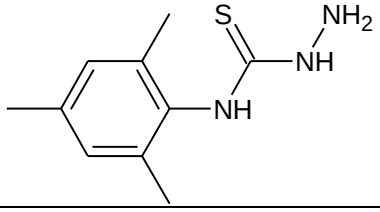	14.4 ± 1.3
68	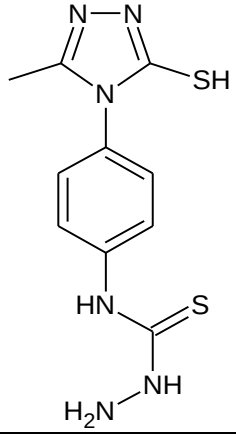	7.1 ± 0.1
69	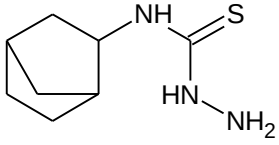	13.6 ± 0.5
70	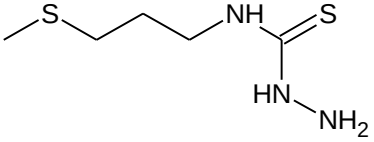	16.8 ± 0.6

Annexe 1. Continued

№	Formula	$IC_{50} \pm SD$ (μM)
71	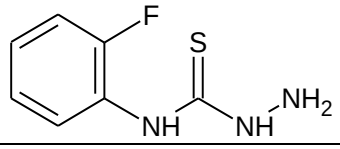	18.7 ± 0.9
72	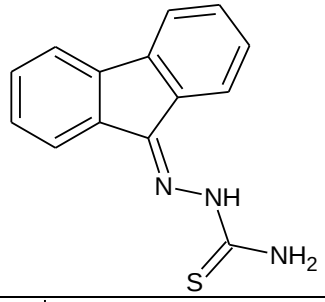	18.4 ± 0.7
73	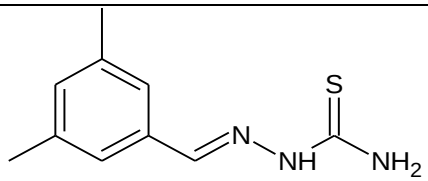	21.6 ± 0.3
74	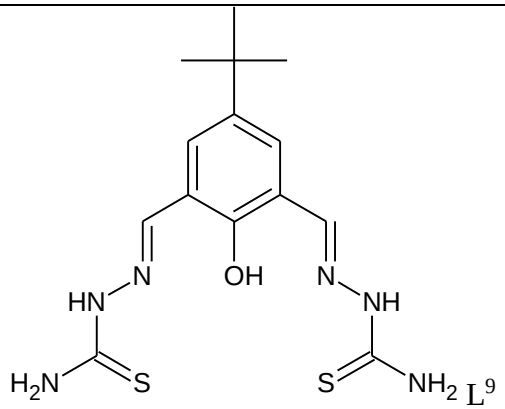	20.3 ± 1.6
75	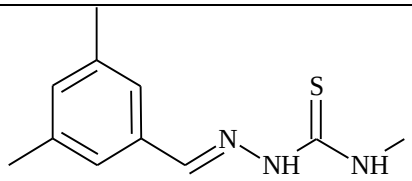	27.8 ± 0.3
76	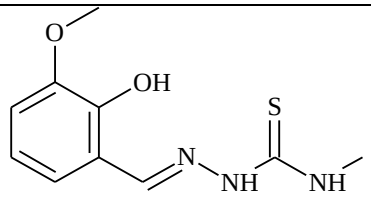	7.7 ± 0.1
77	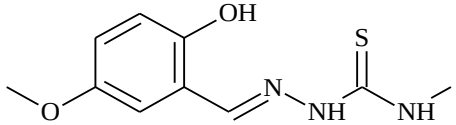	9.8 ± 0.1

Annexe 1. Continued

№	Formula	$IC_{50} \pm SD$ (μM)
78	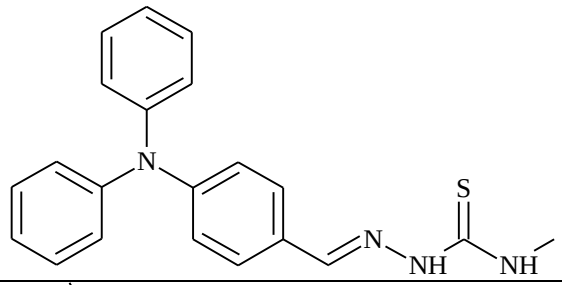	21.2 ± 0.4
79	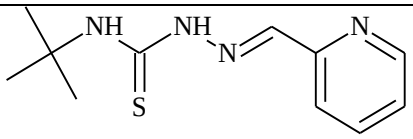 L^{11}	18.5 ± 0.2
80	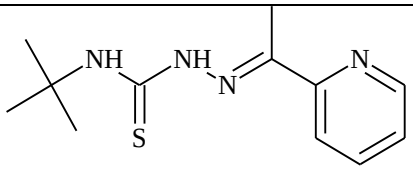 L^{12}	12.5 ± 0.1
81	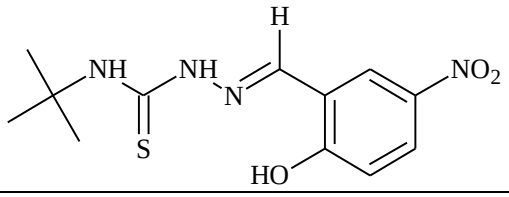	9.6 ± 0.1
82	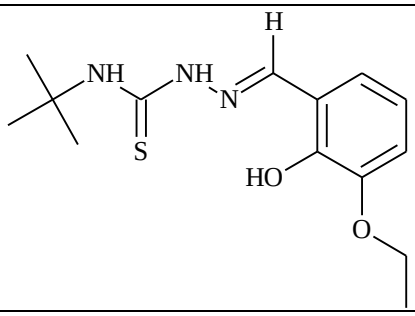	5.6 ± 0.1
83	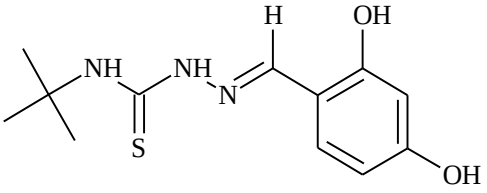	5.2 ± 0.1
84	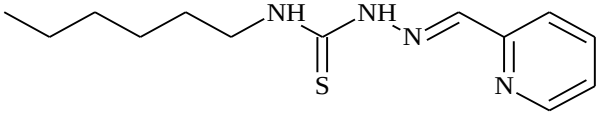 L^{14}	15.6 ± 0.3

Annexe 1. Continued

№	Formula	$IC_{50} \pm SD$ (μM)
85	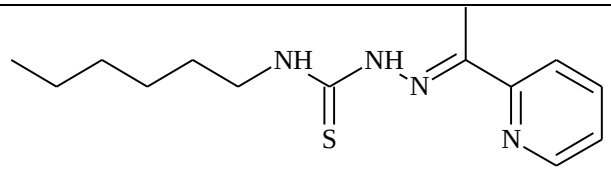 L[15]	10.2 ± 0.6
86	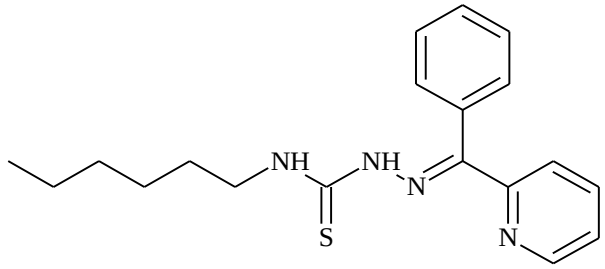 L[16]	23.3 ± 0.4
87	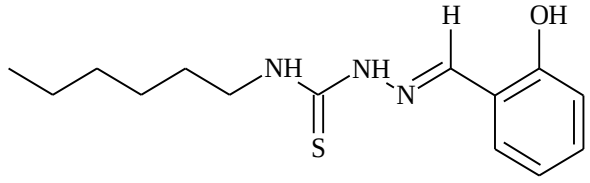 L[17]	0.4 ± 0.1
88	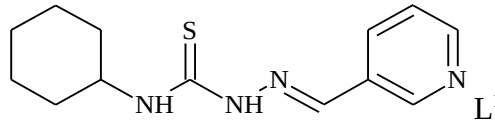 L[18]	21.0 ± 0.3
89	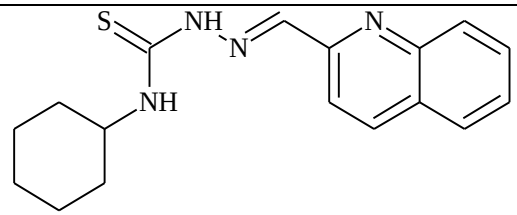 L21	27.9 ± 0.4
90	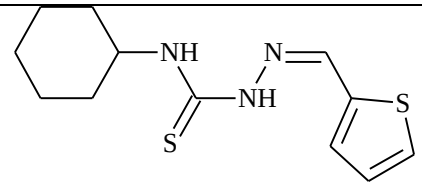	28.6 ± 0.3
91	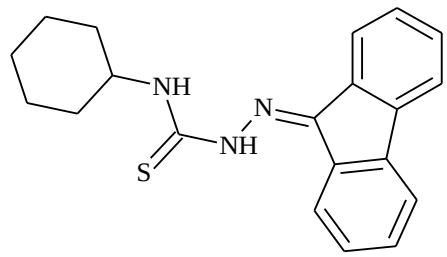 L[22]	26.0 ± 1.1

Annexe 1. Continued

№	Formula	$IC_{50} \pm SD$ (μM)
92	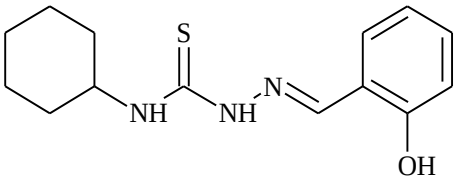 L^{23}	6.7 ± 0.4
93	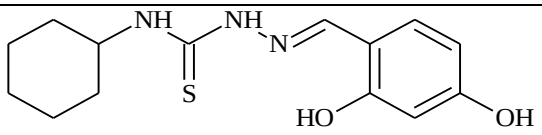 L^{24}	4.8 ± 0.3
94	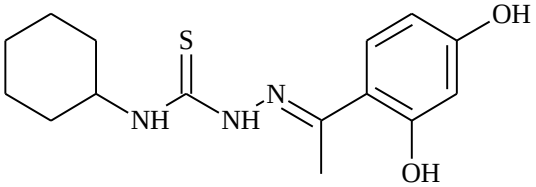 L^{25}	3.6 ± 0.1
95	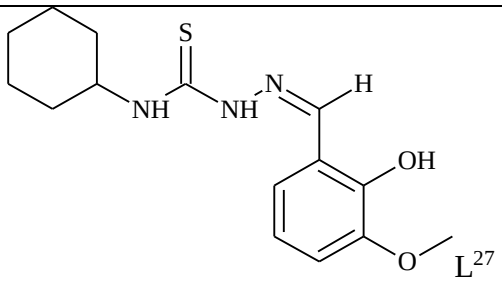 L^{27}	22.3 ± 0.6
96	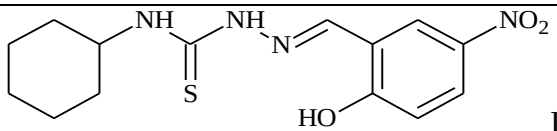 L^{28}	23.1 ± 0.4
97	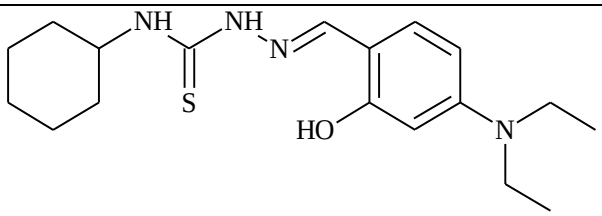 L^{31}	4.5 ± 0.4
98	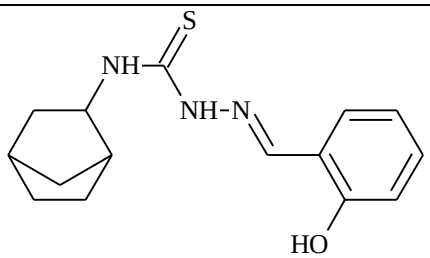 L^{34}	25.9 ± 1.1

Annexe 1. Continued

№	Formula	IC_{50} ± SD (μM)
99	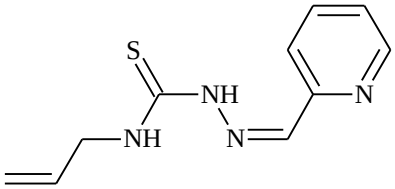 L^{35}	14.2 ± 0.8
100	$L^{35}\cdot HCl$	9.8 ± 1.0
101	$L^{35}\cdot HNO_3$	12.9 ± 0.4
102	$2L^{35}\cdot H_2SO_4$	12.3 ± 0.9
103	$L^{35}\cdot HClO_4$	12.4 ± 0.1
104	$L^{35}\cdot NH_2SO_3H$	12.8 ± 0.3
105	$L^{35}\cdot ClCH_2COOH$	13.4 ± 0.8
106	$L^{35}\cdot Cl_2CHCOOH$	10.9 ± 0.1
107	$L^{35}\cdot Cl_3CCOOH$	12.1 ± 0.7
108	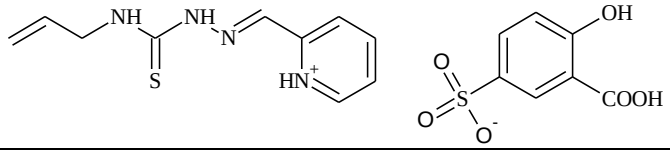	15.0 ± 0.3
109	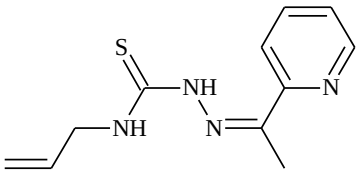 L^{36}	11.6 ± 0.3
110	$L^{36}\cdot HCl$	28.6 ± 0.2
111	$L^{36}\cdot HNO_3$	18.1 ± 0.5
112	$2L^{36}\cdot H_2SO_4$	29.8 ± 0.6
113	$L^{36}\cdot HClO_4$	16.2 ± 0.3
114	$L^{36}\cdot NH_2SO_3H$	21.3 ± 0.1
115	$L^{36}\cdot Cl_2CHCOOH$	15.1 ± 0.4
116	$L^{36}\cdot Cl_3CCOOH$	13.6 ± 0.7
117	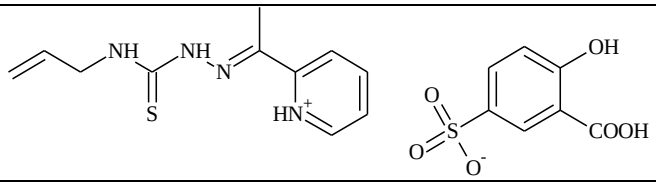	18.4 ± 0.5
118	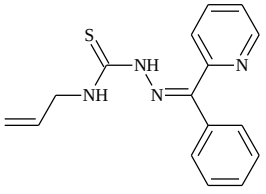 L^{37}	18.7 ± 0.4

Annexe 1. Continued

№	Formula	$IC_{50} \pm SD$ (μM)
119	$L^{37} \cdot HCl$	13.6 ± 0.8
120	$L^{37} \cdot HNO_3$	17.3 ± 0.7
121	$2L^{37} \cdot H_2SO_4$	17.5 ± 0.8
122	$L^{37} \cdot HClO_4$	19.0 ± 0.7
123	$L^{37} \cdot NH_2SO_3H$	32.7 ± 1.6
124	$L^{37} \cdot ClCH_2COOH$	7.2 ± 0.5
125	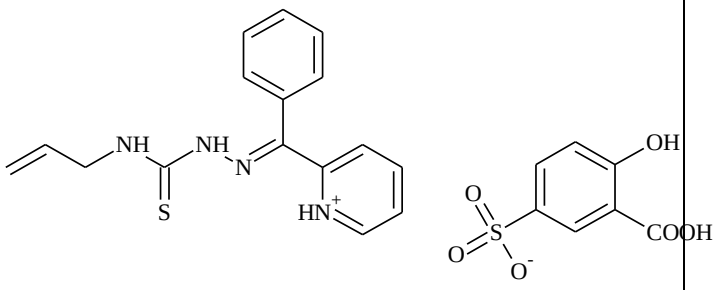	8.9 ± 0.9
126	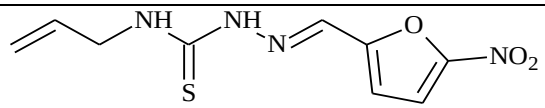	22.1 ± 0.2
127	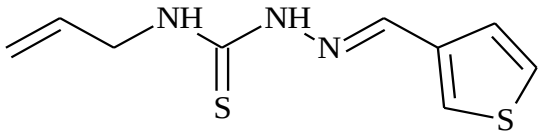	17.5 ± 0.4
128	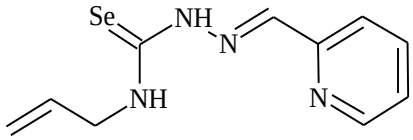	14.6 ± 0.7
129	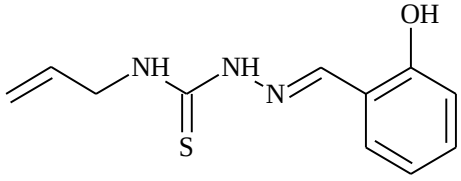 L^{38}	13.8 ± 0.4
130	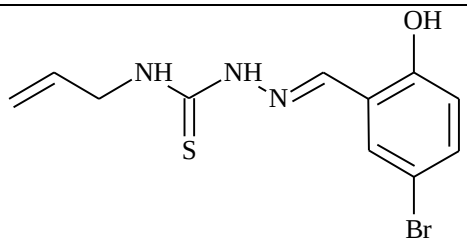 L^{40}	8.5 ± 0.6

Annexe 1. Continued

№	Formula	$IC_{50} \pm SD$ (μM)
131	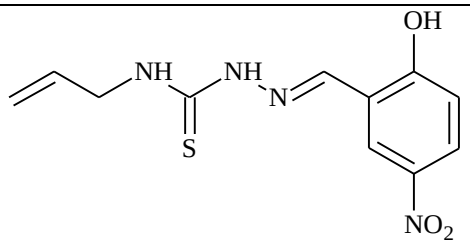 L^{41}	8.0 ± 0.2
132	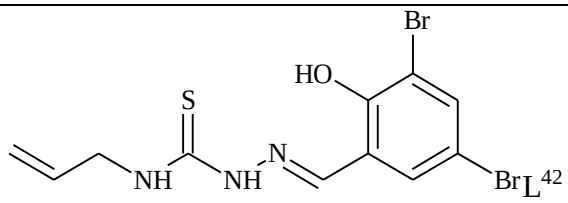 L^{42}	11.9 ± 0.1
133	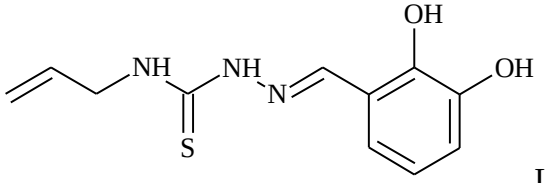 L^{43}	5.7 ± 0.5
134	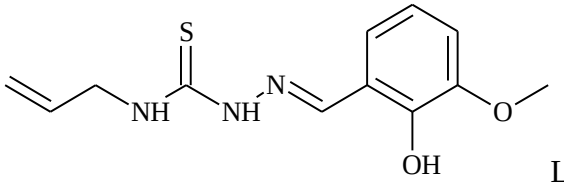 L^{44}	20.0 ± 0.1
135	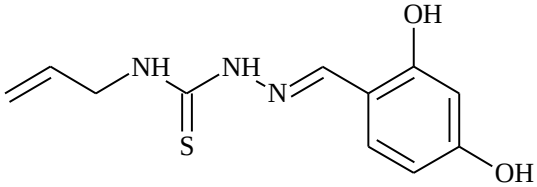 L^{45}	5.5 ± 0.8
136	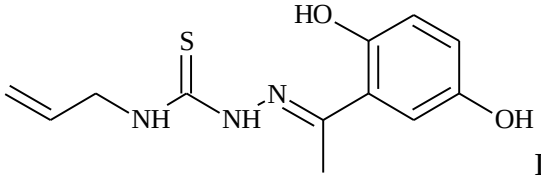 L^{46}	11.5 ± 0.1
137	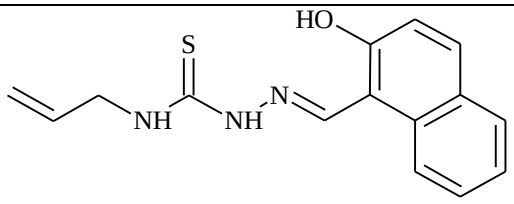 L^{47}	13.6 ± 0.2

Annexe 1. Continued

№	Formula	$IC_{50} \pm SD$ (μM)
138	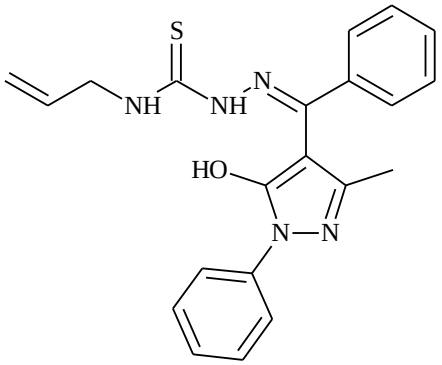 L^{48}	19.7 ± 0.9
139	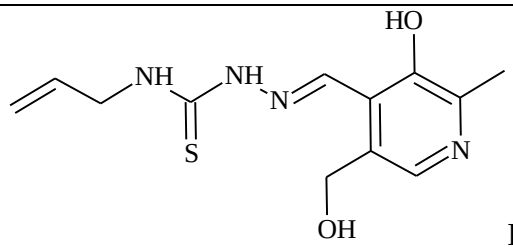 L^{49}	16.7 ± 0.2
140	$L^{49} \cdot HCl$	13.5 ± 0.2
141	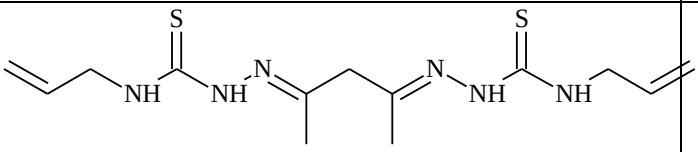	18.9 ± 0.7
142	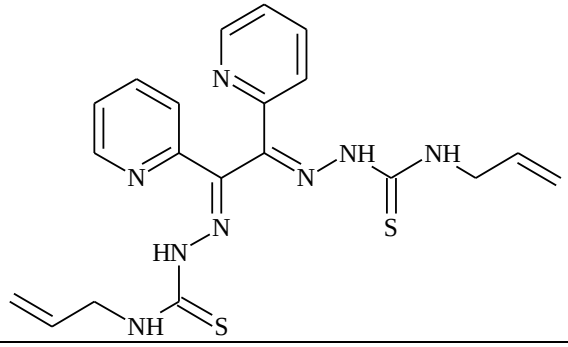	13.1 ± 0.4
143	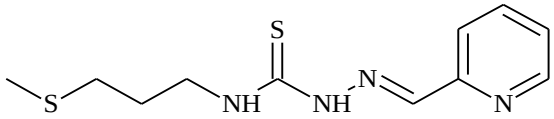 L^{54}	32.4 ± 1.3
144	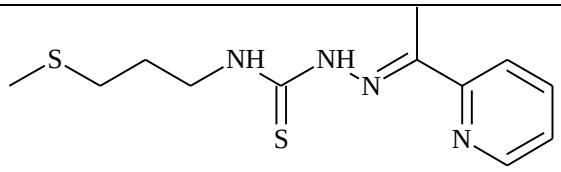 L^{55}	23.5 ± 0.1

Annexe 1. Continued

№	Formula	$IC_{50} \pm SD$ (μM)
145	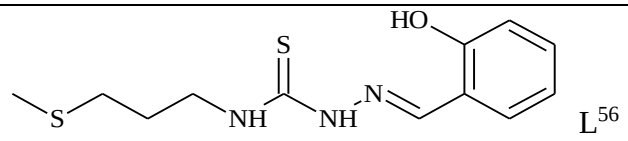 L^{56}	15.2 ± 0.1
146	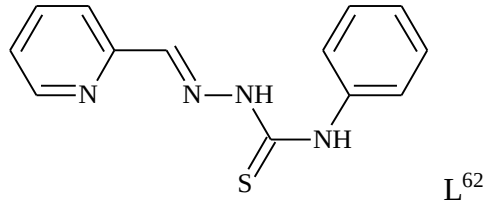 L^{62}	14.9 ± 0.4
147	$2L^{62} \cdot H_2SO_4$	10.0 ± 0.1
148	$L^{62} \cdot HCl$	10.8 ± 0.2
149	$L^{62} \cdot HNO_3$	9.4 ± 0.3
150	$L^{62} \cdot HClO_4$	9.9 ± 0.1
151	$L^{62} \cdot Cl_2CHCOOH$	6.6 ± 0.2
152	$L^{62} \cdot NH_2SO_3H$	6.4 ± 0.2
153	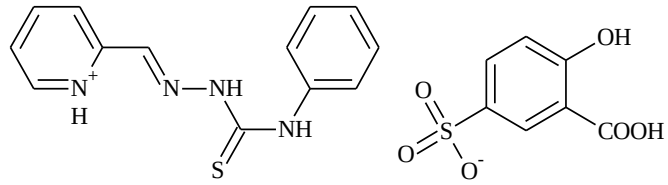	8.6 ± 0.9
154	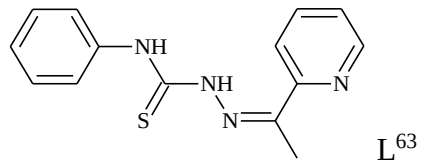 L^{63}	13.6 ± 0.3
155	$L^{63} \cdot HNO_3$	11.2 ± 0.6
156	$L^{63} \cdot HCl$	15.6 ± 0.1
157	$L^{63} \cdot NH_2SO_3H$	10.8 ± 0.2
158	$L^{63} \cdot Cl_2CHCOOH$	10.6 ± 0.3
159	$L^{63} \cdot HClO_4$	10.9 ± 0.7
160	$2L^{63} \cdot H_2SO_4$	11.0 ± 0.4
161	$L^{64} \cdot HClO_4$	23.6 ± 0.3
162	$L^{64} \cdot HNO_3$	25.6 ± 0.4
163	$L^{64} \cdot HCl$	20.1 ± 0.1
164	$2L^{64} \cdot H_2SO_4$	15.0 ± 0.7
165	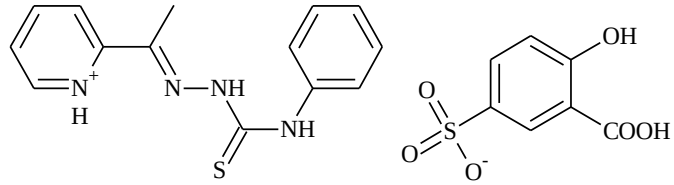	12.1 ± 0.6

Annexe 1. Continued

№	Formula	$IC_{50} \pm SD$ (μM)
166	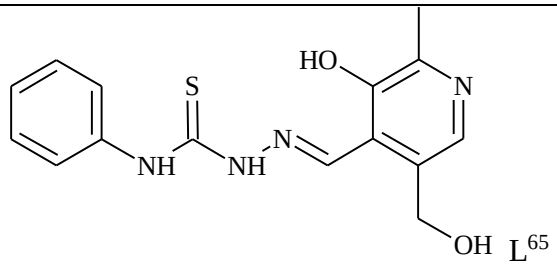 L^{65}	14.1 ± 0.4
167	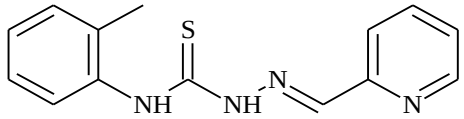	11.2 ± 0.1
168	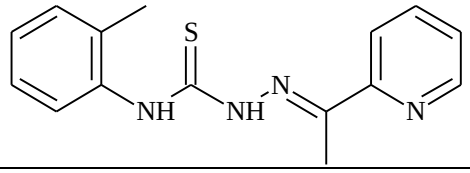	10.7 ± 0.5
169	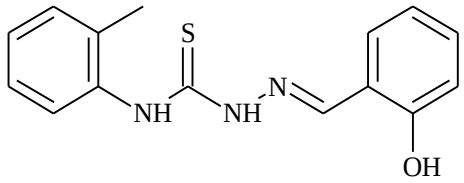	9.3 ± 0.1
170	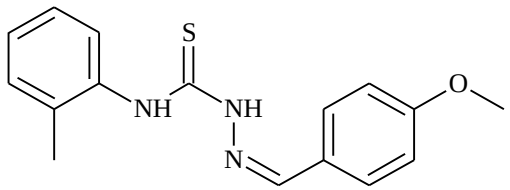	13.0 ± 0.1
171	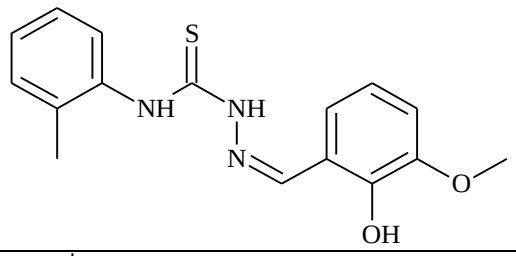	15.2 ± 0.3
172	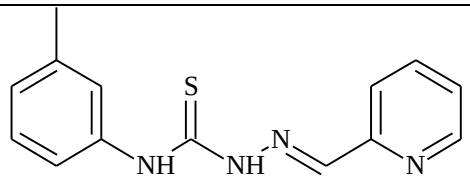	12.3 ± 0.8

Annexe 1. Continued

№	Formula	$IC_{50} \pm SD$ (μM)
173	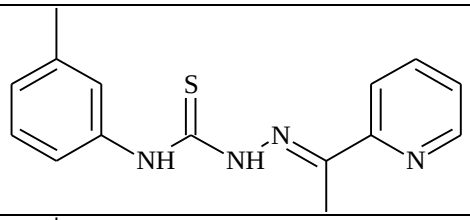	5.1 ± 0.1
174	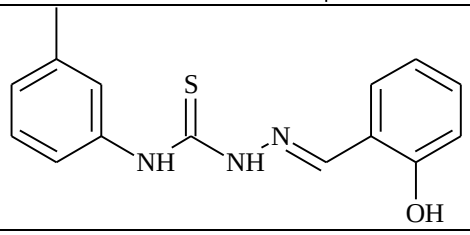	10.0 ± 0.4
175	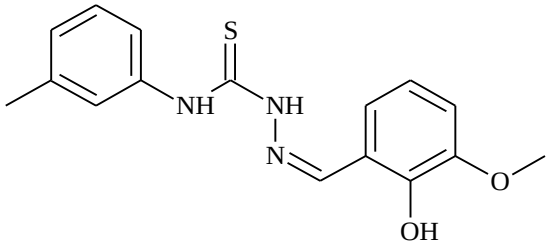	10.0 ± 0.7
176	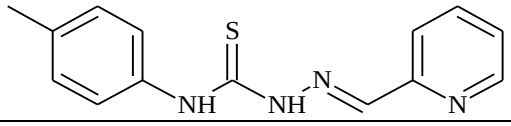	9.3 ± 0.1
177	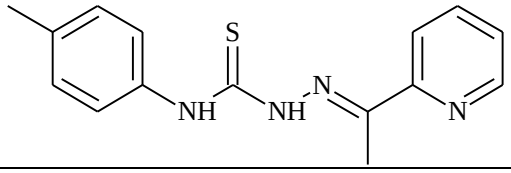	17.8 ± 0.5
178	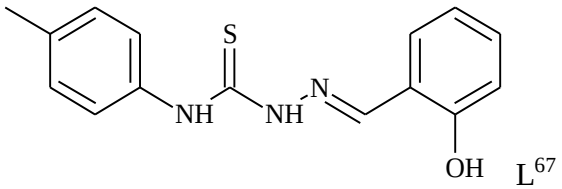	8.6 ± 0.2
179	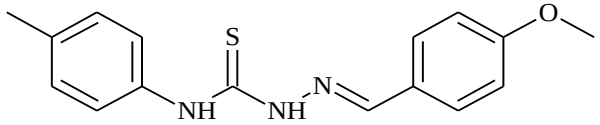	9.3 ± 0.2
180	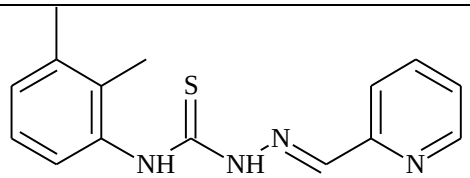	8.7 ± 0.1

L^{67}

Annexe 1. Continued

№	Formula	$IC_{50} \pm SD$ (μM)
181	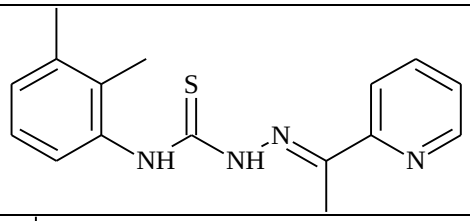	15.6 ± 0.2
182	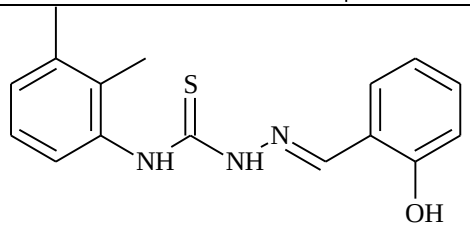 L^{68}	7.8 ± 0.4
183	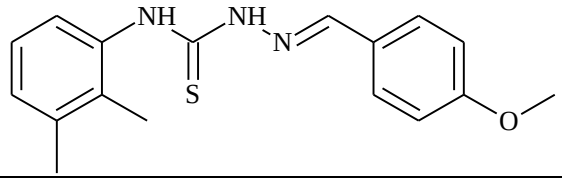	9.7 ± 0.2
184	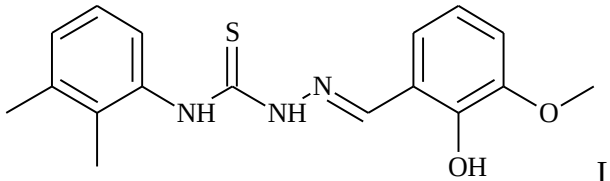 L^{69}	10.1 ± 0.4
185	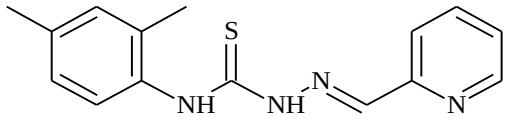	7.2 ± 0.2
186	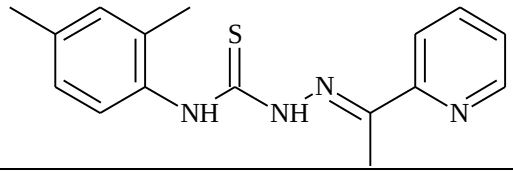	9.1 ± 0.2
187	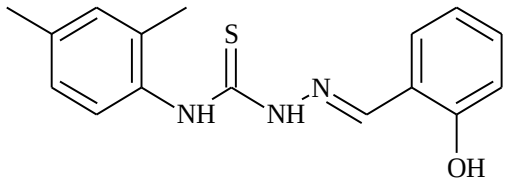	10.2 ± 0.5
188	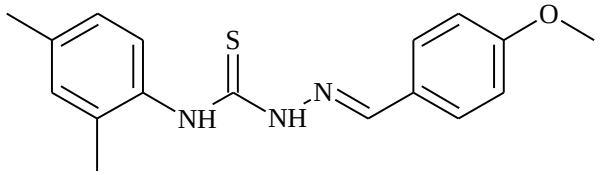	10.0 ± 0.2

Annexe 1. Continued

№	Formula	$IC_{50} \pm SD$ (μM)
189	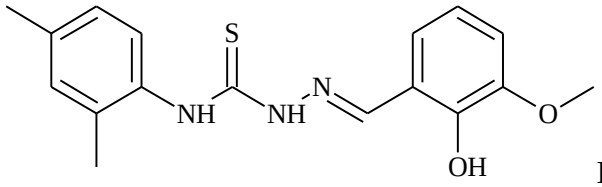 L^{73}	11.2 ± 0.3
190	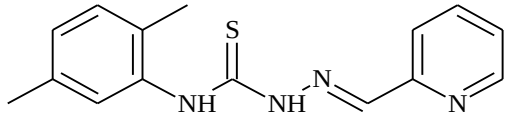	9.4 ± 0.5
191	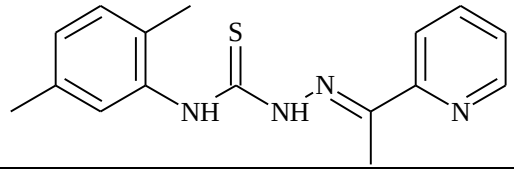	17.7 ± 0.3
192	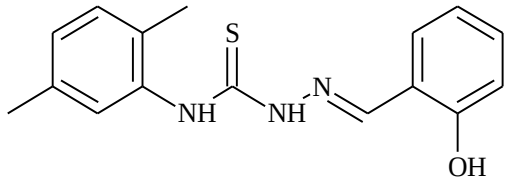	9.8 ± 0.9
193	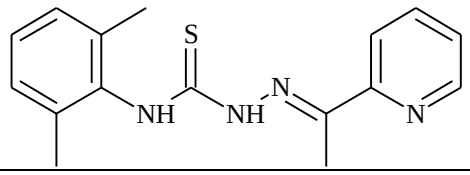	19.9 ± 0.6
194	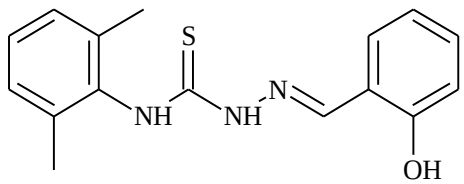 L^{74}	12.8 ± 0.1
195	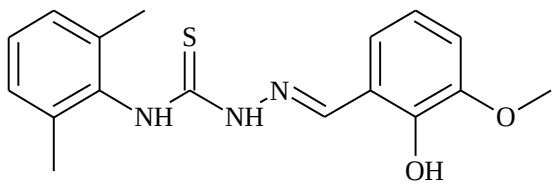	13.1 ± 0.8
196	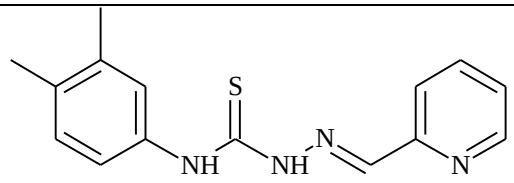	10.3 ± 0.3

Annexe 1. Continued

№	Formula	$IC_{50} \pm SD$ (μM)
197	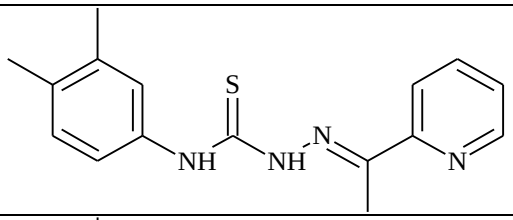	15.8 ± 0.2
198	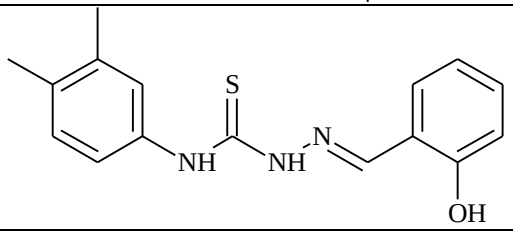	8.6 ± 0.2
199	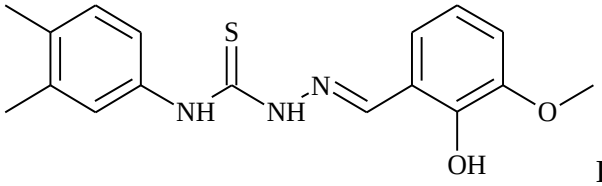 L^{75}	10.6 ± 0.5
200	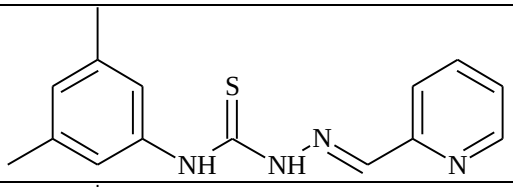	12.3 ± 0.9
201	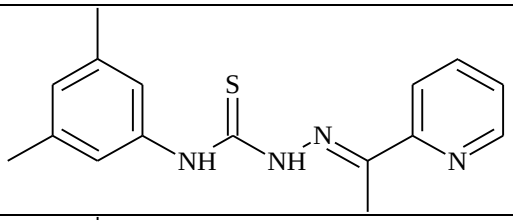	22.1 ± 0.5
202	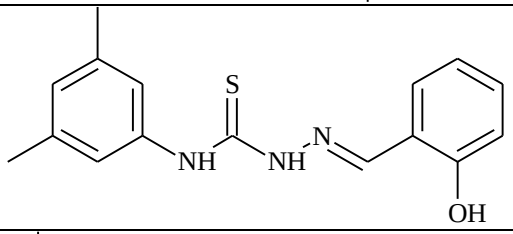	15.4 ± 0.6
203	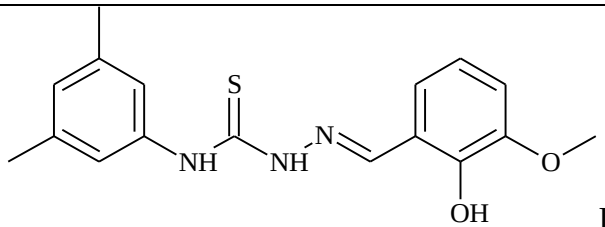 L^{76}	11.2 ± 0.1

Annexe 1. Continued

№	Formula	$IC_{50} \pm SD$ (μM)
204	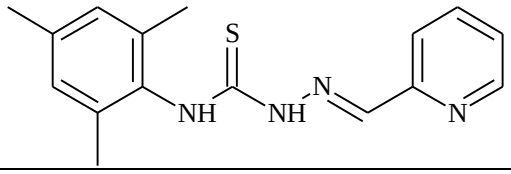	18.2 ± 0.2
205	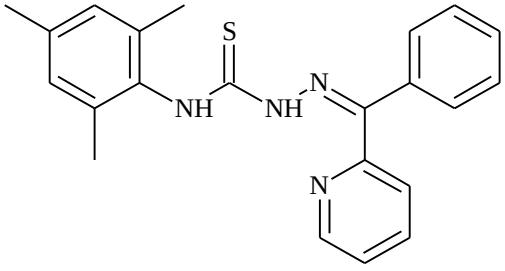	8.9 ± 0.1
206	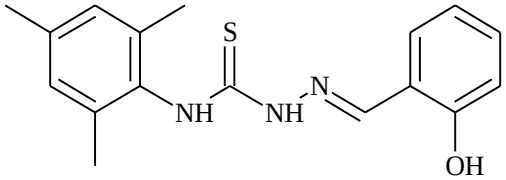 L^{77}	11.9 ± 0.8
207	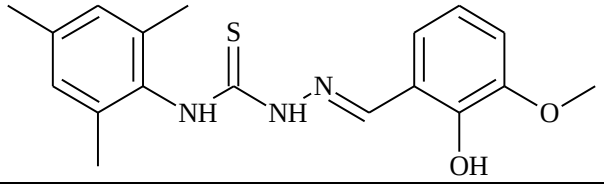	11.8 ± 0.4
208	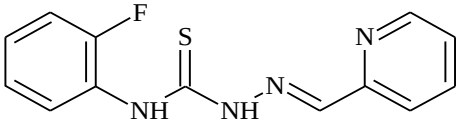 L^{78}	25.1 ± 1.7
209	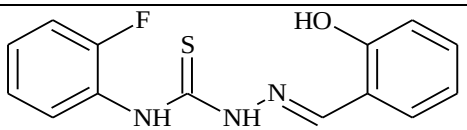 L^{80}	11.6 ± 0.9
210	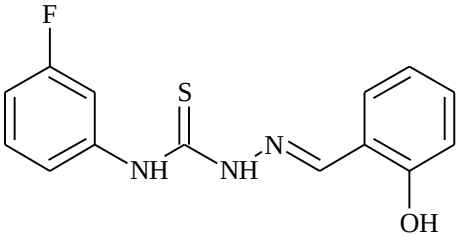 L^{82}	4.3 ± 0.3

Annexe 1. Continued

№	Formula	$IC_{50} \pm SD$ (μM)
211	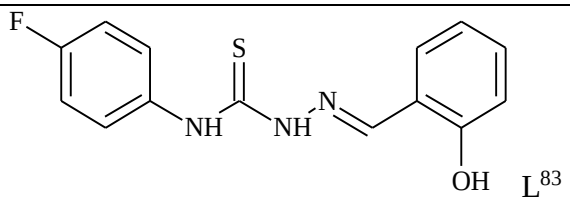 L^{83}	8.6 ± 0.8
212	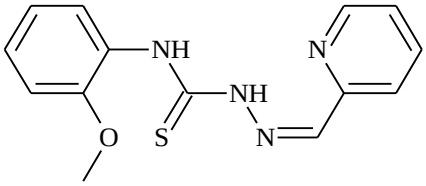	6.3 ± 0.1
213	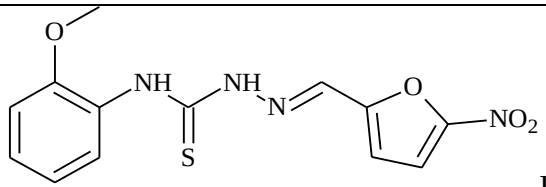 L^{86}	15.5 ± 0.1
214	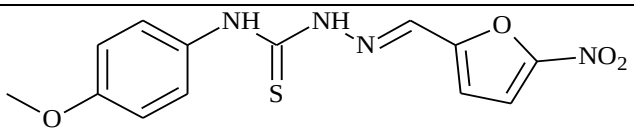	15.1 ± 0.2
215	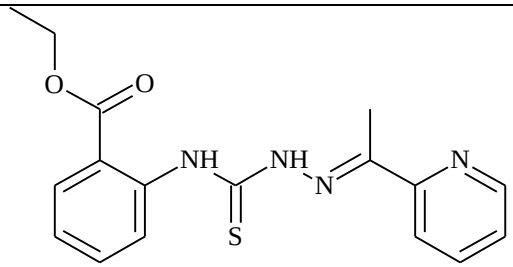	22.5 ± 0.4
216	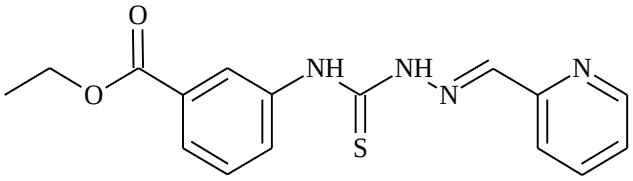 L^{99}	13.1 ± 0.1
217	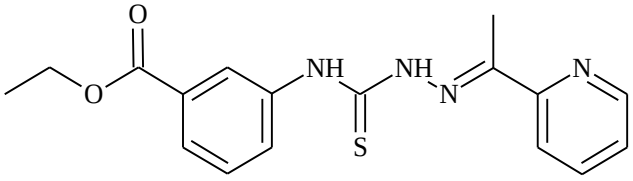 L^{100}	11.5 ± 0.4

Annexe 1. Continued

№	Formula	$IC_{50} \pm SD$ (μM)
218	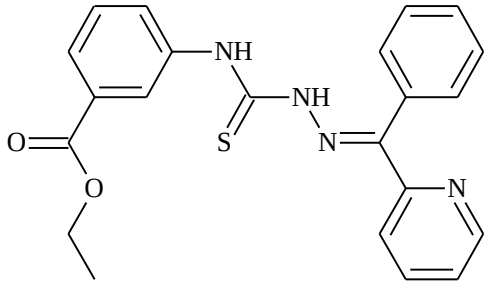 L^{101}	16.4 ± 0.8
219	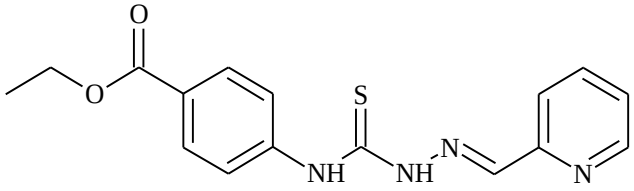 L^{102}	14.3 ± 0.6
220	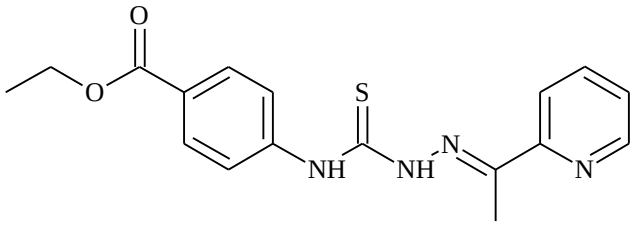 L^{103}	15.8 ± 0.4
221	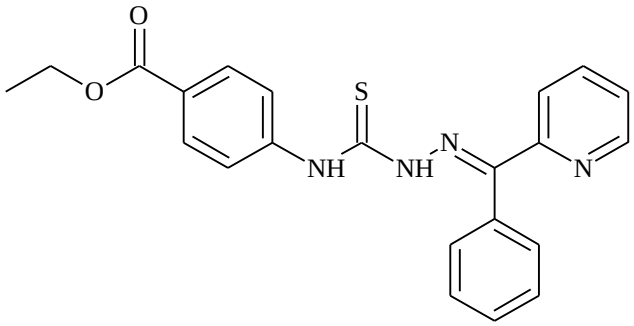 L^{104}	11.9 ± 0.2
222	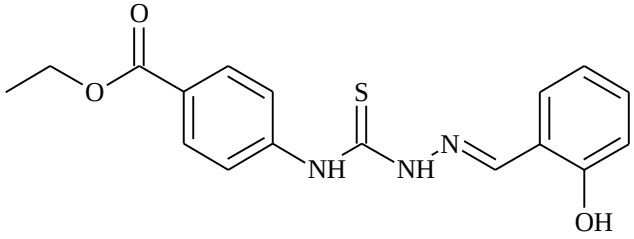 L^{106}	16.7 ± 0.8

Annexe 1. Continued

№	Formula	$IC_{50} \pm SD$ (μM)
223	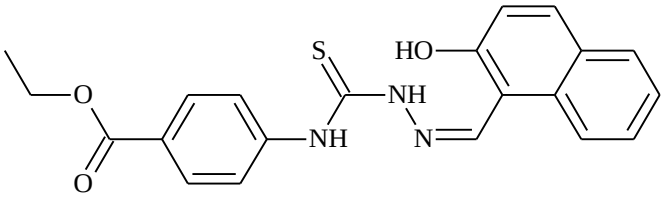 L^{110}	9.3 ± 0.1
224	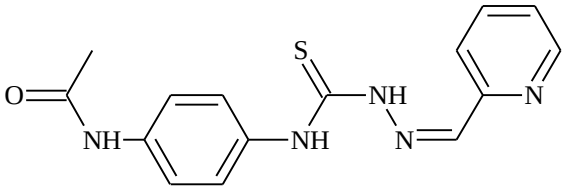 L^{111}	13.4 ± 0.3
225	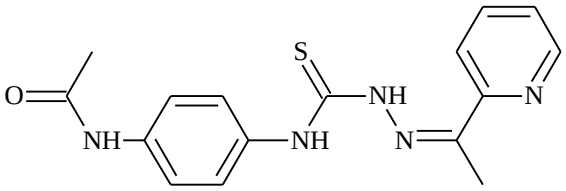 L^{112}	8.5 ± 0.4
226	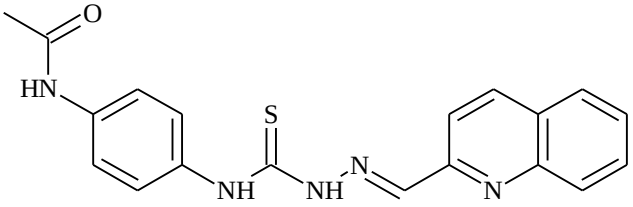 L^{113}	13.1 ± 0.5
227	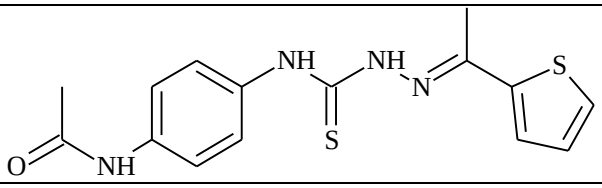	14.6 ± 0.1
228	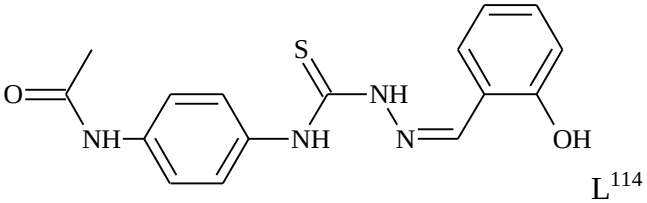 L^{114}	6.6 ± 0.1

Annexe 1. Continued

№	Formula	$IC_{50} \pm SD$ (μM)
229	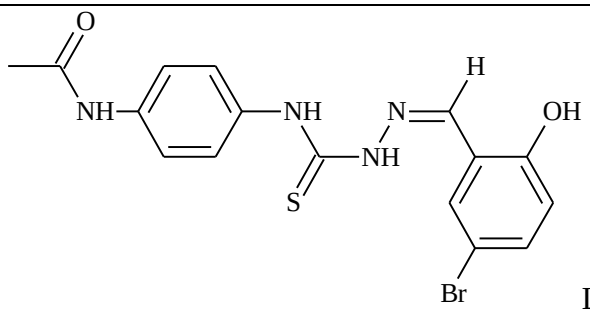 L^{115}	14.9 ± 0.1
230	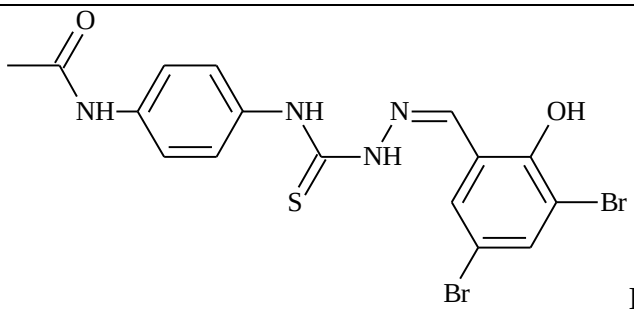 L^{116}	17.4 ± 0.7
231	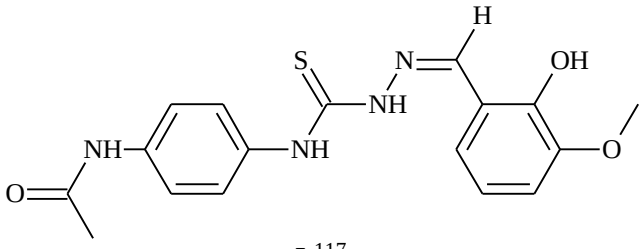 L^{117}	15.8 ± 0.2
232	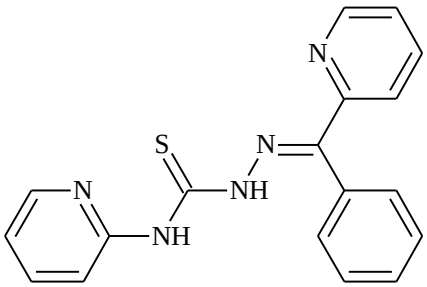 L^{118}	11.3 ± 0.4
233	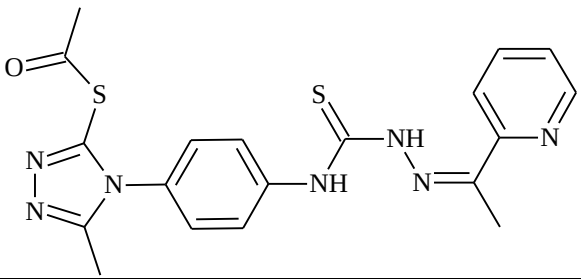	11.0 ± 0.4

Annexe 1. Continued

№	Formula	$IC_{50} \pm SD$ (μM)
234	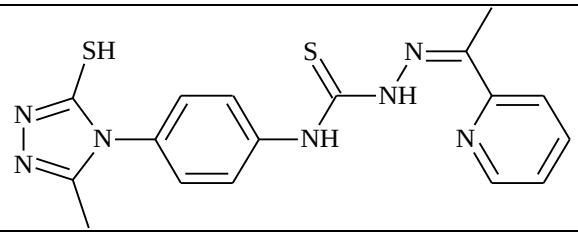	7.0 ± 0.3
235	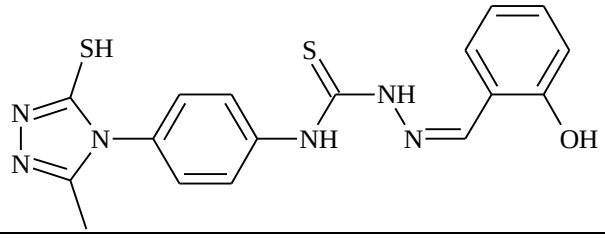	14.8 ± 0.5
236	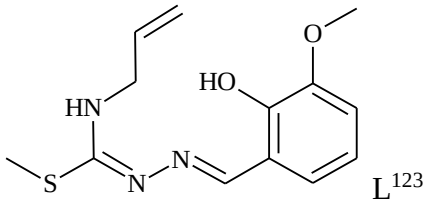 L^{123}	8.8 ± 0.3
237	$L^{123} \cdot HI$	7.7 ± 0.4
238	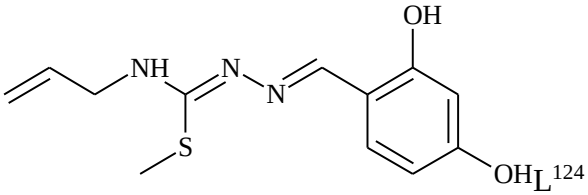 L^{124}	13.1 ± 0.8
239	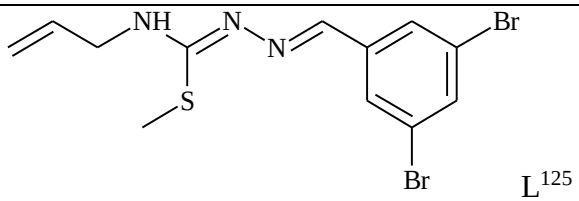 L^{125}	30.1 ± 0.5
240	$L^{126} \cdot HI$	8.7 ± 0.5
241	$L^{130} \cdot HI$	13.7 ± 0.6
242	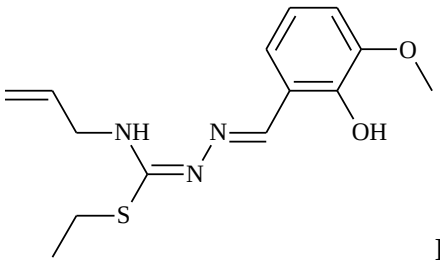 L^{131}	6.9 ± 0.4
243	$L^{131} \cdot HI$	8.6 ± 0.4
244	$L^{132} \cdot HI$	6.2 ± 0.2

Annexe 1. Continued

№	Formula	IC_{50} ± SD (μM)
245	L^{133}·HI	28.5 ± 1.0
246	L^{135}·HI	17.8 ± 0.1
247	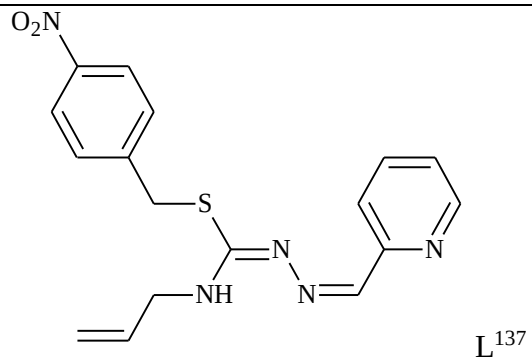 L^{137}	32.4 ± 0.4
248	L^{137}·HBr	23.9 ± 1.2

Annexe 2. The influence of the most active tested complexes on $ABTS^{\bullet+}$

№	Formula	IC_{50} ±SD (μM)
1	$Zn(L^{7})_2Cl_2$	2.9 ± 0.1
2	$Zn(L^{18}\text{-}H)_2$	14.1 ± 0.4
3	$Zn(L^{19}\text{-}H)Cl\cdot H_2O$	21.6 ± 1.0
4	$Zn(L^{20}\text{-}H)_2$	13.9 ± 0.4
5	$Zn(L^{20}\text{-}H)(OAc)\cdot H_2O$	15.8 ± 0.3
6	$Zn(L^{21}\text{-}H)OAc$	17.3 ± 0.1
7	$Zn(L^{23}\text{-}H)Cl$	7.5 ± 0.1
8	$Zn(L^{23}\text{-}H)(OAc)$	7.1 ± 0.1
9	$Zn(L^{30}\text{-}2H)\cdot 2H_2O$	15.9 ± 1.1
10	$Zn(L^{38}\text{-}H)Cl$	9.2 ± 1.1
11	$Zn(L^{80}\text{-}H)_2$	1.8 ± 0.1
12	$Zn(L^{99}\text{-}H)Cl\cdot H_2O$	11.5 ± 0.1
13	$Zn(L^{102}\text{-}H)Cl\cdot H_2O$	23.4 ± 0.5
14	$Zn(L^{106}\text{-}2H)\cdot H_2O$	6.8 ± 0.9
15	$Zn(L^{118}\text{-}H)Cl$	6.7 ± 0.1
16	$Zn(L^{137}\text{-}H)Cl$	4.4 ± 0.1
17	$Zn(L^{137}\text{-}H)Br$	26.6 ± 0.5
18	$[Cu(L^{5})_2]Br_2$	5.5 ± 0.3
19	$[Cu(L^{4})_2]Br_2$	9.1 ± 0.8
20	$[Cu(L^{4})_2]Cl_2$	16.1 ± 0.5
21	$[Cu(L^{5})_2](NO_3)_2$	14.3 ± 0.2
22	$[Cu(L^{5})_2](ClO_4)_2$	21.9 ± 0.1
23	$Cu(L^{5}\text{-}H)_2$	4.4 ± 0.1
24	$[Cu(L^{6})_2]Cl_2$	5.9 ± 0.1
25	$[Cu(L^{6})_2](NO_3)_2$	15.9 ± 0.3
26	$[Cu(L^{6})_2](ClO_4)_2$	6.3 ± 0.1
27	$Cu(L^{6}\text{-}H)_2$	5.1 ± 0.3
28	$Cu(L^{7})_2(NO_3)_2$	19.0 ± 0.2
29	$Cu(L^{7})_2Cl_2$	16.1 ± 0.3
30	$Cu(L^{7})_2SO_4$	18.5 ± 0.4
31	$Cu(L^{7})_2(CH_3COO)_2$	19.0 ± 0.3
32	$Cu(L^{8})(L^{8}\text{-}H)(OAc)$	16.7 ± 0.5
33	$Cu(L^{12}\text{-}H)Cl$	16.4 ± 0.9
34	$Cu(L^{12}\text{-}H)(NO_3)$	23.8 ± 0.2

Annexe 2. Continued

№	Formula	IC_{50} ±SD (μM)
35	$Cu(L^{18}\text{-}H)Cl\cdot H_2O$	25.1 ± 0.6
36	$Cu(L^{18}\text{-}H)(OAc)\cdot H_2O$	25.5 ± 0.1
37	$Cu(L^{21}\text{-}H)Cl\cdot H_2O$	25.8 ± 1.0
38	$Cu(L^{21}\text{-}H)ClO_4\cdot H_2O$	8.1 ± 0.3
39	$Cu(L^{21}\text{-}H)Br\cdot H_2O$	14.9 ± 1.3
40	$Cu(L^{23}\text{-}H)Cl\cdot H_2O$	14.7 ± 0.1
41	$Cu(L^{23}\text{-}H)Br\cdot H_2O$	21.7 ± 0.3
42	$Cu(L^{23}\text{-}2H)\cdot H_2O$	10.8 ± 0.2
43	$Cu(L^{23}\text{-}H)(NO_3)\cdot H_2O$	14.9 ± 0.4
44	$Cu(L^{23}\text{-}H)(ClO_4)\cdot H_2O$	5.9 ± 0.4
45	$Cu(L^{24}\text{-}H)(NO_3)$	6.4 ± 0.1
46	$Cu(L^{24}\text{-}H)Cl$	7.1 ± 0.7
47	$Cu(L^{24}\text{-}H)Br$	11.9 ± 0.9
48	$Cu(L^{25}\text{-}H)NO_3\cdot H_2O$	20.7 ± 0.8
49	$Cu(L^{26}\text{-}H)NO_3$	1.9 ± 0.3
50	$Cu(L^{26}\text{-}H)Cl$	6.5 ± 0.4
51	$Cu(L^{27}\text{-}H)(ClO_4)\cdot H_2O$	13.4 ± 0.1
52	$Cu(L^{27}\text{-}H)Br\cdot H_2O$	5.9 ± 0.1
53	$Cu(L^{27}\text{-}2H)\cdot 2H_2O$	10.4 ± 0.2
54	$Cu(L^{27}\text{-}H)(NO_3)$	12.2 ± 0.5
56	$Cu(L^{28}\text{-}H)(NO_3)$	20.1 ± 0.2
57	$Cu(L^{31}\text{-}H)Br$	1.8 ± 0.2
58	$Cu(L^{31}\text{-}H)Cl$	11.4 ± 0.9
59	$Cu(L^{31}\text{-}H)(NO_3)$	13.6 ± 0.6
60	$Cu(L^{34}\text{-}2H)(H_2O)$	16.1 ± 0.8
61	$Cu(L^{36})(NO_3)_2$	29.8 ± 1.2
62	$Cu(L^{36}\text{-}H)(OAc)$	26.8 ± 0.5
63	$Cu(Im)(L^{38}\text{-}H)(NO_3)$	5.8 ± 0.1
64	$Cu(3.5Br_2Py)(L^{38}\text{-}H)(NO_3)$	7.5 ± 0.5
65	$Cu(4\text{-}Pic)(L^{38}\text{-}H)(NO_3)$	5.8 ± 0.1
66	$Cu(3\text{-}Pic)(L^{38}\text{-}H)(NO_3)$	3.4 ± 0.8
67	$Cu(2.2'\text{-}BPy)(L^{38}\text{-}2H)$	10.2 ± 0.1
68	$Cu(1.10\text{-}Phen)(L^{38}\text{-}2H)$	22.8 ± 0.6
69	$Cu(1.10\text{-}Phen)(L^{39})(NO_3)_2$	7.7 ± 0.7
70	$Cu(L^{42}\text{-}H)NO_3\cdot H_2O$	18.7 ± 0.8

Annexe 2. Continued

№	Formula	IC_{50} ±SD (μM)
71	Cu(1.10-Phen)(L^{42}-H)NO_3	19.9 ± 0.1
72	Cu(2.2'-BPy)(L^{42}-H)NO_3	13.4 ± 0.5
73	Cu(1.10-Phen)(L^{42}-2H)	14.8 ± 0.7
74	Cu(2.2'-BPy)(L^{42}-2H)	19.7 ± 0.6
75	Cu(4-Pic)(L^{42}-2H)	16.8 ± 0.7
76	Cu(3-Pic)(L^{42}-2H)	23.9 ± 0.8
77	Cu(Py)(L^{42}-2H)	18.7 ± 0.1
78	Cu(L^{43}-H)NO_3	7.1 ± 0.1
79	Cu(L^{44}-H)Cl	24.6 ± 0.3
80	Cu(L^{44}-2H)H_2O	13.9 ± 0.3
81	Cu(1.10-Phen)(L^{44}-2H)	5.2 ± 0.2
82	Cu(2.2'-BPy)(L^{44}-2H)	7.3 ± 0.2
83	Cu(Im)(L^{44}-2H)	6.9 ± 0.8
84	Cu(3.5-Br_2Py)(L^{44}-2H)	7.0 ± 0.8
85	Cu(3.4-Lut)(L^{44}-2H)	7.6 ± 0.3
86	Cu(4-Pic)(L^{44}-2H)	18.7 ± 0.6
87	Cu(3-Pic)(L^{44}-2H)	12.8 ± 0.6
88	Cu(Py)(L^{44}-2H)	8.4 ± 0.5
89	Cu(L^{44}-H)$NO_3 \cdot H_2O$	21.5 ± 0.2
90	Cu(2.2'-BPy)(L^{44}-H)NO_3	6.8 ± 0.2
91	Cu(3.5-Br_2Py)(L^{44}-H)NO_3	6.7 ± 0.5
92	Cu(Py)(L^{44}-H)NO_3	16.4 ± 0.4
93	Cu(4-Pic)(L^{44}-H)NO_3	12.8 ± 0.2
94	Cu(3-Pic)(L^{44}-H)NO_3	18.7 ± 0.5
95	Cu(3.4-Lut)(L^{44}-H)NO_3	3.2 ± 0.1
96	Cu(Im)(L^{44}-H)NO_3	8.6 ± 0.7
97	Cu(1.10-Phen)(L^{44}-H)NO_3	7.8 ± 0.3
98	Cu(L^{45}-H)Cl	12.8 ± 0.2
99	Cu(L^{45}-2H)H_2O	6.5 ± 0.8
100	Cu(2.2'-BPy)(L^{45}-2H)	7.4 ± 0.8
101	Cu(3.4-Lut)(L^{45}-2H)	4.5 ± 0.2
102	Cu(4-Pic)(L^{45}-2H)	23.9 ± 0.9
103	Cu(3-Pic)(L^{45}-2H)	17.3 ± 0.8
104	Cu(L^{45}-H)NO_3	8.6 ± 0.3
105	Cu(L^{46}-H)NO_3	17.4 ± 0.3

Annexe 2. Continued

№	Formula	IC_{50} ±SD (μM)
106	$Cu(L^{46}\text{-}H)Cl$	17.8 ± 0.8
107	$Cu(L^{47}\text{-}H)Cl$	14.2 ± 0.6
108	$Cu(L^{47}\text{-}H)NO_3$	14.4 ± 0.4
109	$Cu(1.10\text{-}Phen)(L^{47}\text{-}H)NO_3$	14.5 ± 0.5
110	$Cu(L^{47}\text{-}2H)H_2O$	18.9 ± 0.8
111	$Cu(2.2'\text{-}BPy)(L^{47}\text{-}2H)$	11.6 ± 0.5
112	$Cu(3.4\text{-}Lut)(L^{47}\text{-}2H)$	8.9 ± 0.1
113	$Cu(3\text{-}Pic)(L^{47}\text{-}2H)$	15.4 ± 0.2
114	$Cu(Py)(L^{47}\text{-}2H)$	9.5 ± 0.7
115	$Cu(L^{48}\text{-}H)(OAc)$	31.4 ± 1.8
116	$Cu(1.10\text{-}Phen)(L^{50}\text{-}H)(NO_3)$	23.0 ± 0.2
117	$Cu(2.2'\text{-}BPy)(L^{50}\text{-}H)(NO_3)$	22.3 ± 0.3
119	$Cu(L^{57})(ClO_4)_2$	16.7 ± 0.3
120	$Cu(L^{58})Br_2$	20.9 ± 1.0
121	$Cu(L^{62}\text{-}H)Cl$	4.5 ± 0.6
122	$Cu(Str)(L^{62}\text{-}H)Cl$	6.2 ± 0.7
123	$Cu(L^{65}\text{-}H)(Cl_2CHCOO)$	26.9 ± 0.4
124	$Cu(1.10\text{-}Phen)(L^{67}\text{-}2H)$	11.8 ± 0.2
125	$Cu(L^{68}\text{-}H)(NO_3)$	19.6 ± 0.5
126	$Cu(L^{68}\text{-}H)Cl$	27.2 ± 0.7
127	$Cu_2(L^{68}\text{-}H)_2SO_4$	13.2 ± 0.8
128	$Cu(2.2'\text{-}BPy)(L^{69}\text{-}2H)$	9.9 ± 0.7
129	$Cu(1.10\text{-}Phen)(L^{69}\text{-}2H)$	2.7 ± 0.2
130	$Cu(Im)(L^{69}\text{-}2H)$	10.9 ± 0.1
131	$Cu(3.5\text{-}Br_2Py)(L^{69}\text{-}2H)$	5.7 ± 0.1
132	$Cu(Str)(L^{69}\text{-}2H)$	10.6 ± 0.3
133	$Cu(L^{73}\text{-}H)Br$	5.7 ± 0.4
134	$Cu(L^{73}\text{-}H)Cl$	15.7 ± 0.3
135	$Cu(L^{73}\text{-}H)NO_3\cdot H_2O$	9.5 ± 0.7
136	$Cu(Im)(L^{73}\text{-}2H)$	10.0 ± 0.2
137	$Cu(2.2'\text{-}BPy)(L^{73}\text{-}2H)$	12.4 ± 0.1
138	$Cu(1.10\text{-}Phen)(L^{73}\text{-}2H)$	7.4 ± 0.1
139	$Cu(3.5\text{-}Br_2Py)(L^{73}\text{-}2H)$	3.3 ± 0.5
140	$Cu(Str)(L^{73}\text{-}2H)$	6.7 ± 0.6
141	$Cu(L^{73}\text{-}2H)(H_2O)$	6.9 ± 0.7

Annexe 2. Continued

№	Formula	IC_{50} ±SD (μM)
142	$Cu(L^{73}\text{-}H)ClO_4$	8.1 ± 0.8
143	$Cu(L^{75}\text{-}H)NO_3 \cdot H_2O$	15.7 ± 0.7
144	$Cu(1.10\text{-}Phen)(L^{75}\text{-}2H)$	10.9 ± 0.1
145	$Cu(3.5\text{-}Br_2Py)(L^{75}\text{-}2H)$	6.3 ± 0.1
146	$Cu(L^{75}\text{-}H)Br$	9.3 ± 0.1
147	$Cu(L^{75}\text{-}H)ClO_4 \cdot 4H_2O$	30.8 ± 0.6
148	$Cu(L^{75}\text{-}H)Cl$	7.5 ± 0.3
149	$Cu(L^{75}\text{-}2H)(H_2O)$	8.5 ± 0.2
150	$Cu(L^{78}\text{-}H)NO_3$	12.8 ± 0.9
151	$Cu(L^{78}\text{-}H)Br$	9.7 ± 0.8
152	$Cu(L^{78}\text{-}H)Cl$	9.1 ± 0.1
153	$Cu(L^{78}\text{-}H)(OAc)$	14.2 ± 0.9
154	$Cu(L^{82}\text{-}H)Cl$	12.1 ± 0.2
155	$Cu(L^{83}\text{-}H)Cl$	13.2 ± 0.3
156	$Cu(L^{83}\text{-}H)NO_3$	24.3 ± 1.5
157	$Cu(L^{84}\text{-}H)NO_3$	19.9 ± 0.7
158	$Cu(L^{84}\text{-}H)Cl$	22.4 ± 0.2
159	$Cu(L^{85}\text{-}H)Cl$	82.5 ± 1.5
160	$Cu(L^{85}\text{-}H)NO_3$	23.0 ± 0.1
161	$Cu(L^{86}\text{-}H)NO_3$	34.1 ± 0.8
162	$Cu(L^{87}\text{-}2H)(H_2O)$	12.3 ± 0.9
163	$Cu(L^{87}\text{-}H)Br$	15.9 ± 0.1
164	$Cu(L^{88}\text{-}H)Cl$	27.5 ± 0.3
165	$Cu(L^{88}\text{-}H)NO_3$	18.8 ± 0.6
166	$Cu(L^{89}\text{-}H)Cl$	11.4 ± 0.4
167	$Cu(L^{90}\text{-}H)NO_3$	14.6 ± 0.5
168	$Cu(L^{90}\text{-}H)Cl$	20.2 ± 0.2
169	$Cu(L^{91}\text{-}H)NO_3$	24.7 ± 0.3
170	$Cu(L^{93}\text{-}H)NO_3$	25.3 ± 0.9
171	$Cu(L^{94}\text{-}H)NO_3$	12.0 ± 0.5
172	$Cu(L^{95}\text{-}H)Cl$	17.6 ± 0.1
173	$Cu(L^{96}\text{-}H)Cl$	19.9 ± 0.3
174	$Cu(L^{96}\text{-}H)NO_3$	20.1 ± 0.2
175	$Cu(L^{102}\text{-}H)Cl$	6.6 ± 0.3
176	$Cu(L^{102}\text{-}H)Br$	9.1 ± 0.2

Annexe 2. Continued

№	Formula	IC_{50} ±SD (μM)
177	$Cu(L^{102}\text{-}H)NO_3 \cdot H_2O$	8.0 ± 0.4
178	$Cu(L^{102}\text{-}H)(OAc) \cdot H_2O \cdot C_2H_5OH$	11.3 ± 0.3
179	$Cu(L^{102}\text{-}H)(ClO_4) \cdot C_2H_5OH$	13.3 ± 0.1
180	$Cu(L^{106}\text{-}H)OAc \cdot H_2O$	10.5 ± 0.4
181	$Cu(L^{106}\text{-}H)ClO_4 \cdot H_2O$	11.5 ± 0.7
182	$Cu(L^{106}\text{-}H)Br$	2.9 ± 0.7
184	$Cu(L^{107}\text{-}H)Cl \cdot H_2O$	13.1 ± 0.6
185	$Cu(L^{107}\text{-}2H) \cdot H_2O$	28.0 ± 0.3
186	$Cu(L^{107}\text{-}H)(NO_3) \cdot H_2O$	15.5 ± 0.9
187	$Cu(L^{107}\text{-}H)(ClO_4) \cdot H_2O$	8.7 ± 0.5
188	$Cu(L^{110}\text{-}2H) \cdot H_2O$	13.5 ± 0.2
189	$Cu(L^{111}\text{-}H)Cl \cdot H_2O$	9.2 ± 0.2
190	$Cu(L^{111}\text{-}H)NO_3 \cdot H_2O$	30.5 ± 0.6
191	$Cu(L^{111}\text{-}H)(OAc) \cdot H_2O$	21.3 ± 0.4
192	$Cu(L^{112}\text{-}H)Cl$	24.3 ± 0.2
193	$Cu(L^{112}\text{-}H)NO_3$	23.3 ± 0.9
194	$Cu(L^{112}\text{-}H)ClO_4 \cdot H_2O$	10.1 ± 0.3
195	$Cu(L^{113}\text{-}H)Br$	18.6 ± 0.3
196	$Cu(L^{113}\text{-}H)Cl$	14.3 ± 0.8
197	$Cu(L^{114}\text{-}H)ClO_4 \cdot H_2O$	28.5 ± 0.4
198	$Cu(L^{114}\text{-}H)Br \cdot H_2O$	32.5 ± 0.7
199	$Cu(L^{114}\text{-}2H)(H_2O)$	12.7 ± 0.4
200	$Cu(L^{114}\text{-}H)Cl \cdot H_2O$	30.3 ± 0.6
201	$Cu(L^{114}\text{-}H)(NO_3) \cdot H_2O$	10.9 ± 0.2
202	$Cu(L^{115}\text{-}2H)(H_2O)$	8.7 ± 0.5
203	$Cu(L^{115}\text{-}H)(OAc) \cdot H_2O$	4.9 ± 0.3
204	$Cu(L^{115}\text{-}H)(NO_3) \cdot H_2O$	6.6 ± 0.3
205	$Cu(L^{115}\text{-}H)(ClO_4) \cdot H_2O$	2.4 ± 0.1
206	$Cu(L^{116}\text{-}H)Br \cdot H_2O$	27.2 ± 0.2
207	$Cu(L^{116}\text{-}2H)(H_2O)$	31.9 ± 0.3
208	$Cu(L^{116}\text{-}2H) \cdot H_2O \cdot C_2H_5OH$	15.0 ± 0.8
209	$Cu(L^{117}\text{-}2H)(H_2O)$	19.1 ± 0.2
210	$Cu(L^{117}\text{-}H)NO_3 \cdot H_2O$	15.1 ± 0.4
211	$Cu(L^{117}\text{-}H)Cl \cdot H_2O$	15.6 ± 0.2
212	$Cu(L^{118}\text{-}H)Cl$	17.1 ± 0.6

Annexe 2. Continued

№	Formula	IC_{50} ±SD (μM)
213	$Cu(4\text{-}Pic)(L^{119})(NO_3)_2$	16.6 ± 0.1
214	$Cu(3.4\text{-}Lut)(L^{119})(NO_3)_2$	10.1 ± 0.1
215	$Cu(1.10\text{-}Phen)(L^{122}\text{-}H)NO_3$	11.6 ± 0.5
216	$Cu(L^{123}\text{-}H)Cl$	20.9 ± 0.3
217	$Cu(L^{124}\text{-}H)Br$	26.2 ± 1.8
218	$Cu(L^{126}\text{-}H)Cl$	13.1 ± 0.5
219	$Cu(L^{126}\text{-}H)NO_3$	12.2 ± 0.4
220	$Cu(L^{126}\text{-}H)ClO_4$	16.3 ± 0.8
221	$Cu(L^{126}\text{-}H)(OAc)$	19.8 ± 0.2
222	$Cu(L^{127}\text{-}H)ClO_4$	11.9 ± 0.7
223	$Cu(L^{130}\text{-}H)Cl$	13.7 ± 0.1
224	$Cu(L^{134})(NO_3)_2$	25.1 ± 0.2
225	$Cu(L^{135}\text{-}H)Cl$	12.5 ± 0.4
226	$Cu(L^{135}\text{-}H)NO_3$	10.3 ± 0.3
227	$Cu(L^{135}\text{-}H)(Cl_2CHCOO)$	13.1 ± 0.4
228	$Cu(L^{135}\text{-}H)(OAc)$	10.1 ± 0.1
229	$Cu(Im)(L^{135}\text{-}H)NO_3$	14.4 ± 0.1
230	$Cu(3.4\text{-}Lut)(L^{135}\text{-}H)NO_3$	11.5 ± 0.2
231	$Cu(L^{137})Br_2$	25.7 ± 0.2
232	$Cu(L^{137})Cl_2$	21.8 ± 0.4
233	$Cu_2(L^{140}\text{-}2H)Cl_2$	8.8 ± 0.6
234	$Cu_2(L^{140}\text{-}2H)Br_2$	9.7 ± 0.2
235	$Cu_2(L^{140}\text{-}2H)(NO_3)_2$	31.9 ± 1.0
236	$Ni(L^{1}\text{-}H)_2$	0.6 ± 0.2
237	$Ni(L^{2}\text{-}H)Cl\cdot 2H_2O$	33.1 ± 0.9
238	$[Ni(L^{4})_2]Cl_2$	1.7 ± 0.3
239	$Ni(L^{4}\text{-}H)_2$	13.4 ± 0.3
240	$[Ni(L^{5})_2]Cl_2$	3.6 ± 0.5
241	$Ni(L^{5}\text{-}H)_2$	2.9 ± 0.6
242	$[Ni(L^{6})_2]Cl_2$	3.7 ± 0.6
243	$Ni(L^{6}\text{-}H)_2$	5.8 ± 0.4
244	$Ni(L^{7})_2Cl_2$	4.8 ± 0.2
245	$Ni(L^{7})_2(NO_3)_2$	5.7 ± 0.7
246	$Ni(L^{7})_2SO_4$	4.8 ± 0.2
247	$Ni(L^{11}\text{-}H)Cl$	11.6 ± 0.3

Annexe 2. Continued

№	Formula	IC_{50} ±SD (μM)
248	$Ni(L^{11}\text{-}H)_2$	2.9 ± 0.1
249	$Ni(L^{11}\text{-}H)Br$	12.2 ± 0.2
250	$Ni(L^{11}\text{-}H)(NO_3)$	11.0 ± 0.5
251	$Ni(L^{11}\text{-}H)(OAc)$	19.1 ± 0.1
252	$Ni(L^{12}\text{-}H)Cl$	6.7 ± 0.1
253	$Ni(L^{12}\text{-}H)Br$	8.1 ± 0.1
254	$Ni(L^{12}\text{-}H)(NO_3)$	16.2 ± 0.3
255	$Ni(L^{12}\text{-}H)(OAc)$	17.4 ± 0.2
256	$Ni(L^{13}\text{-}H)Cl$	13.0 ± 0.1
257	$Ni(L^{14}\text{-}H)Cl$	18.5 ± 0.1
258	$Ni(L^{14}\text{-}H)(OAc)$	16.7 ± 0.4
259	$Ni(L^{15}\text{-}H)NO_3$	18.3 ± 0.2
260	$Ni(L^{15}\text{-}H)Br$	24.5 ± 0.1
261	$Ni(L^{16}\text{-}H)(NO_3)$	16.7 ± 0.1
262	$Ni(L^{17}\text{-}H)(NO_3)$	5.7 ± 0.1
263	$Ni(L^{17}\text{-}H)Br$	5.3 ± 0.3
264	$Ni(L^{17}\text{-}H)(OAc)$	7.7 ± 0.1
265	$Ni(L^{17}\text{-}H)_2$	6.9 ± 0.1
266	$Ni(L^{17}\text{-}H)Cl$	19.8 ± 0.4
267	$Ni(L^{18}\text{-}H)_2$	11.2 ± 0.7
268	$Ni(L^{18}\text{-}H)(OAc)$	7.2 ± 0.1
269	$Ni(L^{18}\text{-}H)(NO_3)$	17.6 ± 0.6
270	$Ni(L^{21}\text{-}H)_2$	19.4 ± 0.1
271	$Ni(L^{23}\text{-}H)_2\cdot 2H_2O$	2.1 ± 0.5
272	$Ni(L^{23}\text{-}H)(OAc)$	3.0 ± 0.7
273	$Ni(L^{23})(L^{23}\text{-}H)Br$	12.3 ± 0.2
274	$Ni(L^{27}\text{-}H)_2$	10.2 ± 0.6
275	$Ni(L^{33})_2Cl_2$	5.0 ± 0.6
276	$Ni(L^{33}\text{-}H)Cl$	15.8 ± 0.4
277	$Ni(L^{33})_2(NO_3)_2$	16.7 ± 0.9
278	$Ni(L^{34}\text{-}H)_2$	3.9 ± 0.1
279	$Ni(L^{38})(L^{38}\text{-}H)Cl$	3.6 ± 0.1
280	$Ni(L^{47})(L^{47}\text{-}H)Cl$	8.5 ± 0.3
281	$Ni(L^{50})_2(NO_3)_2$	19.6 ± 0.1
282	$Ni(L^{50}\text{-}H)Cl$	30.6 ± 0.8

Annexe 2. Continued

№	Formula	IC_{50} ±SD (μM)
283	$Ni(L^{52})_2(NO_3)_2$	29.2 ± 0.2
284	$Ni(L^{54})_2Cl_2$	2.7 ± 0.1
285	$Ni(L^{55})(L^{55}\text{-}H)Cl$	9.1 ± 0.1
286	$Ni(L^{55})(L^{55}\text{-}H)(NO_3)$	8.7 ± 0.1
287	$Ni(L^{55}\text{-}H)Cl$	8.7 ± 0.4
288	$Ni(L^{55}\text{-}H)(NO_3)$	9.7 ± 0.2
289	$Ni(L^{58})Cl_2$	19.1 ± 0.4
290	$Ni(L^{59})Cl_2$	15.2 ± 0.4
291	$Ni(L^{60}\text{-}H)Cl$	22.7 ± 0.6
292	$Ni(L^{61}\text{-}H)Cl$	15.1 ± 0.1
293	$Ni(L^{68}\text{-}H)_2$	7.2 ± 0.6
294	$Ni(L^{73}\text{-}H)_2$	2.9 ± 0.1
295	$Ni(L^{73}\text{-}2H)(H_2O)$	11.3 ± 0.6
296	$Ni(L^{74}\text{-}H)Cl$	9.6 ± 0.3
297	$Ni(L^{75}\text{-}H)Cl$	13.2 ± 0.4
298	$Ni(L^{75}\text{-}2H)(H_2O)$	15.6 ± 0.3
299	$Ni(L^{76}\text{-}2H)(H_2O)$	17.6 ± 0.4
300	$Ni(L^{76}\text{-}H)_2$	12.7 ± 0.3
301	$Ni(L^{77}\text{-}2H)(H_2O)$	14.3 ± 0.2
302	$Ni(L^{80}\text{-}H)_2$	8.1 ± 0.1
303	$Ni(L^{80}\text{-}H)Cl$	14.8 ± 0.9
304	$Ni(L^{82}\text{-}H)_2$	2.9 ± 0.5
305	$Ni(L^{83}\text{-}H)_2$	1.5 ± 0.1
306	$Ni(L^{87}\text{-}H)_2$	12.2 ± 0.2
307	$Ni(L^{99}\text{-}H)Cl$	20.4 ± 0.9
308	$Ni(L^{102}\text{-}H)Cl$	3.7 ± 0.6
309	$Ni(L^{102}\text{-}H)NO_3\cdot H_2O$	25.1 ± 0.7
310	$Ni(L^{103}\text{-}H)Cl$	8.4 ± 0.1
311	$Ni(L^{103}\text{-}H)Br\cdot H_2O$	19.7 ± 0.8
312	$Ni(L^{104}\text{-}H)Cl$	14.9 ± 0.1
313	$Ni(L^{105}\text{-}H)Cl$	20.5 ± 0.1
314	$Ni(L^{106}\text{-}2H)\cdot H_2O$	6.7 ± 0.1
315	$Ni(L^{107}\text{-}H)Cl$	22.3 ± 0.1
316	$Ni(L^{107}\text{-}2H)\cdot H_2O$	25.9 ± 0.5
317	$Ni(L^{111}\text{-}H)Cl$	29.7 ± 0.1

Annexe 2. Continued

№	Formula	IC_{50} ±SD (μM)
318	$Ni(L^{111}\text{-}H)(OAc)$	29.6 ± 0.7
319	$Ni(L^{111}\text{-}H)Br\cdot H_2O$	25.6 ± 0.2
320	$Ni(L^{112}\text{-}H)Cl$	24.0 ± 0.1
321	$Ni(L^{114}\text{-}H)_2\cdot H_2O$	14.3 ± 0.2
322	$Ni(L^{114}\text{-}H)Cl\cdot H_2O$	8.9 ± 0.5
323	$Ni(L^{114}\text{-}H)(OAc)$	2.8 ± 0.6
324	$Ni(L^{115}\text{-}H)(NO_3)\cdot H_2O$	14.5 ± 0.6
325	$Ni(L^{115}\text{-}H)(OAc)$	13.2 ± 0.3
326	$Ni(L^{115}\text{-}H)_2\cdot H_2O\cdot C_2H_5OH$	4.1 ± 0.4
327	$Ni(L^{116}\text{-}H)Cl$	28.8 ± 0.6
328	$Ni(L^{116}\text{-}H)(OAc)\cdot H_2O$	22.3 ± 0.4
329	$Ni(L^{116}\text{-}H)(NO_3)\cdot H_2O$	12.3 ± 0.3
330	$Ni(L^{117}\text{-}H)(OAc)\cdot H_2O$	6.9 ± 0.2
331	$Ni(L^{120})_2(ClO_4)_2$	25.1 ± 0.1
332	$Ni(L^{120})_2(NO_3)_2$	21.5 ± 0.4
333	$Ni(L^{121})_2(NO_3)_2$	21.1 ± 0.4
334	$Ni(L^{121})_2(ClO_4)_2$	22.0 ± 0.5
335	$Ni(L^{123})(L^{123}\text{-}H)NO_3$	15.5 ± 0.1
336	$Ni(L^{123})(L^{123}\text{-}H)I$	8.3 ± 0.3
337	$Ni(L^{125})(L^{125}\text{-}H)I$	13.5 ± 0.2
338	$Ni(L^{126}\text{-}H)_2$	6.0 ± 0.4
339	$Ni(L^{127})(L^{127}\text{-}H)ClO_4$	5.2 ± 0.7
340	$Ni(L^{127}\text{-}H)_2$	8.6 ± 0.5
341	$Ni(L^{129})_2I_2$	16.7 ± 0.2
342	$Ni(L^{130})(L^{130}\text{-}H)ClO_4$	8.0 ± 0.2
343	$Ni(L^{130})(L^{130}\text{-}H)I$	6.2 ± 0.6
344	$Ni(L^{131}\text{-}H)_2$	12.0 ± 0.6
345	$Ni(L^{133})_2(NO_3)_2$	27.3 ± 0.7
346	$Ni(L^{134})_2(NO_3)_2$	23.2 ± 0.4
347	$Ni(L^{134})_2I_2$	11.6 ± 0.3
348	$Ni(L^{135}\text{-}H)(OAc)$	7.2 ± 0.5
349	$Ni_2(L^{140}\text{-}2H)(ClO_4)_2$	22.6 ± 0.3
350	$Co(L^{1}\text{-}H)_2Cl$	21.4 ± 0.3
351	$Co(L^{2}\text{-}H)_2Cl\cdot 4H_2O$	22.4 ± 0.6
352	$Co(L^{5}\text{-}H)_3$	3.8 ± 0.9

Annexe 2. Continued

№	Formula	IC_{50} ±SD (μM)
353	$[Co(L^5)_3]Cl_3$	12.2 ± 0.8
354	$[Co(L^5)_3]Br_3$	3.7 ± 0.2
355	$Co(L^6\text{-}H)_3$	12.1 ± 0.4
356	$[Co(L^6)_3]Cl_3$	2.3 ± 0.2
357	$[Co(L^6)_3]Br_3$	2.3 ± 0.4
358	$[Co(L^6)_3](NO_3)_3$	2.7 ± 0.3
359	$Co(L^7)_2Cl_2$	22.8 ± 0.2
360	$Co(L^{13}\text{-}H)_2(NO_3)$	20.8 ± 0.1
361	$Co(L^{13}\text{-}H)_2Cl$	19.4 ± 0.2
362	$Co(L^{20}\text{-}H)_2(NO_3)$	8.9 ± 0.4
363	$Co(L^{23}\text{-}H)_2Cl$	7.3 ± 0.5
364	$Co(L^{23}\text{-}H)_2(OAc)$	3.7 ± 0.3
365	$Co(L^{29}\text{-}H)_2Cl$	22.8 ± 0.2
366	$Co(L^{38}\text{-}H)_2Cl$	21.4 ± 0.6
367	$Co(L^{38}\text{-}H)_2(NO_3)$	8.7 ± 0.3
368	$Co(L^{46}\text{-}H)_2NO_3$	7.6 ± 0.6
369	$Co(L^{47}\text{-}H)_2NO_3$	8.5 ± 0.8
370	$Co(L^{48}\text{-}H)_2Cl$	12.4 ± 0.7
371	$Co(L^{48}\text{-}H)_2NO_3$	13.8 ± 0.1
372	$Co(L^{56}\text{-}H)_2(NO_3)$	18.0 ± 0.2
373	$Co(L^{58})Cl_2$	8.1 ± 0.5
374	$Co(L^{58})(NO_3)_2$	7.3 ± 0.3
375	$Co(L^{59})(NO_3)_2$	18.0 ± 0.3
376	$Co(L^{68}\text{-}H)_2(NO_3)$	14.2 ± 0.2
377	$Co(L^{73}\text{-}H)_2Cl$	8.3 ± 0.1
378	$Co(L^{73}\text{-}H)_2(NO_3)$	12.0 ± 0.2
379	$Co(L^{75}\text{-}H)_2Cl$	7.5 ± 0.5
380	$Co(L^{75}\text{-}H)_2(NO_3)$	11.1 ± 0.2
381	$Co(L^{80}\text{-}H)_2Br$	11.4 ± 0.2
382	$Co(L^{80}\text{-}H)_2(NO_3)$	1.9 ± 0.1
383	$Co(L^{80}\text{-}H)_2Cl$	2.1 ± 0.2
384	$Co(L^{82}\text{-}H)_2(NO_3)$	4.6 ± 0.7
385	$Co(L^{83}\text{-}H)_2(NO_3)$	2.6 ± 0.6
386	$Co(L^{85}\text{-}H)_2Cl$	18.7 ± 0.3
387	$Co(L^{86}\text{-}H)_2Cl$	12.8 ± 0.4

Annexe 2. Continued

№	Formula	IC_{50} ±SD (μM)
388	$Co(L^{87}\text{-}H)_2Cl$	9.7 ± 0.1
389	$Co(L^{91}\text{-}H)_2Cl$	3.7 ± 0.5
390	$Co(L^{92}\text{-}H)_2Cl$	9.0 ± 0.2
391	$Co(L^{97}\text{-}H)_2Cl$	14.8 ± 0.7
392	$Co(L^{106}\text{-}H)_2NO_3$	10.7 ± 0.2
393	$Co(L^{107}\text{-}H)_2NO_3$	11.2 ± 0.6
394	$Co(L^{111}\text{-}H)_2NO_3$	6.0 ± 0.2
395	$Co(L^{111}\text{-}H)_2Br$	6.1 ± 0.4
396	$Co(L^{111}\text{-}H)_2Cl$	6.2 ± 0.4
397	$Co(L^{111}\text{-}H)_2OAc$	7.7 ± 0.7
398	$Co(L^{114}\text{-}H)_2NO_3\cdot H_2O$	6.5 ± 0.1
399	$Co(L^{114}\text{-}H)_2Br$	12.0 ± 0.1
400	$Co(L^{114}\text{-}H)_2Cl$	17.8 ± 0.2
401	$Co(L^{114}\text{-}H)_2(OAc)$	21.2 ± 0.7
402	$Co(L^{114}\text{-}H)_2Br\cdot H_2O$	17.1 ± 0.8
403	$Co(L^{122}\text{-}H)_2NO_3$	7.1 ± 0.2
404	$Co(L^{122}\text{-}H)_2Cl$	23.2 ± 0.6
405	$Co(L^{122}\text{-}H)_2Br$	24.4 ± 0.7
406	$Co(L^{122}\text{-}H)_2I$	21.7 ± 0.6
407	$Co(L^{123}\text{-}H)_2NO_3$	20.9 ± 0.7
408	$Co(L^{123}\text{-}H)_2I$	19.2 ± 0.1
409	$Co(L^{123}\text{-}H)_2Cl$	23.1 ± 0.4
410	$Co(L^{124}\text{-}H)_2I$	10.3 ± 0.4
411	$Co(L^{126}\text{-}H)_2NO_3$	14.5 ± 0.5
412	$Co(L^{126}\text{-}H)_2Br$	7.5 ± 0.3
413	$Co(L^{126}\text{-}H)_2I$	15.3 ± 0.7
414	$Co(L^{127}\text{-}H)_2NO_3$	16.5 ± 0.9
415	$Co(L^{130}\text{-}H)_2NO_3$	19.3 ± 0.3
416	$Co(L^{130}\text{-}H)_2I$	30.1 ± 0.4
417	$Co(L^{131}\text{-}H)_2I$	19.0 ± 0.6
418	$Co(L^{131}\text{-}H)_2Br$	17.9 ± 0.1
419	$Co(L^{131}\text{-}H)_2(OAc)$	23.2 ± 0.7
420	$Co(L^{132}\text{-}H)_2I$	16.0 ± 0.4
421	$Co(L^{133}\text{-}H)_2I$	25.7 ± 0.5
422	$Co(L^{133}\text{-}H)_2NO_3$	19.9 ± 0.1

Annexe 2. Continued

№	Formula	IC_{50} ±SD (μM)
423	$Co(L^{133}\text{-}H)_2Cl$	25.9 ± 0.4
424	$Co(L^{135}\text{-}H)_2Cl$	9.3 ± 0.1
425	$Co(L^{135}\text{-}H)_2I$	7.5 ± 0.1
426	$[Fe(L^{6})_3]Br_3$	2.1 ± 0.7
427	$[Fe(L^{6})_3]Cl_3$	2.8 ± 0.3
428	$Fe(L^{19}\text{-}H)_2(NO_3)$	23.4 ± 0.7
429	$Fe(L^{23}\text{-}H)_2Cl$	2.1 ± 0.1
430	$Fe(L^{34}\text{-}H)_2Cl$	8.6 ± 0.2
431	$Fe(L^{38}\text{-}H)_2(NO_3)$	2.4 ± 0.1
432	$Fe(L^{49}\text{-}H)_2Cl$	8.2 ± 0.2
433	$Fe(L^{49}\text{-}H)_2Br$	6.2 ± 0.3
434	$Fe(L^{56}\text{-}H)_2(NO_3)$	27.6 ± 0.5
435	$Fe(L^{60}\text{-}H)_2Cl$	24.6 ± 0.8
436	$Fe(L^{65}\text{-}H)_2(NO_3)$	14.2 ± 0.4
437	$Fe(L^{65}\text{-}H)_2Cl$	7.9 ± 0.4
438	$Fe(L^{65}\text{-}H)_2Br$	8.7 ± 0.1
439	$Fe(L^{73}\text{-}H)_2Cl$	5.4 ± 0.5
440	$Fe(L^{73}\text{-}H)(NO_3)_2(H_2O)$	18.6 ± 0.4
441	$Fe(L^{73}\text{-}H)_2(NO_3)$	6.2 ± 0.6
442	$Fe(L^{80}\text{-}H)_2(NO_3)$	10.2 ± 0.2
443	$Fe(L^{80}\text{-}H)_2Cl$	2.1 ± 0.2
444	$Fe(L^{82}\text{-}H)_2(NO_3)$	6.5 ± 0.1
445	$Fe(L^{83}\text{-}H)_2(NO_3)$	3.8 ± 0.1
446	$Fe(L^{86}\text{-}H)_2NO_3$	10.4 ± 0.1
447	$Fe(L^{87}\text{-}H)_2NO_3$	20.4 ± 0.1
448	$Fe(L^{106}\text{-}H)_2NO_3$	4.9 ± 0.2
449	$Fe(L^{106}\text{-}H)_2Br$	4.0 ± 0.4
450	$Fe(L^{111}\text{-}H)_2Br$	8.8 ± 0.1
451	$Fe(L^{122}\text{-}H)_2NO_3$	10.0 ± 0.2
452	$Fe(L^{122}\text{-}H)_2Cl$	9.4 ± 0.3
453	$Fe(L^{123}\text{-}H)_2NO_3$	9.6 ± 0.5
454	$Fe(L^{124}\text{-}H)_2NO_3$	7.5 ± 0.6
455	$Fe(L^{126}\text{-}H)_2NO_3$	2.1 ± 0.1
456	$Fe(L^{130}\text{-}H)_2NO_3$	12.5 ± 0.1
457	$Fe(L^{131}\text{-}H)_2NO_3$	4.0 ± 0.1

Annexe 2. Continued

№	Formula	IC_{50} ±SD (μM)
458	$Fe(L^{133}\text{-}H)_2NO_3$	27.4 ± 0.4
459	$Fe(L^{133}\text{-}H)_2Br$	20.8 ± 1.0
460	$Fe(L^{135}\text{-}H)_2NO_3$	7.3 ± 0.1
461	$Fe(L^{136}\text{-}H)_2Cl$	22.3 ± 0.2
462	$Mn(L^{18}\text{-}H)_2$	6.7 ± 0.6
463	$Mn(L^{20}\text{-}H)_2$	13.9 ± 0.4
464	$Mn(L^{21}\text{-}H)_2$	7.7 ± 0.6
465	$Mn(L^{23}\text{-}H)_2$	22.6 ± 0.3
466	$Mn(L^{29}\text{-}H)_2$	9.4 ± 0.5
467	$Mn(L^{61}\text{-}H)_2$	32.1 ± 1.5
468	$K_2Mn(L^{73}\text{-}2H)_2$	10.1 ± 0.3
469	$Mn(L^{102}\text{-}H)_2$	14.0 ± 0.3
470	$Mn(L^{103}\text{-}H)_2$	14.8 ± 0.8
471	$Mn(L^{106}\text{-}2H)_2$	8.7 ± 0.2
472	$Cr(L^{47}\text{-}H)_2NO_3$	0.9 ± 0.1
473	$Cr(L^{122}\text{-}H)_2NO_3$	1.2 ± 0.1
474	$Cr(L^{127}\text{-}H)_2NO_3$	1.4 ± 0.3

Dr. Olga Garbuz, Prof.Valentin Gudumac,

Acad.Ion Toderaș, Acad. Aurelian Gulea

PROPRIETĂȚILE ANTIOXIDATIVE A COMPUȘILOR SINTETICI ȘI NATURALI. MECANISME DE ACȚIUNE.

MONOGRAFIE

Bun de tipar 10. 04. 2023. Formatul 70x100 $^{1}/_{12}$.
Coli de tipar 28,0. Coli editoriale 9,2.
Comanda 20/23. Tirajul 50 ex.

Centrul Editorial-Poligrafic al USM
str. Al. Mateevici, 60, Chişinău, MD 2009